The role of enteric glia in acute gut inflammation

Doctoral thesis

to obtain a doctorate (PhD)

from the Faculty of Medicine

of the University of Bonn

Patrick Leven

from Remscheid, Germany

2024

Written with authorization of

the Faculty of Medicine of the University of Bonn

First reviewer: Prof. Dr. rer. nat. Sven Wehner

Second reviewer: PD Walker S. Jackson, PhD

Day of oral examination: 07.10.2024

From the Clinic and Policlinic for general, visceral, thoracic and vascular surgery

Director: Prof. Dr. med. J. C. Kalff

Table of content

List of abbreviations

18S	18S ribosomal RNA
3‘	3-prime end
6-OHDA	6-hydroxydopamine
Acta2	Actin α 2
ADP	Adenosine diphosphate
AG	Research Group
Ano1	Anoctamin 1
ANOVA	Analysis of variance
AR	Adrenergic receptors
Areg	Amphiregulin
Arg1	Arginase 1
ATP	Adenosine triphosphate
Az	Aktenzeichen (official government ID)
BMDM	Bone-marrow derived macrophages
bp	Base pair
BSA	Bovine serum albumin
Btc	Betacellulin
c	Caecum
C57/BL6	C57Bl/6N inbred mouse strain
$CaCl_2$	Calcium chloride
CCL	C-C chemokine ligand
Cd164	Cluster of differentiation 164
cDNA	Complementary DNA
ChAT	Choline acetyltransferase
ChAT-Cre	B6;129S6-Chattm2(Cre)Lowl/J mice
CM	Conditioned media
Cnn1	Calponin 1
CNS	Central nervous system
Cre	Cre recombinase
CSF	Colony-stimulating factor
CT	Cycle threshold
Ctrl	Control
Cx3cr1	C-X3-C motif chemokine receptor 1
Cx43	Connexin-43 hemi channels
CXCL	C-X-C chemokine ligand
DAMP	Danger-associated molecular pattern
DEG	Differentially expressed genes
DFG	German research foundations
DMEM	Dulbecco’s modified Eagle’s medium
DMSO	Dimethyl sulfoxide
dNTP	Deoxynucleoside triphosphate
DTT	Dithiothreitol
EC	Epithelial cell
EGC	Enteric glial cell
EGF	Epidermal growth factor
Elavl4/ Hu/D	Embryonic lethal abnormal vision-like RNA binding protein 4
ELISA	Enzyme-linked immunosorbent assay
EN	Enteric neurons

ENS	Enteric nervous system
ENTPDase	Ectonucleoside triphosphate diphosphohydrolase
ex	Extracellular
FACS	Fluorescence-activated cell sorting
FBS	Fetal bovine serum
FCS	Fetal calf serum
FFPE	Formalin-fixed paraffin-embedded tissue
FGF	Fibroblast growth factor
FoV	Field of view
Fw	Forward primer
GAPDH	Glyceraldehyde-3-Phosphate Dehydrogenase
GC	Geometric center
GDNF	Glial-derived neurotrophic factor
GFAP	Glial fibrillary acidic protein
GI	Gastrointestinal
GIT	Gastrointestinal transit
GO	Gene ontology
GPCR	G-protein-coupled receptor
h/ hu	Human
HA	Hemagglutinin
HBSS	Hanks balanced salt solution
Hcn4	K/Ca hyperpolarization-activated cyclic nucleotide-gated channel 4
HKG	Housekeeping genes
HRP	Horseradish peroxidase
Hsp90ab1	Heat shock protein 90 α family class B member 1
i.p.	Intraperitoneally
IBD	Inflammatory bowel disease
ICC	Interstitial cells of Cajal
IEG	Immediate early gene
IgG	Immunoglobulin-G
IHC	Immunohistochemistry
IL	Interleukin
IL1R1	Interleukin-1 receptor type 1
IM	Intestinal manipulation
IOC	Intestinal organotypic culture
IP	Immunoprecipitation
Itgam/Cd11b	Integrin α M
JellyOP	Jellyfish opsin
JellyOP$^{flox/+}$	CD1-Gt(ROSA)26Sor$^{em1(CAG-JellyOp-eGFP)}$ mouse
KCl	Potassium chloride
kDA	Kilo Dalton
Ki67	Kiel 67 (Proliferation marker)
KO	Knock-out
Lap	Laparotomy
LoxP	Target location for Cre recombinase
LPS	Lipopolysaccharide
Map2	Microtubule-associated protein 2
MAPK	Mitogen-activated protein kinase
ME	Muscularis externa
ME-Macs	Muscularis externa macrophages

$MgCl_2$	Magnesium chloride
MM	Muscularis macrophages
MPO	Myeloid peroxidase
mRNA	Messenger RNA
MS	Multiple sclerosis
ms	Mouse
mtRnr2	Mitochondrially encoded 16S RNA gene
MTT	Tetrazolium dye
MW	Molecular weight
n.d.	Not detectable
NaCl	Sodium chloride
NaH_2PO_4	Monosodium phosphate
$NaHCO_3$	Sodium bicarbonate
NB	Neurobasal medium
NE	Norepinephrine
Nes	Nestin
ns	Not significant
Olfr	Olfactory receptor
P2X2	Purinergic receptor P2X
p75	Nerve growth factor p75
PAMP	Pathogen-associated molecular patterns
PBS	Phosphate buffered saline
PC	Principal component
PCA	Principal component analysis
PCR	Polymerase chain reaction
Pen	Penicillin
PFA	Paraformaldehyde
Plp1	Proteolipid protein 1
PNS	Peripheral nervous system
POI	Postoperative ileus
QC	Quality control
qPCR	Quantitative real-time PCR
rb	Rabbit
RCAN	Regulator of calcineurin
RiboTag	HA-tagged Rpl22 subunit of the ribosome
RNA	Ribonucleic acid
RNase	Ribonuclease
RNA-Seq	RNA-sequencing
Rpl22	Large subunit ribosomal protein 22
$Rpl22^{HA/+}$	B6N.129-Rpl22tm1.1Psam/J mice
Rplp1	Ribosomal protein lateral stalk subunit P1
rpm	Revolutions per minute
RPMI	Roswell Park Memorial Institute medium
RT	Room temperature
Rv	Reverse primer
s.c.	Subcutaneously
S100b	S100 calcium-binding protein B
SB	Small bowel
scRNA-Seq	Single-cell RNA-sequencing
SDS	Sodium-dodecyl-sulfate
SDS-PAGE	SDS-Polyacrylamide gel electrophoresis

SEM	Standard error of the mean
siRNA	Silencing RNA
Slc1a3	Glutamate Aspartate Transporter
SMC	Smooth muscle cell
SNS	Sympathetic nervous system
Sox10	SRY Box transcription factor 10
$Sox10^{iCreERT2}$	B6-Tg(Sox10-icre/ERT2)388Wdr/J mice
st	Stomach
Strep	Streptomycin
STX	Sympathetic denervation/sympathectomized
Syn1	Synapsin 1
Syt4	Synaptotagmin 4
Tac1	Tachykinin 1
TH	Tyrosine hydroxylase
TNFα	Tumor necrosis factor α
Tris/HCl	Tris(hydroxymethyl)aminomethane hydrochloride
Tubb3	βIII-Tubulin
Uchl1	Ubiquitin carboxy-terminal hydrolase L1
WB	Western blot
WT	Wild type

List of figures

Ethic proposals and animal testing applications

Animal experiments performed at the University Hospital Bonn were approved by the appropriate authorities of North-Rhine-Westphalia, Germany under the following file numbers: 81-02.04.2018.A344, 81-02.04.2016.A367, 81-02-04-02018.A221, and 84-02.04.2017.A114.

Sample collection at the University Hospital Bonn from surgical material was carried out after prior consultation with the patients and under ethics approval from the ethics committee North-Rhine-Westphalia, Germany: Accession number 266_14.

1. Abstract

Background: Enteric glia, a heterogeneous type of neuroglia of the enteric nervous system, are contributors to the etiology of several immune-related gut diseases, such as the acute motility disorder postoperative ileus (POI). These cells are tightly integrated into the tissue and require dedicated novel approaches to analyze their cell-specific transcriptomes. While other tissue-resident cells, such as *muscularis externa* (*ME*) macrophages, have been analyzed, enteric glia and their modes of activation, such as their switch to a reactive phenotype during postoperative trauma, are still elusive. Herein, immediate signals from the sympathetic nervous system (SNS) acting on enteric glia might be the initial trigger of their reactivity. As IL-1 receptor signaling, and the release of ATP after trauma are important drivers of POI symptoms, their actions on enteric glia might exacerbate the initial reactivity and promote a gliosis phenotype.

Methods: Glial *RiboTag* mice, created by crossing *Sox10*^{iCreERT2} with *Rpl22*$^{HA/+}$ mice, were used to generate cell-specific mRNA. Mice (*C57/Bl6*, glial *RiboTag*, *IL-1R1*$^{flox/}$ *GFAP*^{Cre}) underwent an established POI mouse model involving laparotomy with or without mechanical disturbance of the small bowel. Postoperative outcome was additionally modified by pharmacological modulation of different pathways. *RiboTag* mice carrying a JellyOP$^{fl/+}$ construct were used for optogenetic stimulation of the G_s protein cascade in enteric glia and analysis of glial-specific transcriptomes. Primary cell cultures from human and murine enteric glia were used to analyze various active compounds related to the adrenergic, IL-1, or ATP pathways. Primary immune cell cultures were used to investigate their interaction with glial-derived factors. *Ex vivo* tissue cultures and calcium imaging were used to elucidate the effects further. Histology and protein analyses were conducted to investigate glial changes regarding acute inflammation and the pathways of choice.

Results: Specific expression of the glial *RiboTag* was validated, and protocols for its isolation from *ME* tissue were optimized. Longitudinal analysis of glial-specific transcriptomes revealed an early postoperative reactivity shaping the inflammatory microenvironment. Modulation of sympathetic signaling affected glial reactivity, especially during disease onset, with β-1/2 adrenoceptors as potential lynchpins of immediate postoperative gliosis. IL-1R1-signaling triggered gliosis in mice and humans accompanied by the upregulation of migratory mediators, while genetic deletion of IL-1R1 in glia

abolished gliosis, changed the immune cell status, and protected from POI. Purinergic receptor activation by ATP triggered gliosis in a P2X2-dependent manner, and Ambroxol was identified as a novel P2X2 antagonist that can ameliorate gliosis and POI symptoms in murine and human specimens.

Conclusions: We developed and refined a distinct protocol enabling time-point- and glia-specific *in vivo* mRNA snapshots. We revealed enteric glia as one of the earliest responding cell types after surgery through their innervation by the SNS, thereby evoking gliosis and POI initiation. This gliosis signature is further exacerbated by glial IL-1R1 signaling and ATP on glial P2X2. Modulation of either of these pathways reduced gliosis, ameliorated POI, and thus offered new avenues of POI prevention and curation.

2. Introduction

2.1 Enteric glia

The intestine is a highly complex organ containing multiple cell types, including diverse muscle, epithelial, immune, and enteric neural cells, that perform various specialized tasks [1]. The mentioned neural cells form the enteric nervous system (ENS), an expansive network of multiple neuronal and glial subtypes in the mucosal, submucosal, and muscle layers of the gastrointestinal tract [2-4]. Initially disregarded in favor of enteric neurons (EN), Gabella was the first to classify enteric glia cells (EGC) as distinct cells [5] and later, together with Jessen and Mirsky, proposed the name enteric glia [6,7]. EGC numbers and their ratio compared to ENs depend on numerous factors [8-10], such as the specific gut region, species, sex, and age, and can be estimated to several hundred million neurons [11] and up to seven times as many EGCs [12]. EGCs have been classified into four groups (Type I-IV) based on their morphology and intestinal location [13], a characterization initially described in guinea pigs that has since been confirmed in other animals [14-17] and partially translated to humans [18-20]. Spatially, EGCs are organized either in submucosal and myenteric plexuses [21], closely associated with ENs in the form of ganglia, or interspersed in the *muscularis externa (ME)* and mucosal layers [12] (**Figure 1**). EGCs express an array of cell-specific markers that can also be found in other glial populations in both peripheral tissues, such as satellite glia [22] or Schwann cells [23], and the central nervous system, such as astrocytes [24] and oligodendrocytes [25]. While they display a remarkable resemblance to astrocytes through their morphology [26] and electrophysiological potential [27], they lack other astrocytic identifiers, such as *Aldh1l1* [28].

Regarding expressional and functional properties, they rather share similarities to oligodendrocytes and neurons of the CNS [16], thus demanding classification as a unique cell type. So far, several markers have been established to describe EGCs, including glial fibrillary acidic protein (GFAP) [6], calcium-binding protein S100 calcium-binding protein β (S100β) [29], proteolipid protein 1 (PLP1) [16], and SRY-box transcription factor 10 (Sox10) [9,30]. However, the expression of those markers varies between different subpopulations, and no marker covers all subtypes, with Sox10 and S100β as the most abundantly (~95% and 85%, respectively) found cellular identifiers across

myenteric glia [15]. In addition to the traditional morphological classification, recent transcriptomic analyses on a single-cell or single-nuclei level suggest the existence of at least 3 or 6 transcriptionally different glial subtypes in mice [31,32] or humans [32-34], respectively.

Functionally, EGCs were initially defined as structural cells that “glued” the nerve structure of the ENS together and provided trophic support for neighboring neurons [35]. However, the view on EGCs has changed dramatically over the last decades, shifting from a passive, supportive to an active role in homeostasis, disease, and recovery[36-41]. It has become evident that EGCs are essential to gut homeostasis [12,42-44] and motility regulation [45-48]. During the past decade, multiple research groups, including ours, have uncovered their distinct influence during inflammatory conditions, wherein EGCs transition to a reactive state, which alters their morphology and impacts their transcriptional profile and functional capabilities [3]. Glial responses depend highly on disease induction, involved mediators, and interaction with other cells, underlining their plasticity [3,4,42,49].

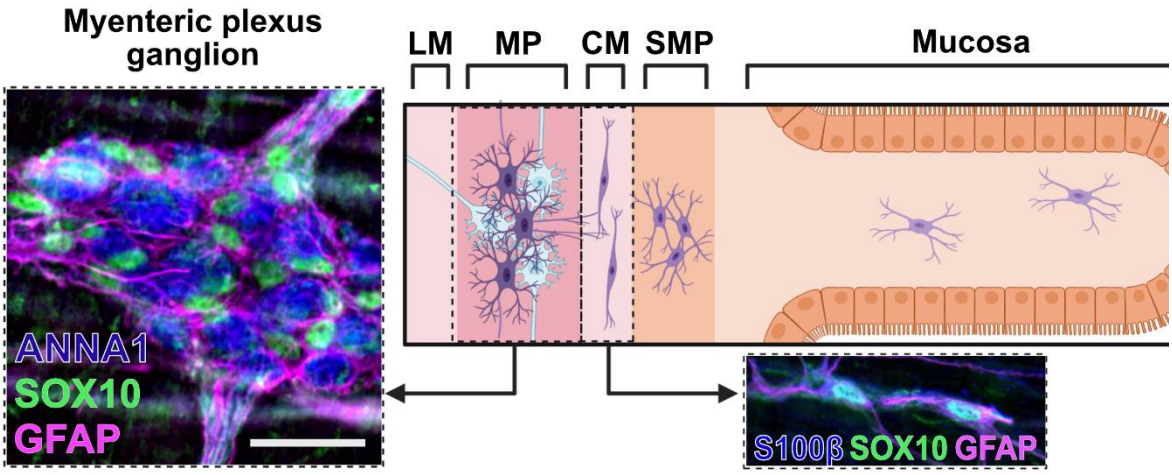

Figure 1. Schematic representation of different intestinal layers in the ileum section of the small bowel with resident EGCs. Depiction of the different layers (mucosa, submucosal plexus (SMP), circular muscle (CM), myenteric plexus (MP), longitudinal muscle (LM)) and EGCs residing in these layers. Arrows point to whole mount stainings of the *muscularis externa (ME)* with either a prominent ganglion in the myenteric plexus (left panel; ANNA1 (blue), SOX10 (green), GFAP (magenta)) or interganglionic EGCs (right panel; S100β (blue), SOX10 (green), GFAP (magenta)). Adapted from [3,4]. Scale bar 50 µm. Created with BioRender.com.

2.2 Postoperative ileus

One clinically relevant model to study the effects of acute surgical trauma and inflammation on enteric glia [50] is the postoperative ileus (POI) model [51]. Complications can arise after each surgical intervention and their degree and outcome depend on various factors, including duration and extent of the surgical procedure, experience of the performing surgeon, comorbidities, or other factors. After around 30% of abdominal surgeries [52], patients develop a transient impairment of gastrointestinal motility, a disorder commonly referred to as postoperative ileus or short POI. The dysfunction can either resolve quickly or persist for multiple days in a prolonged form. Clear nominal distinctions between them in the clinic, as well as defining diagnostics, are still inconsistent [53]. POI is characterized by symptoms ranging from nausea, vomiting, decreased food intake, over discomfort through abdominal bloating, and impaired motility [54], to an increased risk of anastomotic leakage [55]. Even though various risk factors are known [56], modern surgical techniques [57], and optimized protocols before and after surgery [58] are applied, few preventive or curative measures for POI are available, with most lacking additional clinical evidence [59-61]. Consequently, patients still recover slowly and need to be hospitalized longer [62], thereby increasing the financial burden of the hospital [63,64]. Mechanistically, POI develops in two phases: an immediate, post-surgery neurogenic phase, and a subsequent inflammatory phase [65,66]. Using animal models of POI, several studies revealed the involvement of a variety of cell types, such as mast cells [67-69], lymphocytes [70], monocytes [71] and macrophages [72-74], extrinsic nerves [75-79], ENs [80,81], and EGCs [50,82], as well as multiple mediators [83] participating during POI development. As inflammatory effects also occur immediately after surgery and neural deficits become apparent later [84], an overlap of these phases seems likely, especially regarding the highly concerted interactions between various cells. As EGCs have been implicated in one of the defining inflammatory pathways of POI in the past [50], but their exact interactions with other cells in shaping the phases of POI have not been investigated, we aimed to characterize their contribution by cell-specific transcriptional studies and identification of EGC-specific released mediators, thus elucidating their role in developing POI.

2.3 Activators and mediators of reactive EGCs

EGCs are surrounded by various other cell types that constantly interact with each other through multiple mediators [49,85-87]. Mainly discussed are their interactions with closely associated resident macrophages [88-90], ENs [91,92], and extrinsic nerves [93,94]. During inflammatory conditions, these interactions and mediators acting on EGCs lead to a switch in expression patterns, morphology, and function toward a so-called reactive phenotype [3]. Multiple models for chronic diseases [88,91,95-100] and acute disorders, such as POI [50,82,89], have recently been used to assess these reactive changes and investigate glial modulation of the inflammatory environment. As they affected various axes in these conditions as well as different other resident and infiltrating cells, they are attributed a prominent role therein, making them a promising therapeutic target [101] for intervening strategies [102]. Notably, many of the reactive changes observed in EGCs during inflammation are similar to previous observations made in astrocytes [103] in a process called gliosis [104]. Therein, neuroinflammation, in both acute [105] and chronic disease states [106,107], leads to astrocyte transition into a reactive state that affects the surrounding tissue, including neurons and microglia. A similar phenotypic switch for EGCs has been speculated for some time [108] and gained traction as a term [109,110] in other disease models [111-113], leading to a definition of specific hallmarks [3]. However, the exact connotation and setup of this gliosis phenotype have not been thoroughly described in an acute, post-surgery setting. Prompted by the phenotypic switch to a reactive state, EGCs release a variety of mediators that affect their microenvironment. Several of them, including the pro-inflammatory mediators IL-6 [50,114,115], IL-7 [116], CCL-2 [50,89,115], CXCL-10 [98], or nitric oxide (NO) [117] are essential in shaping the inflammatory response. EGCs also secrete macrophage colony-stimulating factor-1 (CSF-1) enabling them to simultaneously recruit immune cells, while also modifying their phenotype in various inflammatory disease conditions [88,89,118,119]. Similarly, the release of neuromodulatory molecules, such as reduced glutathione (GSH) [92] or the prostaglandins 15dPGJ2 [120] and PGE2 [95], influence neighboring ENs, while the release of S-Nitrosoglutathione (GSNO) [17,121] or glial-derived neurotrophic factor (GDNF) [97,122-125] ambivalently affects barrier integrity during health and disease [126]. The ability of EGCs to secrete a broad variety of molecules and thus shape their surroundings makes them an interesting player in the investigation of intestinal inflammation.

Previous studies uncovered several different pathways driving EGC reactivity and gliosis. A major mediator relevant to glial reactivity in POI [71,127,128] is the cytokine interleukin-1 (IL-1). Interestingly, EGCs are both a source of IL-1β [114,115,129] and a recipient through the expression of IL-1 receptor 1 (IL1R1) [50,88,108,130]. Here, IL-1β exacerbates the inflammatory reaction by triggering the release of other pro-inflammatory cytokines, and pharmacological or pan-genetic disruption of IL-1 signaling greatly diminishes POI symptoms [50]. Of note, IL-1β also originates from infiltrating leukocytes, showing yet another interaction with more loosely associated and transient entities [131]. A second important mediator acting on EGCs are purines, such as adenosine triphosphate (ATP), which, under homeostasis ensures gut equilibrium by controlling motility, blood flow, and neuronal interaction [132,133]. However, trauma and pathogenic mechanisms increase extracellular ATP levels to a pathological degree, resulting in more prominent disease symptoms [134-136]. ATP binding to glial purinergic receptors [14,137-140] and ATP released by EGCs [141] influences neurons [91,142-144] and affects motility [48]. Co-released with ATP from extrinsic nerve endings and ENs, norepinephrine (NE) plays an important role in inflammatory diseases [145,146] as one of the central neurochemicals released by the sympathetic nervous system (SNS) [147].

2.4 Influence of the sympathetic nervous system on acute inflammation

The role of the SNS in inflammation has been studied extensively and its outcome depends on specific factors of the underlying disease [148]. In mice affected by POI, we observed improved postoperative motility and an ameliorated inflammatory reaction after a preoperative chemical disruption of SNS innervation [73]. Since the SNS is immediately activated by the surgical incision of the skin [65] and EGCs can be direct targets of SNS signaling [93,149], an early influence of the SNS on EGC reactivity during surgical trauma seems feasible. While both chemical denervation and pharmacological application of SNS mediators have successfully been used to analyze their effects during inflammation [73,150,151], they are accompanied by involuntary systemic effects and modulation of several cell types. To specifically address the reactivity of EGCs after activation of adrenergic pathways and gain insight into their downstream-activated genes and modulated cell types, we generated a specific transgenic mouse – the JellyOP mouse. These mice, initially generated by the group of Philipp Sasse [152] and

modified to include a LoxP site, combine our Sox10^{iCreERT2} mouse line with a line carrying JellyOP-GFP$^{flox/+}$. This construct, containing a jellyfish opsin [153], enables cell-specific activation of G_s proteins [154] similar to pharmacological stimulation with isoprenaline [152]. Optogenetic approaches like these have garnered increasing attention in various fields [155] and have recently been used to modify intestinal diseases such as colitis [156]. In this thesis, optogenetic activation was performed on laparotomized animals by application of blue light (**Figure 2**), which initiates a G_s signaling cascade that resembles the transmitter-mediated stimulation by β-adrenergic agonists. By using a glia-specific Cre driver, we circumvented unspecific effects on other cells occurring during pharmacological modulation, thereby enabling us to precisely stimulate G_s signaling in EGCs.

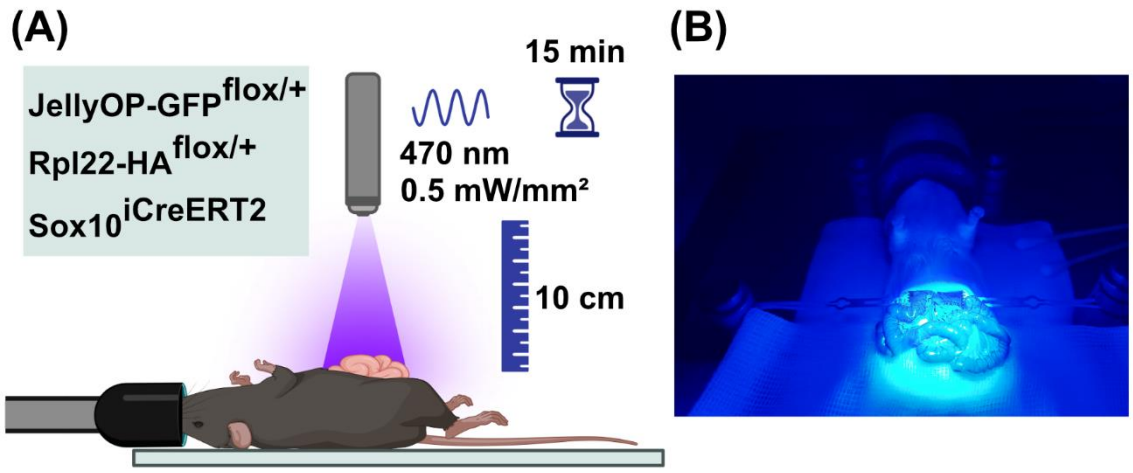

Figure 2. Optogenetic activation of G_s signaling to mimic the activation of β-adrenergic pathways in EGCs. (A) Mice carrying JellyOP-GFP$^{flox/+}$, Rpl22-HA$^{flox/+}$, and Sox10^{iCreERT2} were sedated and underwent a laparotomy and small bowel eventration. The bowel was illuminated with a blue light source (470 nm, 0.5 mW/mm²) at a distance of 10 cm for 15 minutes before the intestine was replaced and animals received standard postoperative care. **(B)** An intraoperative image of the optogenetic activation with blue light as described in (A). The image was created with BioRender.com.

2.5 EGC-specific transcriptomes: the *RiboTag* approach

EGCs are relatively large [8], often multiple processed [15] cells that are highly interconnected and tightly integrated into their surrounding tissue [11]. While traditional methods of obtaining cell-specific mRNA, such as fluorescence-activated cell sorting (FACS), work for spherical and small immune cells, such as lymphocytes, granulocytes, or monocytes [157], EGC morphology and tissue integration could lead to insufficient cell separation and loss of information in cell processes [158]. Even though recent efforts have been made, EGCs so far lack a unifying cell surface marker and thus require a fluorescent reporter signal to forego intracellular staining [159]. In addition, FACS harbors a general problem wherein the extensive cell preparation can lead to a shift in the molecular profile [160,161]. Modern methods such as single-cell RNA-sequencing [162] can circumvent these issues; however, they can be biased during isolation [163], have a limited sequencing depth, and are generally quite expensive [164].

One solution to circumvent these difficulties and facilitate cell-specific mRNA isolation was the creation of a genetic model, the *RiboTag* method, by Sanz and colleagues [158,165]. This method utilizes the Cre/LoxP system, which enables the transcriptional induction of hemagglutinin-tagged ribosomes (Rpl22-HA$^{flox/flox}$) by cell-specific Cre recombinase expression. Using an inducible, at adulthood glia-specific Sox10$^{iCre-ERT2}$ mouse line [166] in conjunction with the *RiboTag* enables immunoprecipitation of cell-specific ribosomes and thus a “snapshot” of actively transcribed mRNA in an *in vivo* situation [158].

Since its inception, the *RiboTag* method has been successfully used for various cell types in the CNS [167-172] and the intestine [82,88,95,113,145,146,173]. Therefore, we decided to optimize it, to decipher transcriptomes of ENS cells, particularly EGCs and cholinergic neurons. After successful establishment, we applied this approach to study POI development longitudinally. Moreover, the combination of the Rpl22-HA$^{flox/flox}$ strain with the Sox10^{iCreERT2}/JellyOP-GFP$^{flox/+}$ strain enabled the acquisition of glial mRNA after cell-specific activation. Notably, we appreciated the ability to capture actively transcribed, time point-specific mRNA from EGCs in POI, thus enabling the visualization of EGC plasticity and reactivity in the disease course.

2.6 Aim of the study

Our previous studies gave the first hints of EGC reactivity in POI; however, the mode of EGC activation as well as their exact molecular responses within the disease course of POI remained unknown. Therefore, we developed the following aims, which have been addressed in the present PhD thesis:

Aim 1: To optimize cell-specific mRNA generation by the *RiboTag* approach from EGCs of the small bowel *muscularis externa*.

Aim 2: To understand the role of the sympathetic nervous system as an immediate trigger of EGC reactivity.

Aim 3: To characterize the molecular responses of IL-1β- and ATP-triggered EGC reactivity.

To achieve **aim 1**, we adapt the *RiboTag* method to be used on cells of the ENS, including EGCs of the *ME* [174]. After the establishment and validation of the technique, we addressed our **2nd aim** and studied the role of the sympathetic nervous system and its primary neurotransmitter NE [175] as an immediate driver of EGC reactivity during the onset phase POI. Finally, in **aim 3**, we elucidated how EGCs shape POI during disease onset, progression, and resolution. Therein, we analyzed ATP [176] or IL-1β [177], known to be released during gut inflammation, and deciphered their potential to trigger EGC reactivity during POI. Ultimately, this PhD thesis was designed to define a specific molecular phenotype, to unveil the molecular cues of EGC reactivity throughout POI progression and provide a deeper insight into the plasticity and function of EGCs. The findings of these studies will yield valuable insight into enteric glial biology in acute intestinal inflammation and potentially other diseases and support the development of targeted approaches to prevent or treat POI.

2.7 References

1. Sharkey KA, Mawe GM. The enteric nervous system. *Physiological Reviews*. 2023;103(2):1487-1564. doi:10.1152/physrev.00018.2022
2. Fung C, Vanden Berghe P. Functional circuits and signal processing in the enteric nervous system. *Cell Mol Life Sci*. 2020;77(22):4505-4522. doi:10.1007/s00018-020-03543-6
3. Seguella L, Gulbransen BD. Enteric glial biology, intercellular signaling and roles in gastrointestinal disease. *Nat Rev Gastroenterol Hepatol*. 2021. doi:10.1038/s41575-021-00423-7
4. Boesmans W, Nash A, Tasnády KR, Yang W, Stamp LA, Hao MM. Development, Diversity, and Neurogenic Capacity of Enteric Glia. *Front Cell Dev Biol*. 2021;9:775102. doi:10.3389/fcell.2021.775102
5. Gabella G. Fine structure of the myenteric plexus in the guinea-pig ileum. *J Anat*. 1972;111(Pt 1):69-97.
6. Jessen KR, Mirsky R. Glial cells in the enteric nervous system contain glial fibrillary acidic protein. *Nature*. 1980;286(5774):736-737. doi:10.1038/286736a0
7. Gabella G. Ultrastructure of the nerve plexuses of the mammalian intestine: the enteric glial cells. *Neuroscience*. 1981;6(3):425-436. doi:10.1016/0306-4522(81)90135-4
8. Gabella G, Trigg P. Size of neurons and glial cells in the enteric ganglia of mice, guinea-pigs, rabbits and sheep. *J Neurocytol*. 1984;13(1):49-71. doi:10.1007/BF01148318
9. Hoff S, Zeller F, Weyhern CWH von, et al. Quantitative assessment of glial cells in the human and guinea pig enteric nervous system with an anti-Sox8/9/10 antibody. *J Comp Neurol*. 2008;509(4):356-371. doi:10.1002/cne.21769
10. Stenkamp-Strahm C, Patterson S, Boren J, Gericke M, Balemba O. High-fat diet and age-dependent effects on enteric glial cell populations of mouse small intestine. *Auton Neurosci*. 2013;177(2):199-210. doi:10.1016/j.autneu.2013.04.014
11. Furness JB. The enteric nervous system and neurogastroenterology. *Nature Reviews Gastroenterology & Hepatology*. 2012;9(5):286-294. doi:10.1038/nrgastro.2012.32
12. Sharkey KA. Emerging roles for enteric glia in gastrointestinal disorders. *J Clin Invest*. 2015;125(3):918-925. doi:10.1172/JCI76303
13. Hanani M, Reichenbach A. Morphology of horseradish peroxidase (HRP)-injected glial cells in the myenteric plexus of the guinea-pig. *Cell Tissue Res*. 1994;278(1):153-160. doi:10.1007/BF00305787
14. Vanderwinden J-M, Timmermans J-P, Schiffmann SN. Glial cells, but not interstitial cells, express P2X7, an ionotropic purinergic receptor, in rat gastrointestinal musculature. *Cell Tissue Res*. 2003;312(2):149-154. doi:10.1007/s00441-003-0716-2

15. Boesmans W, Lasrado R, Vanden Berghe P, Pachnis V. Heterogeneity and phenotypic plasticity of glial cells in the mammalian enteric nervous system. *Glia*. 2015;63(2):229-241. doi:10.1002/glia.22746

16. Rao M, Nelms BD, Dong L, et al. Enteric glia express proteolipid protein 1 and are a transcriptionally unique population of glia in the mammalian nervous system. *Glia*. 2015;63(11):2040-2057. doi:10.1002/glia.22876

17. Savidge TC, Newman P, Pothoulakis C, et al. Enteric glia regulate intestinal barrier function and inflammation via release of S-nitrosoglutathione. *Gastroenterology*. 2007;132(4):1344-1358. doi:10.1053/j.gastro.2007.01.051

18. Kapitza C, Chunder R, Scheller A, et al. Murine Esophagus Expresses Glial-Derived Central Nervous System Antigens. *Int J Mol Sci*. 2021;22(6). doi:10.3390/ijms22063233

19. Liu YA, Chung YC, Pan ST, et al. 3-D imaging, illustration, and quantitation of enteric glial network in transparent human colon mucosa. *Neurogastroenterol Motil*. 2013;25(5):e324-38. doi:10.1111/nmo.12115

20. Graham KD, López SH, Sengupta R, et al. Robust, 3-Dimensional Visualization of Human Colon Enteric Nervous System Without Tissue Sectioning. *Gastroenterology*. 2020;158(8):2221-2235.e5. doi:10.1053/j.gastro.2020.02.035

21. Gershon MD. The enteric nervous system. *Annu Rev Neurosci*. 1981;4:227-272. doi:10.1146/annurev.ne.04.030181.001303

22. Chu Y, Jia S, Xu K, et al. Single-cell transcriptomic profile of satellite glial cells in trigeminal ganglion. *Front Mol Neurosci*. 2023;16:1117065. doi:10.3389/fnmol.2023.1117065

23. Wolbert J, Li X, Heming M, et al. Redefining the heterogeneity of peripheral nerve cells in health and autoimmunity. *Proceedings of the National Academy of Sciences*. 2020;117(17):9466-9476. doi:10.1073/pnas.1912139117

24. Batiuk MY, Martirosyan A, Wahis J, et al. Identification of region-specific astrocyte subtypes at single cell resolution. *Nat Commun*. 2020;11(1):1220. doi:10.1038/s41467-019-14198-8

25. Huang H, He W, Tang T, Qiu M. Immunological Markers for Central Nervous System Glia. *Neurosci Bull*. 2023;39(3):379-392. doi:10.1007/s12264-022-00938-2

26. Reichenbach A, Siegel A, Senitz D, Smith TG. A comparative fractal analysis of various mammalian astroglial cell types. *Neuroimage*. 1992;1(1):69-77. doi:10.1016/1053-8119(92)90008-b

27. Hanani M, Francke M, Härtig W, Grosche J, Reichenbach A, Pannicke T. Patch-clamp study of neurons and glial cells in isolated myenteric ganglia. *Am J Physiol Gastrointest Liver Physiol*. 2000;278(4):G644-51. doi:10.1152/ajpgi.2000.278.4.G644

28. Boesmans W, Rocha NP, Reis HJ, Holt M, Vanden Berghe P. The astrocyte marker Aldh1L1 does not reliably label enteric glial cells. *Neuroscience Letters*. 2014;566:102-105. doi:10.1016/j.neulet.2014.02.042

29. Ferri GL, Probert L, Cocchia D, Michetti F, Marangos PJ, Polak JM. Evidence for the presence of S-100 protein in the glial component of the human enteric nervous system. *Nature*. 1982;297(5865):409-410. doi:10.1038/297409a0

30. Young HM, Bergner AJ, Müller T. Acquisition of neuronal and glial markers by neural crest-derived cells in the mouse intestine. *J Comp Neurol*. 2003;456(1):1-11. doi:10.1002/cne.10448

31. Zeisel A, Hochgerner H, Lönnerberg P, et al. Molecular Architecture of the Mouse Nervous System. *Cell*. 2018;174(4):999-1014.e22. doi:10.1016/j.cell.2018.06.021

32. Drokhlyansky E, Smillie CS, van Wittenberghe N, et al. The Human and Mouse Enteric Nervous System at Single-Cell Resolution. *Cell*. 2020;182(6):1606-1622.e23. doi:10.1016/j.cell.2020.08.003

33. Elmentaite R, Kumasaka N, Roberts K, et al. Cells of the human intestinal tract mapped across space and time. *Nature*. 2021;597(7875):250-255. doi:10.1038/s41586-021-03852-1

34. Fawkner-Corbett D, Antanaviciute A, Parikh K, et al. Spatiotemporal analysis of human intestinal development at single-cell resolution. *Cell*. 2021;184(3):810-826.e23. doi:10.1016/j.cell.2020.12.016

35. Rühl A. Glial cells in the gut. *Neurogastroenterol Motil*. 2005;17(6):777-790. doi:10.1111/j.1365-2982.2005.00687.x

36. Sunardi M, Cirillo C. Mini-review: "Enteric glia functions in nervous tissue repair: Therapeutic target or tool?". *Neuroscience Letters*. 2023;812:137360. doi:10.1016/j.neulet.2023.137360

37. Seguella L, Palenca I, Franzin SB, Zilli A, Esposito G. Mini-review: Interaction between intestinal microbes and enteric glia in health and disease. *Neuroscience Letters*. 2023;806:137221. doi:10.1016/j.neulet.2023.137221

38. Linan-Rico A, Ochoa-Cortes F, Schneider R, Christofi FL. Mini-review: Enteric glial cell reactions to inflammation and potential therapeutic implications for GI diseases, motility disorders, and abdominal pain. *Neuroscience Letters*. 2023;812:137395. doi:10.1016/j.neulet.2023.137395

39. Le Berre C, Naveilhan P, Rolli-Derkinderen M. Enteric glia at center stage of inflammatory bowel disease. *Neuroscience Letters*. 2023;809:137315. doi:10.1016/j.neulet.2023.137315

40. Thomasi B, Gulbransen B. Mini-review: Intercellular communication between enteric glia and neurons. *Neuroscience Letters*. 2023;806:137263. doi:10.1016/j.neulet.2023.137263

41. Prochera A, Rao M. Mini-Review: Enteric glial regulation of the gastrointestinal epithelium. *Neuroscience Letters*. 2023;805:137215. doi:10.1016/j.neulet.2023.137215

42. Rosenberg HJ, Rao M. Enteric glia in homeostasis and disease: From fundamental biology to human pathology. *iScience*. 2021;24(8):102863. doi:10.1016/j.isci.2021.102863

43. Ochoa-Cortes F, Turco F, Linan-Rico A, et al. Enteric Glial Cells: A New Frontier in Neurogastroenterology and Clinical Target for Inflammatory Bowel Diseases. *Inflamm Bowel Dis*. 2016;22(2):433-449. doi:10.1097/MIB.0000000000000667

44. Bubeck M, Becker C, Patankar JV. Guardians of the gut: influence of the enteric nervous system on the intestinal epithelial barrier. *Front Med (Lausanne)*. 2023;10:1228938. doi:10.3389/fmed.2023.1228938

45. Rao M, Rastelli D, Dong L, et al. Enteric Glia Regulate Gastrointestinal Motility but Are Not Required for Maintenance of the Epithelium in Mice. *Gastroenterology*. 2017;153(4):1068-1081.e7. doi:10.1053/j.gastro.2017.07.002

46. Aubé A-C, Cabarrocas J, Bauer J, et al. Changes in enteric neurone phenotype and intestinal functions in a transgenic mouse model of enteric glia disruption. *Gut*. 2006;55(5):630-637. doi:10.1136/gut.2005.067595

47. Nasser Y, Fernandez E, Keenan CM, et al. Role of enteric glia in intestinal physiology: effects of the gliotoxin fluorocitrate on motor and secretory function. *Am J Physiol Gastrointest Liver Physiol*. 2006;291(5):G912-27. doi:10.1152/ajpgi.00067.2006

48. McClain J, Grubišić V, Fried D, et al. Ca2+ responses in enteric glia are mediated by connexin-43 hemichannels and modulate colonic transit in mice. *Gastroenterology*. 2014;146(2):497-507.e1. doi:10.1053/j.gastro.2013.10.061.

49. Progatzky F, Pachnis V. The role of enteric glia in intestinal immunity. *Curr Opin Immunol*. 2022;77:102183. doi:10.1016/j.coi.2022.102183

50. Stoffels B, Hupa KJ, Snoek SA, et al. Postoperative ileus involves interleukin-1 receptor signaling in enteric glia. *Gastroenterology*. 2014;146(1):176-87.e1. doi:10.1053/j.gastro.2013.09.030

51. Kalff JC, Schraut WH, Simmons RL, Bauer AJ. Surgical manipulation of the gut elicits an intestinal muscularis inflammatory response resulting in postsurgical ileus. *Ann Surg*. 1998;228(5):652-663. doi:10.1097/00000658-199811000-00004

52. Wolthuis AM, Bislenghi G, Fieuws S, van Buck Overstraeten A de, Boeckxstaens G, D'Hoore A. Incidence of prolonged postoperative ileus after colorectal surgery: a systematic review and meta-analysis. *Colorectal Dis*. 2016;18(1):O1-9. doi:10.1111/codi.13210

53. Wells CI, Milne TGE, Seo SHB, et al. Post-operative ileus: definitions, mechanisms and controversies. *ANZ J Surg*. 2022;92(1-2):62-68. doi:10.1111/ans.17297

54. Sommer NP, Schneider R, Wehner S, Kalff JC, Vilz TO. State-of-the-art colorectal disease: postoperative ileus. *Int J Colorectal Dis*. 2021;36(9):2017-2025. doi:10.1007/s00384-021-03939-1

55. Peters EG, Dekkers M, van Leeuwen-Hilbers FW, et al. Relation between postoperative ileus and anastomotic leakage after colorectal resection: a post hoc analysis of a prospective randomized controlled trial. *Colorectal Dis*. 2017;19(7):667-674. doi:10.1111/codi.13582

56. Vather R, O'Grady G, Bissett IP, Dinning PG. Postoperative ileus: mechanisms and future directions for research. *Clin Exp Pharmacol Physiol*. 2014;41(5):358-370. doi:10.1111/1440-1681.12220

57. Abernethy EK, Aly EH. Post-operative Ileus after Minimally Invasive Colorectal Surgery: a summary of current strategies for prevention and management. *Dig Surg*. 2024. doi:10.1159/000537805

58. Hedrick TL, McEvoy MD, Mythen MMG, et al. American Society for Enhanced Recovery and Perioperative Quality Initiative Joint Consensus Statement on Postoperative Gastrointestinal Dysfunction Within an Enhanced Recovery Pathway for Elective Colorectal Surgery. *Anesth Analg*. 2018;126(6):1896-1907. doi:10.1213/ANE.0000000000002742

59. Chen H-T, Hung K-C, Huang Y-T, et al. Efficacy of electroacupuncture in improving postoperative ileus in patients receiving colorectal surgery: a systematic review and meta-analysis. *Int J Surg*. 2024;110(2):1113-1125. doi:10.1097/JS9.0000000000000848

60. Cui Y, Zhang C, Zhang H, et al. Effect evaluation of different preventive measures for ileus after abdominal operation: A systematic review and network meta-analysis. *Heliyon*. 2024;10(4):e25412. doi:10.1016/j.heliyon.2024.e25412

61. Emile SH, Horesh N, Garoufalia Z, Gefen R, Ray-Offor E, Wexner SD. Strategies to reduce ileus after colorectal surgery: A qualitative umbrella review of the collective evidence. *Surgery*. 2024;175(2):280-288. doi:10.1016/j.surg.2023.10.005

62. Nazzani S, Bandini M, Preisser F, et al. Postoperative paralytic ileus after major oncological procedures in the enhanced recovery after surgery era: A population based analysis. *Surg Oncol*. 2019;28:201-207. doi:10.1016/j.suronc.2019.01.011

63. Mao H, Milne TGE, O'Grady G, Vather R, Edlin R, Bissett I. Prolonged Postoperative Ileus Significantly Increases the Cost of Inpatient Stay for Patients Undergoing Elective Colorectal Surgery: Results of a Multivariate Analysis of Prospective Data at a Single Institution. *Dis Colon Rectum*. 2019;62(5):631-637. doi:10.1097/DCR.0000000000001301

64. Vather R, Josephson R, Jaung R, Robertson J, Bissett I. Development of a risk stratification system for the occurrence of prolonged postoperative ileus after colorectal surgery: a prospective risk factor analysis. *Surgery*. 2015;157(4):764-773. doi:10.1016/j.surg.2014.12.005

65. Boeckxstaens GE, Jonge WJ de. Neuroimmune mechanisms in postoperative ileus. *Gut*. 2009;58(9):1300-1311. doi:10.1136/gut.2008.169250

66. Kalff JC, Buchholz BM, Eskandari MK, et al. Biphasic response to gut manipulation and temporal correlation of cellular infiltrates and muscle dysfunction in rat. *Surgery*. 1999;126(3):498-509.

67. The FO, Bennink RJ, Ankum WM, et al. Intestinal handling-induced mast cell activation and inflammation in human postoperative ileus. *Gut*. 2008;57(1):33-40. doi:10.1136/gut.2007.120238

68. Jonge WJ de, The FO, van der Coelen D, et al. Mast cell degranulation during abdominal surgery initiates postoperative ileus in mice. *Gastroenterology*. 2004;127(2):535-545. doi:10.1053/j.gastro.2004.04.017

69. Snoek SA, Dhawan S, van Bree SH, et al. Mast cells trigger epithelial barrier dysfunction, bacterial translocation and postoperative ileus in a mouse model. *Neurogastroenterology & Motility*. 2012;24(2):172-e91. doi:10.1111/j.1365-2982.2011.01820.x

70. Engel DR, Koscielny A, Wehner S, et al. T helper type 1 memory cells disseminate postoperative ileus over the entire intestinal tract. *Nat Med*. 2010;16(12):1407-1413. doi:10.1038/nm.2255

71. Farro G, Stakenborg M, Gomez-Pinilla PJ, et al. CCR2-dependent monocyte-derived macrophages resolve inflammation and restore gut motility in postoperative ileus. *Gut*. 2017;66(12):2098-2109. doi:10.1136/gutjnl-2016-313144

72. Wehner S, Behrendt FF, Lyutenski BN, et al. Inhibition of macrophage function prevents intestinal inflammation and postoperative ileus in rodents. *Gut*. 2007;56(2):176-185. doi:10.1136/gut.2005.089615

73. Mallesh S, Schneider R, Schneiker B, et al. Sympathetic Denervation Alters the Inflammatory Response of Resident Muscularis Macrophages upon Surgical Trauma and Ameliorates Postoperative Ileus in Mice. *IJMS*. 2021;22(13):6872. doi:10.3390/ijms22136872

74. Enderes J, Mallesh S, Schneider R, et al. A Population of Radio-Resistant Macrophages in the Deep Myenteric Plexus Contributes to Postoperative Ileus Via Toll-Like Receptor 3 Signaling. *Front Immunol*. 2020;11:581111. doi:10.3389/fimmu.2020.581111

75. Hong G-S, Zillekens A, Schneiker B, et al. Non-invasive transcutaneous auricular vagus nerve stimulation prevents postoperative ileus and endotoxemia in mice. *Neurogastroenterology & Motility*. 2019;31(3):e13501. doi:10.1111/nmo.13501

76. Fukuda H, Tsuchida D, Koda K, Miyazaki M, Pappas TN, Takahashi T. Inhibition of sympathetic pathways restores postoperative ileus in the upper and lower gastrointestinal tract. *J Gastroenterol Hepatol*. 2007;22(8):1293-1299. doi:10.1111/j.1440-1746.2007.04915.x

77. Stakenborg N, Wolthuis AM, Gomez-Pinilla PJ, et al. Abdominal vagus nerve stimulation as a new therapeutic approach to prevent postoperative ileus. *Neurogastroenterol Motil*. 2017;29(9). doi:10.1111/nmo.13075

78. Chapman SJ, Helliwell JA, Naylor M, Tassinari C, Corrigan N, Jayne DG. Noninvasive vagus nerve stimulation to reduce ileus after major colorectal surgery: early development study. *Colorectal Dis*. 2021;23(5):1225-1232. doi:10.1111/codi.15561

79. Costes LMM, van der Vliet J, van Bree SHW, Boeckxstaens GE, Cailotto C. Endogenous vagal activation dampens intestinal inflammation independently of splenic innervation in postoperative ileus. *Auton Neurosci*. 2014;185:76-82. doi:10.1016/j.autneu.2014.07.006

80. Tsuchida Y, Hatao F, Fujisawa M, et al. Neuronal stimulation with 5-hydroxytryptamine 4 receptor induces anti-inflammatory actions via α7nACh receptors on muscularis macrophages associated with postoperative ileus. *Gut*. 2011;60(5):638-647. doi:10.1136/gut.2010.227546

81. Stakenborg N, Labeeuw E, Gomez-Pinilla PJ, et al. Preoperative administration of the 5-HT4 receptor agonist prucalopride reduces intestinal inflammation and shortens postoperative ileus via cholinergic enteric neurons. *Gut*. 2019;68(8):1406-1416. doi:10.1136/gutjnl-2018-317263

82. Mazzotta E, Grants I, Villalobos-Hernandez E, et al. BQ788 reveals glial ETB receptor modulation of neuronal cholinergic and nitrergic pathways to inhibit intestinal motility: Linked to postoperative ileus. *Br J Pharmacol*. 2023;180(19):2550-2576. doi:10.1111/bph.16145

83. Wehner S, Vilz TO, Stoffels B, Kalff JC. Immune mediators of postoperative ileus. *Langenbecks Arch Surg*. 2012;397(4):591-601. doi:10.1007/s00423-012-0915-y

84. Farro G, Gomez-Pinilla PJ, Di Giovangiulio M, et al. Smooth muscle and neural dysfunction contribute to different phases of murine postoperative ileus. *Neurogastroenterol Motil*. 2016;28(6):934-947. doi:10.1111/nmo.12796

85. Yoo BB, Mazmanian SK. The Enteric Network: Interactions between the Immune and Nervous Systems of the Gut. *Immunity*. 2017;46(6):910-926. doi:10.1016/j.immuni.2017.05.011

86. Chow AK, Gulbransen BD. Potential roles of enteric glia in bridging neuroimmune communication in the gut. *Am J Physiol Gastrointest Liver Physiol*. 2017;312(2):G145-G152. doi:10.1152/ajpgi.00384.2016

87. Wang H, Foong JPP, Harris NL, Bornstein JC. Enteric neuroimmune interactions coordinate intestinal responses in health and disease. *Mucosal Immunol*. 2022;15(1):27-39. doi:10.1038/s41385-021-00443-1

88. Grubišić V, McClain JL, Fried DE, et al. Enteric Glia Modulate Macrophage Phenotype and Visceral Sensitivity following Inflammation. *Cell Rep*. 2020;32(10):108100. doi:10.1016/j.celrep.2020.108100

89. Stakenborg M, Abdurahiman S, Simone V de, et al. Enteric glial cells favor accumulation of anti-inflammatory macrophages during the resolution of muscularis inflammation. *Mucosal Immunol*. 2022;15(6):1296-1308. doi:10.1038/s41385-022-00563-2

90. Viola MF, Chavero-Pieres M, Modave E, et al. Dedicated macrophages organize and maintain the enteric nervous system. *Nature*. 2023;618(7966):818-826. doi:10.1038/s41586-023-06200-7

91. Brown IAM, McClain JL, Watson RE, Patel BA, Gulbransen BD. Enteric glia mediate neuron death in colitis through purinergic pathways that require connexin-43 and nitric oxide. *Cell Mol Gastroenterol Hepatol*. 2016;2(1):77-91. doi:10.1016/j.jcmgh.2015.08.007

92. Abdo H, Derkinderen P, Gomes P, et al. Enteric glial cells protect neurons from oxidative stress in part via reduced glutathione. *The FASEB Journal*. 2010;24(4):1082-1094. doi:10.1096/fj.09-139519

93. Gulbransen BD, Bains JS, Sharkey KA. Enteric glia are targets of the sympathetic innervation of the myenteric plexus in the guinea pig distal colon. *J Neurosci*. 2010;30(19):6801-6809. doi:10.1523/JNEUROSCI.0603-10.2010

94. Smith-Edwards KM, Edwards BS, Wright CM, et al. Sympathetic Input to Multiple Cell Types in Mouse and Human Colon Produces Region-Specific Responses. *Gastroenterology*. 2021;160(4):1208-1223.e4. doi:10.1053/j.gastro.2020.09.030

95. Morales-Soto W, Gonzales J, Jackson WF, Gulbransen BD. Enteric glia promote visceral hypersensitivity during inflammation through intercellular signaling with gut nociceptors. *Sci Signal*. 2023;16(812):eadg1668. doi:10.1126/scisignal.adg1668

96. Grubišić V, Perez-Medina AL, Fried DE, et al. NTPDase1 and -2 are expressed by distinct cellular compartments in the mouse colon and differentially impact colonic physiology and function after DSS colitis. *American Journal of Physiology-Gastrointestinal and Liver Physiology*. 2019;317(3):G314-G332. doi:10.1152/ajpgi.00104.2019

97. Gonzalez Acera M, Bubeck M, Mascia F, et al. Dynamic, Transient, and Robust Increase in the Innervation of the Inflamed Mucosa in Inflammatory Bowel Diseases. *Cells*. 2021;10(9). doi:10.3390/cells10092253

98. Progatzky F, Shapiro M, Chng SH, et al. Regulation of intestinal immunity and tissue repair by enteric glia. *Nature*. 2021;599(7883):125-130. doi:10.1038/s41586-021-04006-z

99. Brown IAM, Gulbransen BD. The antioxidant glutathione protects against enteric neuron death in situ, but its depletion is protective during colitis. *American Journal of Physiology-Gastrointestinal and Liver Physiology*. 2018;314(1):G39-G52. doi:10.1152/ajpgi.00165.2017

100. Dora D, Ferenczi S, Stavely R, et al. Evidence of a Myenteric Plexus Barrier and Its Macrophage-Dependent Degradation During Murine Colitis: Implications in Enteric Neuroinflammation. *Cell Mol Gastroenterol Hepatol*. 2021;12(5):1617-1641. doi:10.1016/j.jcmgh.2021.07.003

101. Gulbransen BD, Christofi FL. Are We Close to Targeting Enteric Glia in Gastrointestinal Diseases and Motility Disorders? *Gastroenterology*. 2018;155(2):245-251. doi:10.1053/j.gastro.2018.06.050

102. Mazzotta E, Villalobos-Hernandez EC, Fiorda-Diaz J, Harzman A, Christofi FL. Postoperative Ileus and Postoperative Gastrointestinal Tract Dysfunction: Pathogenic Mechanisms and Novel Treatment Strategies Beyond Colorectal Enhanced Recovery After Surgery Protocols. *Front Pharmacol*. 2020;11:583422. doi:10.3389/fphar.2020.583422

103. Liddelow SA, Barres BA. Reactive Astrocytes: Production, Function, and Therapeutic Potential. *Immunity*. 2017;46(6):957-967. doi:10.1016/j.immuni.2017.06.006

104. Burda JE, Sofroniew MV. Reactive gliosis and the multicellular response to CNS damage and disease. *Neuron*. 2014;81(2):229-248. doi:10.1016/j.neuron.2013.12.034

105. Hara M, Kobayakawa K, Ohkawa Y, et al. Interaction of reactive astrocytes with type I collagen induces astrocytic scar formation through the integrin-N-cadherin pathway after spinal cord injury. *Nat Med*. 2017;23(7):818-828. doi:10.1038/nm.4354

106. das Neves SP, Sousa JC, Sousa N, Cerqueira JJ, Marques F. Altered astrocytic function in experimental neuroinflammation and multiple sclerosis. *Glia*. 2021;69(6):1341-1368. doi:10.1002/glia.23940

107. Liddelow SA, Guttenplan KA, Clarke LE, et al. Neurotoxic reactive astrocytes are induced by activated microglia. *Nature*. 2017;541(7638):481-487. doi:10.1038/nature21029

108. Boyen GBT von, Steinkamp M, Reinshagen M, Schäfer K-H, Adler G, Kirsch J. Proinflammatory cytokines increase glial fibrillary acidic protein expression in enteric glia. *Gut*. 2004;53(2):222-228. doi:10.1136/gut.2003.012625

109. Neunlist M, Rolli-Derkinderen M, Latorre R, et al. Enteric glial cells: recent developments and future directions. *Gastroenterology*. 2014;147(6):1230-1237. doi:10.1053/j.gastro.2014.09.040

110. Gulbransen BD, Sharkey KA. Novel functional roles for enteric glia in the gastrointestinal tract. *Nat Rev Gastroenterol Hepatol*. 2012;9(11):625-632. doi:10.1038/nrgastro.2012.138

111. Filippis D de, Esposito G, Cirillo C, et al. Cannabidiol reduces intestinal inflammation through the control of neuroimmune axis. *PLoS One*. 2011;6(12):e28159. doi:10.1371/journal.pone.0028159

112. Cossais F, Leuschner S, Barrenschee M, et al. Persistent Increased Enteric Glial Expression of S100β is Associated With Low-grade Inflammation in Patients With Diverticular Disease. *J Clin Gastroenterol*. 2019;53(6):449-456. doi:10.1097/MCG.0000000000001011

113. Delvalle NM, Dharshika C, Morales-Soto W, Fried DE, Gaudette L, Gulbransen BD. Communication Between Enteric Neurons, Glia, and Nociceptors Underlies the Effects of Tachykinins on Neuroinflammation. *Cell Mol Gastroenterol Hepatol*. 2018;6(3):321-344. doi:10.1016/j.jcmgh.2018.05.009

114. Liñán-Rico A, Turco F, Ochoa-Cortes F, et al. Molecular Signaling and Dysfunction of the Human Reactive Enteric Glial Cell Phenotype: Implications for GI Infection, IBD, POI, Neurological, Motility, and GI Disorders. *Inflamm Bowel Dis*. 2016;22(8):1812-1834. doi:10.1097/MIB.0000000000000854

115. Rosenbaum C, Schick MA, Wollborn J, et al. Activation of Myenteric Glia during Acute Inflammation In Vitro and In Vivo. *PLoS One*. 2016;11(3):e0151335. doi:10.1371/journal.pone.0151335

116. Kermarrec L, Durand T, Gonzales J, et al. Rat enteric glial cells express novel isoforms of Interleukine-7 regulated during inflammation. *Neurogastroenterol Motil*. 2019;31(1):e13467. doi:10.1111/nmo.13467

117. Turco F, Sarnelli G, Cirillo C, et al. Enteroglial-derived S100B protein integrates bacteria-induced Toll-like receptor signalling in human enteric glial cells. *Gut*. 2014;63(1):105-115. doi:10.1136/gutjnl-2012-302090

118. Muller PA, Koscsó B, Rajani GM, et al. Crosstalk between Muscularis Macrophages and Enteric Neurons Regulates Gastrointestinal Motility. *Cell*. 2014;158(5):1210. doi:10.1016/j.cell.2014.08.002

119. Schneider KM, Blank N, Alvarez Y, et al. The enteric nervous system relays psychological stress to intestinal inflammation. *Cell*. 2023;186(13):2823-2838.e20. doi:10.1016/j.cell.2023.05.001

120. Abdo H, Mahé MM, Derkinderen P, Bach-Ngohou K, Neunlist M, Lardeux B. The omega-6 fatty acid derivative 15-deoxy-$\Delta^{12,14}$-prostaglandin J2 is involved in neuroprotection by enteric glial cells against oxidative stress. *J Physiol*. 2012;590(11):2739-2750. doi:10.1113/jphysiol.2011.222935

121. Cheadle GA, Costantini TW, Lopez N, Bansal V, Eliceiri BP, Coimbra R. Enteric glia cells attenuate cytomix-induced intestinal epithelial barrier breakdown. *PLoS One*. 2013;8(7):e69042. doi:10.1371/journal.pone.0069042

122. Meir M, Flemming S, Burkard N, et al. Glial cell line-derived neurotrophic factor promotes barrier maturation and wound healing in intestinal epithelial cells in vitro. *Am J Physiol Gastrointest Liver Physiol*. 2015;309(8):G613-24. doi:10.1152/ajpgi.00357.2014.

123. Meir M, Kannapin F, Diefenbacher M, et al. Intestinal Epithelial Barrier Maturation by Enteric Glial Cells Is GDNF-Dependent. *Int J Mol Sci*. 2021;22(4). doi:10.3390/ijms22041887

124. Meir M, Burkard N, Ungewiß H, et al. Neurotrophic factor GDNF regulates intestinal barrier function in inflammatory bowel disease. *J Clin Invest*. 2019;129(7):2824-2840. doi:10.1172/JCI120261

125. Anitha M, Gondha C, Sutliff R, et al. GDNF rescues hyperglycemia-induced diabetic enteric neuropathy through activation of the PI3K/Akt pathway. *Journal of Clinical Investigation*. 2006;116(2):344-356. doi:10.1172/JCI26295

126. Biskou O, Meira de-Faria F, Walter SM, et al. Increased Numbers of Enteric Glial Cells in the Peyer's Patches and Enhanced Intestinal Permeability by Glial Cell Mediators in Patients with Ileal Crohn's Disease. *Cells*. 2022;11(3):335. doi:10.3390/cells11030335

127. Wehner S, Schwarz NT, Hundsdoerfer R, et al. Induction of IL-6 within the rodent intestinal muscularis after intestinal surgical stress. *Surgery*. 2005;137(4):436-446. doi:10.1016/j.surg.2004.11.003

128. Stein K, Lysson M, Schumak B, et al. Leukocyte-Derived Interleukin-10 Aggravates Postoperative Ileus. *Front Immunol*. 2018;9:2599. doi:10.3389/fimmu.2018.02599

129. Murakami M, Ohta T, Ito S. Lipopolysaccharides enhance the action of bradykinin in enteric neurons via secretion of interleukin-1beta from enteric glial cells. *J Neurosci Res*. 2009;87(9):2095-2104. doi:10.1002/jnr.22036

130. Tjwa ETTL, Bradley JM, Keenan CM, Kroese ABA, Sharkey KA. Interleukin-1beta activates specific populations of enteric neurons and enteric glia in the guinea pig ileum and colon. *Am J Physiol Gastrointest Liver Physiol*. 2003;285(6):G1268-76. doi:10.1152/ajpgi.00073.2003

131. Hupa KJ, Stein K, Schneider R, et al. AIM2 inflammasome-derived IL-1β induces postoperative ileus in mice. *Sci Rep*. 2019;9(1):10602. doi:10.1038/s41598-019-46968-1

132. Christofi FL. Purinergic receptors and gastrointestinal secretomotor function. *Purinergic Signalling*. 2008;4(3):213-236. doi:10.1007/s11302-008-9104-4

133. Caputi V, Marsilio I, Cerantola S, et al. Toll-Like Receptor 4 Modulates Small Intestine Neuromuscular Function through Nitrergic and Purinergic Pathways. *Front Pharmacol*. 2017;8:350. doi:10.3389/fphar.2017.00350

134. Idzko M, Ferrari D, Eltzschig HK. Nucleotide signalling during inflammation. *Nature*. 2014;509(7500):310-317. doi:10.1038/nature13085

135. Di Virgilio F, Dal Ben D, Sarti AC, Giuliani AL, Falzoni S. The P2X7 Receptor in Infection and Inflammation. *Immunity*. 2017;47(1):15-31. doi:10.1016/j.immuni.2017.06.020

136. Di Virgilio F, Sarti AC, Falzoni S, Marchi E de, Adinolfi E. Extracellular ATP and P2 purinergic signalling in the tumour microenvironment. *Nature Reviews Cancer*. 2018;18(10):601-618. doi:10.1038/s41568-018-0037-0

137. Galligan JJ. Purinergic signaling in the gastrointestinal tract. *Purinergic Signalling*. 2008;4(3):195-196. doi:10.1007/s11302-008-9109-z

138. Mendes CE, Palombit K, Tavares-de-Lima W, Castelucci P. Enteric glial cells immunoreactive for P2X7 receptor are affected in the ileum following ischemia and reperfusion. *Acta Histochem*. 2019;121(6):665-679. doi:10.1016/j.acthis.2019.06.001

139. Boesmans W, Cirillo C, van den Abbeel V, et al. Neurotransmitters involved in fast excitatory neurotransmission directly activate enteric glial cells. *Neurogastroenterol Motil*. 2013;25(2):e151-60. doi:10.1111/nmo.12065

140. Fung C, Boesmans W, Cirillo C, Foong JPP, Bornstein JC, Vanden Berghe P. VPAC Receptor Subtypes Tune Purinergic Neuron-to-Glia Communication in the Murine Submucosal Plexus. *Front Cell Neurosci*. 2017;11:118. doi:10.3389/fncel.2017.00118

141. Vieira C, Ferreirinha F, Magalhães-Cardoso MT, Silva I, Marques P, Correia-de-Sá P. Post-inflammatory Ileitis Induces Non-neuronal Purinergic Signaling Adjustments of Cholinergic Neurotransmission in the Myenteric Plexus. *Front Pharmacol*. 2017;8:811. doi:10.3389/fphar.2017.00811

142. Gulbransen BD, Sharkey KA. Purinergic neuron-to-glia signaling in the enteric nervous system. *Gastroenterology*. 2009;136(4):1349-1358. doi:10.1053/j.gastro.2008.12.058

143. gomes p, chevalier j, Boesmans W, et al. ATP-dependent paracrine communication between enteric neurons and glia in a primary cell culture derived from embryonic mice. *Neurogastroenterol Motil*. 2009;21(8):870-e62. doi:10.1111/j.1365-2982.2009.01302.x

144. Cerantola S, Caputi V, Marsilio I, et al. Involvement of Enteric Glia in Small Intestine Neuromuscular Dysfunction of Toll-Like Receptor 4-Deficient Mice. *Cells*. 2020;9(4). doi:10.3390/cells9040838

145. Matheis F, Muller PA, Graves CL, et al. Adrenergic Signaling in Muscularis Macrophages Limits Infection-Induced Neuronal Loss. *Cell*. 2020;180(1):64-78.e16. doi:10.1016/j.cell.2019.12.002

146. Gabanyi I, Muller PA, Feighery L, Oliveira TY, Costa-Pinto FA, Mucida D. Neuro-immune Interactions Drive Tissue Programming in Intestinal Macrophages. *Cell*. 2016;164(3):378-391. doi:10.1016/j.cell.2015.12.023

147. Duan H, Cai X, Luan Y, et al. Regulation of the Autonomic Nervous System on Intestine. *Front Physiol*. 2021;0:1075. doi:10.3389/fphys.2021.700129

148. Brinkman DJ, Hove AS ten, Vervoordeldonk MJ, Luyer MD, Jonge WJ de. Neuroimmune Interactions in the Gut and Their Significance for Intestinal Immunity. *Cells*. 2019;8(7). doi:10.3390/cells8070670

149. Nasser Y, Ho W, Sharkey KA. Distribution of adrenergic receptors in the enteric nervous system of the guinea pig, mouse, and rat. *J Comp Neurol*. 2006;495(5):529-553. doi:10.1002/cne.20898

150. Deng L, Guo H, Wang S, et al. The Attenuation of Chronic Ulcerative Colitis by (R)-salbutamol in Repeated DSS-Induced Mice. *Oxid Med Cell Longev*. 2022;2022:9318721. doi:10.1155/2022/9318721

151. Hove AS ten, Mallesh S, Zafeiropoulou K, et al. Sympathetic activity regulates epithelial proliferation and wound healing via adrenergic receptor α2A. *Sci Rep*. 2023;13(1):17990. doi:10.1038/s41598-023-45160-w

152. Makowka P, Bruegmann T, Dusend V, et al. Optogenetic stimulation of Gs-signaling in the heart with high spatio-temporal precision. *Nat Commun*. 2019;10(1):1281. doi:10.1038/s41467-019-09322-7

153. Koyanagi M, Takano K, Tsukamoto H, Ohtsu K, Tokunaga F, Terakita A. Jellyfish vision starts with cAMP signaling mediated by opsin-G(s) cascade. *Proceedings of the National Academy of Sciences*. 2008;105(40):15576-15580. doi:10.1073/pnas.0806215105

154. Bailes HJ, Zhuang L-Y, Lucas RJ. Reproducible and sustained regulation of Gαs signalling using a metazoan opsin as an optogenetic tool. *PLoS One*. 2012;7(1):e30774. doi:10.1371/journal.pone.0030774

155. Armbruster A, Mohamed AM, Phan HT, Weber W. Lighting the way: recent developments and applications in molecular optogenetics. *Curr Opin Biotechnol*. 2024;87:103126. doi:10.1016/j.copbio.2024.103126

156. Schiller M, Azulay-Debby H, Boshnak N, et al. Optogenetic activation of local colonic sympathetic innervations attenuates colitis by limiting immune cell extravasation. *Immunity*. 2021;54(5):1022-1036.e8. doi:10.1016/j.immuni.2021.04.007

157. Prinyakupt J, Pluempitiwiriyawej C. Segmentation of white blood cells and comparison of cell morphology by linear and naïve Bayes classifiers. *Biomed Eng Online*. 2015;14:63. doi:10.1186/s12938-015-0037-1

158. Sanz E, Yang L, Su T, Morris DR, McKnight GS, Amieux PS. Cell-type-specific isolation of ribosome-associated mRNA from complex tissues. *Proc Natl Acad Sci U S A*. 2009;106(33):13939-13944. doi:10.1073/pnas.0907143106

159. Grubišić V, Gulbransen BD. Astrocyte Cell Surface Antigen 2 and Other Potential Cell Surface Markers of Enteric glia in the Mouse Colon. *ASN Neuro*. 2022;14:17590914221083203. doi:10.1177/17590914221083203

160. Llufrio EM, Wang L, Naser FJ, Patti GJ. Sorting cells alters their redox state and cellular metabolome. *Redox Biology*. 2018;16:381-387. doi:10.1016/j.redox.2018.03.004

161. Binek A, Rojo D, Godzien J, et al. Flow Cytometry Has a Significant Impact on the Cellular Metabolome. *J Proteome Res*. 2019;18(1):169-181. doi:10.1021/acs.jproteome.8b00472

162. Papalexi E, Satija R. Single-cell RNA sequencing to explore immune cell heterogeneity. *Nature Reviews Immunology*. 2018;18(1):35-45. doi:10.1038/nri.2017.76

163. Zhang MJ, Ntranos V, Tse D. Determining sequencing depth in a single-cell RNA-seq experiment. *Nat Commun*. 2020;11(1). doi:10.1038/s41467-020-14482-y

164. Ziegenhain C, Vieth B, Parekh S, et al. Comparative Analysis of Single-Cell RNA Sequencing Methods. *Mol Cell*. 2017;65(4):631-643.e4. doi:10.1016/j.molcel.2017.01.023

165. Sanz E, Bean JC, Carey DP, Quintana A, McKnight GS. RiboTag: Ribosomal Tagging Strategy to Analyze Cell-Type-Specific mRNA Expression In Vivo. *Curr Protoc Neurosci*. 2019;88(1):e77. doi:10.1002/cpns.77

166. Laranjeira C, Sandgren K, Kessaris N, et al. Glial cells in the mouse enteric nervous system can undergo neurogenesis in response to injury. *J Clin Invest*. 2011;121(9):3412-3424. doi:10.1172/JCI58200

167. Hornstein N, Torres D, Das Sharma S, Tang G, Canoll P, Sims PA. Ligation-free ribosome profiling of cell type-specific translation in the brain. *Genome Biol*. 2016;17(1). doi:10.1186/s13059-016-1005-1

168. Kaczmarczyk L, Schleif M, Dittrich L, et al. Distinct translatome changes in specific neural populations precede electroencephalographic changes in prion-infected mice. *PLoS Pathog*. 2022;18(8):e1010747. doi:10.1371/journal.ppat.1010747

169. Gould TW, Dominguez B, Winter F de, et al. Glial cells maintain synapses by inhibiting an activity-dependent retrograde protease signal. *PLoS Genet*. 2019;15(3):e1007948. doi:10.1371/journal.pgen.1007948

170. Itoh N, Itoh Y, Tassoni A, et al. Cell-specific and region-specific transcriptomics in the multiple sclerosis model: Focus on astrocytes. *Proc Natl Acad Sci U S A*. 2018;115(2):E302-E309. doi:10.1073/pnas.1716032115

171. Kaczmarczyk L, Reichenbach N, Blank N, et al. Slc1a3-2A-CreERT2 mice reveal unique features of Bergmann glia and augment a growing collection of Cre drivers and effectors in the 129S4 genetic background. *Sci Rep*. 2021;11(1):5412. doi:10.1038/s41598-021-84887-2

172. Rakers C, Schleif M, Blank N, et al. Stroke target identification guided by astrocyte transcriptome analysis. *Glia*. 2019;67(4):619-633. doi:10.1002/glia.23544

173. Muller PA, Matheis F, Schneeberger M, Kerner Z, Jové V, Mucida D. Microbiota-modulated CART+ enteric neurons autonomously regulate blood glucose. *Science*. 2020;370(6514):314-321. doi:10.1126/science.abd6176

174. Leven P, Schneider R, Siemens KD, Jackson WS, Wehner S. Application of a RiboTag -based approach to generate and analyze mRNA from enteric neural cells. *Neurogastroenterology & Motility*. 2021. doi:10.1111/nmo.14309

175. Leven P, Schneider R, Schneider L, et al. β-adrenergic signaling triggers enteric glial reactivity and acute enteric gliosis during surgery. *J Neuroinflammation*. 2023;20(1):255. doi:10.1186/s12974-023-02937-0

176. Schneider R, Leven P, Glowka T, et al. A novel P2X2-dependent purinergic mechanism of enteric gliosis in intestinal inflammation. *EMBO Mol Med*. 2021;13(1):e12724. doi:10.15252/emmm.202012724

177. Schneider R, Leven P, Mallesh S, et al. IL-1-dependent enteric gliosis guides intestinal inflammation and dysmotility and modulates macrophage function. *Commun Biol*. 2022;5(1):811. doi:10.1038/s42003-022-03772-4

3. Publications

3.1 Publication 1: *Leven et al. 2021*, Application of a *RiboTag*-based approach to generate and analyze mRNA from enteric neural cells,

DOI:10.1111/nmo.14309

Received: 26 February 2021 | Revised: 22 November 2021 | Accepted: 29 November 2021

DOI: 10.1111/nmo.14309

TECHNICAL NOTE

Neurogastroenterology & Motility NGM WILEY

Application of a *RiboTag*-based approach to generate and analyze mRNA from enteric neural cells

Patrick Leven[1] | Reiner Schneider[1] | Kevin D. Siemens[1] | Walker S. Jackson[2] | Sven Wehner[1]

[1]Department of Surgery, University Hospital Bonn, Bonn, Germany

[2]Department of Biomedical and Clinical Sciences, Wallenberg Center for Molecular Medicine, Linköping University, Linköping, Sweden

Correspondence
Sven Wehner, Department of Surgery, University Hospital Bonn, Bonn, Germany.
Email: Sven.Wehner@ukbonn.de

Funding information
Cluster of Excellence - ImmunoSensation2, Grant/Award Number: EXC2151-190873048; Deutsche Forschungsgemeinschaft, Grant/Award Number: 388159768 and WE4205/3-1

Abstract

Background: Transcriptional profiling of specific intestinal cell populations under health and disease is generally based on traditional sorting approaches followed by gene expression analysis. Therein, specific cell populations are identified either by expressing reporter genes under a cell type-specific promotor or by specific surface antigens. This method provides adequate results for blood-derived and tissue-resident immune cells. However, in stromal cell analysis, cellular stress due to digestion often results in degraded RNA. Particularly, ramified cells integrated into the tissue, such as enteric neurons and glial cells, suffer from these procedures.

These cell types are involved in various intestinal processes, including a prominent immune-regulatory role, which requires suitable approaches to generate cell-specific transcriptional profiles.

Methods: *Sox10*^{iCreERT2} and choline acetyltransferase (*ChAT*^{Cre}) mice were crossed with mice labeling the ribosomal Rpl22 protein upon Cre activity with a hemagglutinin tag (Rpl22-HA, termed *RiboTag*). This approach enabled cellular targeting of enteric glia and neurons and the immediate isolation of cell-specific mRNA from tissue lysates without the need for cell sorting.

Key results: We verified the specific expression of Rpl22-HA in enteric glia and neurons and provided gene expression data demonstrating a successful enrichment of either Sox-10$^+$ glial or ChAT$^+$ neuronal mRNAs by the *RiboTag*-mRNA procedure using qPCR and RNA-Seq analysis.

Conclusions and inferences: We present a robust and selective protocol that allows the generation of cell type-specific transcriptional in vivo snapshots of distinct enteric cell populations that will be especially useful for various intestinal disease models involving peripheral neural cells.

KEYWORDS
enteric nervous system, gut homeostasis, gut inflammation, *RiboTag*

1 | INTRODUCTION

1.1 | Enteric neural cells

The intestine is a vast organ containing multiple cell types, including specialized epithelial, immune, and enteric neural cells with different subtypes. The latter form the enteric nervous system (ENS), a network of various subtypes of enteric neurons and enteric glia that differ in shape, function, and location, spanning the entire intestinal length.[1,2]

Several types of enteric neurons (ENs) exist in the ENS, and the majority express choline acetyltransferase (ChAT).[3] These cholinergic ENs are a prerequisite for developing a healthy gut[4] and vital for intestinal motility[5] and intestinal epithelium maintenance.[6]

Besides ENs, the ENS also harbors enteric glial cells (EGCs), a transcriptionally distinct type of glia in different shapes depending on their subtype,[2] which expresses similar molecular markers as other glia populations like Schwann cells and oligodendrocytes.[7] Similar to ENs, several distinct subtypes of EGC exist in the gut, yet over 95% of all EGCs express *Sox10*.[8] Recent studies of us and others revealed that glia are involved in several gastrointestinal processes such as motility,[9] intestinal inflammation,[10] neurophysiological homeostasis, and barrier functions.[2]

Traditionally, sorting techniques, such as fluorescence-associated cell sorting (FACS), are utilized to generate data from specific cell types and gain a deeper understanding of those mechanisms. However, the common usage of antigens for sorting specific ENS cells exhibits several issues. Most conventional markers require extensive cell preparation or a fluorescent reporter signal. Additionally, these markers are often limited to niche subtypes, such as p75 for neural stem cells,[11] that demand prior *in vitro* cultivation before the sorting procedure.[12] This, together with the prerequisite sample preparation, mechanical and/or enzymatic disruption, and the sorting procedure itself introduces significant changes in cell composition (Figure 1A)[13,14] thereby complicating FACS. Moreover, neural cells possess a complex anatomical structure that is disrupted during sample preparation, causing loss of mRNA in cell processes,[15] which limits RNA analysis. Another viable approach is the analysis of cell-specific transcriptomes via single-cell RNA-sequencing[16] (scRNA-Seq; Figure 1A). This method is highly specific but includes a steep monetary cost, isolation-based handling bias, and its poor sequencing depth majorly limits comparison of different experimental conditions.[17]

As a solution to analyze tightly integrated and morphologically challenging cell types, Sanz et al. developed a method to extract mRNA from a specific cell type without prior cell separation—the *RiboTag* method[15] wherein a transgenic Cre/loxP system is used to produce ribosomes with an Rpl22-haemagglutinin tag (*RiboTag*; Figure 1B) in the Cre-expressing cell type. This enables specific targeting and isolation of mRNA from *in vivo* cell populations by immune-precipitation (IP; Figure 1C). In the CNS, this method has been successfully applied for glia[18,19] and neurons.[20] Meanwhile, the *RiboTag* approach was adapted to several cell types and peripheral tissues, for example, to analyze intestinal macrophages,[21] by modifying the protocol toward unique cellular and extracellular matrix composition.[17] Recently, first steps in utilizing the *RiboTag* approach for enteric neural cells have been undertaken.[22–24] As the enteric nervous system has been shown to closely interact with the intestinal immune system and becomes transcriptionally active during inflammation, we utilized this method with either $Sox10^{iCreERT2}$ or $ChAT^{Cre}$ mice to create the *RiboTag* in EGC or $ChAT^{+}$ neurons, respectively (Figure 1B).

Key Points

- The RiboTag approach using enteric neural Cre-lines is a valid tool to generate in vivo "snapshots" of actively transcribed mRNA and will be invaluable in elucidating the role of these cell types in gut homeostasis and diseases.

In this technical note, we provide a selective protocol including a comprehensive quantitative expression-based quality control in support of the *RiboTag* method as an appropriate tool to generate transcriptional *in vivo* snapshots of ENS cells without the need for elaborate sorting-based isolation.

2 | MATERIALS AND METHODS

For a more convenient overview, all chemicals used in the analysis, including vendors and additional information, can be found in Tables S1 and S2.

2.1 | Animals

10- to 12-week-old male $ChAT^{Cre}$ (B6;129S6-Chattm2(cre)Lowl/J) or $Sox10^{iCreERT2}$ (B6-Tg(Sox10-icre/ERT2)388Wdr/J) were crossbred with $Rpl22^{HA/+}$ (B6N.129-Rpl22tm1.1Psam/J) mice. All animals were maintained under pathogen-free conditions, and experiments were carried out in accordance with German federal law (Az.: 81–02.04.2016 A367).

$Sox10^{iCreERT2}/Rpl22^{HA/+}$ animals received intraperitoneal injections of 100 µl Tamoxifen [MP Biomedicals,] dissolved in 10% ethanol, 90% sterile corn oil (final concentration 10 mg ml^{-1}) for three days. Animals rested at least for one week after the final injection before any experiments were performed.

2.2 | Immunohistochemistry

The terminal ileum and terminal colon were opened longitudinally, fixed with 4% PFA for 20 min (for ChAT stainings, overnight), and washed with Krebs-Henseleit buffer, and mucosal-free *muscularis externa* whole mounts were prepared, permeabilized (1% Triton X-100/PBS; RT, 20 min), and blocked with (5% donkey serum, 0.25% Triton

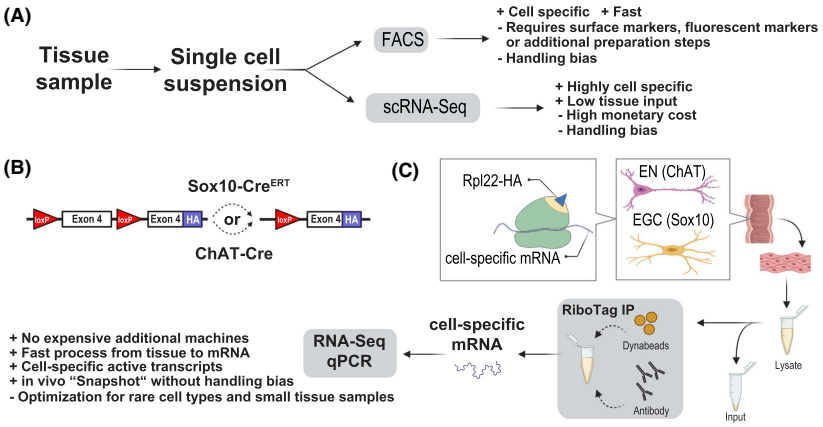

FIGURE 1 Comparative overview of RNA analysis methods. (A) Generation of specific cell population samples by fluorescence-based cell sorting and single-cell RNA-Seq analysis and their dis-/advantages. (B) Genetic overview of the Cre/Rpl22-HA construct (*RiboTag*). Excision of endogenous, loxP flanked Exon 4 of the *Rpl22* gene by either tamoxifen-inducible *Sox10*^{iCreERT2} or ChAT^{Cre} and subsequent expression of HA-tagged *Rpl22* rRNA and tagged ribosomes. (C) *RiboTag* workflow: Schematic of a ribosome with *Rpl22* subunit and incorporated HA-Tag carrying cell-specific mRNA, targeted cell types and their tissue location and workflow of sample preparation, IP and *RiboTag* approach advantages

TABLE 1 Antibodies

Host	Target	Fluorophore	Clone	Supplier	Art. No.	Application
Goat	Sox10	---	Polyclonal	Santa Cruz Biotech	*discontinued*	IHC
Goat	ChAT	---	Polyclonal	Merck	AB144P	IHC
Rabbit	HA	---	C29F4	Cell signaling	3724S	IHC/WB
Mouse	β-Actin	---	AC–74	Merck	A5316	WB
Mouse	HA	---	16-B–12	Biolegend	901514	IP
Donkey	Rabbit	Alexa647	Polyclonal	Dianova	711–606–152	IHC
Donkey	Goat	Alexa488	Polyclonal	Thermo Scientific	A–11055	IHC
Donkey	Mouse	DyLight 800	Polyclonal	Thermo Scientific	SA5-10172	WB
Donkey	Rabbit	IRDye 680	Polyclonal	Li-Cor	926–68073	WB

X-100/PBS; RT, 1 h). Primary and secondary antibodies (Table 1) were incubated overnight at 4°C and 1.5 h at RT, respectively. Stained whole mount preparations were mounted with ImmuMount (Fisher Scientific; 10662815), and microscopy was performed on a Nikon Eclipse TE2000-E and a Leica SP8 AOTF confocal microscope.

2.3 | Western blot

The protein concentration of lysates was determined by a BCA protein assay kit [Thermo Scientific]. SDS-PAGE was performed with 100 µg of protein. The primary and secondary antibodies (Table 1) were incubated overnight at 4°C and 1 h at RT, respectively.

2.4 | *RiboTag* method

RiboTag IP was performed according to Sanz et al. 2019, adapted for intestinal tissue as follows: Small bowel whole intestinal tissue was placed in ice-cold Krebs-Henseleit buffer (Table 2), and muscle layer mechanically separated from the mucosal layer. Swift separation and cooling, whenever possible, are crucial to increase yield and integrity. Separated layers were placed in RNA*later* [Thermo Scientific; AM7020] to further protect the tissue from inherent intestinal enzymes. Muscle layer (~100 mg) was lysed on a Precellys homogenizer [Bertin Instruments] (3x 5000 rpm, 45 s; 5 min intermediate incubation on ice) in pre-cooled homogenization buffer (Table 2), centrifuged (10 minutes, 10000 g, 4°C), and supernatants saved. Cleared lysate (50 µl) saved as "Input" control. Anti-HA antibody (5 µl; 1 mg mL^{-1}; Table 1) was added to each sample and incubated (4 hours, 4°C, 7 rpm). Antibody bound lysates were added to 200 µL of homogenization buffer equilibrated A/G dynabeads [Thermo Scientific; 88802] and incubated (overnight, 4°C, 7 rpm). Beads were washed thrice with high salt buffer (5 min each, 4°C, 7 rpm) (Table 2). Magnetic separation was performed on a pre-cooled magnet on ice for 1 min. Ribosomes containing specific mRNA were eluted from beads, and RNA was extracted using a Qiagen micro kit [Qiagen, Hilden, NRW, DE; 74004].

TABLE 2 IP buffer

Buffer	Components	
Krebs-Henseleit	NaCl 120 mM	Glucose 17.5 mM
	KCl 5.9 mM	$2(H_2O)CaCl_2$ 2.5 mM
	$NaHCO_3$ 15.5 mM	$6(H_2O)MgCl_2$ 1.17 mM
	NaH_2PO_4 1.4 mM	
Homogenization (lysis)	50 mM Tris/HCl	100 mM KCl
	1% NP–40	12 mM $MgCl_2$
	1 mg mL^{-1} Heparin	1 mM DTT
	100 µg mL^{-1} Cycloheximide	1x Protease Inhibitor P8340
	200 u mL^{-1} RNAsin	
High salt buffer (washing)	50 mM Tris/HCl	300 mM KCl
	1% NP–40	12 mM $MgCl_2$
	100 µg mL^{-1} Cycloheximide	0.5 mM DTT

TABLE 3 Primer pairs for qPCR analysis

Gene	Forward primer	Reverse primer
18S	GTAACCCGTTGAACCCCATT	CCATCCAATCGGTAGTAGCG
ChAT	TCATTAATTTCCGCCGTCTC	AGTCCCGGTTGGTGGAGTC
Syn1	ATTCTCTGTGGACATGGAAGTT	AATGACCAAACTTCGGTAGTCT
Map2	CAAAGAGAACGGGATCAACG	CAGGCTGGTCCTTGTGTTG
Tubb3	GTCAGCATGAGGGAGATCGT	GCAGGTCTGAGTCCCCTACA
Nestin	AGATCGCTCAGATCCTGGAA	AGGTGTCTGCAAGCGAGAGT
Sox10	GGACTACAAGTACCAACCTCGG	GGACTGCAGCTCTGTCTTTGG
Cd11b	TCCGGTAGCATCAACAACAT	GGTGAAGTGAATCCGGAACT
S100b	TGGTTGCCCTCATTGATGTCT	CCCATCCCCATCTTCGTCC
GFAP	ACATCGAGATCGCCACCTAC	CCTTCTGACACGGATTTGGT

2.5 | cDNA synthesis and qPCR analysis

For cDNA synthesis, 10 µL of purified RNA was transcribed with the Applied Biosystems™ High-Capacity cDNA Reverse Transcription Kit [Applied Biosystems; 10400745] according to the manufacturer's instruction manual. For qPCR analyses, cDNA (1:10 diluted) was combined with Power SYBR™ Green PCR Master Mix [Applied Biosystems; 4367659] and analyzed by qPCR (Table 3).

2.6 | RNA-Seq analysis

RNA-Seq libraries were prepared with QuantSeq 3′ mRNA-Seq Library Prep Kit [Lexogen, Greenland]. All libraries were sequenced (single-end 50 bp, 10 M reads) on an Illumina Hiseq 2500. RNA-Seq data were analyzed with "Partek Flow" software using a standard Lexogen pipeline (Lexogen 12112017), and Ensemble transcripts release 99 for mm10 mouse alignment. Briefly, the pipeline contained two adapter trimming and a base trimming step with respective subsequent quality controls (QC), followed by alignment using star2.5.3, a post-alignment QC, and a quantification to an annotation model. Counts were normalized, followed by a principal component analysis and lastly a gene set analysis. A file containing the code for each step of the pipeline is provided as supplement (Supplementary document 1).

3 | RESULTS

3.1 | HA expression in EGCs and ChAT-positive ENs

First, we aimed to verify the specific expression of the *RiboTag* (Rpl22-HA) in targeted cell types, and we analyzed HA expression by immunofluorescence microscopy in muscularis whole mounts. Colocalization of HA-tag and cell-specific markers, Sox10 (Figure 2A) or ChAT (Figure 3A) in the respective mouse lines, could be observed. Colocalization for Sox10/HA was roughly 85% in small bowel and 90% in colon whole mounts (Figure 2A). A small fraction of cells in observed ganglions showed HA expression, but not Sox10 expression. Whole mounts from $ChAT^{Cre}$/ $Rpl22^{HA/+}$ animals showed a high specificity of HA with around 90% (small bowel) and 95% (colon) of HA-positive cells double positive for HA/ChAT (Figure 3A). Moreover, in stainings of both tissues for HA and Nos1, no co-localization could be observed (data not shown). In turn,

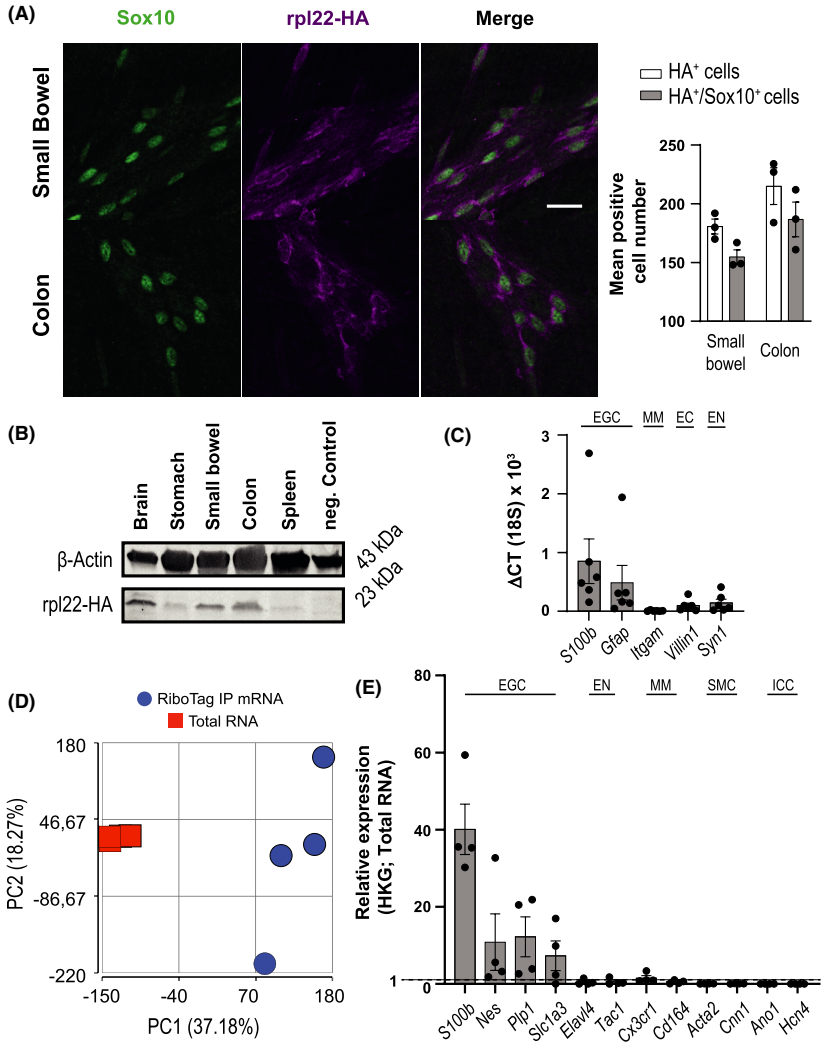

FIGURE 2 Expression of Rpl22-HA in EGCs and glia marker enrichment. (A) Immunohistological analysis of HA expression in whole mounts of small bowel and colon *muscularis externa* and histological analysis of HA specificity by quantification of mean HA^+ and $HA^+/Sox10^+$ cells per field of view ± SEM ($n = 3$; mean counts from 5 images per n). Tissue was stained for common glial cell nucleus marker Sox10 (green) and HA (magenta). Scale bar represents 25 μm. (B) SDS-PAGE of $Sox10^{iCreERT2}$/Rpl22-HA organ lysates (1: brain; 2: stomach; 3: small bowel *muscularis externa* (SB); 4: colon *muscularis externa* (colon); 5: spleen; 6: neg. control (WT brain)). Membranes were stained for Rpl22-HA (23 kDa) and housekeeping protein β-actin (43 kDa). ($n = 3$) (C) qPCR analysis of *RiboTag* IP mRNA from $Sox10^{iCreERT2}$/Rpl22-HA mice for EGC = enteric glial cell marker (*S100b*, *Gfap*), a EN = enteric neuron marker (*Synapsin1 (Syn1)*), a EC = epithelial cell marker (*Villin1*), and a MM = muscularis macrophage marker (*Itgam/Cd11b*) ($n = 6$). Data are represented as mean ΔCT to 18S RNA ± SEM. (D) Principal component analysis (PCA) of $Sox10^{iCreERT2}$/Rpl22-HA *RiboTag* IP mRNA (blue circles) and corresponding total RNA samples (red squares). (E) RNA-Seq analysis of *RiboTag* IP samples normalized to the mean expression of housekeeping genes (HKG; *β-actin*, *Hsp90ab1*, *Rplp1*. *GAPDH*, *mtRnr2*) and folded to corresponding total RNA ± SEM. EGC = enteric glial cell marker (*S100b*, *Nestin*, *Plp1*, *Slc1a3/Glast*), EN = enteric neuron marker (*Elavl4/Hu/D*, *Tac1*), MM = muscularis macrophage marker (*Cx3cr1*, *Cd164*), SMC = smooth muscle cell marker (*Acta2*, *Cnn1*) and, ICC = interstitial cells of cajal marker (*Ano1*, *Hcn4*). ($n = 4$ *RiboTag* IP; $n = 4$ total RNA)

Rpl22-HA protein expression was assessed by Western blotting, revealing high expression in intestinal and brain lysates of used mouse strains, whereas only small amounts were present in the spleen resulting either from $Sox10^+$ astrocyte-like glia cells[25] or $ChAT^+$ T cells,[26] respectively. In the brain of wild-type mice, no HA-tag was detected (Figures 2B and 3B).

3.2 | Cell-specific marker enrichment verification

Next, we assessed the specificity by measuring mRNA levels of target cells and other cell type markers, known to be abundantly present in the tissue samples. PCR analyses of precipitated mRNA from $Sox10^{iCreERT2}$/$Rpl22^{HA/+}$ mice showed strong enrichment of

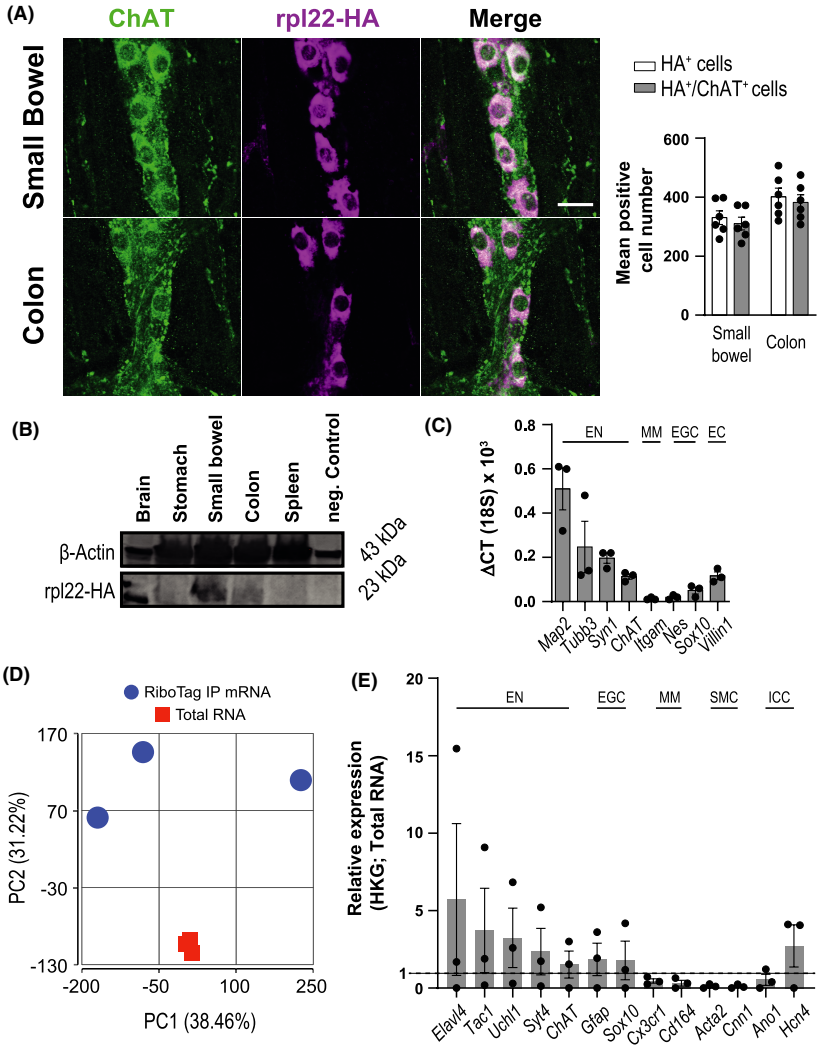

FIGURE 3 Expression of Rpl22-HA in EN and neuronal marker enrichment.(A) Immunohistological analysis of HA expression in whole mounts of small bowel and colon *muscularis externa* and histological analysis of HA specificity by quantification of mean HA^+ and HA^+/$ChAT^+$ cells per field of view ±SEM (n = 6; mean counts from 3 images per n). Tissue was stained for acetylcholine transferase ChAT (green) and HA (magenta). Scale bar represents 25 μm. (B) SDS-PAGE of $ChAT^{Cre}$/Rpl22-HA organ lysates lysates (1: brain; 2: stomach; 3: small bowel *muscularis externa* (SB); 4: colon *muscularis externa* (colon); 5: spleen; 6: neg. control (WT brain)). Membranes were stained for Rpl22-HA (23 kDa) and housekeeping protein β-actin (43 kDa). (*n* = 3) (C) qPCR analysis of *RiboTag* IP mRNA from $ChAT^{Cre}$/Rpl22-HA mice for EN = enteric neuron marker (*Microtubule-associated protein 2 (Map2)*, *βIII-Tubulin (Tubb3)*, *ChAT*, *Synapsin1 (Syn1)*), a MM = muscularis macrophage marker (*Itgam/Cd11b*), an EC = epithelial cell marker (*Villin1*), and EGC = enteric glial cell marker (*Nestin*, *Sox10*) (*n* = 3). Data are represented as mean ΔCT to 18S RNA ±SEM. (D) Principal component analysis (PCA) of $ChAT^{Cre}$/Rpl22-HA *RiboTag* IP mRNA (blue circles) and corresponding total RNA samples (red squares). (E) RNA-Seq analysis of *RiboTag* IP samples normalized to the mean expression of housekeeping genes (HKG; *β-actin*, *Hsp90ab1*, *Rplp1*. *GAPDH*, *mtRnr2*) and folded to corresponding total RNA ± SEM. EN = enteric neuron marker (*Elavl4/Hu/D*, *Tac1*, *Uchl1/Pgp9.5*, *Syt4*, *ChAT*), EGC = enteric glial cell marker (*Gfap*, *Sox10*), MM = muscularis macrophage marker (*Cx3cr1*, *Cd164*), SMC = smooth muscle cell marker (*Acta2*, *Cnn1*), and ICC = interstitial cells of cajal marker (*Ano1*, *Hcn4*). (*n* = 3 *RiboTag* IP; *n* = 3 total RNA)

glial markers (*S100b*, *Gfap)* while pan-leukocyte (*Itgam/Cd11b)* and neuronal marker *(Syn1)* were not enriched (Figure 2C). Additionally, we performed a 3´-end bulk RNA-Seq analysis. A principal component analysis (PCA) of the immunoprecipitated (*RiboTag*) mRNA from $Sox10^{iCreERT2}$/$Rpl22^{HA/+}$ mice and corresponding total RNA samples revealed a strong correlation within the groups (total RNA vs *RiboTag* mRNA) and a distinct clustering between them (Figure 2D). Furthermore, the RNA sequencing emphasized an enrichment of glia-associated genes (*S100b*, *Plp1*, *Nestin*, *Slc1a3/Glast*), while genes of immune cells (*Cx3cr1*, *Cd164*), smooth muscle cells (*Acta2*, *Cnn1*), interstitial cells of cajal (ICC) (*Ano1*, *Hcn4*), and neurons (*Elavl4/Hu/D*, *Tac1*) were not enriched (Figure 2E).

Consistently, we tested *RiboTag*-isolated mRNA from ChAT^{Cre}/Rpl22$^{HA/+}$ mice as well for the enrichment of target cell genes. Herein, we detected an enrichment of neuronal markers (*ChAT*, *Synapsin-1*, *Map2*, *and Tubb3*) in the precipitated mRNA while immune cell (*Itgam/Cd11b)* and glial cells marker (*Nestin*, *Sox10*) were not enriched (Figure 3C). Additionally, we performed a 3´-end bulk RNA-Seq analysis on these samples. A PCA analysis revealed a clustering within groups, but not between them (*RiboTag* IP mRNA vs total RNA; Figure 3D). Neuronal genes were enriched in the *RiboTag* mRNA (*Elavl4/Hu/D*, *Tac1*, *Uchl1/Pgp9.5*, *Syt4*, *and ChAT*), while marker for immune cells (*Cx3cr1*, *Cd164*), ICCs (*Ano1*), and smooth muscle cells (*Acta2*, *Cnn1*) was not enriched (Figure 3E).

Interestingly, expression of glial markers *Gfap* and *Sox10*, as well as ICC marker *Hcn4*, is slightly enriched in ChAT neuron mRNA (Figure 3E).

Applied methods showed a successful enrichment of targeted mRNAs in both mouse lines after the *RiboTag* approach.

4 | DISCUSSION

Originally, the *RiboTag* approach was developed to overcome technical limitations of FACS-based isolation methods of reactive astrocytes[27] and stressed neurons,[20] in the CNS. Their peripheral counterparts in the intestine are EGCs and ENs, respectively, and have been identified as important regulators of intestinal inflammation and homeostasis.[9,10,28] In line, Delvalle et al. already uncovered distinct glial alterations during a mouse colitis model,[24] while Gabanyi et al. gained critical understanding in neuronal transcription patterns with a pan-neuronal (Snap-25) *RiboTag* analysis[21] and revealed distinct subsets of neurons.[29] Due to limited information on the transcriptional responses of certain enteric neural cells in vivo, we developed an optimized *RiboTag* protocol for intestinal tissue that enables enrichment of specific high-quality RNA for further processing by comprehensive NGS methods. Thereby, we were able to reproducibly assess cell-specific mRNA of abundant (Sox-10^{+}) and less abundant (ChAT^{+} neurons) enteric neural cell, representing ~45% or 90% of the overall EN or EGC population,[30] respectively. HA signal was highly co-localized to the respective cell types, only present in tissues of genetically modified animals and showed an enrichment of genes depicting the chosen cell type. With the exception of some glial and ICC markers in the ChATCre/Rpl22HA/+ line, off-target cell marker expression was not enriched. While technical issues could be responsible for the presence of those markers, we rather suggest that glial gene expression in ChAT^{Cre}/Rpl22$^{HA/+}$ mice is a remnant feature from their shared neural progenitors.[31] Furthermore, recent studies in zebra fish gut show an expression of ICC marker *Hcn4* in enteric neurons,[32] in line with the expression in our ChAT neurons, suggesting a use of this channel in mice EN.

Although the *RiboTag* approach brings significant advantages into the intestinal research field, it has some limitations. Low amounts of tissue or isolation of mRNA from rare cell types might prove difficult, but additional steps, such as sample pooling, can assist acquiring sufficient amounts of RNA. Examples for clinically relevant but limited intestinal tissue are surgically resected regions, for example, tumors or anastomosis, or selective regions like Peyer's patches. Notably, regions such as the mucosa in which epithelial cells outnumber other stromal cell populations, like glia or neurons, are difficult to analyze (results not shown) and a *RiboTag* approach might not be the proper method to target these low abundance targets. Since inconsistent RNA amounts can lead to underperforming samples, experimental setups should be adjusted for sufficient samples to gain a solid statistical relevance of the results. Furthermore, the need for transgenic modification creates a strong dependence on the availability and specificity of Cre-mouse lines and, by that, limits this method to transgenic animal studies. Additionally, alternative methods to analyze specific RNA from cells, such as droplet-based collection of reporter-labeled nuclei or single-cell RNA sequencing, are emerging and might provide further avenues for future analyses or a means to emphasize *RiboTag* generated data.[33–35] Moreover, while the *RiboTag* approach is excellent for transcriptomic analysis of mRNA, other RNAs such as long noncoding RNAs cannot be analyzed with this approach.

In conclusion, the *RiboTag* method is a versatile, specific, and appropriate preclinical approach to analyze transcription patterns of complex tissues in the intestine and will be extremely valuable to delve deeper into the functional role of neural cells in the gut.

ACKNOWLEDGEMENTS

We thank Bianca Schneiker, Mariola Lysson for their technical assistance with animal handling and sample preparation. We also thank the Next Generation Sequencing Core and the Bioinformatics Core of the University Clinic Bonn for their assistance. We thank Professor Vassilis Pachnis for kindly providing the *Sox10^{iCreERT2}* mouse line. Workflow overview and graphical summary were created with *BioRender* software. This work was in part financed by the german research society (DFG; Grant WE4205/3-1) and the cluster of excellence “Immunosensation2” (EXC2151-190873048). We would like to thank the Microscopy Core Facility of the Medical Faculty at the University of Bonn for providing help, services, and devices funded by the Deutsche Forschungsgemeinschaft (DFG, German Research Foundation)—Project number 388159768.

AUTHOR CONTRIBUTIONS

PL and KDS performed the research; PL, RS, SW, and WSJ designed the study; SW and WSJ contributed essential reagents or tools; PL, RS, and SW analyzed the data and wrote the paper.

CONFLICT OF INTERESTS

The authors declare no competing interests.

DATA AVAILABILITY STATEMENT

The data that support the findings of this study are available from the corresponding author upon reasonable request.

ORCID

Patrick Leven https://orcid.org/0000-0002-6768-2523
Reiner Schneider https://orcid.org/0000-0002-7194-2703
Walker S. Jackson https://orcid.org/0000-0002-3003-5509
Sven Wehner https://orcid.org/0000-0002-8632-7631

REFERENCES

1. Fung C, Vanden BP. Functional circuits and signal processing in the enteric nervous system. *Cell Mol Life Sci*. 2020;77(22):4505-4522. doi:10.1007/S00018-020-03543-6
2. Seguella L, Gulbransen BD. Enteric glial biology, intercellular signalling and roles in gastrointestinal disease. *Nat Rev Gastroenterol Hepatol*. 2021;18(8):571-587. doi:10.1038/S41575-021-00423-7
3. Qu ZD, Thacker M, Castelucci P, Bagyánszki M, Epstein ML, Furness JB. Immunohistochemical analysis of neuron types in the mouse small intestine. *Cell Tissue Res*. 2008;334(2):147-161. doi:10.1007/S00441-008-0684-7
4. Johnson CD, Aj BA, Jf P, et al. Deletion of choline acetyltransferase in enteric neurons results in postnatal intestinal dysmotility and dysbiosis. *Faseb J*. 2018;32(9):4744-4752. doi:10.1096/Fj.201701474rr
5. Porter AJ, Wattchow DA, Brookes SJH, Costa M. Cholinergic and nitrergic interneurones in the myenteric plexus of the human colon. *Gut*. 2002;51(1):70-75. doi:10.1136/Gut.51.1.70
6. Gross ER, Gershon MD, Margolis KG, Gertsberg ZV, Cowles RA. Neuronal serotonin regulates growth of the intestinal mucosa in mice. *Gastroenterology*. 2012;143(2):408-417. doi:10.1053/j.gastro.2012.05.007
7. Rao M, Nelms BD, Dong L, et al. Enteric glia express proteolipid protein 1 and are a transcriptionally unique population of glia in the mammalian nervous system. *Glia*. 2015;63(11):2040-2057. doi:10.1002/Glia.22876
8. Boesmans W, Lasrado R, Vanden Berghe P, Pachnis V. Heterogeneity and phenotypic plasticity of glial cells in the mammalian enteric nervous system. *Glia*. 2015;63(2):229-241. doi:10.1002/Glia.22746
9. Ochoa-Cortes F, Turco F, Linan-Rico A, et al. Enteric glial cells: a new frontier in neurogastroenterology and clinical target for inflammatory bowel diseases. *Inflamm Bowel Dis*. 2016;22(2):433-449. doi:10.1097/Mib.0000000000000667
10. Stoffels B, Kj H, Sa S, et al. Postoperative ileus involves interleukin-1 receptor signaling in enteric glia. *Gastroenterology*. 2014;146(1):176-187. doi:10.1053/J.Gastro.2013.09.030
11. Bixby S, Gm K, Jt M, Nm J, Sj M. Cell-Intrinsic differences between stem cells from different regions of the peripheral nervous system regulate the generation of neural diversity. *Neuron*. 2002;35(4):643-656. doi:10.1016/S0896-6273(02)00825-5
12. Bn R, Zhang D, La S, et al. Enteric neural cells from hirschsprung disease patients form ganglia in autologous aneuronal colon. *Cell Mol Gastroenterol Hepatol*. 2016;2(1):92-109. doi:10.1016/J.Jcmgh.2015.09.007
13. Em L, Wang L, Fj N, Gj P. Sorting cells alters their redox state and cellular metabolome. *Redox Biol*. 2018;16:381-387. doi:10.1016/J.Redox.2018.03.004
14. Binek A, Rojo D, Godzien J, et al. Flow cytometry has a significant impact on the cellular metabolome. *J Proteome Res*. 2019;18(1):169-181. doi:10.1021/Acs.Jproteome.8b00472
15. Sanz E, Yang L, Su T, Dr M, Gs M, Amieux PS. Cell-type-specific isolation of ribosome-associated mrna from complex tissues. *Proc Natl Acad Sci U S A*. 2009;106(33):13939-13944. doi:10.1073/Pnas.0907143106
16. Papalexi E, Satija R. Single-cell rna sequencing to explore immune cell heterogeneity. *Nat Rev Immunol*. 2018;18(1):35-45. doi:10.1038/Nri.2017.76
17. Mj Z, Ntranos V, Tse D. Determining sequencing depth in a single-cell rna-seq experiment. *Nat Commun*. 2020;11(1):774. doi:10.1038/S41467-020-14482-Y
18. Tw G, Dominguez B, De WF, et al. Glial cells maintain synapses by inhibiting an activity-dependent retrograde protease signal. *Plos Genet*. 2019;15(3):e1007948. doi:10.1371/Journal.Pgen.1007948
19. Itoh N, Itoh Y, Tassoni A, et al. Cell-specific and region-specific transcriptomics in the multiple sclerosis model: focus on astrocytes. *Proc Natl Acad Sci U S A*. 2018;115(2):E302-E309. doi:10.1073/Pnas.1716032115
20. Hornstein N, Torres D, Das Sharma S, Tang G, Canoll P, Pa S. Ligation-free ribosome profiling of cell type-specific translation in the brain. *Genome Biol*. 2016;17(1):149. doi:10.1186/S13059-016-1005-1
21. Gabanyi I, Muller PA, Feighery L, Oliveira TY, Costa-Pinto FA, Mucida D. Neuro-immune interactions drive tissue programming in intestinal macrophages. *Cell*. 2016;164(3):378-391. doi:10.1016/j.cell.2015.12.023
22. Grubišić V, Jl M, De F, et al. Enteric glia modulate macrophage phenotype and visceral sensitivity following inflammation. *Cell Rep*. 2020;32(10):108100. doi:10.1016/J.Celrep.2020.108100
23. Pa M, Matheis F, Schneeberger M, Kerner Z, Jové V, Mucida D. Microbiota-modulated cart+ enteric neurons autonomously regulate blood glucose. *Science*. 2020;370(6514):314-321. doi:10.1126/Science.Abd6176
24. Nm D, Dharshika C, Morales-Soto W, De F, Gaudette L, Gulbransen BD. Communication between enteric neurons, glia, and nociceptors underlies the effects of tachykinins on neuroinflammation. *Cell Mol Gastroenterol Hepatol*. 2018;6(3):321-344. doi:10.1016/J.Jcmgh.2018.05.009
25. Ta L, Zhu L, Ms B. Spleen glia are a transcriptionally unique glial subtype interposed between immune cells and sympathetic axons. *Glia*. 2021;69(7):1799-1815. doi:10.1002/Glia.23993
26. Ding X, Wang H, Qian X, et al. Panicle-shaped sympathetic architecture in the spleen parenchyma modulates antibacterial innate immunity. *Cell Rep*. 2019;27(13):3799-3807. doi:10.1016/J.Celrep.2019.05.082
27. Rakers C, Schleif M, Blank N, et al. Stroke target identification guided by astrocyte transcriptome analysis. *Glia*. 2019;67(4):619-633. doi:10.1002/Glia.23544
28. Puzan M, Hosic S, Ghio C, Koppes A. Enteric nervous system regulation of intestinal stem cell differentiation and epithelial monolayer function. *Sci Rep*. 2018;8(1):6313. doi:10.1038/S41598-018-24768-3
29. Pa M, Schneeberger M, Matheis F, Kerner Z, Mucida D. Microbiota–modulated enteric neuron translational profiling uncovers a cart+ glucoregulatory subset; 2020. Accessed September 3, 2020.
30. Beck M, Schlabrakowski A, Schrödl F, Neuhuber W, Brehmer A. Chat and nos in human myenteric neurons: co-existence and co-absence. *Cell Tissue Res*. 2009;338(1):37-51. doi:10.1007/S00441-009-0852-4
31. Kulkarni S, Micci M-A, Leser J, et al. Adult enteric nervous system in health is maintained by a dynamic balance between neuronal apoptosis and neurogenesis. *Proc Natl Acad Sci*. 2017;114(18):E3709-E3718. doi:10.1073/Pnas.1619406114
32. Fujii K, Nakajo K, Egashira Y, et al. Gastrointestinal neurons expressing Hcn4 regulate retrograde peristalsis. *Cell Rep*. 2020;30(9):2879-2888. doi:10.1016/J.Celrep.2020.02.024
33. Morarach K, Mikhailova A, Knoflach V, et al. Diversification of molecularly defined myenteric neuron classes revealed by single-cell rna sequencing. *Nat Neurosci*. 2021;24(1):34-46. doi:10.1038/S41593-020-00736-X
34. Obata Y, Castaño Á, Boeing S, et al. Neuronal programming by microbiota regulates intestinal physiology. *Nature*. 2020;578(7794):284-289. doi:10.1038/S41586-020-1975-8

35. Drokhlyansky E, Cs S, Van Wittenberghe N, et al. The human and mouse enteric nervous system at single-cell resolution. *Cell*. 2020;182(6):1606-1622. doi:10.1016/J.Cell.2020.08.003

SUPPORTING INFORMATION

Additional supporting information may be found in the online version of the article at the publisher's website.

How to cite this article: Leven P, Schneider R, Siemens KD, Jackson WS, Wehner S. Application of a *RiboTag*-based approach to generate and analyze mRNA from enteric neural cells. *Neurogastroenterology & Motility*. 2022;34:e14309. doi:10.1111/nmo.14309

3.2 Publication 2: *Leven and Schneider et al. 2023*, β-adrenergic signaling triggers enteric glial reactivity and acute enteric gliosis during surgery, DOI:10.1186/s12974-023-02937-0

Leven *et al. Journal of Neuroinflammation* (2023) 20:255
https://doi.org/10.1186/s12974-023-02937-0

Journal of Neuroinflammation

RESEARCH Open Access

β-adrenergic signaling triggers enteric glial reactivity and acute enteric gliosis during surgery

Patrick Leven[1†], Reiner Schneider[1*†], Linda Schneider[1], Shilpashree Mallesh[1], Pieter Vanden Berghe[2], Philipp Sasse[3], Jörg C. Kalff[1] and Sven Wehner[1*]

Abstract

Background Enteric glia contribute to the pathophysiology of various intestinal immune-driven diseases, such as postoperative ileus (POI), a motility disorder and common complication after abdominal surgery. Enteric gliosis of the intestinal *muscularis externa* (*ME*) has been identified as part of POI development. However, the glia-restricted responses and activation mechanisms are poorly understood. The sympathetic nervous system becomes rapidly activated by abdominal surgery. It modulates intestinal immunity, innervates all intestinal layers, and directly interfaces with enteric glia. We hypothesized that sympathetic innervation controls enteric glia reactivity in response to surgical trauma.

Methods *Sox10*^{iCreERT2}/*Rpl22*$^{HA/+}$ mice were subjected to a mouse model of laparotomy or intestinal manipulation to induce POI. Histological, protein, and transcriptomic analyses were performed to analyze glia-specific responses. Interactions between the sympathetic nervous system and enteric glia were studied in mice chemically depleted of TH^{+} sympathetic neurons and glial-restricted *Sox10*^{iCreERT2}/*JellyOP*$^{fl/+}$/*Rpl22*$^{HA/+}$ mice, allowing optogenetic stimulation of β-adrenergic downstream signaling and glial-specific transcriptome analyses. A laparotomy model was used to study the effect of sympathetic signaling on enteric glia in the absence of intestinal manipulation. Mechanistic studies included adrenergic receptor expression profiling in vivo and in vitro and adrenergic agonism treatments of primary enteric glial cell cultures to elucidate the role of sympathetic signaling in acute enteric gliosis and POI.

Results With ~4000 differentially expressed genes, the most substantial enteric glia response occurs early after intestinal manipulation. During POI, enteric glia switch into a reactive state and continuously shape their microenvironment by releasing inflammatory and migratory factors. Sympathetic denervation reduced the inflammatory response of enteric glia in the early postoperative phase. Optogenetic and pharmacological stimulation of β-adrenergic downstream signaling triggered enteric glial reactivity. Finally, distinct adrenergic agonists revealed β-1/2 adrenoceptors as the molecular targets of sympathetic–driven enteric glial reactivity.

Conclusions Enteric glia act as early responders during post-traumatic intestinal injury and inflammation. Intact sympathetic innervation and active β-adrenergic receptor signaling in enteric glia is a trigger of the immediate glial

†Patrick Leven and Reiner Schneider are contributed equally to the work.

*Correspondence:
Reiner Schneider
Reiner.Schneider@ukbonn.de
Sven Wehner
Sven.Wehner@ukbonn.de
Full list of author information is available at the end of the article

postoperative inflammatory response. With immune-activating cues originating from the sympathetic nervous system as early as the initial surgical incision, adrenergic signaling in enteric glia presents a promising target for preventing POI development.

Keywords Enteric glia, *RiboTag*, Gut inflammation, Postoperative ileus, Sympathetic nervous system, Neuroimmunology, Adrenergic Signaling

Background

The enteric nervous system (ENS), consisting of enteric neurons and enteric glia, is a branch of the autonomous nervous system that governs various functions throughout the alimentary tract, such as gastric motility, fluid homeostasis, and blood flow [1]. Enteric glia are diverse neuroglia, displaying several subtypes based on morphology and location in intestinal structures [1]. Most enteric glia also show a unique co-expression pattern of SRY-Box transcription factor 10 (SOX10) together with either the glial markers S100B or glial fibrillary acidic protein (GFAP) [2], or proteolipid protein 1 (PLP1) [2, 3].

At first, enteric glia were mainly considered solely as neuron-supporting cell populations of the ENS, providing nutrition and protection for enteric neurons [1]. More recent studies provided new insights into enteric glia involvement in gastrointestinal (GI) homeostasis [1] and discovered their vital role in chronic [4] and acute [5] gut inflammation. Enteric glia switch to a reactive state during gut inflammation, altering their morphology, expression pattern, and functional character [1]. So far, broader enteric glial reactivity in POI has only been analyzed in vivo in the full tissue context, also described as a POI-related "enteric gliosis", but cell-intrinsic molecular responses of enteric glia and their primary activating mechanism were still missing. We termed the reactive inflammatory tissue state of the muscularis externa tissue "enteric gliosis" [5] as it shares molecular expression patterns with tissue gliosis in the central nervous system (CNS). Notably, this CNS gliosis is defined by the reactivity of glial cells, such as microglia, oligodendrocytes, and most importantly, astrocytes [6], the counterpart to enteric glia, which become activated during neuroinflammation in chronic disease states [7, 8] and after neurological traumata [9].

Part of the enteric gliosis state are reactive enteric glia, which modulate their microenvironment by secreting cytokines and chemokines like interleukin (IL)-6, C–C motif chemokine ligand (CCL)-2 [5, 10], and C–X–C motif chemokine ligand (CXCL)-10 [11], pro-inflammatory molecules, such as nitric oxide [12], and molecules that elicit an anti-inflammatory response, including glial cell-derived neurotrophic factor (GDNF) [13] and S-Nitrosoglutathione [14].

Although a comprehensive picture of reactive enteric glia in intestinal inflammation is still missing, recent studies provide evidence about stimuli being able to induce gliosis in the gut. These include lipopolysaccharide (LPS) [15], cytokines such as interleukin (IL)-1β [10], tumor necrosis factor (TNF)α [16], and interferon-gamma (IFNγ) [17], as well as purines, e.g., ADP [4] or ATP [5]. The latter is released by both intrinsic and extrinsic enteric neurons innervating the gut and is co-released with norepinephrine (NE) from sympathetic neurons. NE is the principal neurotransmitter of the sympathetic nervous system (SNS) [18], known to interact with enteric glia through adrenergic receptors [19]. More recently, several publications highlighted the involvement of the SNS in inflammation-based infectious [20] and non-infectious bowel diseases [21] and its ambivalent effect on the inflammatory milieu, depending on the disease stage, neurotransmitter concentration, and receptor binding [22].

We recently showed that the SNS affects the postoperative inflammatory immune cell milieu in postoperative ileus (POI) and functionally impacts the disease progression [23]. POI is a frequent transient GI-motility disorder and complication of abdominal surgery. Patients with POI suffer from nausea, abdominal distension pain, reduced oral food tolerance, delayed recovery, and finally, an extended hospitalization phase with a high medico-economic burden on our health care systems [24]. A prominent response to abdominal surgery is a dysbalance of the sympathetic and parasympathetic inputs of the intestine towards sympathetic overactivation. Notably, this sympathetic overactivity is already induced by the skin incision [25], and the subsequent surgical manipulation of the intestine (or other visceral organs) enhances this overactivity. Hallmarks of enteric gliosis have been identified as part of POI (5, 10, 26) and are discussed to be of potential value for therapeutic interventions in POI and other intestinal inflammation-driven diseases [26]. As SNS-released mediators directly act on enteric glia [19, 27], we hypothesized that adrenergic signaling might be an early trigger of acute postoperative enteric glial reactivity in the onset phase of POI.

To test this hypothesis, we used $Sox10^{iCreERT2}/Rpl22^{HA/+}$ mice to extract cell-specific mRNA from hemagglutinin-labeled ribosomes of enteric glia [28, 29]

within three phases of POI: the immediate initiation phase, the manifestation, and the resolution phase. We found striking evidence of strong enteric glial reactivity in the immediate postoperative phase. Furthermore, we discovered that laparotomy, the first step of abdominal surgery, which does not include manipulation of any other visceral organs, is sufficient to trigger enteric glial activation in the intestine. Sympathetic denervation studies, live calcium imaging in ex vivo ganglia, enteric glia-restricted optogenetic activation of β-adrenergic downstream signaling in *Sox10*^{iCreERT2}*/JellyOP*$^{fl/+}$*/Rpl22*$^{HA/+}$ mice, and stimulation of primary EGC cultures gave insight into the distinct β-adrenergic signaling pathways triggering enteric glial reactivity in POI.

Materials and methods

Materials

Animals

Sox10^{iCreERT2} (*B6-Tg(Sox10-icre/ERT2)388Wdr/J*) mice were crossbred with *Rpl22*$^{HA/+}$ (*B6N.129-Rpl22tm1.1Psam/J*)/tdTomato (*B6;129S6-Gt(ROSA)26Sortm14(CAG-tdTomato)Hze*) mice. Additionally, *Sox10*^{iCreERT2}*/RiboTag/tdTomato* were crossbred with *JellyOP* mice (*CD1-Gt(ROSA)26Sor*$^{em1(CAG-JellyOp-eGFP)}$; Additional file 1: Method S2, S3) [30] for optogenetic activation experiments. Animals were housed under SPF conditions in the central housing facility or our laboratory (Immunpathophysiology, University Hospital Bonn, Bonn, Germany). Male mice (10–12 weeks) were used in the intestinal manipulation and laparotomy experiments, and mice of both sexes (10–20 weeks) were used for optogenetic activation experiments and pharmacological modification with reserpine and tyramine carried out under German federal law (Az.: 81-02.04.2016 A367 and 81-02-04-02018.A221, 84–02.04.2017.A114).

Inducible Cre was activated by intraperitoneal injections of 100 µl Tamoxifen [MP Biomedicals, Irvine, CA, USA] dissolved in 10% ethanol and 90% sterile corn oil (final concentration 10 mg/ml) for three consecutive days. Experiments were performed one week after the last injection.

Calcium imaging studies were conducted on female *Wnt1-Cre; R26R-GCaMP3* mice as approved by the Animal Ethics Committee of the University of Leuven (Belgium) in the laboratory of Pieter Vanden Berghe.

In vivo optogenetic activation of adrenergic signaling in enteric glia

Sox10^{iCreERT2}*/RiboTag/tdTomato/JellyOP* animals and *JellyOP*-negative littermate controls received pain medication (Tramadol [Grünenthal, Aachen, NRW, DE]; i.p.) 15 min before surgery. During surgery, animals were anesthetized with Isoflurane and kept on a heating pad to stabilize body temperature. After abdominal shaving, the abdominal cavity was opened (2 cm incision) along the *linea alba* and held open by clamps while the small bowel was gently lifted and placed on gauze. The *JellyOP* construct was activated with supramaximal blue light (470 nm, > 0.5 mW/mm^2) at a distance of 10 cm for 15 min with regular moisturization with saline. Activation of the *JellyOP* construct triggers a G_s signaling cascade downstream from 1D4, that resembles activation by β-adrenergic stimulation. The intestine was gently replaced, and the opened cavity was sutured. Animals were replaced in their cages and slowly woke from the narcosis under heating lamps during the following 30 min. Animals received further pain medication orally (Tramadol [Aliud Pharma, Laichingen, BW, DE]) via their water supply.

Post-operative ileus (POI) model

Animals received pain medication (Tramadol [Grünenthal, Aachen, NRW, DE]; i.p.) 15 min before surgery. During surgery, animals were anesthetized with Isoflurane and kept on a heating pad to stabilize body temperature. After abdominal shaving, the abdominal cavity was opened (2 cm incision) along the *linea alba* and held open by clamps, while the small bowel was gently lifted and placed on gauze (Fig. 1A). The small bowel was mechanically manipulated by light pressure with moist cotton swaps in a rolling motion towards the *Caecum* (2x). The intestine was gently replaced, and the opened cavity was sutured. Additionally, we performed a modified laparotomy model in which no manipulation was performed. Animals were replaced in their cages and slowly woke from the narcosis under a red light during the following 30 min. Animals received further pain medication orally (Tramadol [Aliud Pharma, Laichingen, BW, DE]) via their water supply.

Gastrointestinal transit

Animals received 100 µl of FITC-dextran [Sigma Aldrich, St. Louis, MO, USA] via gavage and rested for 90 min without additional food or water. Subsequently, animals were sacrificed, intestines eventrated, and separated into segments (stomach 1; small bowel 2–11, ~ 3 cm each; caecum 12; colon 13–15, ~ 2 cm each). Segments were flushed with Krebs–Henseleit buffer (Additional file 1: Table S1), and eluates were analyzed for FITC fluorescence. The geometric center was calculated to generate GI-transit time for naïve, Lap 24 h, IM 24 h, and IM 72 h animals.

Sympathetic denervation

Sox10^{iCreERT2}/Rpl22$^{HA/+}$mice were injected with 250 µl 6-Hydroxydopamine (6-OHDA; 80 mg/kg body weight in saline [Sigma Aldrich, St. Louis, MO, USA]) for three consecutive days as described before [23]. Animals rested for fourteen days after the final injection before subsequent experiments were performed.

Pharmaceutical adrenergic modulation (reserpine and tyramine)

*Sox10^{iCreERT2}/Rpl22$^{HA/+}$*mice were injected s.c. with 100 µl reserpine (20 mg/kg body weight in saline [#83,580, Sigma Aldrich, St. Louis, MO, USA]) adapted from [31] and kept for 24 h. Animals subsequently underwent laparotomy as described above (with and without prior administration of reserpine) and were sacrificed 3 h later.

Sox10^{iCreERT2}/Rpl22$^{HA/+}$ mice were injected i.p. with 100 µl tyramine (100 mg/kg body weight in saline [#W421501, Sigma Aldrich, St. Louis, MO, USA]) adapted from [32] or 100 µl saline and sacrificed 3 h later.

Primary murine enteric glial cell (EGC) cultures

Primary EGC cultures were generated from small bowel *muscularis externa (ME)* of 8–12-week-old *Sox10^{iCreERT2}/Rpl22$^{HA/+}$/Ai14$^{fl/fl}$* mice. Briefly, the intestine was eventrated, flushed with oxygenated Krebs–Henseleit buffer (cell culture; Additional file 1: Table S1), dissected into 3–5 cm long segments, and transferred to ice-cold, oxygenated Krebs–Henseleit buffer. *ME* tissue was mechanically separated from the mucosal layer, centrifuged (300 g, 5 min), and digested in dissociation buffer (Additional file 1: Table S1) in a water bath (15 min, 37 °C, 150 rpm). The enzymatic reaction was stopped by the addition of 5 ml DMEM + 10% FBS [Sigma Aldrich, St. Louis, MO, USA], centrifugation (300 g, 5 min), and resuspension in proliferation media (Additional file 1: Table S1). Cells were kept in proliferation media for 7 days (37 °C, 5% CO_2) before dissociation with trypsin (0.25%, 5 min, 37 °C) [Thermo Fisher Scientific, Waltham, MA, USA] and seeding on Poly-L-Ornithine [Sigma Aldrich, St. Louis, MO, USA] coated 6-well plates at 50% confluence in differentiation media (Additional file 1: Table S1). Cells were differentiated for seven days before treatment with norepinephrine (NE; 10 µM, 100 µM), adrenergic receptor (AR) agonists (β-AR/isoprenaline (1 µM, 10 µM); α2a-AR/guanfacine (10 µM); β3-AR/CL-316243 (10 µM) [all Tocris Bioscience, Bristol, UK]), or forskolin [#HY-15371, MedChemExpress, Monmouth Junction, NJ, USA] in PBS for 3 h or 24 h. Cell culture constituted mainly of enteric glia (> 85%) and small amounts of fibroblasts (< 10%), described in more detail in [5]. Conditioned media was used for ELISA analysis, and cells were processed for RNA analysis.

In vitro optogenetic activation of adrenergic signaling in enteric glial cell cultures

JellyOP$^{fl/+}$ animals were used to isolate primary enteric glial cells as described above. Cells were transfected with 1 µl (1.69×10^8 VG/ml) of an rAAV2/1-hGFAP-NLS-Cre virus construct ("AAV-GFAP-Cre"; Additional file 1: Method S4) to activate the JellyOP construct and subsequently differentiated for seven days. Differentiated cells were subjected to four consecutive 1 min pulses of blue light (470 nm, 32 µW/mm^2) in a custom-built illuminator for cell culture plates. Media from illuminated and dark-kept cells was used for ELISA.

Calcium imaging

Female *Wnt1-Cre;R26R-GCaMP3* mice were killed by cervical dislocation, as approved by the Animal Ethics Committee of the University of Leuven (Belgium). These mice express the fluorescent Ca^{2+} indicator GCaMP3 in all enteric neurons and glia [33, 34].

The ileum was carefully removed, opened along the mesenteric border, and pinned flat in a sylgard-lined dissection dish in cold O_2/CO_2 (95%/5%) suffused Krebs buffer (120.9 mM NaCl; 5.9 mM KCl; 1.2 mM $MgCl_2$;

(See figure on next page.)

Fig. 1 Enteric glia react to mechanical stimuli and transition into an acute gliosis state. **A** Schematic description of the surgical procedure (intestinal manipulation, IM) with follow-up *RiboTag* approach in *Sox10^{iCreERT2}/Rpl22$^{HA/+}$* enteric glia and immunohistological image of HA (green) and SOX10 (magenta) co-expression in *ME*. Scale bar (100 µm). The *RiboTag* procedure was performed 3 h, 24 h, or 72 h after surgery. **B** Confocal images of SOX10 (magenta) and Ki67 (green) expression in whole mounts of small bowel *ME* at different time points. Scale bar (100 µm). **C** Histological analysis (mean ± SEM) of SOX10$^+$ and SOX10$^+$ Ki67$^+$ cells per field of view (n = 6–14 animals per time point; mean counts of 5 images per n ± SEM; two-way ANOVA, to naive *** < 0.01, between IM24/IM72h ### < 0.01). **D** Principal component analysis (PCA) of a bulk RNA-Seq of *Sox10^{iCreERT2}/Rpl22$^{HA/+}$ RiboTag* mRNA at different time points. **E** Volcano plot for actively transcribed genes at IM3h in *Sox10^{iCreERT2}/Rpl22$^{HA/+}$*enteric glia with significantly differentially transcribed genes (p-value < 0.05, > ± twofold) marked in red (upregulated) and blue (downregulated) and annotation of notable genes. **F** Venn diagrams of the top 50 induced genes at IM3h, IM24h, and IM72h separated into clusters. **G** Analysis of enriched GO-terms in mRNA from *Sox10^{iCreERT2}/Rpl22$^{HA/+}$*enteric glia for POI hallmarks related to migration and inflammatory response. **H** RNA-Seq heat maps for naïve and IM3h samples of *Sox10^{iCreERT2}/Rpl22$^{HA/+}$RiboTag* mRNA and total RNA "acute enteric gliosis" induction and an indication of genes related to key POI hallmarks. (n = 3–4 animals per time point)

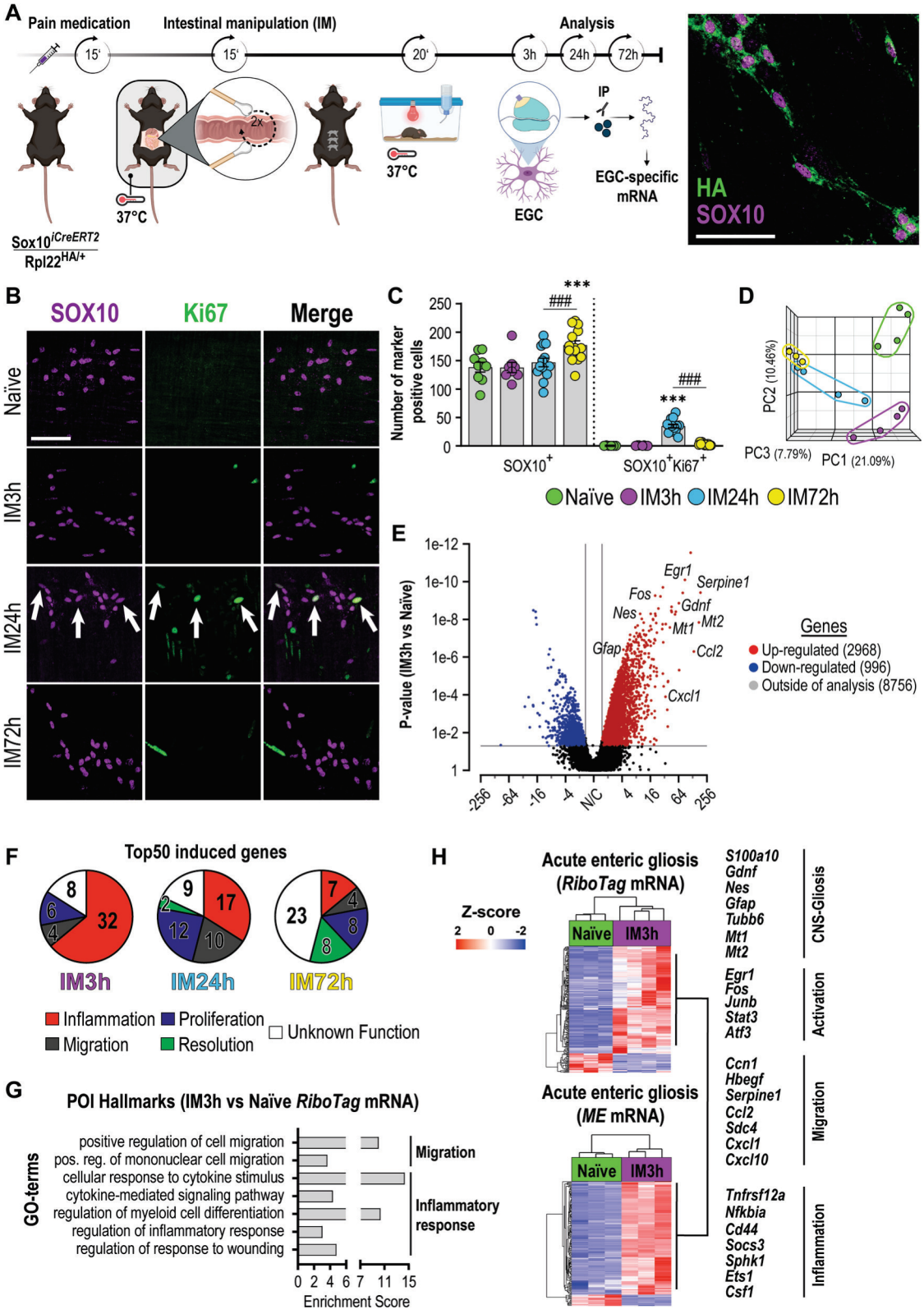

Fig. 1 (See legend on previous page.)

1.2 mM NaH_2PO_4; 14.4 mM $NaHCO_3$; mM 11.5 Glucose; 2.5 mM $CaCl_2$). The mucosa, submucosa, and circular muscle were removed by microdissection to expose the myenteric plexus. These preparations were stabilized over an inox ring using a matched o-ring [35], which was mounted in a cover glass bottom chamber on the microscope stage. 3D recordings of the GCaMP3 were made on an inverted spinning disk confocal microscope (Nikon Ti—Andor Revolution—Yokogawa CSU-X1 Spinning Disk [Andor, Belfast, UK]) with a Nikon 20×lens (NA 0.8), excitation 488 nm and detection 525/50 nm. A Piezo Z Stage controller (PI) was used to record fast 3D stacks at 2 Hz. Tissues were constantly supplied with oxygenated Krebs buffer via a gravity-fed perfusion system that allowed instantaneous switching between control and high K^+, Substance P (10^{-5} M, to identify the glia network, [36]) or isoprenaline (10^{-5} M) containing Krebs buffer. The tissues were constantly perfused by O_2/CO_2 (95%/5%) suffused Krebs buffer containing 2 µM nifedipine to prevent most of the muscle contractions.

Analysis of calcium imaging

All calcium image analysis was performed with custom-written routines (available via [37]) in Igor Pro [Wavemetrics, Lake Oswego, OR, USA]. Image registration was performed in Fiji using the descriptor-based registration algorithm developed by Preibish et al. [38]. Registered images were further analyzed in Igor 8, and regions of interest were drawn to extract temporal information. Peak amplitude calculation was performed using custom-written procedures as previously described [37, 39]. The average Ca^{2+} signal intensity was calculated, normalized to the initial GCaMP3 signal, and reported as F/F_0.

Immunohistochemistry

Immunohistochemistry was performed on terminal ileum parts. Briefly, the ileum was placed in Sylgard gel-covered Petri dishes and opened along the mesentery. After fixation with 4% PFA for 20 min, mucosal-free *ME* whole mounts were prepared through mechanical separation of both layers. Next, whole mounts were permeabilized (1% Triton X-100/PBS; RT, 20 min) and blocked with (5% donkey serum, 0.25% Triton X-100/PBS; RT, 1 h) before antibody incubation (primary: 4 °C, overnight; secondary: 1.5 h, RT; Additional file 1: Table S2).

Microscopy imaging

Widefield images used for quantitative analysis of proliferation, numbers of SOX10 positive cells, and MPO infiltration were obtained on a Nikon Eclipse TE2000-E with a magnification of 20×and a field of view of 397 µm×317 µm or a Nikon Eclipse T*i*2 with a magnification of 20×and a field of view of 769 µm×769 µm. Representative images are confocal slices obtained with a Leica SP8 AOTF confocal microscope using a 40×objective.

Hanker-Yates histology

Hanker-Yates staining was performed on the terminal ileum. Briefly, the ileum was pinned to Sylgard gel-covered Petri dishes and opened along the mesentery. After fixation with pure ethanol for 10 min, mucosal-free *ME* whole mounts were prepared by mechanically separating both layers. Before mounting, whole mounts were subjected to Hanker-Yates myeloperoxidase staining solution (RT, 10 min).

Western Blot

A BCA protein assay kit [Thermo Fisher Scientific, Waltham, MA, USA] was used to assess protein lysate concentrations. SDS-PAGE was performed with 100 µg of protein. The primary and secondary antibodies (Additional file 1: Table S2) were incubated overnight at 4 °C and 1 h at RT, respectively.

ELISA

Conditioned media from EGC cultures treated with NE or agonists for the indicated time points was collected, centrifuged (5000*g*, 5 min), and snap-frozen in liquid nitrogen. According to the manufacturer's instruction manual, media was analyzed for IL-6 release with an ELISA kit [R&D Systems, Abingdon, GB].

RiboTag approach

RiboTag immunoprecipitation was performed according to a previously established protocol (Additional file 1: Method S1, [28]). Briefly, the muscle layer of the whole small bowel tissue was mechanically separated from the mucosal layer and placed in RNA*later* [Thermo Fisher Scientific, Waltham, MA, USA]. Muscle tissue was lysed on a Precellys homogenizer [Bertin Instruments, Montigny-le-Bretonneux, FR] (3×5000 rpm, 45 s; 5 min intermediate incubation on ice) in pre-cooled homogenization buffer (Additional file 1: Table S1), centrifuged (10 min, 10,000*g*, 4 °C), and supernatants saved. "Input" controls were generated from 50 µl cleared lysate. Samples were incubated with anti-HA antibody (5 µl; 1 mg/ml; Additional file 1: Table S2; 4 h, 4 °C, 7 rpm). Lysate/Antibody conjugates were added to 200 µl of washed A/G dynabeads [Thermo Fisher Scientific, Waltham, MA, USA] and incubated (overnight, 4 °C, 7 rpm). Beads were washed thrice with high salt buffer (Additional file 1: Table S1). Ribosomes containing specific mRNA were eluted from beads, and RNA was extracted with a Qiagen micro kit.

cDNA Synthesis and quantitative PCR Analysis

Purified RNA (10 µg) was transcribed with the Applied Biosystems™ High-Capacity cDNA Reverse Transcription Kit [Applied Biosystems, Foster City, CA, USA] according to the manufacturer's instruction manual. cDNA (1:10 diluted) was added to SYBR™ Green PCR Master Mix [Applied Biosystems, Foster City, CA, USA] and analyzed by qPCR [Applied Biosystems, Foster City, CA, USA] (Additional file 1: Table S3).

RNA-Seq analysis

Libraries were prepared with QuantSeq 3′ mRNA-Seq Library Prep Kit [Lexogen, Greenland, NH, USA] and sequenced (single-end 50 bp, 10 M reads) on an Illumina Hiseq 2500. "Partek Flow" software was used to analyze RNA-Seq data (Lexogen pipeline 12,112,017), and Ensemble transcripts release 99 for mm10 mouse alignment. The pipeline consisted of two adapter trimming and a base-trimming step with subsequent quality controls (QC). Reads were aligned with star2.5.3, followed by a post-alignment QC, and quantification to an annotation model. Normalized counts were subjected to principal component and gene set analysis. Pipeline information can be found within our uploaded sequencing files (*GSE198889*).

Statistical analysis

Statistical analysis was performed with Prism 9.0 [GraphPad, San Diego, CA, USA] using Student's t-test, multiple unpaired t-test, one-way, or two-way ANOVA as indicated in the figure legends. Significance to controls is resembled by *, while significance to other samples is indicated by #. All plots are mean ± SEM. Animals for experiments were age- and sex-matched and randomly assigned to the experimental groups.

Results

Intestinal inflammation induces enteric gliosis during post-operative ileus development

In a previous study, we re-defined the inflammatory state of the post-operative *ME*, containing reactive enteric glia, based on a publication-based gene selection associated with the term "gliosis" in the CNS [5] and termed this condition "enteric gliosis". As the underlying gene selection only defined the overall transcriptional inflammatory responses of the enteric glial-containing tissue but did not reflect individual cell-type-specific changes of enteric glia, we aimed to precisely determine their reactivity and better understand their role during acute inflammation. Therefore, we assessed the transcriptional changes of enteric glia by a *RiboTag* approach. The *RiboTag,* in conjunction with a *Sox10*^{iCreERT2} system (Fig. 1A, [28]), enabled the isolation of actively transcribed mRNA from enteric glia-specific HA-tagged ribosomes and subsequent RNA-Seq analysis with glial mRNA (Additional file 2: Fig. S1A). Enteric glia reactivity was induced through a standardized model of intestinal inflammation resulting in post-operative ileus (POI). A proper tissue response was confirmed by our previously defined enteric gliosis gene panel [5]. POI progresses in three stages, and the selection of representative time points 3 h, 24 h, and 72 h after intestinal manipulation (IM) enabled us to define the molecular responses within the early/immediate phase (IM3h), inflammatory/manifestation phase (IM24h), and recovery/resolution phase (IM72h). IM (Fig. 1A) triggered acute gut inflammation in the *muscularis externa* (*ME*) (Additional file 2: Fig. S1B), with a decrease in gastrointestinal motility (Additional file 2: Fig. S1C) and an induction of a substantial influx of infiltrating leukocytes (Additional file 2: Fig. S1D) peaking at IM24h, confirming that *Sox10*^{iCreERT2} *RiboTag* mice develop POI. The existence of enteric gliosis was shown by increased protein expression of GFAP and vimentin (VIM) during POI progression (Additional file 2: Fig. S1E). Notably, the number of Sox10^{+}Ki67^{+} enteric glia in the *ME* increased at IM24h (35 ± 3 vs. 0.17 ± 0.15 cells/ field of view) but not at IM3h (0.5 ± 0.18 cells/ field of view). SOX10^{+} Ki67^{+} enteric glia numbers dropped to baseline levels at IM72h (3 ± 0.6 cells/ field of view) (Fig. 1B, C), indicating the presence of a timely-limited trigger of glial cell proliferation in the acute phase of inflammation. Supportively, total numbers of SOX10^{+} enteric glia increased at IM72h compared to naïve and IM24h time points (Fig. 1C), showing that molecular features of proliferation indeed resulted in increased EGC numbers in the recovery phase. These changes coincided with POI hallmarks and an overall strong transcriptional response related to inflammation in the *ME* (Additional file 2: Fig. S1B).

Principal component analysis of *RiboTag* samples revealed a clear separation of gene expression patterns at investigated POI time points (Fig. 1D). Volcano plots comparing naïve with IM samples showed the most substantial enteric glial activation at IM3h with 2968 genes up- and 996 genes down-regulated (Fig. 1E), compared to IM24h (101 up- and 1703 down-regulated genes) and IM72h (42 up- and 2218 down-regulated genes) (Additional file 2: Fig. S1F, G). Validation of the top 50 induced genes at all disease time points with gene databanks (*GeneCards* and *Mouse Genome Informatics*) revealed a change of enteric glia toward an inflammation-related cell type (Fig. 1F). Enteric glia displayed a strong expression of inflammatory genes (32 of the top 50; e.g., metallothioneins *Mt1* and *Mt2*, *Tnfrsf12a*, *Nfkbia*, *Sphk1*) in the initial phase that declined during POI progression and was replaced by a strong expression of migratory

(10 of the top 50; e.g., *Ccl2*, *Ccl6*, *Ccl9*) and proliferation-associated genes (12 of the top 50; e.g., *Mcm3*, *Chaf1a*) at IM24h. A so far undefined resolution phenotype arose at IM72h (8 resolution genes of the top 50), showing the induction of olfactory receptors (e.g., *Olfr373*, *Olfr95*, *Olfr1254*), implicated in gut inflammation [40] (Fig. 1F). Notably, the number of actively transcribed genes pulled down with the *RiboTag* approach was also the highest during disease onset at IM3h (12,720 genes) compared to IM24h (8129 genes) and IM72h (3599 genes) (Additional file 2: Fig. S1H). The high transcriptional activity at IM3h aligns with the early enteric glial reactivity. GO analyses showed the enrichment of genes associated with multiple immunological aspects and POI hallmarks, including migration regulation, cytokine signaling, and myeloid cell differentiation (Fig. 1G). To define inflammation-induced enteric glial activation on a transcriptional level, we generated the novel gene ontology (GO) term "acute enteric gliosis" (Additional file 1: Table S4). Therein, we validated the expression of published gliosis genes, previously defined by our group [5], in the *RiboTag* data set and added highly induced genes at IM3h (> tenfold vs. naïve; e.g., *Serpine1, Mt2, Gdnf*) together with genes that were only detected in samples at the IM3h time point (naïve 0 counts; IM3h > 5 counts per sample; e.g., *Fosl, Ucn2, Areg*). Notably, around half of the published gliosis genes are also expressed by enteric glia during POI (Additional file 1: Fig. S1I, Additional file 2: Table S4). Application of this novel GO term showed strong induction of gliosis genes in enteric glia 3 h after manipulation with a steep decline at IM24h and IM72h (Additional file 2: Fig. S1J). To test the applicability of the "acute enteric gliosis" GO term as an indicator of acute enteric gliosis in the full *ME* tissue, we analyzed an RNA-Seq data set generated of total *ME* from POI mice. The resulting heat map mirrored the prominent induction of gliosis genes from our *RiboTag* analysis at IM3h (Additional file 2: Fig. S1K), with most of the upregulated gliosis genes induced exclusively in the early disease phase (IM3h, 94 genes), some overlapping genes at IM3h and IM24h (49 genes; Additional file 2: Fig. S1L) and only one induced gene overlapping between IM3h and IM72h. Highly induced genes at IM3h included known astrogliosis genes (*Gfap*, *Nes, Mt1, Mt2, Gdnf*), early response genes (*Egr1*, *Fos*), migration factors (*Ccl2*, *Cxcl1, Cxcl10, Serpine1*), and inflammatory factors (*Nfkbia, Socs3, Sphk1, Cd44*) (Fig. 1H). Notably, almost no acute enteric gliosis gene panel genes were upregulated in the *ME* at later postoperative time points, supporting its usefulness as an acute enteric gliosis marker panel.

These data provide evidence of the strong plasticity of enteric glia during acute intestinal inflammation, wherein an acute immune-reactive phenotype is a very early event. At the disease peak, 24 h after surgery, enteric glial reactivity switched towards a phenotype supporting migration and proliferation, which further declined towards a resolution type at IM72h.

Sympathetic signaling triggers acute enteric glia gliosis

The rapid transition of enteric glia into an inflammatory phenotype raised the question of which mechanisms might trigger this immediate enteric glial activation. A previous study from our group showed that extracellular ATP levels quickly rose after abdominal surgery, thereby triggering an enteric glial immune activation during POI [5]. As ATP is co-stored with norepinephrine (NE) in synaptic vesicles of sympathetic nerves and intestinal sympathetic activity is known to become immediately over-activated during surgery, we hypothesized that sympathetic pathways might contribute to the acute enteric gliosis phenotype. We performed a comparative GO-term analysis and found enriched expression of genes associated with “beta-2-adrenergic receptor binding” and “adrenergic signaling pathway” (Fig. 2A). Interestingly, the enrichment scores were comparable with GO terms linked to IL-1 signaling and ATP-guided expression changes, albeit drastically lower than general ATP binding, both pathways known to activate enteric glia upon surgery [5, 41]. Heat maps of differentially expressed genes related to G-protein-coupled receptor

(See figure on next page.)

Fig. 2 Acute enteric gliosis is modulated by sympathetic innervation. **A** Analysis of enriched GO-terms in mRNA from *Sox10*^{iCreERT2}/*Rpl22*$^{HA/+}$ enteric glia 3 h after IM for POI hallmarks related to gliosis triggering pathways. **B** Heat map for the GO-term "GPCR signaling" in naïve and IM3h samples of mRNA from *Sox10*^{iCreERT2}/*Rpl22*$^{HA/+}$ enteric glia and with selected genes highlighted. **C** Schematic description of chemical sympathetic denervation of C57BL6 mice with three consecutive intraperitoneal 6-OHDA injections (days 1–3). After 14 days, mice underwent IM. *ME* was isolated three hours later (IM3h) for qPCR and RNA sequencing. **D** Confocal images of immunohistological stainings of TUBB3 (magenta) and TH (green) expression in whole mounts of control (saline) and 6-OHDA treated (sympathectomized/STX) small bowel *ME* 17 days after injection. (n = 6 animals per condition). Scale bar (100 µm). **E** qPCR analysis showing fold changes of mRNA levels (mean ± SEM) from IM3h/Saline and IM3h/STX mice for enteric gliosis-related genes ($2^{-\Delta\Delta CT}$, *18S*, IM3h + saline; n = 6 animals per condition; Student’s t-test, * < 0.05, ** < 0.01). **F** Analysis of enriched POI hallmark GO-terms in IM3h/Saline total RNA and comparatively reduced in IM3h/STX samples related to inflammatory response and migration. **G** RNA-Seq heat map of our “acute enteric gliosis” GO-term for naïve and IM3h samples treated with saline or 6-OHDA (STX), and an indication of STX-affected genes (black line)

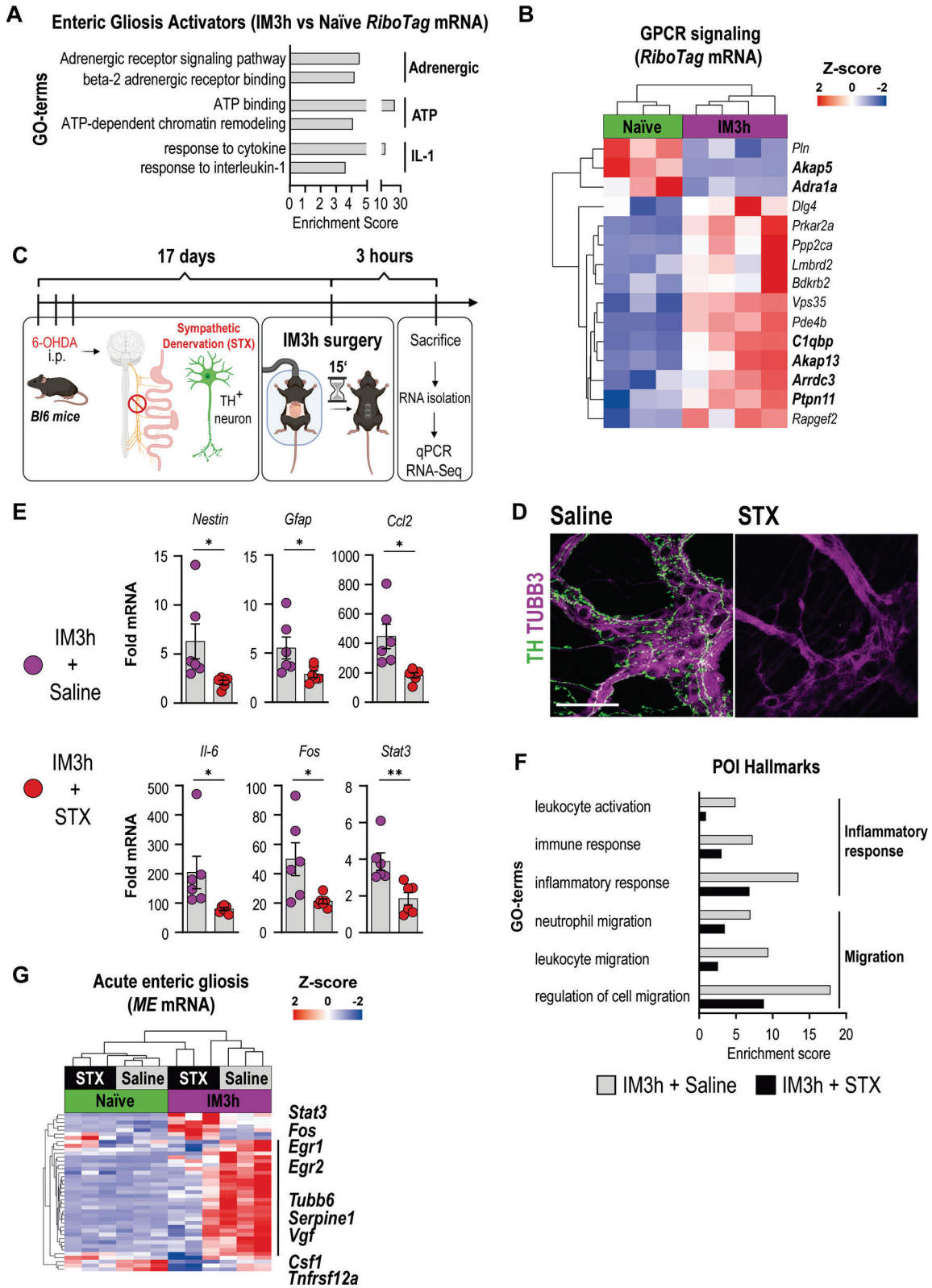

Fig. 2 (See legend on previous page.)

(GPCR) signaling showed a clear pattern between naïve and IM3h enteric glia in our *RiboTag* mice (Fig. 2B). Activation of enhanced adrenergic signaling was confirmed in *ME* tissue samples, depicting a similar gene expression pattern for adrenergic signaling activity (Additional file 2: Fig. S2A).

Since acute gliosis triggered changes in genes related to adrenergic signaling, we theorized that ablation of the intestinal sympathetic innervation affects acute enteric gliosis. To test this hypothesis, we chemically ablated sympathetic neurons (sympathectomy/STX). Denervation was facilitated by the established model of i.p. injection of 6-Hydroxydopamine (6-OHDA), starting 17 days before surgery (Fig. 2C), resulting in a complete depletion of TH^+ neurons within the *ME* of C57BL6 wildtype mice (Fig. 2D). A proof-of-concept analysis by qPCR of *ME* RNA samples from IM3h animals showed a significant reduction of gliosis markers (*Nestin, Gfap*), early response genes (*Stat3, Fosb*), and pro-inflammatory mediators (*Il-6, Ccl2*) in denervated animals (Fig. 2E). Next, we re-analyzed an RNA-Seq data set published by our group [23] for a more comprehensive study of early inflammation. GO term analysis on genes related to POI hallmarks revealed a decrease in genes associated with migration (e.g., leukocytes and neutrophils) and inflammation (e.g., immune and inflammatory response and leukocyte activation) after STX (Fig. 2F). Additionally, we also detected substantial alterations in gene clusters related to changes in the ENS, previously shown to be upregulated at IM3h in our *RiboTag* mice (Additional file 2: Fig. S2B), suggesting a direct effect of denervation on enteric glial reactivity and communication during gut inflammation (Additional file 2: Fig. S2C).

Consequently, we used the "acute enteric gliosis" GO term to investigate the transcriptional status of enteric glia and affected tissue after STX. While only a minority of genes were altered between naïve mice with and without 6-OHDA treatment, strong differences were observed in the majority of enteric gliosis genes at IM3h following STX, highlighting SNS involvement in the development of acute post-operative enteric gliosis (Fig. 2G).

These data suggest that increased sympathetic inputs, known to start simultaneously with surgery, immediately trigger enteric glial reactivity and modulate inflammatory and migratory gene expression.

Sympathetic innervation triggers enteric glial reactivity already in the absence of intestinal manipulation

Earlier work showed that inflammation within the small intestinal *ME* already occurs upon abdominal incision without surgical manipulation of the visceral organs. As intestinal sympathetic over-activation is known to start with the abdominal incision [42], we speculated that sympathetic projections of TH^+ neurons, innervating the *ME,* might also signal to enteric glia by an immediate release of NE after the abdominal incision, thereby directly activating enteric glia. Confocal microscopy revealed close proximity of TH^+ nerve fibers with MAP^+ neurons and $GFAP^+$ enteric glia in myenteric ganglia (Fig. 3A), anatomically supporting the idea of a direct SNS to enteric glia communication. To test this hypothesis, we subjected *Sox10*^{iCreERT2} *RiboTag* mice to a laparotomy without eventration or manipulation of the intestine (Fig. 3B). FOS expression, an early cellular activation marker, and a representative enteric gliosis gene was not detected in $SOX10^+$ enteric glia in naïve mice. At the same time, laparotomy elicited FOS immunoreactivity in myenteric ganglia, including $SOX10^+$ expressing enteric glia (arrows, Fig. 3C). Notably, intestinal manipulation aggravated FOS immunoreactivity in the *ME*, particularly in enteric glia (marked by arrows, Additional file 2: Fig. S3A). These data show that an enteric glial activation already occurs immediately after the surgical incision without surgical manipulation of the intestine, while the latter is a potent enhancer of enteric glial reactivity. To confirm that a laparotomy is sufficient to trigger acute enteric gliosis genes, we performed a laparotomy in *Sox10*^{iCreERT2} *RiboTag* mice. We detected the induction of representative acute enteric gliosis genes (i.e., *Il6*, *Ccl2,* and *Stat3*) compared to naïve animals (Fig. 3D). Consequently, we used 6-OHDA in *RiboTag* mice to test whether sympathetic innervation triggers the laparotomy-induced enteric gliosis genes. Analogous to our wildtype mice, 6-OHDA depleted the TH^+ neuronal processes in *RiboTag* mice and left the glial network intact (Fig. 3E). In line with our hypothesis, *Il6*, *Ccl2*, and *Stat3* gene expression levels were reduced in enteric glia in STX mice compared to saline-treated controls (Fig. 3F). Notably, cellular and functional POI hallmarks also occur in laparotomized mice, although to a lesser extent, with a distinct increase in infiltrating myeloperoxidase$^+$ cells (Additional file 2: Fig. S3B) and reduced gastrointestinal motility compared to naïve mice (Additional file 2: Fig. S3C).

Overall, these data uncovered that the SNS contributes to the induction of genes involved in acute enteric glial reactivity already after the initial abdominal incision, which is further aggravated by mechanical manipulation of the intestine.

NE triggers acute enteric gliosis and activates enteric glia via β-adrenergic receptors

As ablation of TH^+ neurons led to a reduced acute enteric gliosis, we next assessed whether NE, the principal postganglionic sympathetic neurotransmitter, induces

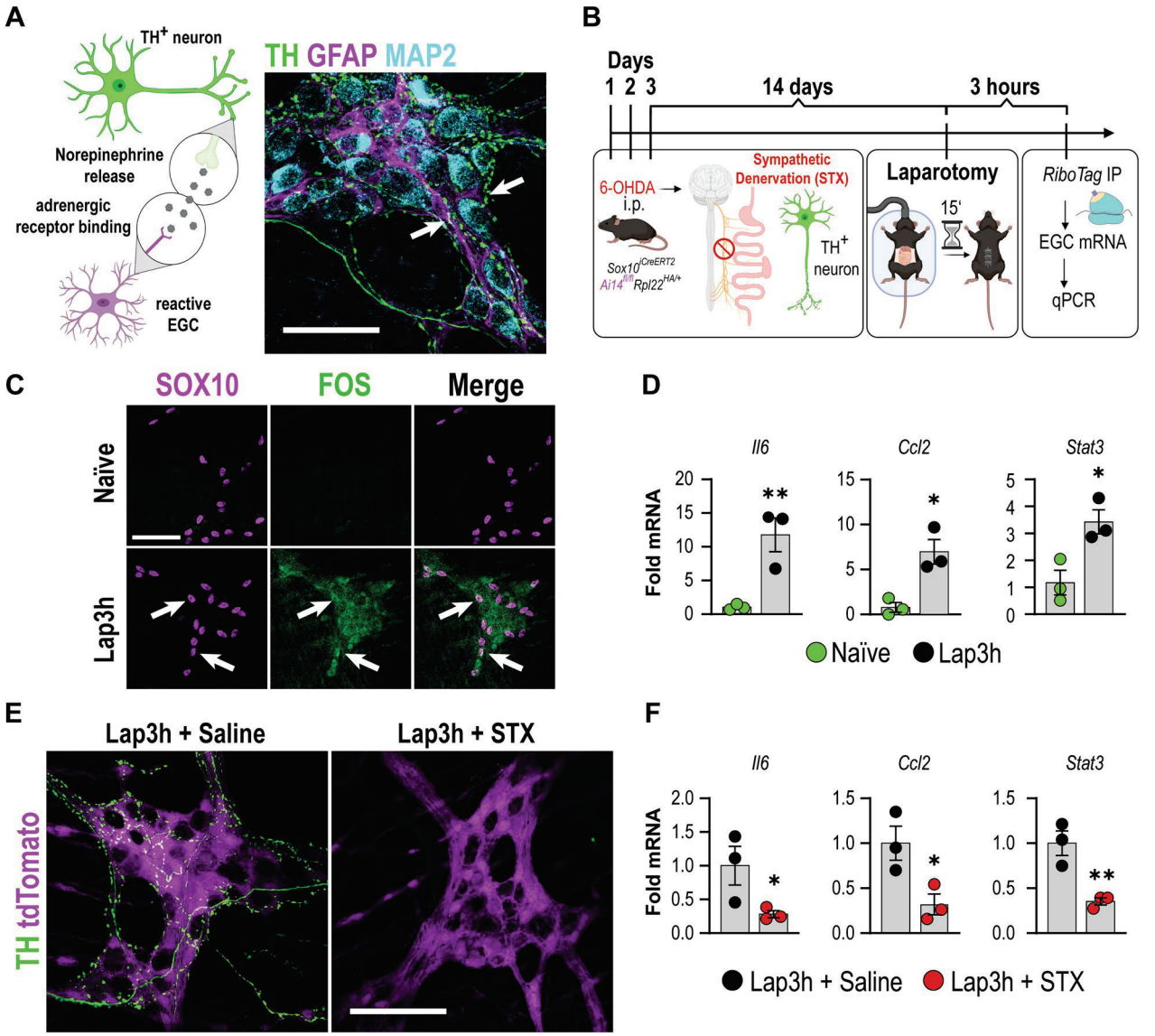

Fig. 3 Enteric glia react before overt inflammation by receiving cues from the sympathetic nervous system. **A** Illustration of our hypothesis of TH$^+$ neuron released NE triggering enteric glial activation and confocal images of immunohistological staining of sympathetic nerve fibers (TH, green), enteric neurons (MAP2; light blue), and enteric glia (GFAP, magenta). Arrows indicate TH$^+$ fibers innervating the *ME*. Scale bar (50 µm). **B** Schematic description of chemical sympathetic denervation of *Sox10*^{iCreERT2}/*Rpl22*$^{HA/+}$ mice with three consecutive intraperitoneal 6-OHDA injections (days 1–3). After 14 days, the mice underwent Lap. *ME* was isolated three hours later (Lap3h), processed according to the RiboTag approach, and analyzed by qPCR. **C** Confocal images of immunohistological stainings of SOX10 (magenta) and FOS (green) expression in whole mounts of naïve and Lap3h small bowel *ME*. (n = 3 animals per condition). Arrows indicate FOS$^+$ SOX10$^+$ enteric glia. Scale bar (100 µm). **D** qPCR analysis showing fold changes of mRNA levels (mean ± SEM) of *Sox10*^{iCreERT2}/*Rpl22*$^{HA/+}$ *RiboTag* mRNA from naïve and Lap3h mice for cytokines (*Ccl2, Il6*) and an early response marker (Stat3) ($2^{-\Delta\Delta CT}$, *18S/Tubb4*, Naïve; n = 3 animals per condition; Student's t-test, * < 0.05, ** < 0.01). **(E)** Confocal images of immunohistological stainings of TH (green) and endogenous SOX10-tdTomato (magenta) expression in whole mounts of Lap3h + Saline and Lap3h + STX small bowel *ME*. (n = 3 animals per condition). Scale bar (100 µm). **F** qPCR analysis showing fold changes of mRNA levels (mean ± SEM) of *Sox10*^{iCreERT2}/*Rpl22*$^{HA/+}$ *RiboTag* mRNA from Lap3h + Saline and Lap3h + STX mice for cytokines (*Ccl2, Il6*), and an early response marker (Stat3) ($2^{-\Delta\Delta CT}$, *Tubb4/Actb/PGK/GAPDH*, Naïve; n = 3 animals per condition; Student's t-test, * < 0.05, ** < 0.01)

enteric glial reactivity. Therefore, we treated primary murine EGC cultures from small bowel *ME* specimens (Fig. 4A) with NE, which caused an almost threefold increase in IL-6 protein release after 3 h (Fig. 4B) that further increased in a dose-dependent manner 24 h after NE treatment (Additional file 2: Fig. S4B). In addition, NE also triggered *Gfap*, *Nestin*, *Stat3, Fos*, and *Ccl2* gene expression 3 h post-treatment (Additional file 2: Fig.

S4C). Notably, the induction of these reactive glia marker genes was transient and disappeared after 24 h (Additional file 2: Fig. S4C), resembling the immediate in vivo enteric glial activation pattern seen in laparotomized and intestinally manipulated mice.

Since NE signals through various adrenergic receptors, we next aimed to characterize their expression profile in primary EGCs to elucidate possible receptors involved in acute enteric gliosis induction. RNA samples of naïve *Sox10*^{iCreERT2} *RiboTag* mice and cultured primary EGCs revealed α2a adrenergic receptor (AR) and the three β-ARs β3 > β1 > β2 as the highest expressed on primary EGCs in vitro and in vivo (Fig. 4C). However, immunocytochemistry of α2a-AR showed no expression in primary EGCs, while it was strongly expressed in non-glial cells in vitro in primary EGC cultures (Additional file 2: Fig. S4D). We next stimulated the three β-ARs and the α2a-AR (as an anticipated negative control) with selective adrenergic agonists in cultured primary EGCs. We analyzed IL-6 and CCL2 release by ELISA and other representative enteric gliosis genes by qPCR. The pan-β-AR agonist isoprenaline elicited IL-6 and CCL2 protein release to the same extent as NE, while neither the α2a-AR-specific agonist (guanfacine) nor the β3-AR-specific agonist (CL-316243) triggered any release (Fig. 4D). Accordingly, isoprenaline and NE significantly induced *Ccl2, Il6, Nestin,* and *Fos* gene expression (Fig. 4E). By immunohistochemistry of *ME* whole-mounts and intestinal cross-sections, we detected β1-AR in GFAP$^+$ ganglia (Fig. 4F**,** Additional file 2: Fig. S4E) and verified the signal with an IgG control (Additional file 2: Fig. S4F). Furthermore, we wanted to investigate the activation of adrenergic signaling cascades upon treatment with isoprenaline. We performed SDS-PAGE and western blotting in combination with an antibody specifically binding to the consensus phosphorylation sequence (RRXS*/T*) of all targets of the activated/phosphorylated form of cAMP-dependent protein kinase A (Fig. 4G), a primary signaling molecule for the adrenergic pathway. Here, we observed a significant increase in the amount of phosphorylated targets after treatment of primary EGCs with 10 µM isoprenaline for 1 h (Fig. 4G), comparable to the activation induced by our positive control treatment forskolin (10 µM).

Since the pan-β-AR agonist isoprenaline, but not the β3-AR-specific agonist, induced a molecular enteric gliosis signature and activated downstream kinases in primary EGCs, we deduced that NE released by the SNS after the onset of surgery activates β1- or β2-AR signaling in enteric glia.

Ex vivo and optogenetic activation of adrenergic downstream signaling triggers enteric glial reactivity

To better understand the in vivo activation of enteric glia by beta-adrenergic signaling in living tissue and in vivo, we utilized several additional models. We first assessed glial responses in an ex vivo approach wherein we used ileal tissue from *Wnt1-Cre;R26R-GCaMP3* mice to test whether isoprenaline (10 µM) would elicit a glial Ca^{2+} response in the myenteric ganglia. Using a local perfusion system, isoprenaline was applied directly onto the ganglion (Fig. 5A; Additional file 3A and B). Additionally, using the same multi-barrel perfusion tip, Substance P (10 µM) was used to identify the glia cell network [36], and high K^+ to identify the neurons (Additional file 2: Fig. S5A). Fourteen ganglia were imaged in separate preparations, and although the responses were variable between recordings and mice, some clear glial cell network activation was seen in a fraction of the recordings (4/14). In contrast, in others (4/14), at least one enteric glial cell in the field of view (FOV) responded (Fig. 5B). In the six other recordings, isoprenaline induced a small contraction, and no cellular (neither neuronal nor glial) Ca^{2+} response could be detected. The relative amplitude

(See figure on next page.)

Fig. 4 NE triggers acute primary enteric gliosis and glial reactivity via β-adrenergic receptors. **A** Schematic of primary EGC cultures from *Sox10*^{iCreERT2}*/Rpl22*$^{HA/+}$*/Ai14*$^{fl/fl}$ mice. **B** ELISA analysis for IL-6 (mean ± SEM) from conditioned medium of cultured EGCs after stimulation with vehicle (PBS) or NE (3 h; 10 µM, 100 µM) (n = 8 distinct cell culture wells per condition; multiple unpaired t-tests, comparison to vehicle, *** < 0.001). **C** qPCR analysis (mean ± SEM) of *Sox10*^{iCreERT2}*/Rpl22*$^{HA/+}$ *RiboTag* mRNA and RNA from cultured primary EGCs for different adrenergic receptors ($2^{-\Delta\Delta CT}$, *Tubb4/Actb/PGK/GAPDH*, n = 5 distinct cell culture wells per condition). **D** ELISA analysis for IL-6 and CCL2 (mean ± SEM) from conditioned medium of cultured primary EGCs after stimulation (3 h) with vehicle (PBS), adrenergic agonists (against: α2a, β3, pan-β (isoprenaline)), and NE (all 10 µM); CCL2: n = 6 distinct cell culture wells per condition; IL-6: n = 9–21 distinct cell culture wells per condition; multiple unpaired t-tests, comparison to vehicle, *** < 0.001). **E** qPCR analysis (mean ± SEM) of cultured primary EGCs for acute gliosis genes after vehicle (PBS), isoprenaline (100 µM), or NE (100 µM) treatment ($2^{-\Delta\Delta CT}$, *18S*, Naïve; n = 4–7 distinct cell culture wells per condition; multiple unpaired t-tests, comparison to vehicle, * < 0.05). **F** Immunohistochemistry of cryo-embedded intestinal specimens stained for GFAP$^+$ enteric glia (magenta) and ADRβ1 (green) in the *ME*; Hoechst was used to detect cell nuclei (white). Arrows indicate double-positive cells. Scale bar (50 µm). **G** Western blot and corresponding densitometry (mean ± SEM) of lysates of primary EGC cultures treated with vehicle, isoprenaline (10 µM), or forskolin (10 µM) stained for phosphorylated cAMP-dependent protein kinase (pPKA) (multiple bands) and β-actin (~ 42 kDa) as loading control (n = 4 cultures from 4 different animals treated with the compounds or vehicle; representative blot shows three technical replicates of one biological repeat per condition); multiple unpaired t-tests, comparison to vehicle, ** < 0.01)

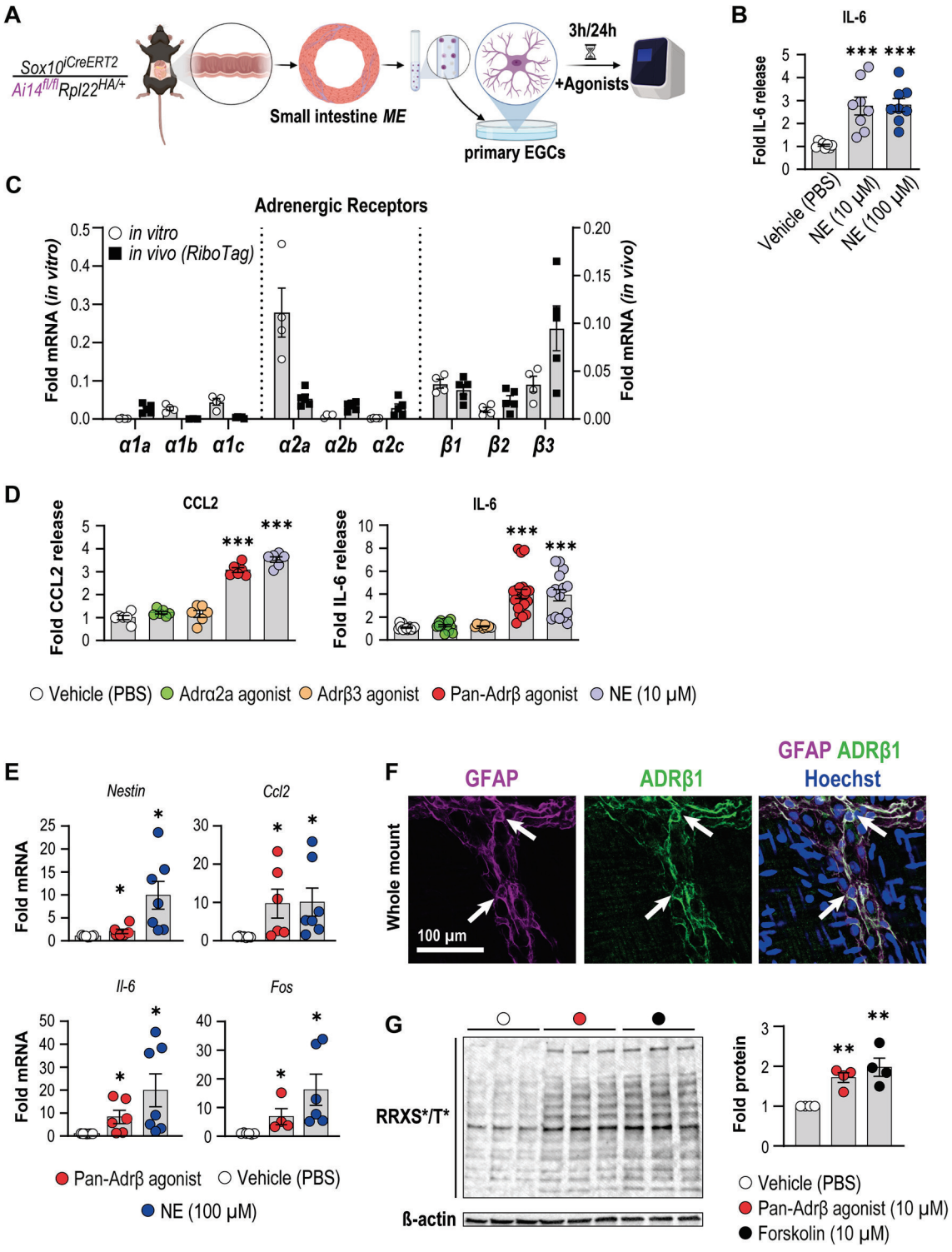

Fig. 4 (See legend on previous page.)

of those glial cells that were responding to isoprenaline showed a small delay in reaction time with half the amplitude (47 ± 6%) of Substance P used to identify them as glial cells (n = 45 cells; Additional file 2: Fig. S5B). Therefore, we assume that β-AR-stimulated enteric glia acquire a reactive state and can react with distinct Ca^{2+} responses.

Furthermore, we attempted to expand on our denervation experiments by pharmacological manipulation of adrenergic signaling. Therefore, we injected reserpine, a long-lasting inhibitor of monoamines and subjected these mice, as well as mice without reserpine injection, to our laparotomy model (Additional file 2: Fig. S5D). Since sympathetic denervation led to reduced gliosis, we expected the injection of reserpine to mimic this effect, but could not detect significant changes between the laparotomy groups with and without reserpine (Additional file 2: Fig. S5E). We next tested if a chemical increase in NE release induces a POI-like phenotype. Therefore, we applied tyramine, an indirect sympathomimetic compound facilitating catecholamine release [31] (Additional file 2: Fig. S5F). However, no significant changes were observed between the tyramine and control group with the chosen administration scheme (Additional file 2: Fig. S5G).

Finally, we addressed the question if β-adrenergic signaling can indeed directly trigger enteric glial reactivity by utilization of an optogenetic tool, the Jellyfish-Opsin (*JellyOP)*-construct, which enables selective optogenetic activation of the adrenergic G_s signaling by blue light stimulation [43]. For cell-type specific expression of JellyOP and GFP after Cre-mediated excision of a floxed stop cassette, a new mouse line (*JellyOP-GFP*$^{fl/+}$) was generated by CRISPR/Cas9 mediated gene-editing of the Rosa26 locus (30). Starting with an in vitro approach, primary EGCs from *JellyOP-GFP*$^{fl/+}$ mice were transfected with an AAV-GFAP-Cre during their seven days of maturation (Fig. 5C) to generate EGFP-expressing *JellyOP* EGCs. These *JellyOP* EGCs were blue light stimulated and analyzed 24 h later for GFAP and GFP expression as well as IL-6 and CCL2 expression by ELISA. Confocal microscopy revealed a strong GFP expression in GFAP$^+$ enteric glia, indicating successful viral transfection and Cre-activity (Fig. 5D) in primary EGCs. In line with the previous isoprenaline treatment, we detected a significant increase in IL-6 and CCL2 release after blue light stimulation (Fig. 5E), proving that optogenetic activation of adrenergic (G_s) downstream signaling in EGCs causes an inflammatory glial phenotype.

Next, we performed an in vivo study with the *JellyOP* system by generating a specific mouse line that utilizes our *Sox10*^{iCreERT2} *RiboTag* approach in conjunction with the *JellyOP-GFP*$^{fl/+}$ mice. The resulting glial *JellyOP RiboTag* mice enable the direct optogenetic activation of enteric glial-restricted adrenergic downstream signaling and assessment of their transcriptome. Immunohistochemistry confirmed the successful expression of the *JellyOP*-GFP construct exclusively in enteric glia of the small intestinal *ME* (Additional file 2:: Fig. S6A). To validate an immediate glial response upon the beginning of surgery, our glial *JellyOP* mice and *JellyOP*-negative litter mates were laparotomized, the small bowel was carefully eventrated, and the jejunum and ileum were illuminated with blue light (Fig. 5F). Immunohistochemistry revealed a strong FOS expression already 1 h after blue light stimulation (Fig. 5G) in glial *JellyOP*-positive animals, while reactivity was almost absent in mice lacking the *JellyOP*.

Interestingly, smooth muscle cell nuclei, identified by their longitudinal shape (Fig. 5G, asteriks) and SOX10-negative ganglionic cells, likely enteric neurons (Fig. 5G, arrowheads), also stained positive for FOS, indicating that these cells become activated due to the glial-specific activation of G_s signaling. Similar FOS histology results were obtained 3 h after stimulation (Additional file 2: Fig. S6B) showing even more cells activated, which is comparable to IM3h whole mount specimens of *JellyOP RiboTag* mice (Additional file 2: Fig. S6C). Strikingly, when we compared blue light-treated glial *JellyOP*-positive and *JellyOP*-negative *RiboTag* mice by qPCR analysis, a strong upregulation of several gliosis panel genes, e.g., *Il6, Fos, Stat3, Gfap,* and *Nestin*, were detected (Fig. 5H). Of note, *Ccl2* expression was only detectable in 2 of 3 glial *JellyOP*-negative *RiboTag* mice, but it was highly expressed in *JellyOP*-positive litter mates (data not shown). To

(See figure on next page.)

Fig. 5 Ex vivo and optogenetic activation of adrenergic downstream signaling triggers enteric glial reactivity. **A** Image frames taken during the acute exposure to isoprenaline (left panel, 10 µM) or Substance P (right panel, 10 µM) in *Wnt1-Cre; R26R-GCaMP3*$^{fl/fl}$ mice. **B** Pie plot depicting the response types observed in the 14 ganglia (n = 4 mice). **C** Schematic of the primary culture preparation, viral transfection, and in vitro activation process of *JellyOP*$^{fl/+}$ mice with blue light. **D** Confocal images of the *JellyOP-GFP* construct in tdTomato-Sox10$^+$ cells seven days after transfection with the AAV-GFAP-Cre. Arrows indicate GFP$^+$/GFAP$^+$ glia. Scale bar (100 µm). **E** ELISA analysis for IL-6 and CCL2 (mean ± SEM) from conditioned medium of cultured primary EGCs from *JellyOP*$^{fl/+}$ mice transfected with an AAV-GFAP-Cre after stimulation with blue light or without stimulation (n = 24–42 separately transfected wells from two distinct isolations; Student's t-test, *** < 0.001). **F** Schematic of the in vivo activation process of *Sox10*^{iCreERT2}*/Rpl22*$^{HA/+}$*/Ai14*$^{fl/+}$*/JellyOP*$^{fl/+}$ mice. **G** Confocal images of IHC for FOS (green) and SOX10 (magenta) in whole mounts of *Sox10*^{iCreERT2}*/Rpl22*$^{HA/+}$*/Ai14*$^{fl/+}$*/JellyOP*$^{fl/+}$ or *Sox10*^{iCreERT2}*/Rpl22*$^{HA/+}$*/Ai14*$^{fl/+}$*/JellyOP*$^{+/+}$ *mice* 1 h after stimulation with blue light. Arrows indicate FOS-positive SOX10 glia. Scale bar (100 µm). **H** qPCR analysis of mRNA (mean ± SEM) from *Sox10*^{iCreERT2}*/Rpl22*$^{HA/+}$*/Ai14*$^{fl/+}$*/JellyOP*$^{fl/+l}$ mice or *Sox10*^{iCreERT2}*/Rpl22*$^{HA/+}$*/Ai14*$^{fl/+}$*/JellyOP*$^{+/+}$ *mice* 3 h after optogenetic activation and laparotomy for gliosis hallmark genes ($2^{-\Delta\Delta CT}$, *18S*, *JellyOP*-negative animals, n = 3–7 animals per genotype; Student's t-test, *** < 0.001, * < 0.05)

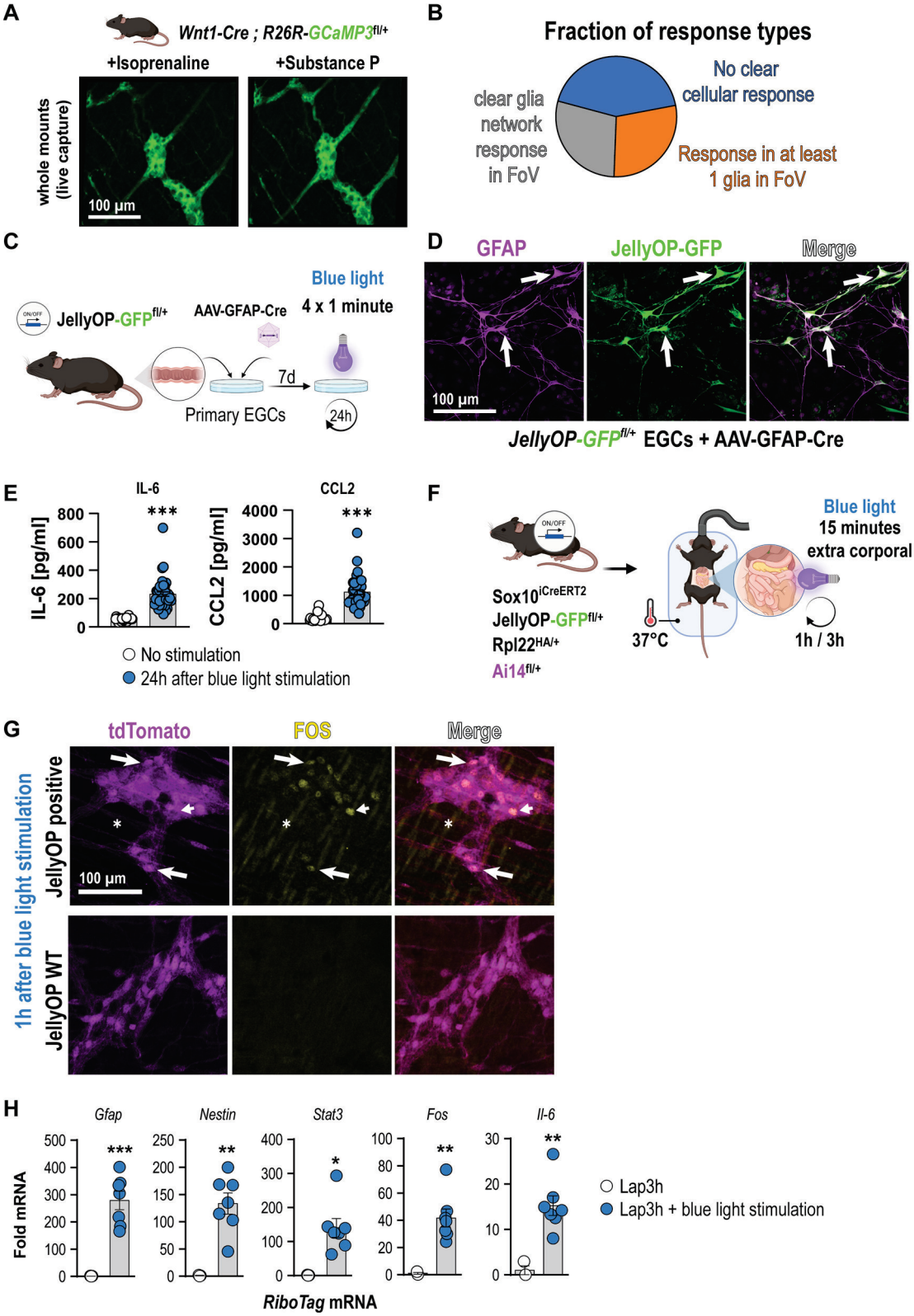

Fig. 5 (See legend on previous page.)

ensure that JellyOP RiboTag mice with a mixed CD1/BL6 background develop a classical POI, we performed IM and analyzed general disease hallmarks. IM evoked a distinct increase in leukocyte infiltration in JellyOP RiboTag mice (Additional file 2: Fig. S6D, SE) and a reduction of gastrointestinal motility (Additional file 2: Fig. S6H) 24 h after surgery compared to naïve littermates. These changes were similar to those observed in mice on a pure BL6 background. Moreover, to validate the gliosis state, we analyzed glial cell proliferation and detected a comparable increase in Ki67 + /SOX10 + cells 24 h after IM (Additional file 2: Fig. S6F, G) as seen before in BL6 mice (Fig. 1B; [5]), solidifying the use of this strain even without backcrossing to a pure BL6 background.

In conclusion, our data show that abdominal surgery immediately induces a transient reactive enteric glia phenotype in the small intestine *ME*. Surgery-induced SNS activity, confirmed by optogenetically induced G_S and chemically induced β-adrenergic stimulation of enteric glia, can trigger this phenotype directly via β1/2-AR signaling immediately after the initial surgical incision. Selective antagonism of these receptors might be a potential future target to modulate enteric glial reactivity and their functional consequences in immune-driven intestinal disorders.

Discussion

Enteric glia are an immuno-active cell type involved in intestinal homeostasis that act on the level of local tissue inflammation. They communicate with neurons and immune cells [44] and are discussed as potential targets in treating or preventing immune-driven intestinal disorders [45]. In our previous studies, we have shown that enteric glia trigger a tissue-related inflammatory state, termed "enteric gliosis", triggered amongst others by immune-mediators IL-1 [41] and ATP [5], finally resulting in postoperative *ME* inflammation and POI. However, the individual molecular mechanism in this disease-specific acute enteric gliosis state and the cellular response of enteric glia remained elusive. Herein, we now selectively analyzed enteric glia-specific transcriptional responses by the *RiboTag* approach [46], a tool to isolate actively transcribed mRNA selectively from a target cell population in the tissue of interest [28]. This technique delivered longitudinal transcriptional data of enteric glia in all relevant POI stages, thereby depicting a compelling transition of enteric glial reactivity within different phases of POI. This transition is structured in three stages: an early transcriptional switch of enteric glia into an inflammatory type, a stage defined by an active release of chemotactic factors (migratory), and an increase in proliferation markers (proliferation), and ultimately a state of tissue regeneration and inflammatory resolution (resolution) (Fig. 6A), which are remarkably similar to the classical POI disease development [25]. Notably, gene expression patterns do not significantly overlap between these phases.

Our Ribotag approach generated a list of 243 early induced and actively transcribed genes that we compiled into a novel GO term, "acute enteric gliosis". We hypothesize that reactive enteric glia are a crucial starting point for the subsequent inflammatory changes in cellular and molecular composition in the *ME* environment [47], thereby resembling a critical time point for potential intervention strategies involving enteric glia. Some of the genes immediately induced in enteric glia by IM confirmed our previous studies, e.g., induction of IL-1 and purinergic target genes [5, 41]. In these studies, we showed that ATP via the P2X2 receptor leads to enteric gliosis and cytokine release [5], and IL-1 signaling evokes enteric glial reactivity that leads to *ME* macrophage recruitment [41]. However, our new findings demonstrate that early enteric glial activation emerges as a multifactorial process requiring a variety of stimuli. Furthermore, other factors that are also well-known markers for glial reactivity in the CNS, including *Ccl2* [48], *Cxcl1* [48, 49], *Mt2* [50], *Nes* [9, 49], and *Il6* [48], can now be directly attributed to enteric glial reactivity in the acutely inflamed small bowel *ME*. Notably, some of these molecules, e.g., CCL2 [51], IL-6 [52], and CXCL1 [53], have already been analyzed for their molecular or immune-modulatory function in POI. Another important chemokine-induced in enteric glia during POI is CXCL10, which was recently implicated during acute infection [11] and is also known in context with CNS gliosis [49]. Moreover, metallothioneins *Mt1* and *Mt2*, essential regulators of oxidative stress in reactive astrocytes of MS patients [54], were highly induced during early inflammation. In addition to the prominently expressed chemotactic factors and immune mediators, we detected others that are novel in this context. For instance, genes of the EGF-family, such as *betacellulin* (*Btc*), previously indicated in ileal growth and homeostasis [55] during health, and *amphiregulin* (*Areg*), implicated in intestinal homeostasis during colitis [56], was induced (*Btc*) or even de novo expressed (*Areg*) upon trauma. Regarding gliosis, we detected an upregulation of *Ier5l* and *Ifrd1*, two genes of the "immediate-early gene" group that regulate cell growth and immune function [57] and include other factors., e.g., *Fos*, *Egr1/2*, *Nr4a1/2*, *Jun*, *Atf3,* and *Fosl*, all strongly induced upon IM. Nevertheless, most (thirty-six) of the top 50 induced genes have inflammatory and chemotactic functions supporting the central role of enteric glia as modulators and initiators of acute inflammatory responses in the gut [1, 44].

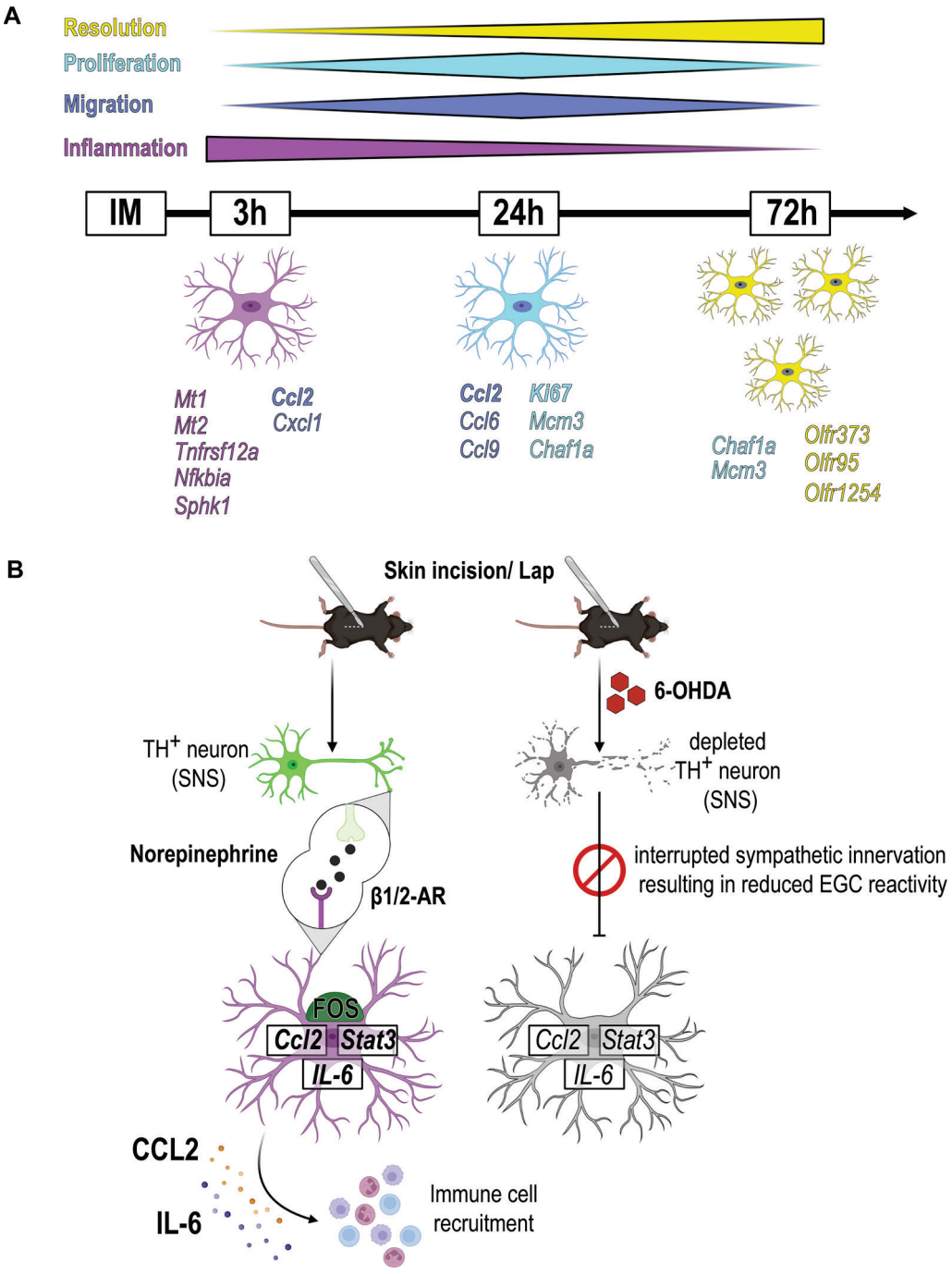

Fig. 6 β-adrenergic signaling in enteric glia triggers enteric glial reactivity and modulates intestinal inflammation in POI. **A** Graphical abstract of the longitudinal analysis of enteric glia after intestinal manipulation (IM) showing a distinct separation into three stages defined by specific hallmarks. Initial reaction (IM3h, magenta) includes an immediate inflammatory reaction and the shaping of the intestinal environment in concert with the initiation of cell migration (blue). This migratory phenotype manifests further 24 h after IM and is accompanied by elevated proliferation (light blue). Finally, inflammatory reactions of enteric glia continuously taper off and are gradually replaced by resolution-related genes (yellow) that initiate a return to the regular intestinal environment. **B** Graphical abstract of SNS activation of enteric glia. Skin incision and laparotomy (in the absence of IM) lead to immediate activation of the SNS, which triggers enteric glial reactivity in the small bowel *ME*. Sympathetic nerve endings in the *ME* release NE, which binds to adrenergic receptors β1 or β2 on myenteric enteric glia. Enteric glia subsequently become reactive (FOS, *Stat3*) and induce upregulation and release of inflammatory mediators (CCL2, IL-6) that in turn modulate immune cells. Chemical disruption of the sympathetic innervation reduces the reactive enteric glia phenotype and the postsurgical inflammatory response

The transcriptional profiling suggests the enormous plasticity of enteric glia in acute inflammation. The high enteric glial plasticity was recently analyzed and discussed by Guyer et al., substantiating the enteric glia potential to manage multiple gut functions [58]. Within the progression of POI, the enteric glia phenotype switches from the initial inflammatory phenotype over a proliferation state towards a so far undefined phenotype. In the proliferation state, we detected a substantial increase in $Ki67^+/SOX10^+$ enteric glia and attributed this cell cycle activation to the POI-related enteric gliosis phenotype. Our countings of the total number of $SOX10^+$ enteric glia could verify the increase in cell numbers 72 h after surgery. Interestingly, recent publications also discuss additional functions of Ki67, such as its role in cell cycle arrest and/or cell synchronization [59, 60]. These functions may play a role in the phenotypic switch of enteric glia during intestinal inflammation in POI.

In the late phase, enteric glia express several olfactory receptors (e.g., *Olfr373* and *Olfr95*) recently shown as "resolution genes" of intestinal inflammation [40, 61] and discussed as potential therapeutic targets to control inflammation and healing [62]. Other OLFRs like OLFR544 [61] or OLFR78 [40] also control gut inflammation, and some were shown to detect and signal to short-chain fatty acids, e.g., butyrate and propionate, produced by luminal bacteria, which act on multiple levels to control intestinal health and disease [63].

Overall, the first part of our study delivers new molecular insight into enteric glial plasticity during intestinal inflammation. While glial reactivity is highly tissue, trigger and disease state dependent, resulting in a different outcome for the cells and their surrounding environment, these distinct molecular signatures will be a valuable starting point for other research. Certainly, enteric glial reactivity varies with treatment conditions in different disease models, including inflammatory bowel diseases [15, 64] or colorectal cancer [65].

Any abdominal surgery starts with the incision of the skin and the abdominal wall before any surgical manipulation of the visceral organs occurs. More than two decades ago, Kalff et al. found that the initial steps of a laparotomy already triggered *ME* inflammation [42]. Accordingly, sympathetic reflexes and activation of the SNS are known to occur early in surgery. The SNS connects to a variety of cells, including enteric ganglia [27] and intestinal macrophages, wherein they exert β2-AR-mediated immune-modulatory function in infectious [20] and immune-driven diseases [21]. Furthermore, sympathetic neurotransmitters, such as NE, regulate motility [66] and control immune cell migration during inflammatory events. As our findings revealed a particular role of enteric glial reactivity within the immediate postoperative phase, when the SNS becomes activated by surgery, and the principal sympathetic neurotransmitter NE is known to modulate the postoperative immune response in POI [23], we were wondering if sympathetic pathways might trigger the early activation of enteric glia.

Indeed, enteric glia responded to the initial bowel wall incision before the actual surgical manipulation of the intestine began. Enteric glia released cytokines such as *Il6* and *Ccl2*, and ablation of SNS nerve fibers ameliorated the acute postsurgical enteric gliosis by reducing cytokine production and early response gene transcription. This diminished glial reactivity was accompanied by a decrease in several POI hallmarks, such as migration and inflammatory response (Fig. 6B).

Further evidence about functional alterations of glial cells to adrenergic stimulation comes from observations in the CNS [67]. The findings of Tong et al. supported the immunomodulatory role of sympathetic inputs, as 6-OHDA-mediated ablations of sympathetic nerves resulted in diminished activation of spinal cord glia [68]. Another study showed that the blockage of β-AR prior to cytotoxic insults to the spinal cord reduced reactive gliosis [69]. SNS neurotransmitters can elicit pro- or anti-inflammatory cytokine release depending on the tissue environment, concentration, and AR binding [70]. In the CNS, for example, NE reduced astrocyte swelling after spinal cord injury [71] and elicited neuroprotective effects in H_2O_2-treated neuron/glia co-cultures [72]. In contrast, preconditioning with NE before ischemic injury exacerbated reactive gliosis [73], and β-2AR agonist treatment increased IL-6 expression after TNFα-induced inflammation in vivo and in vitro [74]. Another pathway triggered by adrenergic activation, partially glimpsed in our experiments, might be the modulation of calcium signaling, which was recently observed in vitro in HEK cells [75] and in vivo in cardiac myocytes [76]. Moreover, adrenergic agonists evoked calcium changes in cultured astrocytes and astrocyte networks in hippocampal slices [77], further prompting future research into this interaction in the gut.

Interestingly, SNS action during inflammation can have opposing effects. While chemical denervation showed beneficial effects during acute inflammation in POI [23] it had adverse effects in chronic intestinal inflammation [78, 79] and mice suffering from physical stress together with colitis [80]. Supporting the beneficial effect of the SNS in chronic inflammation, a recent study by Schiller et al. showed that repeated optogenetic stimulation of TH^+ fibers attenuated symptoms of DSS colitis by reducing immune cell abundance [81]. In IBD patients, the use of β-blockers is associated with an increased relapse risk [82]. Based on the spontaneous increase in glial calcium signaling upon β-adrenergic stimulation, the immediate

induction of reactive glia marker genes after blue light activation of a downstream G_s cascade that mimics β-adrenergic pathways [43] in our *JellyOP* experiments, and the observation that a chemical sympathetic denervation improves symptoms of POI [23], we believe that sympathetic actions in acute inflammatory conditions are rather detrimental. To this end, we expected a more profound insight from our in vivo experiments with reserpine and tyramine application. However, the tested conditions, adapted from previous publications that used these drugs in vivo [31, 32], failed to show changes in POI symptoms and transcriptional glial reactivity compared to the control groups. The lack of strong pharmacological in vivo studies for both compounds, particularly in gastrointestinal physiology and immunology, thus warrants a need for further studies. These should include in-depth pharmacological analyses, comparisons of different administration routes, use of different drug concentrations, time points, and durations before a clear statement about the mode of action of reserpine and tyramine in sympathetic in vivo modulation within the intestine can be claimed.

Our study emphasizes that adrenergic signaling is complex and exerts distinct roles in different cell types, organs, and diseases to control cellular reactivity during inflammation. This knowledge might also be of clinical relevance, e.g., in the application of adrenergic blockers in patients suffering or expected to suffer from acute or chronic intestinal inflammatory diseases. Depending on the nature of the underlying disease, adrenergic blockers can evoke beneficial or detrimental health effects.

As chemical denervation ameliorated postoperative glial reactivity and reduced acute enteric gliosis, we propose SNS-based neurotransmitter release acting on enteric glia as the mechanism of their early activation, a state aggravated by the manipulation of the intestine and additional signaling cascades such as ATP and IL1 signaling. Imura et al. provided supporting evidence of an adrenergic signaling-induced reactive astrocyte phenotype upon stimulation with isoprenaline [83] accompanied by an increased β-AR expression in reactive astrocytes in vivo. Our findings suggest β1- or β2-AR as the relevant receptors to propagate SNS-stimulated inflammatory changes in enteric glia, as the pan-β-AR agonist isoprenaline, but not β3-AR agonism evoked a cytokine release. Applying β2-AR agonist salbutamol also ameliorated DSS-induced ulcerative colitis [84]. Interestingly, antagonists against β-ARs reduced both cardiac inflammation (metoprolol) [85] and ulcerative colitis (propranolol) [86]. Further studies utilizing additional β-AR-specific agonists (e.g., isoprenaline or salbutamol), antagonists (e.g., metoprolol and propranolol), or glial-specific AR-knockouts can help to decipher inflammation-driven diseases involving glial activation as part of their pathophysiology.

It should be noted that adrenergic signaling-induced enteric glial reactivity might not, per se, be a purely detrimental factor in inflammation. Enteric glia appear to be highly plastic during inflammation. While initial NE interaction aggravates the acute enteric glial reactivity, prolonged NE exposure, as it occurs during prolonged or chronic inflammation, might drive enteric glia to a beneficial phenotype and partially explain the positive influence of the SNS during those stages [78, 79, 84]. Moreover, the inflammatory environment changes during the disease course, altering the cellular and molecular composition and thus might also affect the responses to adrenergic signaling. For instance, in the presence of TNFα, NE binding to β-ARs inhibited further TNFα and downstream IL-6 secretion, while adrenergic signaling in the absence of TNFα directly stimulated IL-6 secretion [70]. Moreover, AR receptor expression is modulated during inflammation, previously shown for astrocytes [83], and in the intestine controlled by sympathetic inputs [23]. As inflammation can be accompanied by a later loss [70], the absence of feedback loops might also explain the differences in adrenergic immune-related responses between acute and chronic inflammation. Notably, differences in the adrenergic reactions might also occur within different locations of the same organ. While chronic intestinal disease models focus on the mucosal layer, the acute postoperative response to surgery is mainly limited to the *ME* [87], which comprises a different cellular composition and more distant localization to the luminal contents of the gut.

Overall, our study delivers an unknown longitudinal insight into enteric glial molecular responses and reactivity during different phases of an acute inflammation-driven intestinal disorder. We introduced sympathetic adrenergic signaling as a priming factor of enteric glial reactivity and a potential therapeutic target. These data are of important future value, as they not only present an interventional target to control inflammation but will also help to understand similarities and differences in enteric glial reactivity in other inflammation-driven diseases, such as IBD and gastrointestinal cancer development.

Abbreviations

EGC	Enteric glial cell
POI	Postoperative ileus
ENS	Enteric nervous system
CNS	Central nervous system
SNS	Sympathetic nervous system
GI	Gastro-intestinal
LPS	Lipopolysacharrid

Lap	Laparotomy
STX	Sympathetectomy (chemical)
NE	Norepinephrine
ME	Muscularis externa
AR	Adrenergic receptor
GO	Gene ontology
IM	Intestinal manipulation
6-OHDA	6-Hydroxydopamine
GFAP	Glial fibrilliary acidic protein
SOX10	SRY-Box transcription factor 10
IL-6	Interleukin-6
IL-1β	Interleukin-1β
CCL2	C–C motif chemokine ligand 2
TNFα	Tumor necrosis factor α
IFNγ	Interferone γ
GDNF	Glial-cell derived neurotrophic factor
PLP1	Proteolipid protein 1

Supplementary Information

The online version contains supplementary material available at https://doi.org/10.1186/s12974-023-02937-0.

Additional file 1: Method S1. RiboTag approach in the muscularis externa. **Method S2.** Construction of the *JellyOP* targeting vector for the mouse Rosa26 locus. **Method S3.** *JellyOP* animal creation. **Method S4.** Recombinant adeno-associated virus (rAAV) preparation. **Table S1.** Buffer and media. **Table S2.** Antibodies. **Table S3.** PCR primer. **Table S4.** Acute enteric gliosis GO-term.

Additional file 2: Figure S1. Characterization of POI in *Sox10*^{iCreERT2}/*Rpl22*$^{HA/+}$ mice. **Figure S2.** Sympathetic signaling is involved in enteric glia functions. **Figure S3.** Laparotomy affects molecular functions. **Figure S4.** Effect of NE and tissue expression of ADRβ1. **Figure S5.** Ex vivo β-adrenergic stimulation elicits enteric glia calcium signaling. **Figure S6.** JellyOP mice with a mixed genetic background develop regular POI.

Additional file 3: Video SA. Isoprenaline. **Video SB.** Substance P.

Acknowledgements

We thank Mariola Lysson, Bianca Schneiker, Patrik Efferz, Frank Holst and Jana Müller for their excellent technical support and animal handling. Moreover, we thank the Bioinformatics Core, the Next Generation Sequencing Core, and the Microscopy Core Facility of the University Hospital Bonn for providing help, services, and devices funded, among others, by the German research council (DFG, German Research Foundation) – Project number 388159768. We would like to thank the Gene-Editing Core Facility of the Medical Faculty at the University of Bonn for the generation of the Gt(ROSA)26Sor$^{em1(CAG-JellyOp-eGFP)}$ mouse line and Vanessa Dusend, Daniela Malan, Wanchana Jangsangthong for generation of targeting constructs and characterization of the JellyOP-GPF fl/+ mouse line. We furthermore thank the Viral Core Facility of the Medical Faculty at the University of Bonn for the production of the rAAV2/1-hGFAP-NLS-Cre. Graphical visualizations were created with *BioRender* software. Furthermore, we would like to express our gratitude to Professor Vassilis Pachnis for kindly providing the Sox10^{iCreERT2} mouse line, Prof. Sasse and Prof. Pfeifer for sharing adrenergic agonists with us, and Prof. Wegner for providing us with a goat Sox10 antibody. Finally, we would like to thank Professor Walker S. Jackson and Dr. Eileen C. Haring for their valuable input on the manuscript.

Author contributions

PL, RS, LS, SM and PVB performed research; PL, RS, and SW designed the study and analyzed the data; PL, RS, LS, PVB, PS, JCK, and SW wrote the manuscript. All authors reviewed the manuscript.

Funding

Open Access funding enabled and organized by Projekt DEAL. This publication was financed by a grant from the German research council (DFG) to SW (WE4204/3-1) and, BonnNI to SW (Q-611.0754), Bonfor to RS (O-112.0066) and the ImmunoSensation^2 Cluster of Excellence (EXC 2151–390873048). PS received support from DFG (SA 1785/7-1, SA 1785/9-1). P. Vanden Berghe receives support from FWO G021.15, G012223N and I000123N (in support of the Cell & tissue Imaging Core (CIC)-Flanders BioImaging). The Andor Revolution Spinning Disk System was obtained via Hercules Grant AKUL/09/50 to P. Vanden Berghe.

Availability of data and materials

The datasets used and analyzed during the current study have been submitted to the GEO database under the accession number *GSE198889* with the following token: cdupiqaotjsnvgf.

Declarations

Ethical approval and consent to participate

Mouse work was conducted under the ethical approval for animal experiments number: Az.81–02.04.2016.A367 and Az.1–02.04.2018.A221. Since no patient data were included in this study, consent to participate is not applicable.

Consent for publication

Not applicable.

Competing interests

SW and JCK receive royalties from Wolter Kluwer for his contribution to the postoperative ileus section of the *UpToDate* library. All other authors declare no competing interests.

Author details

[1]Department of Surgery, University Hospital Bonn, Venusberg-Campus 1, 53127 Bonn, Germany. [2]Laboratory for Enteric NeuroScience (LENS), Translational Research Center for Gastrointestinal Disorders (TARGID), University of Leuven, Louvain, Belgium. [3]Institute of Physiology I, Medical Faculty, University of Bonn, Bonn, Germany.

Received: 27 May 2022 Accepted: 27 October 2023
Published online: 08 November 2023

References

1. Seguella L, Gulbransen BD. Enteric glial biology, intercellular signalling and roles in gastrointestinal disease. Nat Rev Gastroenterol Hepatol. 2021. https://doi.org/10.1038/s41575-021-00423-7.
2. Boesmans W, Lasrado R, Vanden Berghe P, Pachnis V. Heterogeneity and phenotypic plasticity of glial cells in the mammalian enteric nervous system. Glia. 2015;63:229–41. https://doi.org/10.1002/glia.22746.
3. Rao M, Nelms BD, Dong L, Salinas-Rios V, Rutlin M, Gershon MD, Corfas G. Enteric glia express proteolipid protein 1 and are a transcriptionally unique population of glia in the mammalian nervous system. Glia. 2015;63:2040–57. https://doi.org/10.1002/glia.22876.
4. Brown IAM, McClain JL, Watson RE, Patel BA, Gulbransen BD. Enteric glia mediate neuron death in colitis through purinergic pathways that require connexin-43 and nitric oxide. Cell Mol Gastroenterol Hepatol. 2016;2:77–91. https://doi.org/10.1016/j.jcmgh.2015.08.007.
5. Schneider R, Leven P, Glowka T, Kuzmanov I, Lysson M, Schneiker B, et al. A novel P2X2-dependent purinergic mechanism of enteric gliosis in intestinal inflammation. EMBO Mol Med. 2021;13: e12724. https://doi.org/10.15252/emmm.202012724.
6. Burda JE, Sofroniew MV. Reactive gliosis and the multicellular response to CNS damage and disease. Neuron. 2014;81:229–48. https://doi.org/10.1016/j.neuron.2013.12.034.
7. das Neves SP, Sousa JC, Sousa N, Cerqueira JJ, Marques F. Altered astrocytic function in experimental neuroinflammation and multiple sclerosis. Glia. 2021;69:1341–68. https://doi.org/10.1002/glia.23940.
8. Liddelow SA, Guttenplan KA, Clarke LE, Bennett FC, Bohlen CJ, Schirmer L, et al. Neurotoxic reactive astrocytes are induced by activated microglia. Nature. 2017;541:481–7. https://doi.org/10.1038/nature21029.
9. Hara M, Kobayakawa K, Ohkawa Y, Kumamaru H, Yokota K, Saito T, et al. Interaction of reactive astrocytes with type I collagen induces astrocytic scar formation through the integrin-N-cadherin pathway after spinal cord injury. Nat Med. 2017;23:818–28. https://doi.org/10.1038/nm.4354.

10. Stoffels B, Hupa KJ, Snoek SA, van Bree S, Stein K, Schwandt T, et al. Postoperative ileus involves interleukin-1 receptor signaling in enteric glia. Gastroenterology. 2014;146:176-87.e1. https://doi.org/10.1053/j.gastro.2013.09.030.
11. Progatzky F, Shapiro M, Chng SH, Garcia-Cassani B, Classon CH, Sevgi S, et al. Regulation of intestinal immunity and tissue repair by enteric glia. Nature. 2021;599:125–30. https://doi.org/10.1038/s41586-021-04006-z.
12. Turco F, Sarnelli G, Cirillo C, Palumbo I, de Giorgi F, D'Alessandro A, et al. Enteroglial-derived S100B protein integrates bacteria-induced Toll-like receptor signalling in human enteric glial cells. Gut. 2014;63:105–15. https://doi.org/10.1136/gutjnl-2012-302090.
13. Meir M, Kannapin F, Diefenbacher M, Ghoreishi Y, Kollmann C, Flemming S, et al. Intestinal epithelial barrier maturation by enteric glial cells is GDNF-dependent. Int J Mol Sci. 2021. https://doi.org/10.3390/ijms22041887.
14. Cheadle GA, Costantini TW, Lopez N, Bansal V, Eliceiri BP, Coimbra R. Enteric glia cells attenuate cytomix-induced intestinal epithelial barrier breakdown. PLoS ONE. 2013;8: e69042. https://doi.org/10.1371/journal.pone.0069042.
15. Liñán-Rico A, Turco F, Ochoa-Cortes F, Harzman A, Needleman BJ, Arsenescu R, et al. Molecular signaling and dysfunction of the human reactive enteric glial cell phenotype: implications for GI infection, IBD, POI, neurological, motility, and GI disorders. Inflamm Bowel Dis. 2016;22:1812–34. https://doi.org/10.1097/MIB.0000000000000854.
16. von Boyen GBT, Steinkamp M, Reinshagen M, Schäfer K-H, Adler G, Kirsch J. Nerve growth factor secretion in cultured enteric glia cells is modulated by proinflammatory cytokines. J Neuroendocrinol. 2006;18:820–5. https://doi.org/10.1111/j.1365-2826.2006.01478.x.
17. Cirillo C, Sarnelli G, Turco F, Mango A, Grosso M, Aprea G, et al. Proinflammatory stimuli activates human-derived enteroglial cells and induces autocrine nitric oxide production. Neurogastroenterol Motil. 2011;23:e372–82. https://doi.org/10.1111/j.1365-2982.2011.01748.x.
18. Duan H, Cai X, Luan Y, Yang S, Yang J, Dong H, et al. Regulation of the autonomic nervous system on intestine. Front Physiol. 2021. https://doi.org/10.3389/fphys.2021.700129.
19. Nasser Y, Ho W, Sharkey KA. Distribution of adrenergic receptors in the enteric nervous system of the guinea pig, mouse, and rat. J Comp Neurol. 2006;495:529–53. https://doi.org/10.1002/cne.20898.
20. Matheis F, Muller PA, Graves CL, Gabanyi I, Kerner ZJ, Costa-Borges D, et al. Adrenergic signaling in muscularis macrophages limits infection-induced neuronal loss. Cell. 2020;180:64-78.e16. https://doi.org/10.1016/j.cell.2019.12.002.
21. Gabanyi I, Muller PA, Feighery L, Oliveira TY, Costa-Pinto FA, Mucida D. Neuro-immune interactions drive tissue programming in intestinal macrophages. Cell. 2016;164:378–91. https://doi.org/10.1016/j.cell.2015.12.023.
22. Brinkman DJ, ten Hove AS, Vervoordeldonk MJ, Luyer MD, de Jonge WJ. Neuroimmune interactions in the gut and their significance for intestinal immunity. Cells. 2019. https://doi.org/10.3390/cells8070670.
23. Mallesh S, Schneider R, Schneiker B, Lysson M, Efferz P, Lin E, et al. Sympathetic denervation alters the inflammatory response of resident muscularis macrophages upon surgical trauma and ameliorates postoperative ileus in mice. IJMS. 2021;22:6872. https://doi.org/10.3390/ijms22136872.
24. Augestad KM, Delaney CP. Postoperative ileus: impact of pharmacological treatment, laparoscopic surgery and enhanced recovery pathways. World J Gastroenterol. 2010;16:2067–74. https://doi.org/10.3748/wjg.v16.i17.2067.
25. Boeckxstaens GE, de Jonge WJ. Neuroimmune mechanisms in postoperative ileus. Gut. 2009;58:1300–11. https://doi.org/10.1136/gut.2008.169250.
26. Mazzotta E, Villalobos-Hernandez EC, Fiorda-Diaz J, Harzman A, Christofi FL. Postoperative ileus and postoperative gastrointestinal tract dysfunction: pathogenic mechanisms and novel treatment strategies beyond colorectal enhanced recovery after surgery protocols. Front Pharmacol. 2020;11: 583422. https://doi.org/10.3389/fphar.2020.583422.
27. Gulbransen BD, Bains JS, Sharkey KA. Enteric glia are targets of the sympathetic innervation of the myenteric plexus in the guinea pig distal colon. J Neurosci. 2010;30:6801–9. https://doi.org/10.1523/JNEUROSCI.0603-10.2010.
28. Leven P, Schneider R, Siemens KD, Jackson WS, Wehner S. Application of a RiboTag-based approach to generate and analyze mRNA from enteric neural cells. Neurogastroenterol Motil. 2021. https://doi.org/10.1111/nmo.14309.
29. Delvalle NM, Dharshika C, Morales-Soto W, Fried DE, Gaudette L, Gulbransen BD. Communication between enteric neurons, glia, and nociceptors underlies the effects of tachykinins on neuroinflammation. Cell Mol Gastroenterol Hepatol. 2018;6:321–44. https://doi.org/10.1016/j.jcmgh.2018.05.009.
30. van Chu T, Weber T, Graf R, Sommermann T, Petsch K, Sack U, et al. Efficient generation of Rosa26 knock-in mice using CRISPR/Cas9 in C57BL/6 zygotes. BMC Biotechnol. 2016;16:4. https://doi.org/10.1186/s12896-016-0234-4.
31. Poll BG, Xu J, Jun S, Sanchez J, Zaidman NA, He X, et al. Acetate, a short-chain fatty acid, acutely lowers heart rate and cardiac contractility along with blood pressure. J Pharmacol Exp Ther. 2021;377:39–50. https://doi.org/10.1124/jpet.120.000187.
32. Olfe J, Domanska G, Schuett C, Kiank C. Different stress-related phenotypes of BALB/c mice from in-house or vendor: alterations of the sympathetic and HPA axis responsiveness. BMC Physiol. 2010;10:2. https://doi.org/10.1186/1472-6793-10-2.
33. Danielian PS, Muccino D, Rowitch DH, Michael SK, McMahon AP. Modification of gene activity in mouse embryos in utero by a tamoxifen-inducible form of Cre recombinase. Curr Biol. 1998;8:1323–6. https://doi.org/10.1016/s0960-9822(07)00562-3.
34. Zariwala HA, Borghuis BG, Hoogland TM, Madisen L, Tian L, de Zeeuw CI, et al. A Cre-dependent GCaMP3 reporter mouse for neuronal imaging in vivo. J Neurosci. 2012;32:3131–41. https://doi.org/10.1523/JNEUROSCI.4469-11.2012.
35. Vanden Berghe P, Kenyon JL, Smith TK. Mitochondrial Ca2+ uptake regulates the excitability of myenteric neurons. J Neurosci. 2002;22:6962–71. https://doi.org/10.1523/JNEUROSCI.22-16-06962.2002.
36. Boesmans W, Hao MM, Fung C, Li Z, van den Haute C, Tack J, et al. Structurally defined signaling in neuro-glia units in the enteric nervous system. Glia. 2019;67:1167–78. https://doi.org/10.1002/glia.23596.
37. Li Z, Hao MM, van den Haute C, Baekelandt V, Boesmans W, Vanden BP. Regional complexity in enteric neuron wiring reflects diversity of motility patterns in the mouse large intestine. Elife. 2019. https://doi.org/10.7554/eLife.42914.
38. Preibisch S, Saalfeld S, Schindelin J, Tomancak P. Software for bead-based registration of selective plane illumination microscopy data. Nat Methods. 2010;7:418–9. https://doi.org/10.1038/nmeth0610-418.
39. Boesmans W, Martens MA, Weltens N, Hao MM, Tack J, Cirillo C, Vanden BP. Imaging neuron-glia interactions in the enteric nervous system. Front Cell Neurosci. 2013;7:183. https://doi.org/10.3389/fncel.2013.00183.
40. Kotlo K, Anbazhagan AN, Priyamvada S, Jayawardena D, Kumar A, Chen Y, et al. The olfactory G protein-coupled receptor (Olfr-78/OR51E2) modulates the intestinal response to colitis. Am J Physiol Cell Physiol. 2020;318:C502–13. https://doi.org/10.1152/ajpcell.00454.2019.
41. Schneider R, Leven P, Mallesh S, Breßer M, Schneider L, Mazzotta E, et al. IL-1-dependent enteric gliosis guides intestinal inflammation and dysmotility and modulates macrophage function. Commun Biol. 2022;5:811. https://doi.org/10.1038/s42003-022-03772-4.
42. Kalff JC, Türler A, Schwarz NT, Schraut WH, Lee KKW, Tweardy DJ, et al. Intra-abdominal activation of a local inflammatory response within the human muscularis externa during laparotomy. Ann Surg. 2003;237:301–15. https://doi.org/10.1097/01.SLA.0000055742.79045.7E.
43. Makowka P, Bruegmann T, Dusend V, Malan D, Beiert T, Hesse M, et al. Optogenetic stimulation of Gs-signaling in the heart with high spatiotemporal precision. Nat Commun. 2019;10:1281. https://doi.org/10.1038/s41467-019-09322-7.
44. Progatzky F, Pachnis V. The role of enteric glia in intestinal immunity. Curr Opin Immunol. 2022;77: 102183. https://doi.org/10.1016/j.coi.2022.102183.
45. Gulbransen BD, Christofi FL. Are we close to targeting enteric glia in gastrointestinal diseases and motility disorders? Gastroenterology. 2018;155:245–51. https://doi.org/10.1053/j.gastro.2018.06.050.
46. Sanz E, Bean JC, Carey DP, Quintana A, McKnight GS. RiboTag: ribosomal tagging strategy to analyze cell-type-specific mRNA expression in vivo. Curr Protoc Neurosci. 2019;88: e77. https://doi.org/10.1002/cpns.77.
47. Wehner S, Vilz TO, Stoffels B, Kalff JC. Immune mediators of postoperative ileus. Langenbecks Arch Surg. 2012;397:591–601. https://doi.org/10.1007/s00423-012-0915-y.

48. Nieves MD, Furmanski O, Doughty ML. Sensorimotor dysfunction in a mild mouse model of cortical contusion injury without significant neuronal loss is associated with increases in inflammatory proteins with innate but not adaptive immune functions. J Neurosci Res. 2021;99:1533–49. https://doi.org/10.1002/jnr.24766.
49. Zamanian JL, Xu L, Foo LC, Nouri N, Zhou L, Giffard RG, Barres BA. Genomic analysis of reactive astrogliosis. J Neurosci. 2012;32:6391–410. https://doi.org/10.1523/JNEUROSCI.6221-11.2012.
50. Mathys H, Davila-Velderrain J, Peng Z, Gao F, Mohammadi S, Young JZ, et al. Single-cell transcriptomic analysis of Alzheimer's disease. Nature. 2019;570:332–7. https://doi.org/10.1038/s41586-019-1195-2.
51. Farro G, Stakenborg M, Gomez-Pinilla PJ, Labeeuw E, Goverse G, Di Giovangiulio M, et al. CCR2-dependent monocyte-derived macrophages resolve inflammation and restore gut motility in postoperative ileus. Gut. 2017;66:2098–109. https://doi.org/10.1136/gutjnl-2016-313144.
52. Wehner S, Schwarz NT, Hundsdoerfer R, Hierholzer C, Tweardy DJ, Billiar TR, et al. Induction of IL-6 within the rodent intestinal muscularis after intestinal surgical stress. Surgery. 2005;137:436–46. https://doi.org/10.1016/j.surg.2004.11.003.
53. Docsa T, Bhattarai D, Sipos A, Wade CE, Cox CS, Uray K. CXCL1 is upregulated during the development of ileus resulting in decreased intestinal contractile activity. Neurogastroenterol Motil. 2020;32: e13757. https://doi.org/10.1111/nmo.13757.
54. Penkowa M, Espejo C, Ortega-Aznar A, Hidalgo J, Montalban X, Martínez Cáceres EM. Metallothionein expression in the central nervous system of multiple sclerosis patients. Cell Mol Life Sci. 2003;60:1258–66. https://doi.org/10.1007/s00018-003-3021-z.
55. Howarth GS, Bastian SEP, Dunbar AJ, Goddard C. Betacellulin promotes growth of the gastrointestinal organs and effects a diuresis in normal rats. Growth Factors. 2003;21:79–86. https://doi.org/10.1080/08977190310001605779.
56. Chen F, Yang W, Huang X, Cao AT, Bilotta AJ, Xiao Y, et al. Neutrophils promote amphiregulin production in intestinal epithelial cells through TGF-β and contribute to intestinal homeostasis. J Immunol. 2018;201:2492–501. https://doi.org/10.4049/jimmunol.1800003.
57. Bahrami S, Drabløs F. Gene regulation in the immediate-early response process. Adv Biol Regul. 2016;62:37–49. https://doi.org/10.1016/j.jbior.2016.05.001.
58. Guyer RA, Stavely R, Robertson K, Bhave S, Mueller JL, Picard NM, et al. Single-cell multiome sequencing clarifies enteric glial diversity and identifies an intraganglionic population poised for neurogenesis. Cell Rep. 2023;42:112194. https://doi.org/10.1016/j.celrep.2023.112194.
59. Miller I, Min M, Yang C, Tian C, Gookin S, Carter D, Spencer SL. Ki67 is a graded rather than a binary marker of proliferation versus quiescence. Cell Rep. 2018;24:1105-1112.e5. https://doi.org/10.1016/j.celrep.2018.06.110.
60. Sun X, Kaufman PD. Ki-67: more than a proliferation marker. Chromosoma. 2018;127:175–86. https://doi.org/10.1007/s00412-018-0659-8.
61. Wu C, Jeong M-Y, Kim JY, Lee G, Kim J-S, Cheong YE, et al. Activation of ectopic olfactory receptor 544 induces GLP-1 secretion and regulates gut inflammation. Gut Microbes. 2021;13:1987782. https://doi.org/10.1080/19490976.2021.1987782.
62. Lee S-J, Depoortere I, Hatt H. Therapeutic potential of ectopic olfactory and taste receptors. Nat Rev Drug Discov. 2019;18:116–38. https://doi.org/10.1038/s41573-018-0002-3.
63. van der Beek CM, Dejong CHC, Troost FJ, Masclee AAM, Lenaerts K. Role of short-chain fatty acids in colonic inflammation, carcinogenesis, and mucosal protection and healing. Nutr Rev. 2017;75:286–305. https://doi.org/10.1093/nutrit/nuw067.
64. Biskou O, Meira de-Faria F, Walter SM, Winberg ME, Haapaniemi S, Myrelid P, et al. Increased numbers of enteric glial cells in the Peyer's patches and enhanced intestinal permeability by glial cell mediators in patients with ileal Crohn's disease. Cells. 2022;11:335. https://doi.org/10.3390/cells11030335.
65. Schonkeren SL, Thijssen MS, Vaes N, Boesmans W, Melotte V. The emerging role of nerves and glia in colorectal cancer. Cancers (Basel). 2021. https://doi.org/10.3390/cancers13010152.
66. Lomax AE, Sharkey KA, Furness JB. The participation of the sympathetic innervation of the gastrointestinal tract in disease states. Neurogastroenterol Motil. 2010;22:7–18. https://doi.org/10.1111/j.1365-2982.2009.01381.x.
67. Madrigal JL. Noradrenaline, Astroglia, and Neuroinflammation. In: Vardjan N, Zorec R, editors. Noradrenergic signaling and astroglia. London: Academic Press; 2017. p. 273–87. https://doi.org/10.1016/B978-0-12-805088-0.00014-1.
68. Tong F, He Q, Du W-J, Yang H, Du D, Pu S, Han Q. Sympathetic nerve mediated spinal glia activation underlies itch in a cutaneous T-cell lymphoma model. Neurosci Bull. 2021. https://doi.org/10.1007/s12264-021-00805-6.
69. Sutin J, Griffith R. Beta-adrenergic receptor blockade suppresses glial scar formation. Exp Neurol. 1993;120:214–22. https://doi.org/10.1006/exnr.1993.1056.
70. Straub RH, Wiest R, Strauch UG, Härle P, Schölmerich J. The role of the sympathetic nervous system in intestinal inflammation. Gut. 2006;55:1640–9. https://doi.org/10.1136/gut.2006.091322.
71. Vardjan N, Horvat A, Anderson JE, Yu D, Croom D, Zeng X, et al. Adrenergic activation attenuates astrocyte swelling induced by hypotonicity and neurotrauma. Glia. 2016;64:1034–49. https://doi.org/10.1002/glia.22981.
72. Yoshioka Y, Negoro R, Kadoi H, Motegi T, Shibagaki F, Yamamuro A, et al. Noradrenaline protects neurons against H2 O2 -induced death by increasing the supply of glutathione from astrocytes via β3 -adrenoceptor stimulation. J Neurosci Res. 2021;99:621–37. https://doi.org/10.1002/jnr.24733.
73. Danková M, Domoráková I, Fagová Z, Stebnický M, Kunová A, Mechírová E. Bradykinin and noradrenaline preconditioning influences level of antioxidant enzymes SOD, CuZn-SOD, Mn-SOD and catalase in the white matter of spinal cord in rabbits after ischemia/reperfusion. Eur J Histochem. 2019. https://doi.org/10.4081/ejh.2019.3045.
74. Laureys G, Gerlo S, Spooren A, Demol F, de Keyser J, Aerts JL. β_2-adrenergic agonists modulate TNF-α induced astrocytic inflammatory gene expression and brain inflammatory cell populations. J Neuroinflammation. 2014;11:21. https://doi.org/10.1186/1742-2094-11-21.
75. Galaz-Montoya M, Wright SJ, Rodriguez GJ, Lichtarge O, Wensel TG. β2-Adrenergic receptor activation mobilizes intracellular calcium via a non-canonical cAMP-independent signaling pathway. J Biol Chem. 2017;292:9967–74. https://doi.org/10.1074/jbc.M117.787119.
76. Maxwell JT, Domeier TL, Blatter LA. β-adrenergic stimulation increases the intra-SR Ca termination threshold for spontaneous Ca waves in cardiac myocytes. Channels (Austin). 2013;7:206–10. https://doi.org/10.4161/chan.24173.
77. Duffy S. Adrenergic calcium signaling in astrocyte networks within the hippocampal slice. J Neurosci. 1995. https://doi.org/10.1523/JNEUROSCI.15-08-05535.1995.
78. Willemze RA, Welting O, van Hamersveld P, Verseijden C, Nijhuis LE, Hilbers FW, et al. Loss of intestinal sympathetic innervation elicits an innate immune driven colitis. Mol Med. 2019. https://doi.org/10.1186/s10020-018-0068-8.
79. Willemze RA, Welting O, van Hamersveld HP, Meijer SL, Folgering JHA, Darwinkel H, et al. Neuronal control of experimental colitis occurs via sympathetic intestinal innervation. Neurogastroenterol Motil. 2018. https://doi.org/10.1111/nmo.13163.
80. Schneider KM, Blank N, Alvarez Y, Thum K, Lundgren P, Litichevskiy L, et al. The enteric nervous system relays psychological stress to intestinal inflammation. Cell. 2023;186:2823-2838.e20. https://doi.org/10.1016/j.cell.2023.05.001.
81. Schiller M, Azulay-Debby H, Boshnak N, Elyahu Y, Korin B, Ben-Shaanan TL, et al. Optogenetic activation of local colonic sympathetic innervations attenuates colitis by limiting immune cell extravasation. Immunity. 2021;54:1022-1036.e8. https://doi.org/10.1016/j.immuni.2021.04.007.
82. Willemze RA, Bakker T, Pippias M, Ponsioen CY, de Jonge WJ. β-Blocker use is associated with a higher relapse risk of inflammatory bowel disease: a Dutch retrospective case-control study. Eur J Gastroenterol Hepatol. 2018;30:161–6. https://doi.org/10.1097/MEG.0000000000001016.
83. Imura T, Shimohama S, Sato M, Nishikawa H, Madono K, Akaike A, Kimura J. Differential expression of small heat shock proteins in reactive astrocytes after focal ischemia: possible role of β-adrenergic receptor. J Neurosci. 1999;19:9768–79. https://doi.org/10.1523/JNEUROSCI.19-22-09768.1999.
84. Deng L, Guo H, Wang S, Liu X, Lin Y, Zhang R, Tan W. The attenuation of chronic ulcerative colitis by (R)-salbutamol in repeated DSS-induced mice. Oxid Med Cell Longev. 2022;2022:9318721. https://doi.org/10.1155/2022/9318721.

85. Clemente-Moragón A, Gómez M, Villena-Gutiérrez R, Lalama DV, García-Prieto J, Martínez F, et al. Metoprolol exerts a non-class effect against ischaemia-reperfusion injury by abrogating exacerbated inflammation. Eur Heart J. 2020;41:4425–40. https://doi.org/10.1093/eurheartj/ehaa733.
86. Ramadan N, El-Menshawy S, Amal Elsayed S, Shireen Sami MO. Protective effects of propranolol and carvedilol on experimentallyinduced ulcerative colitis in male albino rat. Eur J Mol Clin Med. 2021. https://doi.org/10.13140/RG.2.2.22062.38724.
87. Snoek SA, Dhawan S, van Bree SH, Cailotto C, van Diest SA, Duarte JM, et al. Mast cells trigger epithelial barrier dysfunction, bacterial translocation and postoperative ileus in a mouse model. Neurogastroenterol Motil. 2012;24:172-e91. https://doi.org/10.1111/j.1365-2982.2011.01820.x.

Publisher's Note

3.3 Publication 3: *Schneider et al. 2021*, A novel P2X2-dependent purinergic mechanism of enteric gliosis in intestinal inflammation, DOI:10.15252/emmm.202012724

Article

SOURCE DATA | TRANSPARENT PROCESS | OPEN ACCESS

EMBO Molecular Medicine

A novel P2X2-dependent purinergic mechanism of enteric gliosis in intestinal inflammation

Reiner Schneider[1], Patrick Leven[1], Tim Glowka[1], Ivan Kuzmanov[1], Mariola Lysson[1], Bianca Schneiker[1], Anna Miesen[1], Younis Baqi[2,3], Claudia Spanier[3], Iveta Grants[4], Elvio Mazzotta[4], Egina Villalobos-Hernandez[4], Jörg C Kalff[1], Christa E Müller[3], Fedias L Christofi[4] & Sven Wehner[1,*]

Abstract

Enteric glial cells (EGC) modulate motility, maintain gut homeostasis, and contribute to neuroinflammation in intestinal diseases and motility disorders. Damage induces a reactive glial phenotype known as "gliosis", but the molecular identity of the inducing mechanism and triggers of "enteric gliosis" are poorly understood. We tested the hypothesis that surgical trauma during intestinal surgery triggers ATP release that drives enteric gliosis and inflammation leading to impaired motility in postoperative ileus (POI). ATP activation of a p38-dependent MAPK pathway triggers cytokine release and a gliosis phenotype in murine (and human) EGCs. Receptor antagonism and genetic depletion studies revealed P2X2 as the relevant ATP receptor and pharmacological screenings identified ambroxol as a novel P2X2 antagonist. Ambroxol prevented ATP-induced enteric gliosis, inflammation, and protected against dysmotility, while abrogating enteric gliosis in human intestine exposed to surgical trauma. We identified a novel pathogenic P2X2-dependent pathway of ATP-induced enteric gliosis, inflammation and dysmotility in humans and mice. Interventions that block enteric glial P2X2 receptors during trauma may represent a novel therapy in treating POI and immune-driven intestinal motility disorders.

Keywords enteric nervous system; gut inflammation; motility disorders; postoperative ileus; purinergic signaling
Subject Categories Digestive System; Immunology; Neuroscience
DOI 10.15252/emmm.202012724 | Received 19 May 2020 | Revised 13 November 2020 | Accepted 16 November 2020 | Published online 17 December 2020
EMBO Mol Med (2021) 13: e12724

Introduction

Enteric glial cells (EGCs) are a unique population of cells in the enteric nervous system (Furness, 2012) playing a pivotal role in the maintenance of gut homeostasis (Sharkey, 2015). They shape the immune environment through interactions with resident immune cells and other cell types (Brierley & Linden, 2014; Yoo & Mazmanian, 2017). In line with this, EGCs secrete neuroprotective (Abdo *et al*, 2010) and immune-modulatory factors (Yoo & Mazmanian, 2017) and targeted ablation of glia (Rao *et al*, 2017) or inhibition (McClain *et al*, 2014) of glial signaling through connexin-43 hemichannel communication between glia can disrupt motility. However, the neuroinflammatory effect of glial ablation is still unclear, as in some cases a fatal bowel inflammation was documented (Bush *et al*, 1998; Cornet *et al*, 2001; Aubé *et al*, 2006) while in a recent study, utilizing a new genetic mouse model, no immune-modulatory effect was observed (Rao *et al*, 2017). In contrast to their immune-modulatory role, several *in vivo* and *in vitro* studies by us and others provide evidence that murine or human EGCs can turn into reactive glia in an immune-stimulated environment, e.g., under LPS presence (Rosenbaum *et al*, 2016; Liñán-Rico *et al*, 2016), after viral protein HIV-1 Tat (Esposito *et al*, 2017) or IL-1 stimulation upon which EGCs release inflammatory mediators like cytokines, nitric oxide or reactive oxygen species (Stoffels *et al*, 2014; Brown *et al*, 2016; Liñán-Rico *et al*, 2016; Rosenbaum *et al*, 2016). EGCs were also shown to interact with bacteria, and they can discriminate between beneficial and harmful bacteria (Turco *et al*, 2014).

Immune responses are often a consequence of tissue damage which leads to the release of intracellular molecules that act as danger-associated molecular patterns (DAMP) and trigger innate immune processes (Yoo & Mazmanian, 2017). One prominent DAMP is ATP that is produced and utilized by all cell types (Idzko *et al*, 2014). In the healthy gut, ATP is involved in intestinal homeostasis, gastrointestinal motility, blood flow and synaptic transmission (Christofi, 2008). However, increased extracellular ATP concentrations resulting from tissue damage and trauma, excessive mechanical stimulation, shear stress in diseased blood vessels, cancer, inflammatory cells or a variety of acute or chronic diseases represent a pathogenic pro-inflammatory mechanism contributing to symptomatology (Idzko *et al*, 2014; Di Virgilio *et al*, 2018).

ATP signaling is complex and is mediated by purinergic receptors to which ATP either binds directly or as an enzymatically metabolized form, e.g., ADP or adenosine (Galligan, 2008). Purinergic

1 Department of Surgery, University of Bonn, Bonn, Germany
2 Faculty of Science, Department of Chemistry, Sultan Qaboos University, Muscat, Oman
3 Pharmaceutical Institute, Pharmaceutical & Medical Chemistry, University of Bonn, Bonn, Germany
4 Department of Anesthesiology, Wexner Medical Center, The Ohio State University, Columbus, OH, USA
*Corresponding author. Tel: +49 228 287 11007; E-mail: sven.wehner@ukbonn.de

receptors are classified broadly into ionotropic P2X, metabotropic P2Y and P1 receptor families. ATP, or other nucleotides can variably activate P2X and P2Y while adenosine activates metabotropic P1 receptors (Galligan, 2008). Recent studies demonstrated the expression of purinergic receptors on EGCs and their role in the regulation of gastrointestinal motility (McClain *et al*, 2014), neuron-to-glia communication (Gulbransen & Sharkey, 2009) and neuronal survival (Brown *et al*, 2016). We have identified P1, P2X and P2Y purinergic receptors in primary human EGCs in primary culture networks and the molecular identity of the reactive hEGC phenotype was revealed by LPS induction (Liñán-Rico *et al*, 2016). Recent progress in the field suggests that EGC may represent "a new frontier in neurogastroenterology and motility" (Ochoa-Cortes *et al*, 2016).

Overall, EGCs modulate motility, maintain gut homeostasis, and contribute to neuroinflammation in intestinal diseases and motility disorders (Gulbransen & Christofi, 2018). The latter includes postoperative gastrointestinal dysfunction and postoperative ileus (POI), a common clinical complication observed upon abdominal surgery that is characterized by a transient impairment of gastrointestinal (GI) function after surgery. POI is associated with increased morbidity in patients, and despite implementation of enhanced recovery protocols for elective colorectal surgery (Hedrick *et al*, 2018), no good treatment option exists. POI remains a huge health care problem costing billions of dollars in extended hospitalizations (Iyer *et al*, 2009). POI is well known to originate from postoperative neuronal dysregulation and is based on an inflammation of the muscularis externa (ME) (Wehner *et al*, 2007). Recently, we demonstrated that this postoperative inflammation involves EGC reactivity (Stoffels *et al*, 2014), but the molecular identity of the induction and trigger mechanisms of EGC activation are not fully understood.

Herein, we tested the hypothesis that surgical manipulation and trauma triggers ATP release that drives enteric gliosis and intestinal inflammation leading to impairment of motility in POI. We accessed the relevance of reactive EGC in human bowel specimens and the well characterized mouse model of acute posttraumatic bowel inflammation resulting in POI. By transferring the discovered mechanistic insights to a clinically relevant treatment option of selective purinergic receptor antagonism with ambroxol, a newly identified P2X2 antagonist "drug", we confirmed the potential therapeutic importance of ATP-activated EGCs for inflammation-induced POI that may be relevant to other motility disorders.

Results

Enteric glial cells respond to injury and inflammation and contribute to damage and regenerative processes (Grubišić & Gulbransen, 2017). Our investigation uncovered a purinergic pathway in reactive murine and human EGCs involved in the response to surgical trauma and inflammation.

ATP induction of a reactive EGC phenotype is dependent on a p38 MAPK signaling pathway

To evaluate enteric glia reactivity, we applied ATP, a trigger of purinergic signaling and an inflammatory mediator, to primary msEGC in culture. Our msEGC cultures were highly enriched in GFAP-expressing cells (mean, $86 \pm 2\%$, Fig EV1A) that also showed Sox10 and S100β immunoreactivity (Fig EV1B) representing the main EGC phenotype seen *in vivo* (Boesmans *et al*, 2015) and enriched glial marker expression (Appendix Fig S1A).

RNA-Seq analysis of the glial transcriptome identified the unique gene dysregulation profile induced by ATP in msEGCs. We found profound changes in msEGC gene expression with 2,027 up-regulated and 2,218 down-regulated genes after ATP stimulation (fold change ≥ 1.5; *P*-value: < 0.05, Fig 1A and principal component analysis shown in Fig EV1C). Therefore, ATP caused up-regulation in 10% and down-regulation in 11% of total glial transcriptome. Induction of genes, known to be expressed in direct response to ATP, including members of the regulator of calcineurin (*RCAN)* (Canellada *et al*, 2008) and *FOS* (Pacheco-Pantoja *et al*, 2016) gene families were confirmed by both RNA-Seq and qPCR (Figs 1H and EV1D). Gene ontology (GO) enrichment analyses demonstrated a general glial activation in ATP-treated msEGCs showing enriched genes for "ATP binding" and "glial proliferation" (Fig 1B and Appendix Fig S1B). Importantly, challenge with ATP induced genes involved in the regulation of cell motility, cytokine response genes (Fig 1C and D and Dataset EV1) and the mitogen-activated protein kinase (MAPK) pathways (Fig 1E and Dataset EV1) underlining the transition of msEGCs to an activated immune phenotype, also referred to as "*gliosis*". The term gliosis is commonly used to describe reactive astrocytes, the CNS counterparts to EGCs. Transcriptionally, gliosis is characterized by the up-regulation of a particular gene set, including, inflammatory response genes. To analyze the reactivity of the EGCs, we created a new GO term for gliosis based on all recent reports discussing CNS gliosis induced by inflammatory stimuli *in vivo* and *in vitro* (Zamanian *et al*, 2012; Hara *et al*, 2017; Liddelow *et al*, 2017; Fujita *et al*, 2018; Mathys *et al*, 2019; Rakers *et al*, 2019; Schirmer *et al*, 2019). Notably, we found that many gliosis-related genes are also regulated in ATP-activated msEGCs (Fig 1F, Appendix Fig S1C and Dataset EV1). Quantitative PCR confirmed the up-regulation of key markers of gliosis including *GFAP* and *NESTIN* (Fig 1G) as well as inflammatory mediators like *CXCL2* and *IL-6* (Fig 1I and J). The latter has been shown to be an important EGC-derived cytokine released upon IL-1β stimulation during surgical trauma (Stoffels *et al*, 2014). Our data confirmed a robust dose-dependent and statistically significant increase in the levels of IL-6, in both mRNA and protein (Fig 1J and K) upon ATP stimulation, indicating a prominent role of IL-6 in activated EGCs, subsequently making it a reliable marker in enteric gliosis and a central part of our further investigations. To efficiently analyze and describe the glia transformation to a reactive phenotype, we chose six targets; *NESTIN* and *GFAP*, two structural glia genes; *IL-6* and *CXCL2*, two inflammatory mediators and *FOSb* and *RCAN*, two transcriptional targets of ATP signaling, as a reliable gliosis marker panel developed from our in silico-based method to further evaluate purinergic enteric gliosis in subsequent studies.

Given that ATP treatment led to an activation of MAPK pathways (Fig 1E), we investigated the involvement of p38-MAPK, an important molecular switch of inflammatory pathways and astrogliosis in the central nervous system (Roy Choudhury *et al*, 2014). ATP was shown to elevate phospho-p38-MAPK protein (Fig EV1E) which is strongly localized in the nucleus of GFAP-positive msEGCs, absent in untreated msEGCs (Fig EV1F). Furthermore, ATP-induced IL-6 protein release was dose-dependently suppressed using the

Expanded View Figures

Figure EV1. ExATP induces gliosis in enteric glia cells.

A Histological analysis of EGC culture purity by quantification of EGCs and fibroblasts *in vitro*. Representative immunofluorescence image shows GFAP (violet)-positive EGCs and α smooth muscle actin (αSMA, green)-positive fibroblasts with DAPI as counterstain. Scale bar 50 μm.

B Representative immunofluorescence image of s100β (violet)- and Sox10 (green)-positive EGCs with DAPI as counterstain. Scale bar 10 μm.

C PCA plot of gene expression by ATP-treated and untreated EGCs. Blue circles represent ATP-treated EGC cultures, and white circles are matching controls; $n = 5–6$, respectively.

D Heat map of ATP-target genes, showing a collection of known target genes of ATP signaling ($n = 5–6$, msEGCs).

E Representative Western blots of phospho-p38-MAPK (pp38) and p38-MAPK (p38) in 1 h ATP-treated EGCs. Actin was used as loading control ($n = 3$, msEGCs).

F Representative images of GFAP (violet)- and phospho-p38-MAPK (pp38, green)-positive msEGCs with or without ATP treatment (100 μM) for 1 h. White arrows show pp38-positive (ATP-treated) or negative (untreated) EGCs. Scale bar is 10 μm.

G Effect of p38 inhibition on ATP-induced IL-6 release. Cells were treated with the p38-MAPK inhibitor SB203580 (1, 5, 10 μM) alone or together with ATP (100 μM) for 24 h. ELISA measurement of IL-6 in msEGCs supernatants ($n = 7–22$, msEGCs).

H Effect of p38 inhibition on ATP induced mRNA expression of gliosis markers in msEGCs. Cells were treated with SB203580 (10 μM) alone or together with ATP (100 μM) for 6 h ($n = 4$, msEGCs).

Data information: In (A), data are represented as percentage + SEM normalized to the total cell numbers, $n = 8$, msEGCs. In (G and H), data are represented as fold induction + SEM. Statistics were done in (G and H) by applying unpaired Student's *t*-test and one-way ANOVA with a subsequent Bonferroni test. * indicates significance to control, and # indicates significance to the ATP treatment with $*/^{\#}P < 0.05$, $^{\#\#}P < 0.01$, and $***/^{\#\#\#}P < 0.001$.

Source data are available online for this figure.

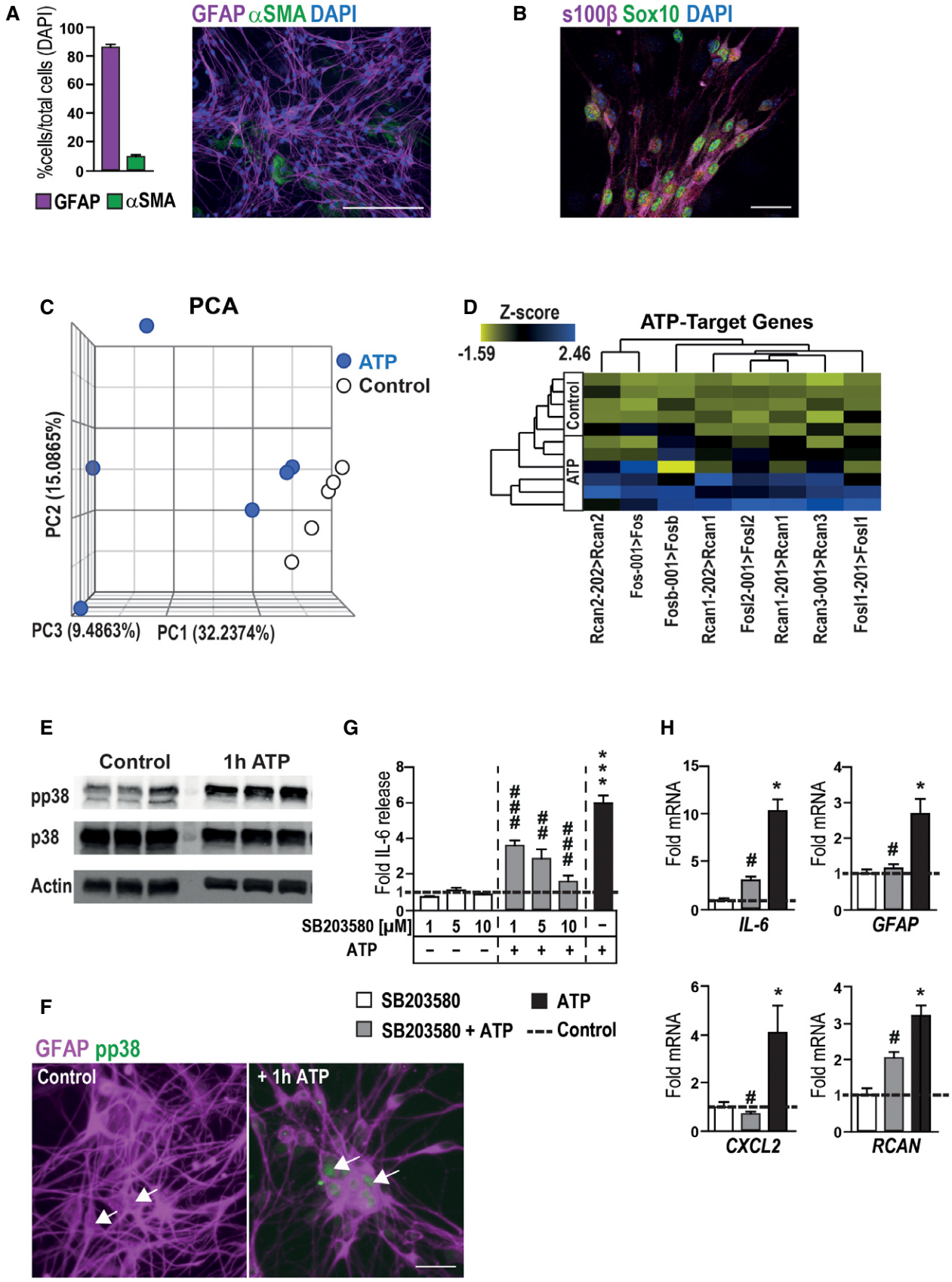

Figure EV1.

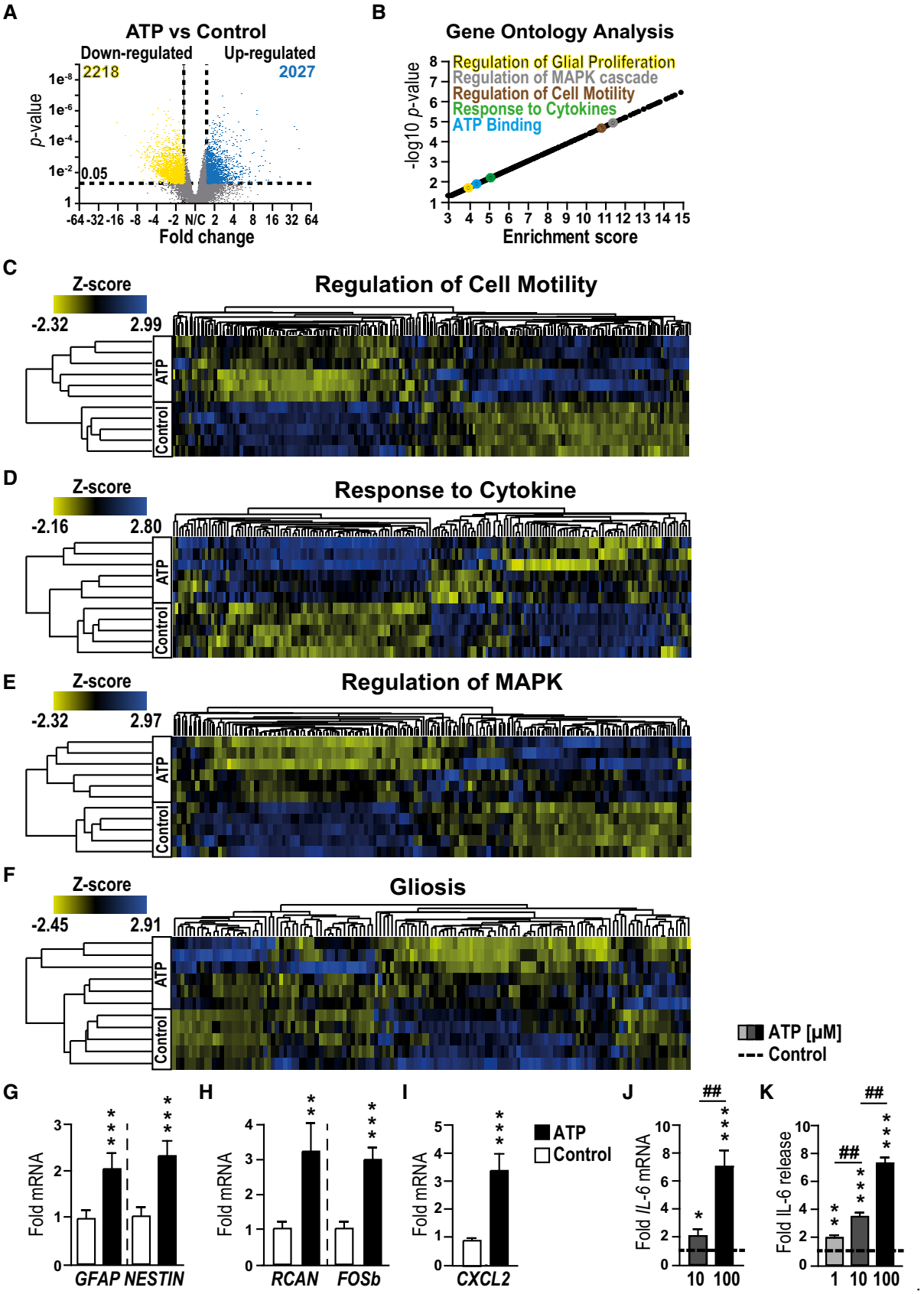
A
ATP vs Control
Down-regulated
2218
Up-regulated
2027
p-value
1e-8
1e-6
1e-4
1e-2
1
0.05
-64 -32 -16 -8 -4 -2 N/C 2 4 8 16 32 64
Fold change
B
Gene Ontology Analysis
Regulation of Glial Proliferation
Regulation of MAPK cascade
Regulation of Cell Motility
Response to Cytokines
ATP Binding
-log10 p-value
3 4 5 6 7 8 9 10 11 12 13 14 15
Enrichment score
C
Regulation of Cell Motility
Z-score
-2.32
2.99
ATP
Control
D
Response to Cytokine
Z-score
-2.16
2.80
ATP
Control
E
Regulation of MAPK
Z-score
-2.32
2.97
ATP
Control
F
Gliosis
Z-score
-2.45
2.91
ATP
Control
ATP [µM]
Control
G
Fold mRNA
GFAP
NESTIN
H
Fold mRNA
RCAN
FOSb
I
Fold mRNA
CXCL2
ATP
Control
J
Fold IL-6 mRNA
10
100
K
Fold IL-6 release
1
10
100

Figure 1.

Figure 1. ATP induces a gliosis in msEGCs.

A Volcano plot showing significantly regulated genes between control and ATP-treated msEGCs.
B Visual representation of GO terms associated with enriched genes in ATP-treated msEGCs compared to control.
C–F Heat maps of indicated GO terms in ATP-treated msEGCs compared to control.
G–I qPCR analysis of indicated gliosis genes in ATP-treated EGCs.
J qPCR analysis of *IL-6* in msEGCs that were treated for 6 h with ATP.
K IL-6 protein levels in supernatants from msEGCs collected after 24 h treatment with ATP.

Data information: In (A), data are shown as fold change > 1.5, *P*-value < 0.05; (n = 5 for untreated and n = 6 for ATP-treated EGCs). In (G–K), data are shown as fold change + SEM. (G–I) n = 6–9, msEGCs. (J) n = 4–9, msEGCs. (K) n = 6–18, msEGCs. In (A–I): ATP concentration was 100 μM. In (J, K), ATP concentration was 1, 10, or 100 μM. Statistics were performed by applying unpaired Student's *t*-test (G–K) and/or one-way ANOVA with a subsequent Bonferroni test (J and K). In (A) a limma-trend pipeline model and in (B) the Fishers exact test were performed. * indicates significance to control, and # indicates significance to ATP treatment with $^{*}P < 0.05$, $^{**/\#\#}P < 0.01$ and $^{***}P < 0.001$.

p38-MAPK-inhibitor SB203580 (Fig EV1G); qPCR confirmed the transcriptional reduction of IL-6 and other gliosis markers like *GFAP*, *CXCL2,* and *RCAN* (Fig EV1H).

Altogether, our data demonstrate that EGC gliosis can be triggered by ATP and induction of enteric gliosis depends on activation of the p38-MAPK signaling pathway.

P2X receptors mediate the ATP-triggered IL-6 release from msEGC

ATP can be enzymatically dephosphorylated and is, together with its metabolites ADP and adenosine, able to signal via multiple purinergic receptors. Those receptors, broadly divided into the P2X, P2Y and P1 classes (Galligan, 2008), make ATP's signaling repertoire rather complex. Many of these receptor subtypes have been identified in enteric glia, although their role in normal or disease states remains unclear (Ochoa-Cortes *et al*, 2016; Grubišić & Gulbransen, 2017; Gulbransen & Christofi, 2018).

As a starting point to pinpoint the purinergic receptor subtype(s) involved in enteric gliosis, we performed pharmacological screening with various agonists and antagonists of the purinergic signaling system. In our analysis, adenosine failed to stimulate IL-6 release from msEGCs, suggesting that the P1 class is not involved in the ATP-induced phenotype (Fig EV2A). Next, we tested the non-selective P2-class antagonist suramin that showed a blockade of ATP-dependent IL-6 release in a concentration-dependent manner (Fig 2A). Similar results were observed with PPADS, another P2 antagonist (Fig EV2B). Additionally, the degradation resistant ATP isoform and P2 agonist ATPγS, dose-dependently increased the IL-6 release with comparable or even stronger efficacy than ATP itself (Fig 2B) and induced the expression of established gliosis marker genes (data not shown). These findings indicated that ATP, but not ADP, AMP, adenosine or inosine are likely involved in ATP-induced EGC gliosis, thereby limiting the involved receptors to members of the P2 class.

Next, a P2 receptor mRNA expression profile in msEGC was determined in cells isolated from $GFAP^{cre}$ x $Ai14^{fl/wt}$ mice, expressing tdTomato in all $GFAP^{+}$ cells. Cells were either directly sorted upon ME digestion or sorted upon an intermediate cell culture period (Fig EV2D, F and G). Highly increased gene expression of *GFAP* and *Sox10* in $tdTomato^{+}$ compared to $tdTomato^{-}$ cells confirmed a successful enrichment of msEGC in both procedures (Fig EV2E). Comprehensive gene expression analyses of purinergic receptors in isolated EGC showed a distinct and comparable *ex vivo* and *in vitro* gene expression profile with three P2X receptor genes reaching the highest levels, exceeding not only P1 (Appendix Fig S2A and B), but also P2Y expression levels by several times. Accordingly, we directed our focus toward these P2X receptors expressed in enteric glia in the order P2X7 > P2X4 > P2X2 (Fig EV2H–K).

P2X2 receptors mediate the ATP-triggered EGC gliosis

P2X7 has been shown to be prominently involved in inflammatory processes. However, neither blockade of P2X7 receptors (Fig 2C) nor its activation with selective agonists (Appendix Fig S2C) could influence IL-6 release in EGCs. While we made the same observation with a P2X4 antagonist, P2X2 antagonism by PSB-1011 (Baqi *et al*, 2011) significantly decreased the ATP-triggered IL-6 release by around 40% (Fig 2C) and demonstrated a dose-dependent inhibitory effect (Fig EV2C). Another P2X2 antagonist (PSB-0711) tested at a lower ATP concentration supported the findings of PSB-1011 (Fig EV2C). PSB-1011 treatment also reduced the gliosis-triggered mRNA expression of *IL-6*, *GFAP,* and *RCAN* (Fig 2D). The absence of cleaved-caspase 3 in msEGCs and no changes in the MTT signal after PSB-1011 treatment confirmed that the reduced IL-6 release and gene expression was not due to apoptosis or reduced cell viability (Appendix Fig S2D and E). To reinforce the pharmacological data with a P2X2 antagonist, we were able to confirm a strong P2X2 immunoreactivity in msEGCs (Fig 2E) with a specific P2X2 signal (Appendix Fig S2F) and used a genetic approach with P2X2-siRNA to block the response. The efficiency of the P2X2 knockdown was confirmed on mRNA (Fig 2F) and protein level (Fig EV2L and M) and it reduced ATP-induced gliosis marker expression on mRNA (Fig 2F) and protein level (Fig 2G).

Together, these pharmacological and siRNA data prove that ATP activates a P2X2 receptor to trigger msEGC gliosis. P1, P2Y or any other highly expressed P2X receptors are not likely to be involved in ATP-triggered EGC gliosis.

Surgical bowel manipulation in a mouse model of postoperative ileus induces ATP-target gene expression and enteric gliosis

The next series of experiments were performed to investigate the role of ATP on EGC in an *in vivo* model of surgical intestinal manipulation (IM, Appendix Fig S3A) that induces enteric neuroinflammation in the ME and subsequently results in impaired gastrointestinal motility, clinically known as POI. Previous work of our group demonstrated that EGC are involved in POI pathogenesis (Stoffels *et al*, 2014). Hallmarks of POI are an increased IL-6 release (Wehner *et al*, 2005), the infiltration of blood-derived immune cells into the

Figure EV2. ATP-induced gliosis is mediated by p38-MAPK and P2X2-purinergic signaling.

A IL-6 release measurement by ELISA of IL-6 in msEGCs. Cells were treated adenosine (1 and 100 μM) or with ATP (100 μM) for 24 h; n = 14–16, msEGCs.

B Protein release measurement by ELISA of IL-6 in msEGCs. Cells were treated with P2 antagonist PPADS (5, 30 μM) alone or together with ATP (10 or 100 μM) for 24 h; n = 11–12, msEGCs.

C Protein release measurement by ELISA of IL-6 in msEGCs. Cells were treated with P2X2 antagonist PSB-1011 (0.2, 2, 20 μM) or PSB-0711 (0.2, 2, 20 μM) alone or together with ATP (10 μM) for 24 h; n = 9–13, msEGCs.

D Schematic overview of the isolation of msEGCs from small bowel muscularis externa of $GFAP^{cre}$-$Ai14^{fl/wt}$ mice: FACS-sorted $tdTomato^{+}$ msEGCs were either analyzed directly (*ME-tissue*) or in cultured msEGCs before tdTomato-FACS-sorting and further analysis; n = 3–6.

E Gene expression analysis by qPCR of *GFAP* and *Sox10* in msEGC cultures (n = 10) and mouse ME tissue (n = 10).

F, G Representative images of co-localization of GFAP (green) and $tdTomato^{+}$ msEGC (red) in the ME and in cultured EGCs. Scale bars 50 μm.

H–K qPCR analysis of P2-purinergic receptors in msEGCs isolated from ME (H, J; n = 3) or from cultured cells (I, K; n = 6), respectively.

L, M Representative Western blots of P2X2 in msEGCs transfected with siRNA-control or siRNA-P2X2 for 72 h together with an optical density measurement, see in M. Actin was used as loading control and normalization (n = 6, msEGCs).

Data information: In (A–C and E), data are represented as fold induction + SEM. In (H–K), data are represented as mean + SEM normalized to *GAPDH* expression. In (M), data are represented as optical density + SEM normalized to actin expression. Statistics were done by applying unpaired Student's t-test in (A-C, M and E) or both by unpaired Student's t-test and one-way ANOVA with a subsequent Bonferroni test in (B and C). * indicates significance to control, and # indicates significance to the ATP treatment with $^{\#}P < 0.05$, **/$^{\#\#}P < 0.01$, and ***/$^{\#\#\#}P < 0.001$.

Source data are available online for this figure.

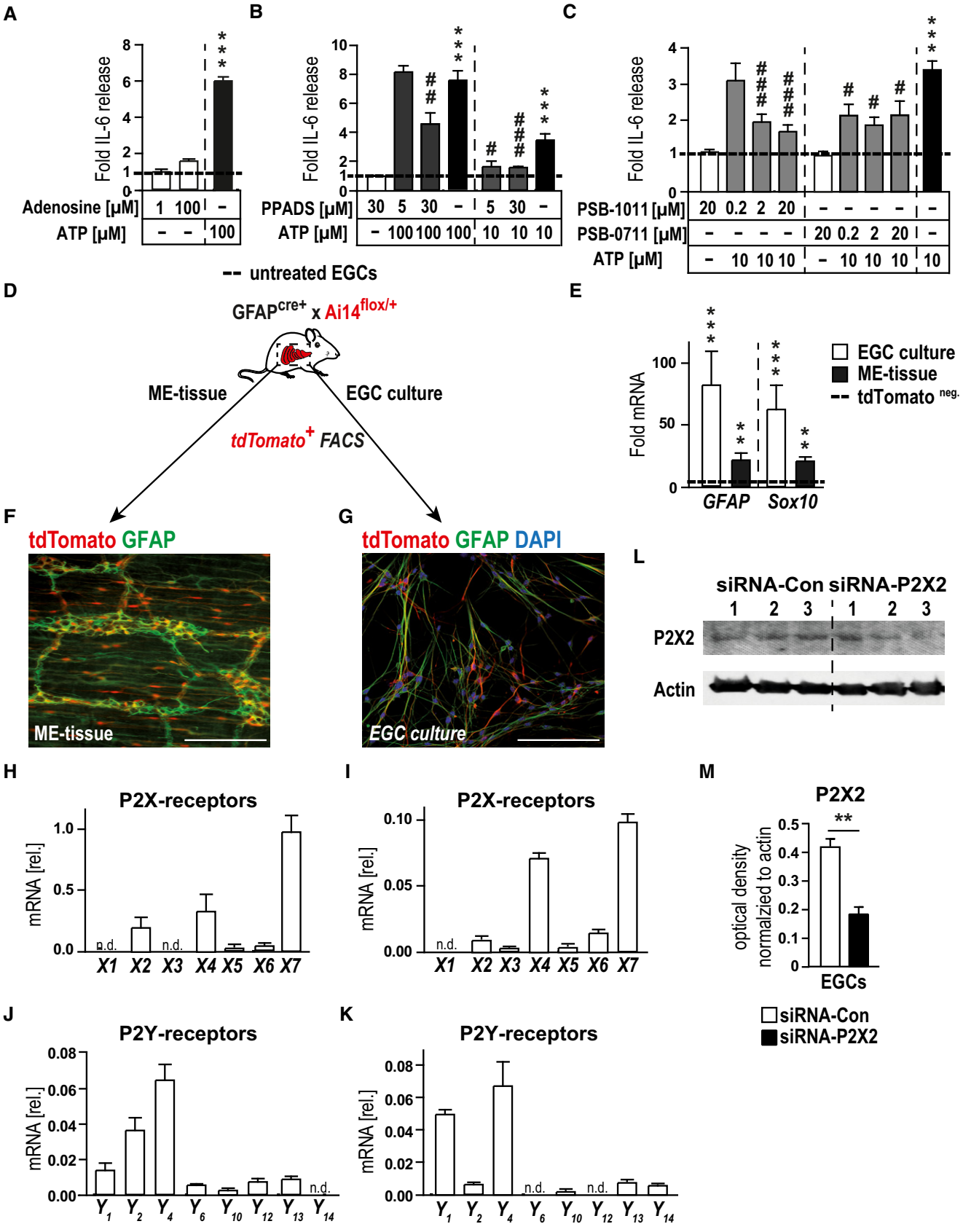

Figure EV2.

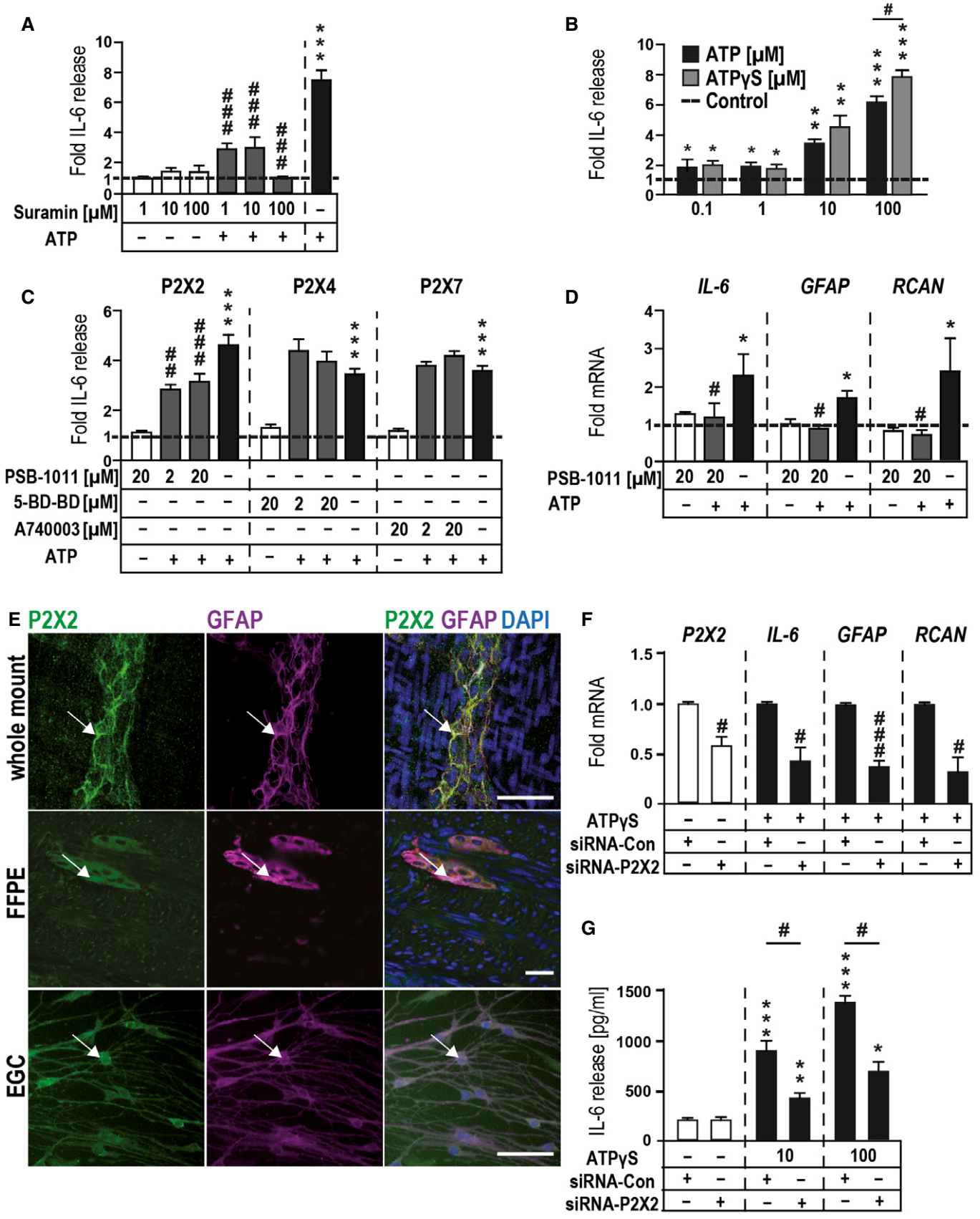
A
Fold IL-6 release
Suramin [µM] 1 10 100 1 10 100 –
ATP – – – + + + +
B
ATP [µM]
ATPγS [µM]
Control
Fold IL-6 release
0.1 1 10 100
C
P2X2 P2X4 P2X7
Fold IL-6 release
PSB-1011 [µM] 20 2 20 – – – – – – – – –
5-BD-BD [µM] – – – – 20 2 20 – – – – –
A740003 [µM] – – – – – – – – 20 2 20 –
ATP – + + + – + + + – + + +
D
IL-6 GFAP RCAN
Fold mRNA
PSB-1011 [µM] 20 20 – 20 20 – 20 20 –
ATP – + + – + + – + +
E
P2X2 GFAP P2X2 GFAP DAPI
whole mount
FFPE
EGC
F
P2X2 IL-6 GFAP RCAN
Fold mRNA
ATPγS – – + + + + + +
siRNA-Con + – + – + – + –
siRNA-P2X2 – + – + – + – +
G
IL-6 release [pg/ml]
ATPγS – – 10 100
siRNA-Con + – + – + –
siRNA-P2X2 – + – + – +

Figure 2.

Figure 2. ATP-induced gliosis is mediated by p38-MAPK and selective purinergic signaling.

A Effect of P2 receptor antagonism on ATP-induced IL-6 release. Cells were treated with P2 antagonist suramin (1, 10, and 100 μM) alone or together with ATP (100 μM) for 24 h.

B ATP-induced IL-6 release in msEGCs measured by ELISA. Cells were treated with the indicated concentrations of ATP and ATPγS for 24 h.

C Effects of P2X antagonists on ATP-induced IL-6 release. Cells were treated for 24 h alone or together with ATP (100 μM) in absence or presence of P2X2, P2X4, and P2X7 antagonists PSB-1011, 5-BD-BD, and A740003, respectively.

D P2X2 antagonism of ATP induced mRNA expression of *IL-6*, *GFAP,* and *RCAN* by qPCR in msEGCs. Cells were treated with the P2X2 antagonist PSB-1011 (20 μM) alone or together with ATP (10 μM) for 6 h.

E Representative confocal images of P2X2 (green)- and GFAP (violet)-positive msEGCs *in vivo* and *in vitro*. White arrows mark double-positive (white) cells. Scale bar 50 μm.

F P2X2-siRNA reduces P2X2-mRNA and dampens the gliosis gene expression after ATPγS (100 μM) treatment for 6 h.

G P2X2-siRNA reduces IL-6 release after ATPγS treatment (10, 100 μM) for 6 h.

Data information: In (A–D and F), data are shown as fold induction + SEM and (G) as IL-6 pg/ml + SEM, (A): n = 10–15, msEGCs; (B): n = 3–15, msEGCs; (C): n = 8–17, msEGCs; (D): n = 4, msEGCs; (E): n = 3–5, msEGCs; (F): n = 3–5, msEGCs; (G): n = 3–5, msEGCs. Statistics in (A–D, F, G) were performed by applying unpaired Student's t-test and/or one-way ANOVA with a subsequent Bonferroni test. * indicates significance to control, and # indicates significance to ATP treatment with $*/^{\#}P < 0.05$, $**/^{\#\#}P < 0.01$, and $***/^{\#\#\#}P < 0.001$.

manipulated ME, activation of resident macrophages, and subsequent impairment of gastrointestinal (GI)-transit (Appendix Fig S3B–D). To evaluate whether ATP is involved in the pathogenic mechanism of POI we first sought to measure ATP release in the peritoneal cavity in the lavage fluid to test whether it was elevated after IM. Here, we detected a time-dependent increase of ATP release after IM (Fig 3A). Simultaneously, gene expression of the ATP degrading enzymes *ENTPD2*, *ENTPD8* and *CD73* decreased, indicating a shift in postoperative ATP metabolism that may favor higher extracellular ATP levels that can further activate EGCs (Fig EV3A). In the early phases of POI, immunohistochemistry showed $FOSb^{+}/Sox10^{+}$ cells in enteric ganglia (Fig EV3B) and strong induction of *FOSb* and *RCAN* gene expression by qPCR (Fig 3H) indicating active ATP signaling in EGC.

RNA-Seq analysis on murine ME specimens isolated 3 or 24 h after IM or from naïve animals showed substantial differences in the gene expression patterns between all tested groups (Figs 3B and EV3C and Dataset EV2). GO enrichment indicated significant regulation of gliosis-associated genes 3 and 24 h after IM and showed similar activation patterns between the postoperative ME and ATP-treated msEGC cultures with alterations in "MAPK", "cell motility", "inflammatory response signaling" and genes involved in "glial development and proliferation" (Fig 3C). Using the previous gliosis gene panel, we confirmed the induction of enteric gliosis during POI progression as demonstrated by gene up-regulation (Fig 3D and Appendix Fig S3F). The strongest response occurred at IM24h. Moreover, a Venn diagram of the gliosis genes displays the similarity of regulated genes *in vivo* and *in vitro* with shared up and down-regulated genes (Appendix Fig S3E), indicating a similar glial activation pattern (Fig 3E). This POI phenotype was confirmed by qPCR showing elevated levels of our established gliosis marker: *GFAP*, *NESTIN*, *IL-6*, *CXCL2*, *FOSb,* and *RCAN* at 3 and 24 h after IM (Fig 3F–H) with a similar increase in IL-6 and CXCL2 protein levels (Fig EV3D).

Next, we analyzed glial proliferation and morphology by immunohistochemistry, defining two hallmarks of gliosis (Buffo *et al*, 2008; Pekny & Pekna, 2016). During disease progression within 24 h the $Ki67^{+}/Sox10^{+}$ EGC numbers increased up to 10-fold and the glial morphology gains a more complex "branchwood" in myenteric ganglia, revealing a postoperative change in the EGC phenotype (Figs 3I and EV3E). Furthermore, using once more the $tdTomato^{+}$-glia-reporter mouse in our POI model, we were able to gain further insights into the glial expression profile after IM (Fig 3J). Interestingly, the expression analysis of gliosis markers in EGC showed a different pattern, as previously seen in whole ME tissue after IM. In line with the proliferation, the highest gene expression was detected at IM24h with impressive levels of up-regulation in gliosis genes, including *GFAP*, *NESTIN*, *IL-6*, *CXCL2*, *RCAN,* and *FOSb* mRNA (Fig 3K–M). These results provided us with an *in vivo* insight of enteric gliosis during acute inflammation demonstrating again the immune response of EGCs in POI, a post-surgical intestinal inflammatory disease.

P2X2 antagonism by ambroxol prevents enteric gliosis

Our next series of experiments tested whether P2X2 antagonism can attenuate or prevent enteric gliosis and improve motility in our mouse model of POI. While the P2X2 antagonists PSB-1011 and PSB-0711 were not applicable for in *in vivo* usage the prospect of future clinical application of a P2X2 antagonist drug to regulate enteric gliosis and protect against developing POI, prompted us to perform a drug library screening to identify a clinically feasible P2X2 antagonist. In this drug screening, ambroxol (Appendix Fig S4A) was identified, as it showed a significant inhibition of ATP-induced calcium influx in 1321N1 astrocytoma cells transfected with the human P2X2 receptor (IC_{50}: 5.69 ± 1.06 μM), but not in cells transfected with P2X1, P2X3, P2X4, or P2X7 receptors (Fig EV4A). Thus, ambroxol was characterized as a potent P2X2 receptor antagonist with selectivity for P2X2 vs the other P2X receptor subtypes.

After confirming that ambroxol inhibited ATP-triggered gliosis marker up-regulation in msEGCs similar to the before used P2X2 antagonists without any apoptotic effects (Appendix Fig S4B–D), we tested ambroxol as a prophylactic treatment in the POI animal model (Fig 4A). Interestingly, we found a reduced postoperative ME gene expression of ATP-gliosis targets *FOSb* and *RCAN* (Fig 4B) as well as *GFAP* and *NESTIN* (Fig 4C) 3 and 24 h after surgery. In line with these findings, postoperative levels of IL-6 and CXCL2 (Figs 4D and EV4B) were also reduced. Simultaneously, other prototypical pro-inflammatory markers in POI, such as *CCL2* or *TNF-α,* were not affected by ambroxol treatment (Fig EV4C). Antagonism with ambroxol had a discrete influence on pro-inflammatory signaling pathways. To validate direct effects of the P2X2 antagonism on EGCs, we quantified glia proliferation at IM24h for both treatment groups. In comparison, ambroxol dampened the proliferation rate

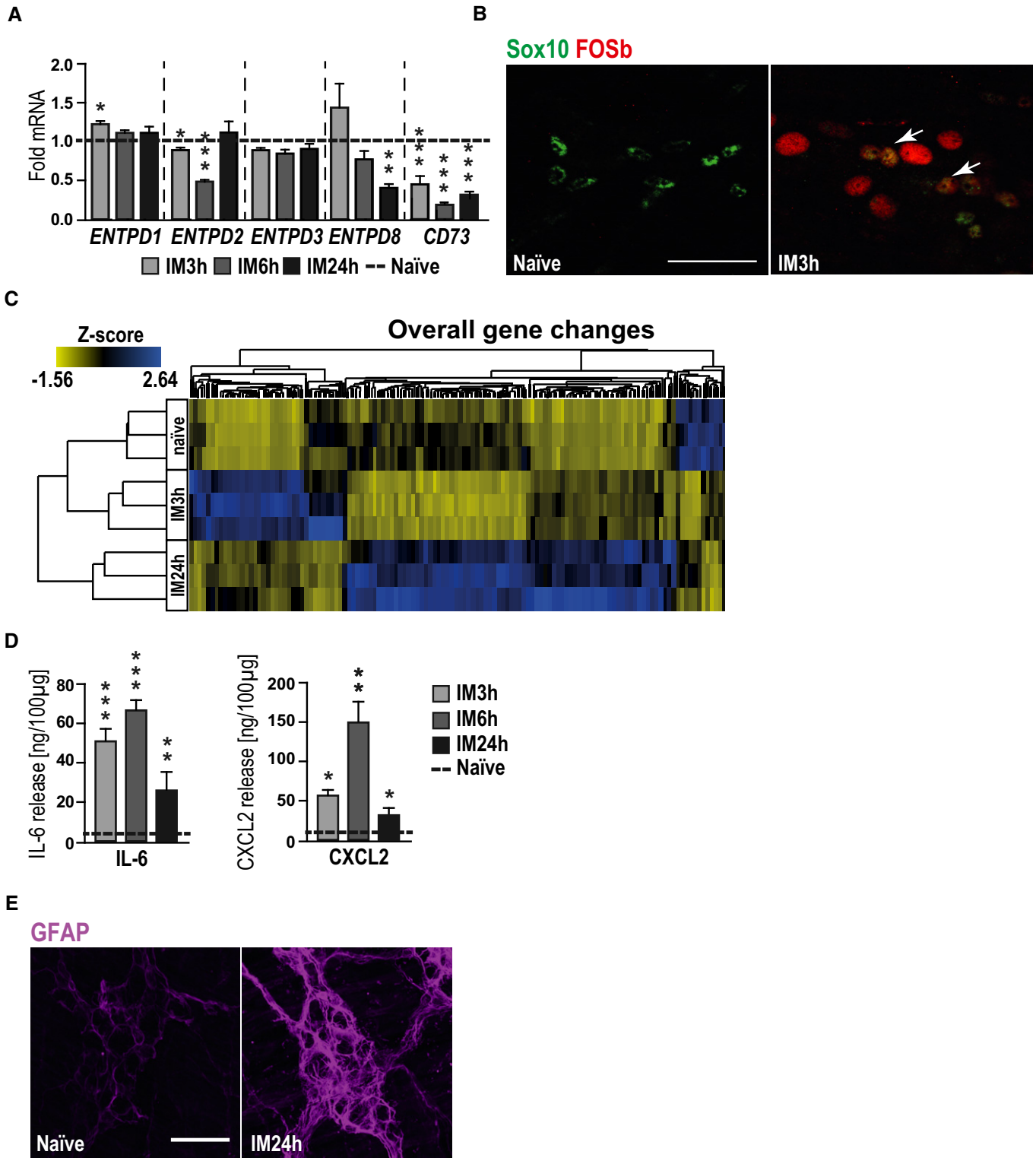
A
Fold mRNA
2.0
1.5
1.0
0.5
0.0
ENTPD1 ENTPD2 ENTPD3 ENTPD8 CD73
IM3h IM6h IM24h Naïve
B
Sox10 FOSb
Naïve
IM3h
C
Z-score
-1.56
2.64
Overall gene changes
naïve
IM3h
IM24h
D
IL-6 release [ng/100µg]
80
60
40
20
0
IL-6
CXCL2 release [ng/100µg]
200
150
100
50
0
CXCL2
IM3h
IM6h
IM24h
Naïve
E
GFAP
Naïve
IM24h

Figure EV3.

Figure EV3. Intestinal inflammation induces enteric gliosis.

A Gene expression of ectonucleotidases in POI mice at indicated disease stages.
B Representative confocal images of the activation marker FOSb (red)- and Sox10 (green)-positive EGCs (white arrows) in ganglia of intestinally manipulated mice (3 h after IM) or naïve mice. Scale bar 50 μm.
C Heat map of all significantly changed genes from POI mice at different disease stages and naïve mice; $n = 3$ for each group.
D Protein release analysis by ELISA of IL-6 or CXCL2 in POI mice at indicated disease stages.
E Representative confocal images of gliosis marker GFAP (violet)-positive EGCs in ganglia of intestinally manipulated mice (24 h after IM) or naïve mice. Scale bar 50 μm.

Data information: In (A), data are represented as fold change + SEM; $n = 7$, POI mice. In (D), data are represented as IL-6/CXCL2 protein in 100 μg tissue + SEM; $n = 7$, POI mice. Statistics were done in (A, D) by applying unpaired Student's *t*-test. * indicates significance to control with $^{*}P < 0.05$, $^{**}P < 0.01$, and $^{***}P < 0.001$.
Source data are available online for this figure.

Figure EV4. P2X2 signaling inhibition by ambroxol improves clinical symptoms in POI.

A Concentration-dependent inhibition of ATP-induced calcium influx in 1321N1-astrocytoma cells with recombinant expression of the human P2X2 receptor. ATP was used in a concentration corresponding to its EC80 value (1 μM). An IC_{50} value for ambroxol of 5.69 ± 1.06 μM ± SEM was determined. Inhibitory potency of ambroxol at P2X receptor subtypes X1-X7. At an initial test concentration of 20 μM, only the P2X2 receptor subtype was blocked by more than 50% indicating P2X2 receptor selectivity and no significant receptor inhibition was detected (n.d.) with other P2 receptor subtypes ($n = 6$).
B Protein release analysis by ELISA of IL-6 and CXCL2 in POI mice treated with ambroxol or vehicle at 24 h.
C Gene expression analysis by qPCR of *CCL2* and *TNFα* in POI mice treated with ambroxol or vehicle at IM3h and 24h; $n = 6$ POI mice.
D Representative FACS gating strategy of infiltrating cells in the ME of mice treated with ambroxol or vehicle. CD45, Ly6C, and CX3CR1 were used to distinguish resident macrophages ($CD45^{+}/Ly6C^{-}/CX3CR1^{+}$), infiltrating monocytes ($CD45^{+}/Ly6C^{+}/CX3CR1^{-}$), and infiltrated monocyte-derived macrophages ($CD45^{+}/Ly6C^{+}/CX3CR1^{+}$); $n = 3$–5 POI mice per group.
E Representative confocal images of GFAP (violet)-positive EGCs and CX3CR1-GFP-positive macrophages (green, white arrows) around ganglia of intestinally manipulated mice treated with ambroxol or vehicle (24 h after IM). Scale bar 50 μm.

Data information: In (B), data are represented as IL-6 or CXCL2 protein in 100 μg tissue + SEM; $n = 6$ POI mice. In (C), data are represented as fold change + SEM. Statistics were done in (B and C) by applying unpaired Student's *t*-test and one-way ANOVA with a subsequent Bonferroni test. * indicates significance to sham animals, and $^{\#}$indicates significance between vehicle and ambroxol treatment with $^{\#}P < 0.05$, $^{**}/^{\#\#}P < 0.01$, and $^{***}P < 0.001$.
Source data are available online for this figure.

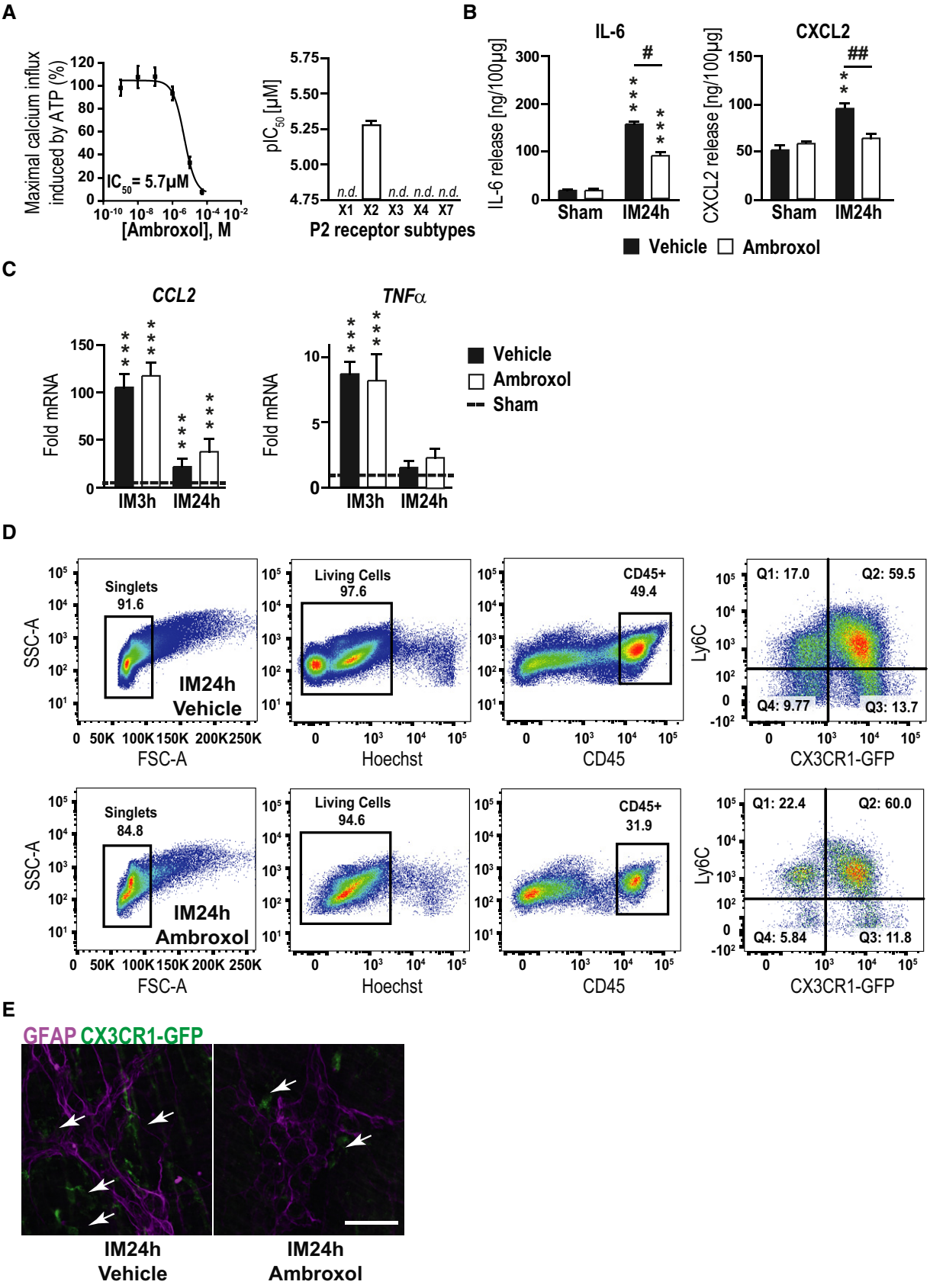
A
Maximal calcium influx induced by ATP (%)
IC50 = 5.7µM
[Ambroxol], M
pIC50 [µM]
n.d.
X1 X2 X3 X4 X7
P2 receptor subtypes
B
IL-6
CXCL2
IL-6 release [ng/100µg]
CXCL2 release [ng/100µg]
Sham
IM24h
Vehicle
Ambroxol
C
CCL2
TNFα
Fold mRNA
IM3h
IM24h
Vehicle
Ambroxol
Sham
D
Singlets 91.6
Living Cells 97.6
CD45+ 49.4
Q1: 17.0
Q2: 59.5
Q4: 9.77
Q3: 13.7
IM24h Vehicle
SSC-A
FSC-A
Hoechst
CD45
Ly6C
CX3CR1-GFP
Singlets 84.8
Living Cells 94.6
CD45+ 31.9
Q1: 22.4
Q2: 60.0
Q4: 5.84
Q3: 11.8
IM24h Ambroxol
E
GFAP CX3CR1-GFP
IM24h Vehicle
IM24h Ambroxol

Figure EV4.

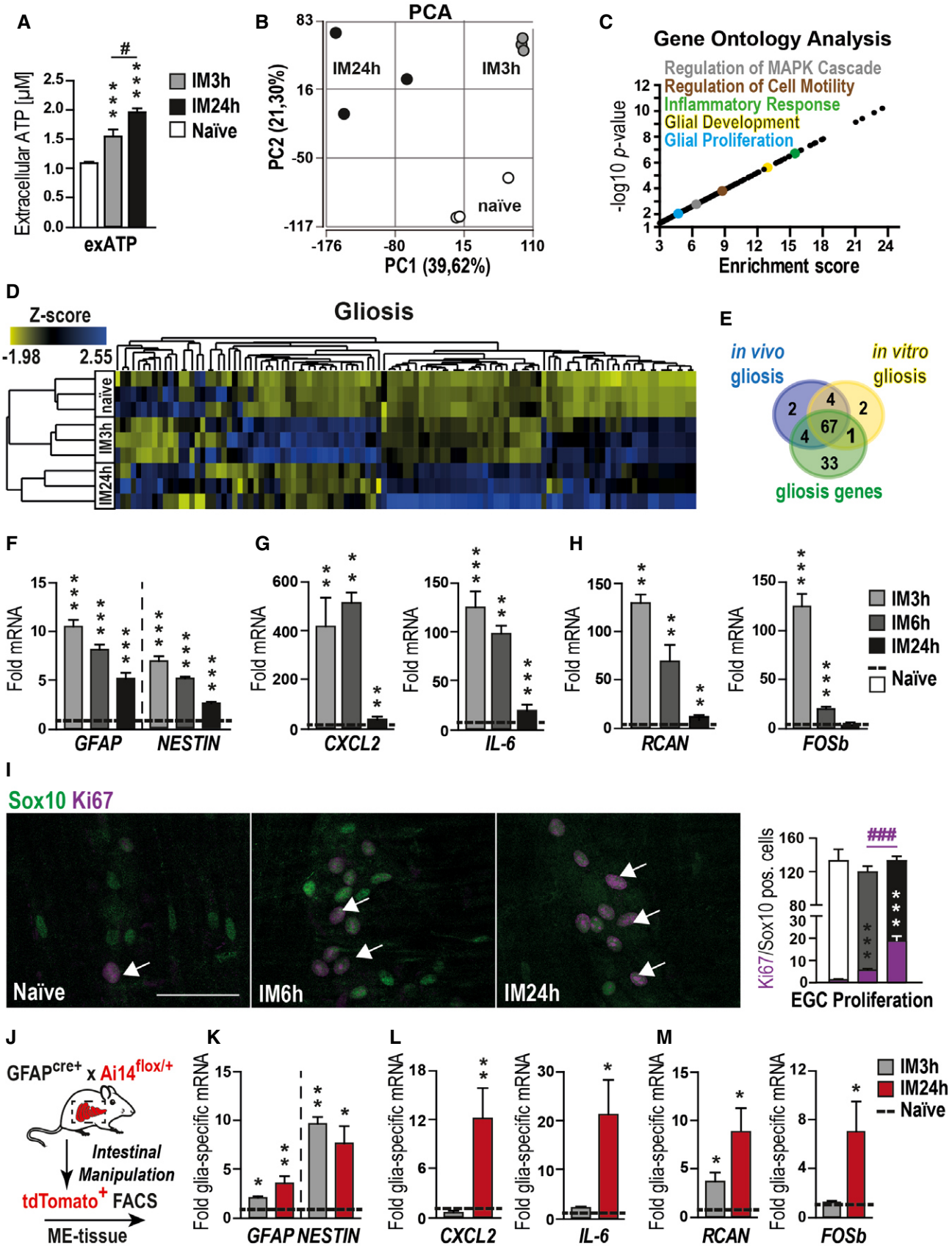
A
Extracellular ATP [µM]
exATP
IM3h
IM24h
Naïve
B
PCA
PC2 (21,30%)
PC1 (39,62%)
IM24h
IM3h
naïve
C
Gene Ontology Analysis
Regulation of MAPK Cascade
Regulation of Cell Motility
Inflammatory Response
Glial Development
Glial Proliferation
-log10 p-value
Enrichment score
D
Z-score
-1.98
2.55
Gliosis
naïve
IM3h
IM24h
E
in vivo gliosis
in vitro gliosis
gliosis genes
F
Fold mRNA
GFAP
NESTIN
G
CXCL2
IL-6
H
RCAN
FOSb
IM3h
IM6h
IM24h
Naïve
I
Sox10 Ki67
Naïve
IM6h
IM24h
Ki67/Sox10 pos. cells
EGC Proliferation
J
GFAPcre+ x Ai14flox/+
Intestinal Manipulation
tdTomato+ FACS
ME-tissue
K
Fold glia-specific mRNA
GFAP NESTIN
L
CXCL2
IL-6
M
RCAN
FOSb
IM3h
IM24h
Naïve

Figure 3.

Figure 3. An ATP-induced enteric gliosis in postoperative bowel inflammation.

A ATP measurement at the indicated postoperative time points in peritoneal lavages of mice that underwent intestinal manipulation (IM) or were naïve.

B PCA plot of gene expression from POI mice at different disease stages and naïve mice; $n = 3$ for each group.

C Visual representation of *P*-value ($-\log_{10}$) against fold enrichment of GO terms associated with enriched genes in mice that underwent IM.

D Heat map of enriched genes connected with GO term gliosis in mice that underwent IM or in naïve animals.

E Venn diagram of gliosis genes expressed *in vitro* and *in vivo*.

F–H qPCR analysis of indicated gliosis marker in mice that underwent IM ($n = 7$).

I Histological analysis of EGC proliferation *in vivo*. Representative confocal images and quantification show Sox10 (green)- and Ki67 (violet)-positive EGCs (white arrows) in the small bowel muscularis externa at naïve, IM6h and 24 h. Scale bar 50 μm.

J Experimental setup for glia-specific RNA analysis. GFAP-cre$^+$ × Ai14-floxed mice underwent IM, and small intestine ME was digested and sorted for tdTomato by FACS to provide glia-specific RNA for qPCR measurements seen in (K-M).

K–M qPCR analysis of indicated gliosis markers in td + glia cells from naïve mice and mice that underwent IM ($n = 5$–7, POI mice).

Data information: In (A), data are represented as mean + SEM; $n = 7$–12, POI mice. In (F–H and K–M), data are represented as fold induction + SEM. In (I), data are represented as mean of double-positive cells per total Sox10-positive cells + SEM; 9–20 whole mount specimens per conditions; $n = 8$, POI mice per group. Statistics were performed by applying unpaired Student's *t*-test (A, C, F–I, K–M). In (C), the Fisher's exact test was performed. * indicates significance to naïve animals, and # indicates significance to the indicated time point with */#$P < 0.05$, **$P < 0.01$, and ***/###$P < 0.001$.

by almost 50%, indicating reduced glial activation during POI (Fig 4E). Finally, we examined a modulatory effect on immune cell infiltration by ambroxol and discovered that ambroxol significantly reduced the number of monocytes (CD45$^+$/Ly6C$^+$/CX3CR1$^-$) and resident (CD45$^+$/Ly6C$^-$/CX3CR1$^+$) or monocytes derived (CD45$^+$/Ly6C$^+$/CX3CR1$^+$) macrophages (CD45$^+$/Ly6C$^{+/-}$/CX3CR1$^+$) in the manipulated ME at 3 h (~ 70% reduction, MPO-histology) and 24 h (~ 50% reduction, MPO-histology and FACS; Figs 4F and G, and EV4D). In addition, histological analysis of the localization of CX3CR1$^+$-cells in context to EGCs showed fewer macrophages surrounding ganglia in the ambroxol-treated group (Fig EV4E). Functionally, ambroxol led to a significant improvement in postoperative gastrointestinal transit time (geometric center ambroxol: 6.8 ± 0.4 vs vehicle: 4.1 ± 0.4, Fig 4H). These data indicated that P2X2 antagonism is an effective strategy to attenuate gliosis to improve clinical symptoms in the mouse POI model and makes ambroxol a relevant P2X2 antagonist drug candidate for future therapeutic approaches.

Human enteric gliosis is blocked by P2X2 antagonism

To determine whether findings in the mouse are translatable to human, we carried out additional experiments in human specimens from surgical patients who underwent pancreatectomy, a procedure in which intense IM is an unavoidable consequence, enabling the collection of small bowel specimen at two different intraoperative time points (Fig 5A). In this series of experiments, we analyzed the expression of gliosis markers and ATP-dependent genes in ME samples of jejunum specimens. Similar to our previous analyses, we performed RNA-Seq analysis in a limited set of patient ME samples to gain more insight into the glial activation status. The PCA showed a distinct difference between the early and late samples (Fig EV5A) and the consecutive GO analysis pointed to a similar activation pattern as previously shown in the murine system with enriched genes for "MAPK cascade", "regulation of cell motility", "immune response" and "glial proliferation" (Fig 5B, Dataset EV3). Consistently, the gliosis panel showed differential gene expression between late and early collected specimens, providing evidence for inflammation-induced enteric gliosis during surgery (Fig 5C). A Venn diagram comparing the murine and the human enteric gliosis genes visualized 37 shared genes between these species (Fig 5D). To strengthen the RNA-Seq data, we validated our gliosis marker panel in 13 more patients. Compared to the foremost collected ME specimens, specimens collected at the later time point showed a strong increase in IL-6-protein (Fig EV5B) and mRNA levels (Fig EV5C) in concordance with the induction of other gliosis markers (Fig EV5C).

To determine the involvement of glia in inflammatory processes occurring after IM in patients, we subjected human EGCs, isolated and purified from single human myenteric ganglia dissociated from ME specimen (hEGC) to ATP and ATPγS *in vitro* stimulation according to our established protocols (Ochoa-Cortes *et al*, 2016). Both treatments induced a more than 12-fold increase in IL-6 protein release after 6 h, which dropped to a still significant two-fold induction after 24 h (Fig 5E). Interestingly, naïve hEGC exhibited a dose-dependent increase in IL-6 release upon stimulation with ARL67156, a selective ectonucleoside triphosphate diphosphohydrolase (ENTPDase) inhibitor (Fig 5F) indicating that ATP levels are tightly regulated by ENTPDases and that their inhibition creates a high-enough endogenous ATP concentration to activate hEGC *in vitro*.

As purinergic activation in hEGC showed similarities to the mouse data, we also investigated human P2X2 signaling. Immunofluorescence microscopy revealed strong P2X2-immunoreactivity in s100β$^+$ hEGCs in myenteric ganglia in intact surgical tissues (Figs 5G and EV5D) and more than 80% of cultured hEGCs (Fig EV5E). Additionally, P2X2 antagonism by PSB-1011 blocked the ATP-triggered IL-6 release in hEGCs (Fig 5H). The antagonistic specificity for the human system of our tested P2X2 inhibitors was also confirmed in HEK293-P2X2 sniffer cells expressing a mutant human P2X2 receptor resistant to desensitization. This process leads to continuous elevation of free intracellular calcium levels upon ATP stimulus in a dose-dependent manner (Appendix Fig S5A). ATP-induced calcium levels were independently reduced by the P2X2 antagonists PSB-1011 (Fig 5I) and PSB-0711 (Fig 5J and Appendix Fig S5B) verifying that these antagonists are able to block responses mediated via hP2X2 *in vitro*. Based on the promising results of ambroxol as a therapeutic in mice, we utilized it further in an experimental approach in hEGC. Ambroxol treatment inhibited dose-dependently ATP-induced calcium influx in HEK293-P2X2 sniffer cells (Appendix Fig S5C) and blocked ATP-triggered IL-6 release in hEGC (Fig 5K).

Together, these data confirm the relevance of ATP-triggered P2X2 signaling in hEGC gliosis and identify ambroxol as a novel

P2X2 antagonist in the human system. To finally confirm the role of ambroxol in human specimens, freshly isolated human full-thickness jejunal samples, underwent an *ex vivo* mechanical alteration in the presence or absence of ambroxol (Fig EV5F). All relevant gliosis genes followed up in this study, were significantly down-regulated in the ambroxol-treated extracorporally manipulated jejunal ME

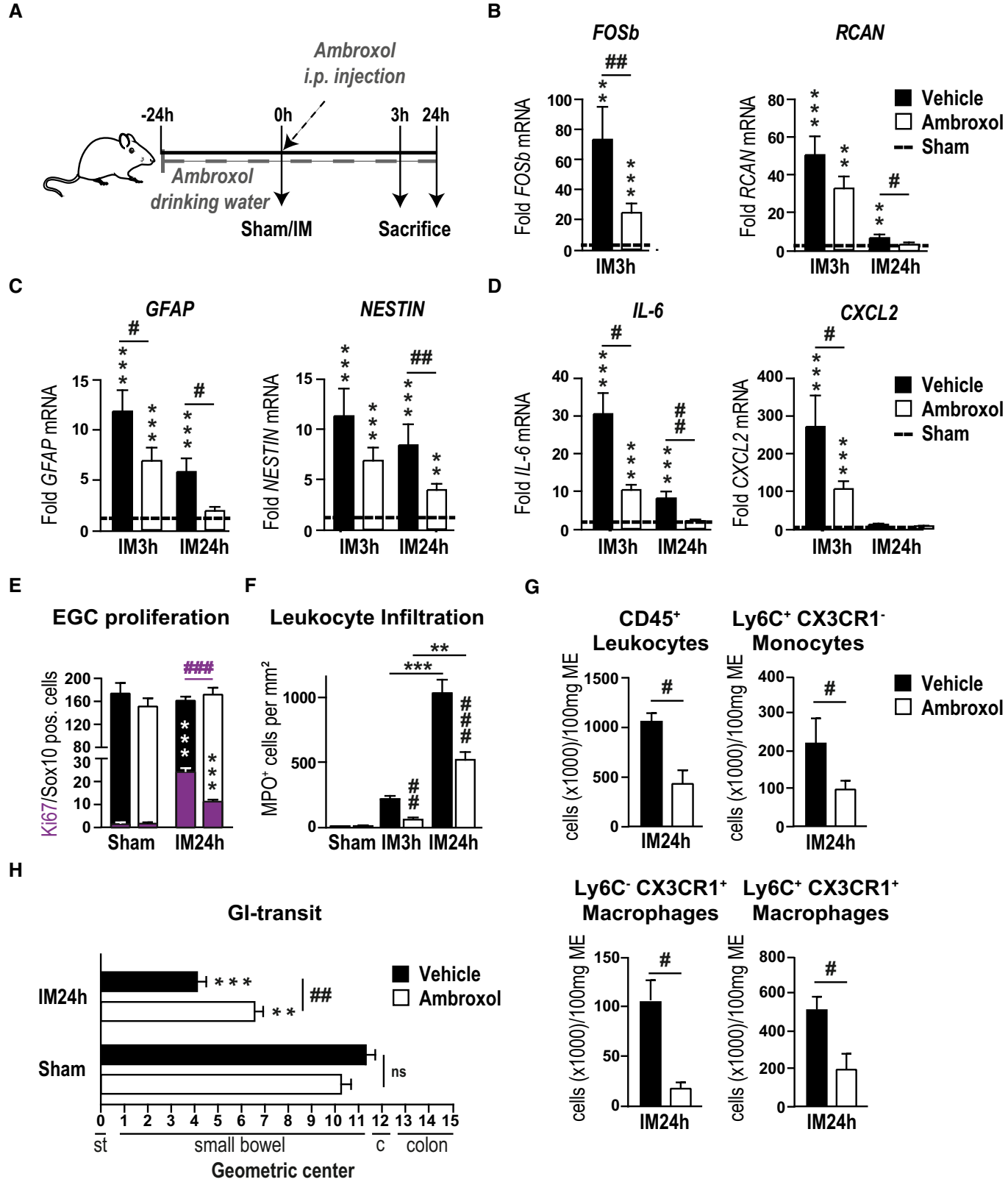

Figure 4.

Figure 4. The novel P2X2 antagonist ambroxol prevents IL-6 release from EGCs.

A Ambroxol treatment scheme. Mice were treated with ambroxol or vehicle and underwent a sham operation (laparotomy) or intestinal manipulation (IM). Small bowel muscularis externa (ME) was isolated and analyzed 3 or 24 h after surgery.

B–D Postoperative gene expression analyses of indicated gliosis marker in the ME.

E Histological analysis of EGC proliferation by quantification of Ki67 (violet)- and Sox10 -positive EGCs at IM24h. Mice were treated as seen in (A).

F Histological counting of infiltrating myeloperoxidase (MPO)-positive leukocytes in the postoperative ME (n = 6–8).

G FACS analysis of infiltrating cells in the ME of mice treated with ambroxol or vehicle. CD45, Ly6C, and CX3CR1 were used to distinguish resident macrophages ($CD45^+/Ly6C^-/CX3CR1^+$), infiltrating monocytes ($CD45^+/Ly6C^+/CX3CR1^-$) and infiltrated monocyte-derived macrophages ($CD45^+/Ly6C^+/CX3CR1^+$).

H Postoperative *in vivo* GI transit measurement in mice treated with ambroxol or vehicle.

Data information: In (B–D), data are represented as fold change + SEM vs the sham groups (n = 6–8, POI mice per group). In (E), data are represented as mean of double-positive cells per total Sox10-positive cells + SEM; six whole mount specimens per conditions; n = 11 mice per IM group and n = 3 per sham group. In (F), data are presented as mean + SEM MPO^+ cells/mm^2 small intestine ME tissue. In (G), data are presented as cells per 100 mg ME tissue + SEM n = 3–5 POI mice per group. In (H), data are presented as mean + SEM; n = 12 mice per group. Statistics were performed by applying unpaired Student's t-test and one-way ANOVA with a subsequent Bonferroni test (B-H). * indicates significance compared to sham animals, and # indicates significance between vehicle and ambroxol treatment with $*/^{\#}P < 0.05$, $**/^{\#\#}P < 0.01$, and $***/^{\#\#\#}P < 0.001$.

(Fig 5L–N) indicating that ambroxol treatment is sufficient to attenuate trauma-induced gliosis.

While future studies, particularly clinical trials, must prove if ambroxol also prevents surgery-induced gliosis in patients, our *ex vivo* human data corroborate its role in dampening gliosis and ATP-driven inflammatory processes and provide proof of concept for translatability of findings on P2X2 from mice to humans.

Discussion

In this study, we aimed to define and better understand the reactive glial phenotype of the enteric nervous system induced by ATP and clarifying its role, beneficial or adverse, concerning inflammation-induced motility disorders, and in particular POI. In this regard, it has been previously shown by our group that activated EGCs contribute to the disease progression in POI (Stoffels *et al*, 2014). However, to this day, the significance of glial reactivity in the pathogenic mechanism remained unclear. We provide evidence to support the hypothesis that surgical manipulation and trauma triggers ATP release that drives enteric gliosis and intestinal inflammation leading to impaired motility and POI.

In general, reactive changes of glial cells are a hallmark of "gliosis" that is known to be induced in the CNS by numerous pathological conditions including traumatic (Andersson *et al*, 2011) or ischemic insults (Roy Choudhury *et al*, 2014) and in neurodegenerative diseases (Pekny & Pekna, 2014). As a predefined-GO term for gliosis did not exist and in order to achieve a more integrative description of a reactive EGC phenotype, we created a non-exclusive list of published genes regulated in reactive astrogliosis (Zamanian *et al*, 2012; Hara *et al*, 2017; Liddelow *et al*, 2017; Fujita *et al*, 2018; Mathys *et al*, 2019; Rakers *et al*, 2019; Schirmer *et al*, 2019). Based on this gene panel, we analyzed EGCs *in vitro* and *in vivo* and termed the glial activation "enteric gliosis". We targeted ATP as a potential trigger mechanism of enteric gliosis. EGCs have been shown to respond to ATP *in situ* (Gulbransen & Sharkey, 2009; Boesmans *et al*, 2019) and *in vitro* (Gomes *et al*, 2009; Boesmans *et al*, 2013) and ATP is a potent trigger of innate immune responses. Increased release of ATP has been observed in multiple acute and chronic inflammatory diseases, including autoimmune diseases (Carta *et al*, 2015), sepsis (Csóka *et al*, 2015), sterile insults (Cauwels *et al*, 2014) and colitis (Grubišić *et al*, 2019). Thus, we hypothesized that increased ATP levels, which occur as a result of tissue damage to the intestine (Galligan, 2008) or extensive gut manipulation during the operation, might trigger an inflammatory response and activation of EGCs. Our comprehensive RNA-Seq analysis confirmed profound transcriptional changes in EGCs upon direct ATP stimulation visualized by a separation of control and ATP-treated EGCs in a PCA plot. The differences in the severity of the activation by purinergic stimuli most likely come from batch differences of primary cells. Moreover, we detected an EGC profile that is comparable to a reactive astrocyte, the CNS counterpart of EGCs (Grubišić & Gulbransen, 2017). In agreement with the up-regulation of genes involved in MAPK signaling, the main switch in astrogliosis (Roy Choudhury *et al*, 2014), p38-MAPK is also induced in ATP-stimulated EGCs and its blockade completely abrogates enteric gliosis. Interestingly, another of our studies revealed the importance of p38-MAPK (Wehner *et al*, 2009) in intestinal inflammation, although its role as a signaling pathway in enteric gliosis had not been investigated before. From these data, we conclude that ATP stimulation induces phenotypical changes in EGCs that are most precisely described by the term enteric gliosis.

So far, ATP's role in gliosis has not been investigated in detail, but previous studies had speculated on the possible involvement of purinergic receptors (Burda & Sofroniew, 2014). Herein, we identified P2X2, one of the highest expressed P2X receptors in murine and in human EGCs (Liñán-Rico *et al*, 2016), as the purinergic receptor responsible for triggering enteric gliosis upon ATP stimulation. In humans and mice, we confirmed by immunohistochemistry, that hEGCs and glia in the intact human myenteric plexus strongly express the P2X2 receptor. While P1 receptors, in general, could be excluded from the list of involved receptors, other P2 receptors that have not been tested in our study either because of their low expression or due to a lack of selective antagonist/agonist could potentially be involved in ATP-triggered gliosis. However, P2X7, the purinergic receptor with the highest expression in msEGCs and the third highest in hEGC (Liñán-Rico *et al*, 2016) that is also expressed on virtually all immune cell types (Di Virgilio *et al*, 2017), is not involved in the ATP-triggered reactive EGC phenotype.

In contrast, ATP signaling induces neuronal death in models of colitis, another intestinal inflammatory disease, by activating a complex involving P2X7 receptors, Pannexin-1, Asc and caspases (Gulbransen *et al*, 2012). It appears that the glial P2X2 gliosis mechanism is unique to postsurgical inflammation. Interestingly, others

Figure EV5. ExATP induces gliosis in human enteric glia.

A PCA plot of gene expression from patient specimens at two different time points of the surgery; $n = 3$ for early and late specimens.

B IL-6 protein measurement in human surgical specimens collected during a pancreaticoduodenectomy at an early and a late time point of surgery. Samples were provided on ice directly from the operation room, and *muscularis externa* (ME) was separated from the lamina propria mucosae; $n = 9$ human patients.

C Gene expression analyses of gliosis marker in human surgical specimens collected during a pancreaticoduodenectomy at an early and a late time point of surgery. The late specimens' mRNA level show an up-regulation of gliosis genes.

D Immunofluorescence microscopy revealed P2X2 expression (green) in a majority of $s100\beta^+$ (violet) hEGCs in intact myenteric ganglia of the human colon. White arrows mark double-positive cells. Scale bar 50 μm.

E Immunofluorescence microscopy revealed P2X2 expression (green) in a majority of $s100\beta^+$ (violet) hEGCs in culture. DAPI counterstained nuclei. Quantification of double-positive cells showed that 75% of cultured hEGCs express P2X2 (marked with +). Scale bar 50 μm.

F Schematic workflow on the collection and processing of surgical specimens collected during a pancreaticoduodenectomy. Samples were provided directly from the operation room in oxygenated Krebs–Henseleit buffer and were mechanically activated *ex vivo*. Immediately after activation, specimens were incubated for 3 h with or without ambroxol (20 μM). Finally, ME was isolated and further processed for qPCR analysis.

Data information: In (B), data are represented as IL-6 protein in 100 μg tissue; $n = 9$ human patients. In (C), data are represented as fold change; $n = 13$ human patients. In (E), data are represented as the percentage of $P2X2^+/s100\beta^+$ cells + SEM; $n = 16$, hEGCs. Statistics were done by applying unpaired Student's *t*-test in (B, C). * indicates significance to control with $^*P < 0.05$, $^{**}P < 0.01$, and $^{***}P < 0.001$.

Source data are available online for this figure.

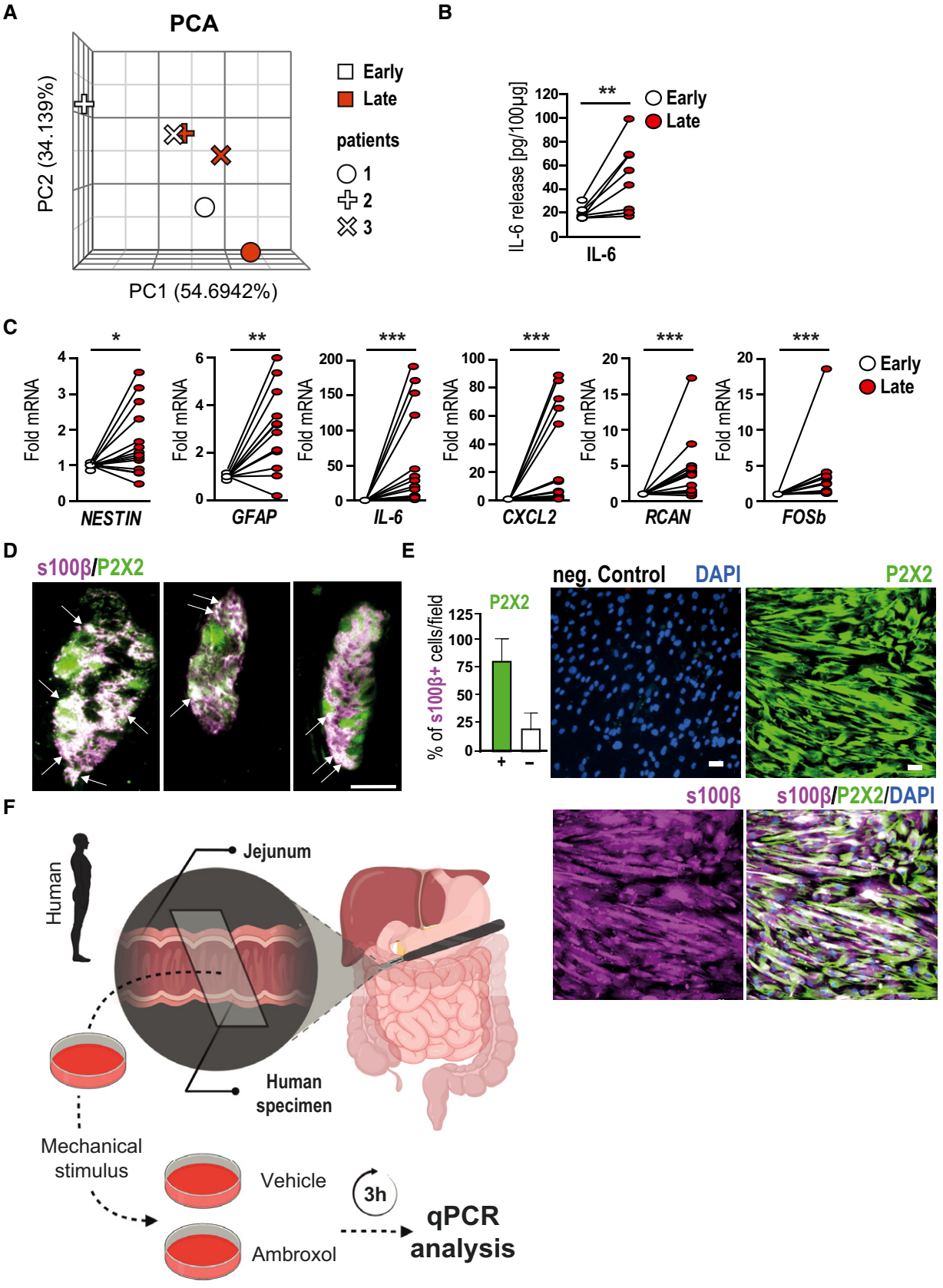
A
PCA
PC2 (34.139%)
PC1 (54.6942%)
Early
Late
patients
1
2
3
B
IL-6 release [pg/100µg]
**
Early
Late
IL-6
C
Fold mRNA
*
**
***
NESTIN
GFAP
IL-6
CXCL2
RCAN
FOSb
Early
Late
D
s100β/P2X2
E
P2X2
% of s100β+ cells/field
neg. Control
DAPI
P2X2
s100β
s100β/P2X2/DAPI
F
Human
Jejunum
Human specimen
Mechanical stimulus
Vehicle
Ambroxol
3h
qPCR analysis

Figure EV5.

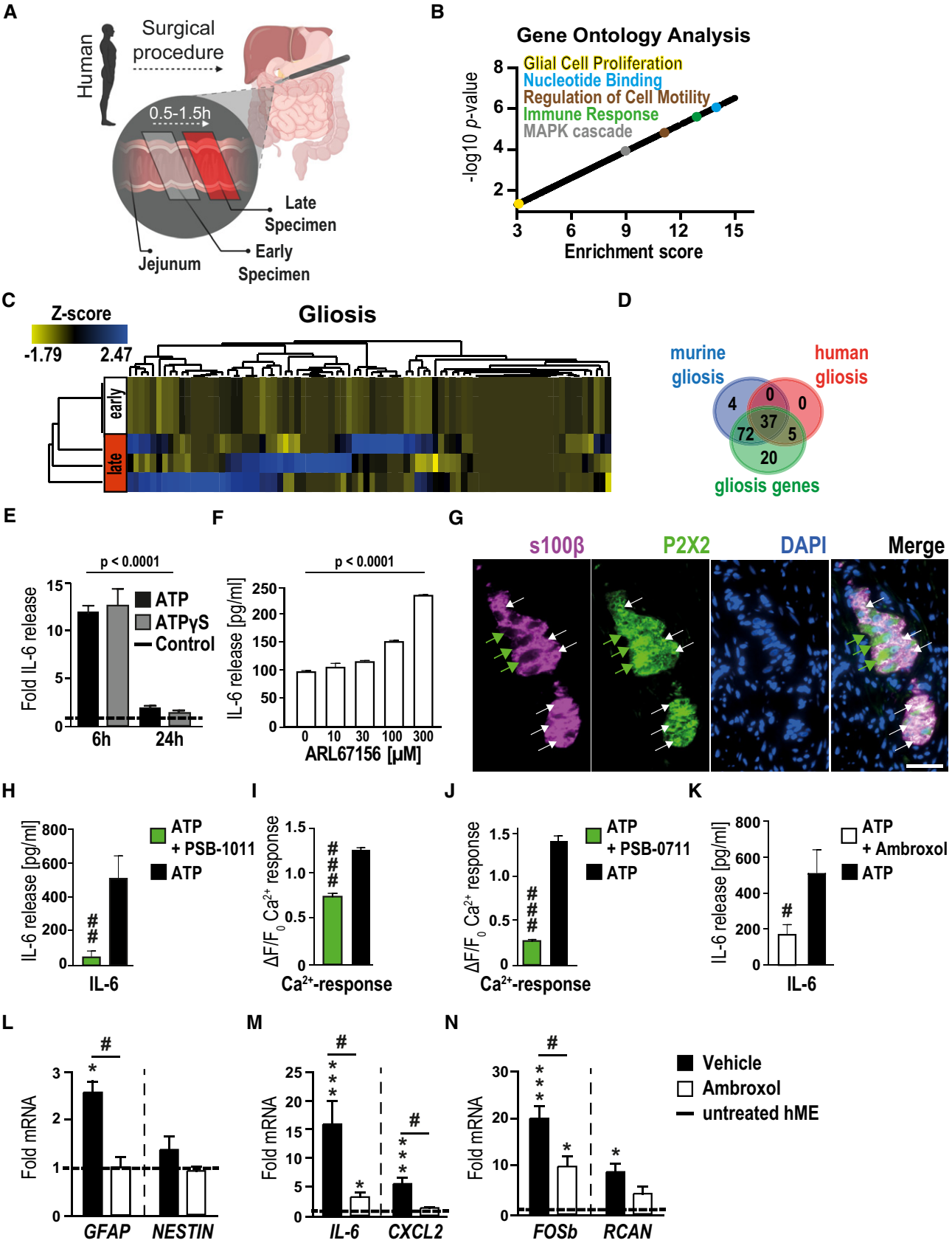
A
Human
Surgical procedure
0.5-1.5h
Late Specimen
Early Specimen
Jejunum
B
Gene Ontology Analysis
Glial Cell Proliferation
Nucleotide Binding
Regulation of Cell Motility
Immune Response
MAPK cascade
-log10 p-value
Enrichment score
C
Z-score
-1.79
2.47
Gliosis
early
late
D
murine gliosis
human gliosis
gliosis genes
4
0
0
37
72
5
20
E
p < 0.0001
Fold IL-6 release
ATP
ATPγS
Control
6h
24h
F
p < 0.0001
IL-6 release [pg/ml]
ARL67156 [μM]
G
s100β
P2X2
DAPI
Merge
H
IL-6 release [pg/ml]
ATP + PSB-1011
ATP
IL-6
I
ΔF/F0 Ca2+ response
Ca2+-response
J
ΔF/F0 Ca2+ response
ATP + PSB-0711
ATP
Ca2+-response
K
IL-6 release [pg/ml]
ATP + Ambroxol
ATP
IL-6
L
Fold mRNA
GFAP
NESTIN
M
Fold mRNA
IL-6
CXCL2
N
Fold mRNA
FOSb
RCAN
Vehicle
Ambroxol
untreated hME

Figure 5.

Figure 5. ATP induces gliosis in hEGC.

A Schematic workflow on the collection and processing of surgical specimens collected during a pancreaticoduodenectomy. Samples were provided on ice directly from the operation room, and the ME was separated from lamina propria mucosae.

B Visual representation of *P*-value ($-\log_{10}$) against fold enrichment of GO terms associated with enriched genes in patient specimen that underwent IM.

C Heat map of enriched genes connected with GO term gliosis in patient specimens that underwent IM at two time points: early and late; $n = 3$ human patients.

D Venn diagram of gliosis genes expressed in human (red) and murine (blue) ME tissue.

E IL-6 protein release in hEGC cultures upon stimulation with ATP (200 μM) or ATPγS (100 μM) after 6-h and 24-h treatment ($n = 4$–6, hEGCs).

F IL-6 protein release in hEGC cultures upon stimulation with NTPDase inhibitor ARL67156 at indicated concentrations; $n = 4$–6, hEGCs.

G Immunofluorescence microscopy revealed P2X2 expression (green) in a majority of $s100\beta^+$ (violet) hEGCs in intact myenteric ganglia of the human colon. White arrows mark double-positive glia cells, and green arrows mark P2X2-positive neurons. Scale bar, 50 μm.

H Effect of the P2X2 antagonism on ATP-induced IL-6 release. ELISA measurement of IL-6 in hEGCs upon treatment with P2X2 antagonist PSB-1011 (20 μM) alone or together with ATP (200 μM) treated for 24 h ($n = 6$, hEGCs).

I PSB-1011 (20 μM) treatment inhibited ATP-triggered calcium responses in HEK cells transfected with P2X2. Data are represented as $\Delta F/F_0$ + SEM; $n = 102$ HEK cells.

J The P2X2 receptor antagonist PSB-0711 (20 μM) nearly abolished the ATP-triggered calcium response in HEK cells transfected with P2X2. $n = 219$ HEK cells.

K Ambroxol blocks ATP-induced IL-6 release in hEGCs; protein release measurement by ELISA of IL-6 in hEGCs. Cells were treated with ATP (200 μM) alone or together with ambroxol (20 μM) for 24 h; $n = 6$, hEGCs.

L–N qPCR analysis of several gliosis and ATP-target genes in the mechanically manipulated surgical specimens incubated in the presence or absence of ambroxol (20 μM) ($n = 7$, 4 human patients).

Data information: In (E, F, H, and K), data are represented as mean IL-6 release + SEM. In (I and J), data are represented as $\Delta F/F_0$ + SEM. In (L–N), data are shown as fold induction + SEM. Statistics were performed by applying unpaired Student's *t*-test and one-way ANOVA with a subsequent Bonferroni test (E and F, H–N), and in (B), the Fisher's exact test was performed. * indicates significance compared to controls, and # indicates significance to ATP treatment or between vehicle and ambroxol with $*/^{\#}P < 0.05$, $^{\#\#}P < 0.01$, and $***/^{\#\#\#}P < 0.001$.

have shown that chronic morphine induced constipation associated with intestinal inflammation involves a glial ATP-connexin signaling pathway (Bhave *et al*, 2017).

In order to analyze the role of enteric gliosis *in vivo* and to access its value as a therapeutic target (Ochoa-Cortes *et al*, 2016; Gulbransen & Christofi, 2018), we chose our established *in vivo* model of intestinal surgical manipulation (IM) that leads to development of POI (Wehner *et al*, 2009; Stoffels *et al*, 2014). Our comprehensive gliosis marker analysis, immune-activation pathway analysis, morphological, proliferation and cytokine release analysis in response to ATP activation allowed us to conclude that abdominal surgery induces enteric gliosis. In line, detection of increased ATP levels in the peritoneal cavity, which is either actively or passively released following cellular damage (Carta *et al*, 2015), clearly indicate that ATP release is part of the postoperative inflammatory cascade (Cauwels *et al*, 2014) and can principally act as a DAMP and an inducer of gliosis. The simultaneous decrease in several nucleotide-catabolizing ecto-enzymes, including CD73 and ENTPD8, shifts the cellular metabolic machinery in favor of elevated extracellular levels of ATP in surgically manipulated bowel to reach levels that are sufficient to induce enteric gliosis *in vivo* via P2X2.

Although the cellular source of ATP remains unknown, the immediate increase in the early phase of POI indicates that it is initially released from resident cells than from infiltrating leukocytes that extravasate into the ME in later stages of POI (Stein *et al*, 2018). These resident cells could be enteric neurons (Gomes *et al*, 2009) or resident macrophages (Riteau *et al*, 2012), as both lie in proximity to EGCs and contain large amounts of ATP that can be actively or passively released upon damage or during inflammation (Oliveira *et al*, 2014). Additionally, the reactive EGCs themselves are another likely local source of ATP release, and we have previously shown that LPS induction of primary hEGCs in culture elevates ATP release by several fold (Liñán-Rico *et al*, 2016). Interestingly, we observed that fewer macrophages surround enteric ganglia upon ambroxol treatment in the POI model. However, it remained unclear if this is due to a general reduction in macrophages or due to a specific reduction in glial activation. Of interest, a recent story revealed direct effects of activated EGCs on macrophage function (Grubišić *et al*, 2020) substantiating our observation that gliosis is connected to monocyte/macrophage infiltration. Notably, we analyzed previous POI samples of $CCR2^{-/-}$ mice published by Stein *et al* (2018) to address the potential role of the infiltrating immune cells in ATP release and glial activation during the later time points in POI. Intriguingly, glial activation was reduced in $CCR2^{-/-}$ POI mice, indicating that the immune infiltrate maintains enteric gliosis after manifestation of POI and it is likely that this mechanism also depends on ATP release (Appendix Fig S4F). However, as $CCR2^{-/-}$ mice did not show improved motility 24 h after surgery but showed elevated—but reduced—gliosis marker expression, we interpret that the initial gliosis induced by resident cell activation alone is sufficient to trigger POI. Interestingly, $CCR2^{-/-}$ mice show disturbances in the resolution of POI at later time points (72 h) (Farro *et al*, 2017), supporting our hypothesis that the infiltrating monocytes contribute to the regenerative gliosis.

In humans, the same set of gliosis marker genes as in mice was time-dependently up-regulated in jejunal ME tissues of patients who underwent pancreaticoduodenectomy, a surgical procedure that unavoidably involves strong intestinal manipulation. After gut manipulation and trauma in patients, we detected a clear increase in gliosis markers in the late stages of the operation indicating that our murine data on enteric gliosis are translatable to humans. Therefore, we conclude that gliosis is a conserved cross-species mechanism regulating the EGC inflammatory response. Moreover, hEGCs exhibited a comparable receptor expression profile and the same functional dependence on P2X2 as msEGC. Further evidence for a conserved enteric gliosis mechanism across different species originates from our recent *in vitro* studies in hEGCs describing an immune phenotype upon LPS and interferon-γ signaling (Liñán-Rico *et al*, 2016) similar to the one seen in msEGC in the present study.

Our findings lead to a new question: What is the purpose of this conserved gliosis; is the induction necessary for regenerative mechanisms or could an initial blockade lead to a less severe disease

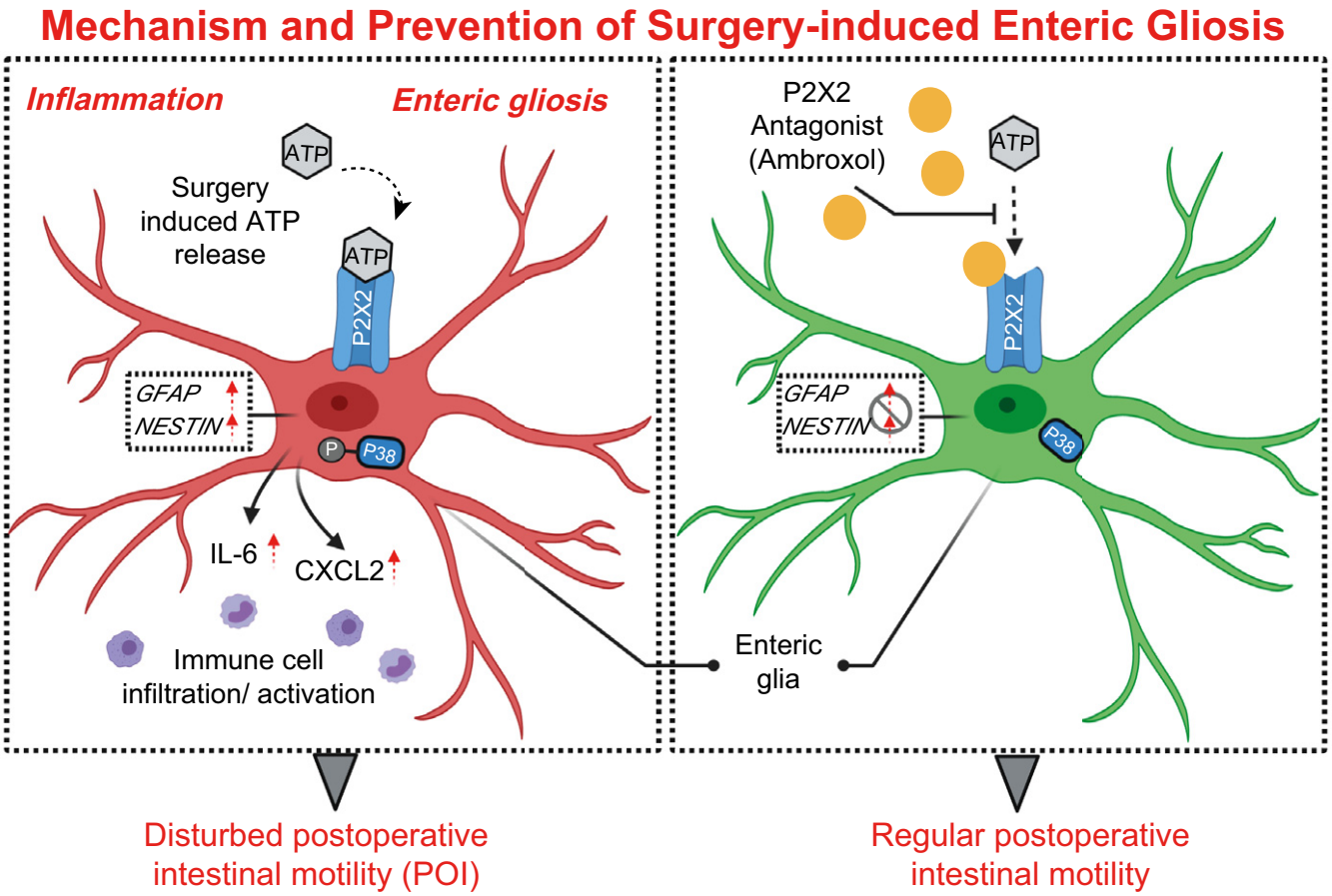

Figure 6. Purinergic mechanism of enteric gliosis in postoperative ileus.

Gut surgical manipulation and trauma cause inflammation and increase ATP release that activates P2X2 receptors on enteric glia and induces a reactive glial phenotype termed "enteric gliosis". In the context of inflammation, ATP activates a P2X2/p38 MAPK pathogenic signaling pathway associated with an increased expression in gliosis markers GFAP, NESTIN, and the release of cytokines like IL-6 and CXCL2. Enteric gliosis exacerbates neuroinflammation, contributes to immune cell infiltration and that causes postoperative motility disturbances and POI. P2X2 antagonism by ambroxol prevents the ATP-triggered enteric gliosis and protects against POI.

outcome? In the CNS, gliosis is targeted by therapeutic approaches in neurodegeneration (Colangelo *et al*, 2014) to minimize for example neuronal apoptosis (Livne-Bar *et al*, 2016). In the ENS, there is no evident view on gliosis yet. The general glial activation/proliferation could serve as damage control and/or regeneration boost by assisting the ENS to regenerate faster after an inflammatory strike, but on the other side targeting EGCs in gastrointestinal immune-driven diseases and motility disorders could also be a new and promising therapeutic approach (Gulbransen & Christofi, 2018). Incidentally, the strong up-regulation of glial proliferation in manipulated mice indicated that EGC do participate in ENS regeneration in later stages of POI as already described in colitis-induced chronic intestinal inflammation (Belkind-Gerson *et al*, 2017), in addition to their immune-modulatory role by, e.g., cytokine release. However, to clarify the potential regenerative role of ATP-induced gliosis in POI, future studies need to focus on the regeneration stages of this disorder, i.e., 72 h and later after surgery. (Stein *et al*, 2018).

An internal compound library screening revealed that the antagonist potency of the oral drug ambroxol is comparable to the experimental organic P2X2 antagonist (Baqi *et al*, 2011) and is suitable for an *in vivo* investigation. Interestingly, ambroxol's immune-modulatory effect is already documented in the clinical treatment of airway inflammation, but its mode of action is still unclear (Beeh *et al*, 2008). Indeed, perioperative ambroxol treatment reduced the postoperative gliosis marker increase and EGC proliferation. It also prevented infiltration of monocytes/macrophages and motility impairment in our POI model. The down-regulation of ATP-target genes *FOSb* and *RCAN* implied a direct antagonistic effect on purinergic activation by ambroxol. Importantly, ambroxol prevented induction of *IL-6* and *CXCL2* but no other inflammatory genes, including *TNFα* and *CCL2*. This demonstrates that ambroxol does not function as a general anti-inflammatory drug as previously speculated (Beeh *et al*, 2008) but instead selectively modulates ATP-triggered pathways in EGCs. In support of ambroxol's immune-modulatory action, a recent study using a P2X2/X3 antagonist (gefapixant), showed a down-regulation of airway inflammation, the main target of ambroxol (Zhang *et al*, 2020), upon ambroxol treatment in a cough hypersensitivity syndrome model. Nevertheless,

ambroxol is also known to affect potassium and calcium channels of neurons (Weiser, 2008) that modulate neuronal activity (Magalhaes *et al*, 2018). As motility is tightly regulated by these channels (Rao, 2020), we cannot exclude any enteric neuronal modulation by ambroxol in parallel to its impact on glial P2X2-dependent signaling.

Given that the purinergic system is a prominent player in inflammation (Burnstock, 2020), selective P2X2 antagonism might be of particular therapeutic relevance in POI or perhaps other gut inflammatory or immune-driven motility disorders. This is supported by animal studies which showed improved clinical symptoms in ambroxol-treated mice in models of neurodegeneration (Migdalska-Richards *et al*, 2016), neuropathic pain (Hama *et al*, 2010) and LPS-induced acute lung injuries (Su *et al*, 2004). Notably, all these diseases lead to activated purinergic signaling (Burnstock, 2020). Finally, the effects of reduced enteric gliosis in humans were supported by *ex vivo* manipulation of jejunal samples from surgical patients demonstrating a direct inhibition of a mechanically induced gliosis-related gene induction by ambroxol. In line with these findings, previous clinical trials done over 30 years ago with ambroxol also revealed an alleviated motility in the ambroxol-treated group (Germouty & Jirou-Najou, 1987) and ongoing clinical studies for Parkinson's Disease (*NCT02941822; (*Silveira *et al*, 2019*)*) highlight the potential of ambroxol in treating a neurodegenerative disease with a connection to gut inflammation (Villumsen *et al*, 2019).

Although we used a broad panel of different techniques, we would like to mention that a final validation of our findings would require the use of a glial-specific P2X2 knock out mouse. Furthermore, some of our analyses are based on whole ME tissue samples including multiple non-glia cell types. Even though we validated most of these findings in enriched EGC cultures, a contribution of other cell types *in vivo* cannot completely be excluded. Nevertheless, future studies should aim to test the clinical efficacy of P2X2 antagonism for the treatment of POI in humans and immune-driven inflammatory diseases, including motility disorders. Ambroxol or yet to be developed highly selective P2X2 antagonists with the implementation of the power of medicinal chemistry and congener drug development (Burnstock *et al*, 2017) are suggested to represent novel candidate drugs in the pipeline.

Subsumed, we provide evidence that ATP is able to induce a reactive EGC phenotype, increased inflammation and enteric gliosis *in vivo* in a P2X2 dependent manner. This mechanism proved to represent a pathogenic mechanism of POI, since ambroxol, a novel P2X2 antagonist, was shown to have efficacy in protecting against postoperative bowel inflammation and motility disturbances in mice and humans. Our "purinergic hypothesis of enteric gliosis in POI" is illustrated in Fig 6.

Materials and Methods

Murine EGC cultures

Primary enteric glia cell cultures were obtained by sacrificing C57BL/6 mice 8–16 weeks of age, extracting the small intestine and cleansing it with 20 ml of oxygenated Krebs–Henseleit buffer (126 mM NaCl; 2.5 mM KCl: 25 mM $NaHCO_3$; 1.2 mM NaH_2PO_4; 1.2 mM $MgCl_2$; 2.5 mM $CaCl_2$, 100 IU/ml Pen, 100 IU/ml Strep and 2.5 μg/ml Amphotericin). The small bowel was cut in 3–5 cm long segments and kept in oxygenated ice-cold Krebs–Henseleit buffer. Each segment was then drawn onto a sterile glass pipette and the ME was stripped with forceps to collect muscle tissue for further digestion steps. After centrifugation (300 *g* for 5 min), the tissue was incubated for 15 min in 5 ml DMEM containing Protease Type1 (0.25 mg/ml, Sigma-Aldrich) and Collagenase A (1 mg/ml, Sigma-Aldrich) in a water bath at 37°C, 150 rpm. The enzymatic digestion was stopped by adding 5 ml DMEM containing 10% FBS (Sigma-Aldrich), centrifugation for 5 min at 300 *g* and resuspended in proliferation medium (neurobasal medium with 100 IU/Pen, 100 μg/ml Strep, 2.5 μg/ml Amphotericin [all Thermo Scientific], FGF and EGF [both 20 ng/ml, Immunotools]). Cells in proliferation media were kept at 37°C, 5% CO_2 for 4 days to promote formation of enteric neurospheres. For experiments, enteric neurospheres were dissociated with trypsin (0.25%, Thermo Scientific) for 5 min at 37°C and distributed at 50% confluency on Poly-Ornithin (Sigma-Aldrich) coated six well plates in differentiation medium (neurobasal medium with 100 IU/Pen, 100 μg/ml Strep, 2.5 μg/ml Amphotericin, B27, N2 [all Thermo Scientific] and EGF [2 ng/ml, Immunotools]). After 7 days in differentiation medium, mature enteric glia cells were treated with ATP (0.1, 1, 10, 100 μM, Sigma), ATPγS (0.1, 1, 10, 100 μM, Sigma), Adenosine (1, 100 μM, Sigma), PPADS (5, 30 μM, TOCRIS), Suramin (1, 10, 100 μM, TOCRIS), A740003 (2, 20 μM, TOCRIS), ambroxol (0.2, 2, 20 μM, TOCRIS), PSB-0711 (2, 20 μM, TOCRIS), PSB-1011 (0.2 2, 20 μM, TOCRIS), 5-BDBD (2, 20 μM, TOCRIS) SB203580 (1, 5, 10 μM, TOCRIS) and further processed for RNA isolation or their conditioned medium used for ELISA or qPCR analysis.

For the siRNA approach, primary msEGCs were differentiated as mentioned above and transfected with a control-siRNA (SIGMA) or P2X2-siRNA (#4390771, Thermo Scientific) lipofectamine (Thermo Scientific) complex for 72 h according to the manufacturer's instructions. Afterward, the transfected cells were treated with ATPγS (10, 100 μM, Sigma) and analyzed by qPCR and ELISA. For Western Blotting, primary msEGCs were lysed in RIPA buffer, centrifuged at maximum speed for 20 min and prepared with loading buffer (Bio-Rad). All samples were processed with the Bio-Rad Western Blot systems (any KD SDS-gels, Trans-Blot Turbo System) and incubated with the mentioned antibodies in Appendix Table S4 overnight at +4°C. Next, the blot was washed three times and incubated with secondary antibodies (Thermo Scientific) for 2 h and imaged with the Bio-Rad ChemiDoc Imaging System.

Human surgical specimens

The human IRB-protocol was approved by the ethics committee of the College of Medicine at The Ohio State University. Informed consent was obtained to procure viable human surgical tissue from colon or small bowel from patients with polyps undergoing a colectomy (sigmoid colon) or patients undergoing Roux-en-Y bypass surgery (jejunum) (Appendix Table S1). Human EGCs (hEGCs) in culture from 14 GI-surgical specimens were used to study gene expression and IL-6-release in hEGCs. Human EGCs were also used for calcium imaging studies and P2X-immunofluorescent labeling.

Collection of patient surgical specimens was also approved by the ethics committee of North-Rhine-Westphalia, Germany

(*Accession number: 266_14*). Informed consent was obtained to procure human surgical tissue from the small bowel (jejunum) from patients undergoing a pancreatectomy at an early and a late time point during the surgical procedure (Appendix Table S2). Human samples were collected and used for RNA-Seq and qPCR analysis.

Preparation of human EGC cultures

Tissue collection was performed by the surgeon and immersed immediately in ice-cold oxygenated Krebs–Henseleit solution and promptly transported to the research facilities within 15 min in coordination with the Clinical Pathology Team (Liñán-Rico *et al*, 2016). For isolating myenteric ganglia, tissue was pinned luminal side facing upward under a stereoscopic microscope and the mucosa, submucosa and most of the circular muscle were dissected away using scissors, and then flipped over to remove longitudinal muscle by dissection.

Myenteric plexus tissue was cut and enzymatically dissociated as described elsewhere (Turco *et al*, 2014; Liñán-Rico *et al*, 2016) with modifications as follows: Myenteric plexus tissue was minced into 0.1–0.2 cm^2 pieces and dissociated in an enzyme solution (0.125 mg/ml Liberase, 0.5 μg/ml Amphotericin B) prepared in Dulbecco's modified Eagle's medium (DMEM)-F12, for 60 min at 37°C with agitation. Ganglia were removed from the enzymatic solution by spinning down (twice), and re-suspending in a mixture of DMEM-F12, bovine serum albumin 0.1%, and DNase 50 μg/ml DNase (once). This solution, containing the ganglia, was transferred to a 100-mm culture dish and isolated single ganglia free of smooth muscle or other tissue components were collected with a micropipette while visualized under a stereoscopic microscope and plated into wells of a 24-well culture plate and kept in DMEM-F12 (1:1) medium containing 10% fetal bovine serum (FBS) and a mixture of antibiotics (penicillin 100 U/ml, streptomycin 100 μg/mL, and amphotericin B 0.25 μg/ml) at 37°C in an atmosphere of 5% CO_2 and 95% humidity.

After cells reach semi-confluence after 3–4 weeks (P1), hEGCs were enriched and purified by eliminating/ separating fibroblasts, smooth muscle and other cells. EGC enrichment and purification was achieved by labeling the isolated cells with magnetic micro beads linked to anti-specific antigen, D7-Fib and passing them through a magnetic bead separation column following the manufacturer instructions (*Miltenyi Biotec Inc*, San Diego, CA). This purification protocol was performed twice (P2 and P3) to reach a cell enrichment of up to 10,000 fold, and 20,000 cells were plated on glass coverslips pre-coated with 20 μg/ml laminin/P-D-Lys in 50 mm bottom glass #0 culture dishes for immunostaining and imaging or 12 well plates for IL-6 release experiments. Cultured hEGCs were kept until confluent and harvested for additional experiments (4–10 days). On the day of the experiment, hEGCs were stimulated as indicated. Parallel to this, cells at each passage were split and seeded in plastic 25 mm^2 culture flasks and used for study in passages 3–6.

Immunochemical Identification of glia in hEGC

To confirm the purity and identity of glial cells in the hEGC cultures, immunofluorescent labeling was done for glial markers (s100β, glial fibrillary acidic protein GFAP), for smooth muscle/epithelial actin and fibroblasts; hEGCs were fixed in 4% paraformaldehyde for 15 min at room temperature, rinsed three times with cold phosphate-buffered saline (PBS) 0.1 M and placed at 4°C until further processing. Cells were treated with 0.5% Triton X, 10% normal donkey serum in PBS to permeabilize the cells and block nonspecific antibody binding for 30 min at room temperature. Primary antibodies were diluted in PBS-0.1% Triton X, and 2% normal donkey serum, and were incubated with cells overnight (18–24 h) at 4°C. Next day preparations were rinsed three times in 0.1 M PBS/1 min and incubated 60 min at room temperature in secondary antibodies diluted in PBS-0.1%, Triton X, and 2% normal donkey serum. Antibodies mentioned in Appendix Table S4 were used for analysis. Alexa Fluor 488 or 568 donkey anti-mouse or anti-rabbit secondary antibodies were used at a dilution of 1:400 (Cambridge, MA). Omission of primary antibodies was used to test for background staining of the secondary antibodies. Pre-absorption of primary antisera with immunogenic peptides abolished immune-reactivity. Data confirmed previous reports by Turco *et al* (2014) and are not shown except for illustrating that all cells express s100β immunoreactivity > 99% of cells.

Ex vivo human specimen experiments

Human surgical tissue for *ex vivo* experiments was collected from four patients undergoing a pancreatectomy. The study was approved by the Ethics Committee at University of Bonn. Human jejunum specimens were collected in ice-cold oxygenated Krebs–Henseleit buffer during the surgical procedure and transported to the laboratory. Full-thickness jejunum specimen were mechanically activated for 30 s and then incubated for 3 h with or without 20 μM ambroxol in oxygenated Krebs–Henseleit buffer. As baseline control a human ME sample was taken before the mechanical activation. After the incubation time, the jejunum specimens were dissected, and only mucosa-free ME was used for further analysis.

For the ethics approval, the IRB-protocol for human enteric glia isolation was approved by the ethics committee of the College of Medicine of the Ohio State University and the collection of patient material for the enteric glia analysis was approved by the ethics committee of North-Rhine-Westphalia, Germany (*Accession Number: 266_14*). Further, all experiments conformed to the principles set out in the WMA Declaration of Helsinki and the Department of Health and Human Services Belmont Report.

Cell lines

Human 1321N1 astrocytoma cells were loaded with a calcium-chelating fluorescent dye (Molecular Devices), either fluo-4 acetoxymethyl ester (fluo-4 AM for cells transfected with P2X2, P2X4, or P2X7 receptor), or Calcium-4 AM or Calcium-5 AM for cells transfected with P2X1 or P2X3, respectively (Baqi *et al*, 2011).

HEK-P2X2 sniffer cells were loaded with 2 μM fluo-4/AM in a humidified incubator for 30 min and washed for 30 min prior to transferring to a perfusion chamber with oxygenated Krebs–Henseleit buffer on the stage of an upright Eclipse FNI Nikon scope equipped with a Andor iXon Ultra high speed camera for real-time Ca^{2+} imaging. Elements software was used for data acquisition. Ambroxol was dissolved in dimethyl sulfoxide (DMSO) and added

to the cells at a final concentration of 20 μM followed by stimulation with ATP at its respective EC_{80} concentration (P2X1 and P2X3 [100 nM], P2X2 and P2X4 [1 μM], P2X7 [1 mM]). The assay volume was 200 μl and the final DMSO concentration was 1%. ATP activation of the receptors led to increased calcium influx and consequently to increased fluorescence, which is blocked by treatment with antagonists.

ELISA

Release of IL-6 and CXCL2 was measured in ME RIPA lysates isolated from small intestine segments at the indicated time points after IM. Release of IL-6 in EGC cultures incubated with various treatments was measured at the indicated time points. All ELISAs were purchased from R&D Systems (*Abingdon*, England) and used according to the manufacturer's instructions. Values were normalized to tissue weights or untreated EGCs. Briefly, for animal tissue, the isolated ME (∼ 50 mg) was lysed with 1xRIPA buffer for 30 min, centrifuged for 30 min at maximum speed and the protein concentration determined with a BCA kit (Thermo Scientific). 100 μg of total protein was used to measure the release of IL-6 or CXCL2 in duplicates. For EGCs, cells were treated with the indicated substances for 24 h, supernatant was collected, centrifuged at 5,000 *g* for 5 min and snap-frozen in liquid nitrogen before processed for the IL-6 ELISA.

RNA-Seq

RNA samples were extracted using the RNeasy Mini Kit (*Qiagen*). RNA-Seq libraries were prepared using the QuantSeq 3′ mRNA-Seq Library Prep Kit (*Lexogen*) according to the manufacturer's instructions by the Genomics Core facility of the University Hospital Bonn. The RNA samples were prepared using the QuantSeq 3′ mRNA-Seq Library Prep Kit for Illumina (*Lexogen*). The method has high strand specificity (>99.9%) and most sequences are generated from the last exon and the 3′ untranslated region. The method generates only one fragment per transcript and the number of reads mapped to a given gene is proportional to its expression. Fewer reads than in classical RNA-seq methods are needed to determine unambiguous gene expression levels, allowing a high level of multiplexing. Library preparation involved reverse transcription of RNA with oligodT primers, followed by removal of RNA and second strand cDNA synthesis with random primers. The resulting fragments containing both linker fragments were PCR amplified with primers that also contain the Illumina adaptors and sample-specific barcodes. All libraries were sequenced (single-end 50 bp) on one lane of the Illumina Hiseq 2500. Only genes with an adjusted *P*-value below 0.05 and a minimum fold change greater than 1.5 were considered to be differentially expressed between conditions.

Immunohistochemistry

Whole mount specimens were mechanically prepared by dissection of the (sub)mucosa, fixed in 4% paraformaldehyde/PBS for 30 min, permeabilized with 0.2% Triton X-100/PBS for 15 min, blocked with 5% donkey serum/PBS for 1 h and incubated with primary IgGs mentioned in Appendix Table S4 at 4°C overnight. After three PBS washing steps, secondary antibodies (Dianova, anti-rat IgG-Cy2 1:800, anti-guinea pig IgG-Cy3, anti-chicken IgY-FITC and anti-rabbit IgG-FITC or - Cy3 1:800 were incubated for 90 min. Specimen were mounted in Fluorogel-Tris and imaged on a Leica confocal imaging system.

Primary cells were fixed in 4% paraformaldehyde/PBS for 30 min, permeabilized with 0.2% Triton X-100/PBS for 15 min, blocked with 3% BSA/BPS for 1 h and incubated with primary IgGs mentioned in Appendix Table S4 at 4°C overnight.

After three PBS washing steps, secondary antibodies (Dianova, anti-mouse IgG-Cy2 1:800, anti-guinea pig IgG-FITC and anti-rabbit IgG-FITC or - Cy3 1:800 were incubated for 60 min. Specimens were mounted in Fluorogel-Tris and imaged using a Leica confocal imaging system.

Postoperative ileus mouse model

Postoperative ileus was induced by standardized intestinal manipulation as described previously.(Stoffels *et al*, 2014) Small bowel was eventrated after median laparotomy and gently rolled twice from oral to aboral using moist cotton swabs. After repositioning of the bowel, the laparotomy wound was closed by a two-layer suture. Two different approaches for the ambroxol administration were used, according to Migdalska-Richards *et al* (2016) animals received ambroxol (4 mM) or vehicle via drinking water starting 24 h before the surgery, until their sacrifice and according to Su *et al* (2004) animals received i.p. injections (45 mg/kg) shortly after surgery.

In vivo gastrointestinal transit

Gastrointestinal transit (GIT) was assessed by measuring intestinal distribution of orally administered fluorescently labeled dextran-gavage 90 min after administration as described previously (Stoffels *et al*, 2014). The gastrointestinal tract was divided into 15 segments (stomach to colon). The geometric center (GC) of labeled dextran distribution was calculated as described previously. The stomach (st) correlates with a GC of 1, the small bowel correlates with a GC of 2–11, the cecum (c) correlates with a GC of 12 and the colon correlates with a GC of 13–15. GIT-measurement was performed with sham and IM24h animals.

ATP measurement

ATP concentration was measured in lavage samples of naïve and POI mice at IM3h and IM24h with an ATP determination Kit (*SIGMA-Aldrich*) according to the manufacturer's instructions.

MTT measurement

MTT signal was measured in EGCs after treating them with ambroxol, PSB1011 and PSB-0711, (all 20 μM) with a MTT assay Kit (*Abcam*) according to the manufacturer's instructions.

MPO^+-cell infiltration

Jejunal mucosa-free ME whole mount specimen were fixed in ethanol and stained with Hanker Yates reagent (Polyscience Europe, Germany) to identify myeloperoxidase expressing cells (MPO^+). The mean number of MPO^+ cells/mm^2 for five random areas per animal

was determined. MPO^+ measurement was performed with naive animals, 3, 6 and 24 h after IM.

Quantitative PCR

Total RNA was extracted from ME specimens at indicated time points after IM using the RNeasy Mini Kit (Qiagen, Hilden, Germany) followed by deoxyribonuclease I treatment (Ambion, Austin, TX). Complementary DNA was synthesized using the High Capacity cDNA Reverse Transcription Kit (Applied Biosystems, Darmstadt, Germany). Expression of mRNA was quantified by real-time RT-PCR with TaqMan probes or primers shown in Appendix Table S3.

Quantitative polymerase chain reaction was performed with SYBR Green PCR Master Mix or TaqMan Gene Expression Master Mix (both Applied Biosystems, Darmstadt, Germany).

Fluorescence activated cell sorting

Fluorescence activated cell sorting (FACS) analysis was performed on isolated ME of the small bowel 24 h after intestinal manipulation treated with ambroxol or vehicle CX3CR1-$GFP^{+/-}$ animals, respectively. Isolation of ME was achieved by sliding small bowel segments onto a glass rod, removing the outer muscularis circumferentially with moist cotton applicators and cutting the ME into fine pieces. ME was digested with a 0.1% collagenase type II (Worthington Biochemical, Lakewood, NJ, USA) enzyme mixture, diluted in HBSS, containing 0.1 mg/ml DNase I (La Roche, Germany), 2.4 mg/ml Dispase II (La Roche, Germany), 1 mg/ml BSA (Applichem), and 0.7 mg/ml trypsin inhibitor (Applichem) for 40 min in a 37°C shaking water bath. Afterward, single cell suspension was obtained using a 70 µm filter mesh. Cells were stained for 30 min at 4°C with the appropriate antibodies. For antibodies used in this study see Appendix Table S4. Flow cytometry analyses were performed on FACSCanto III (BD Biosciences), and data were analyzed with FlowJo software (Tree Star, Ashland, OR, USA).

Animals

Experiments were performed using 8–12-week-old mice kept in a pathogen-free animal facility with standard rodent food and tap water ad libitum. C57/BL/6J, CX3CR1-$GFP^{+/-}$ or $GFAP^{cre} \times Ai14^{floxed}$ mice were used for all experiments and were purchased from Jackson Laboratories directly or bred in our animal facility. All experiments were performed in accordance to the federal law for animal protection and approved by appropriate authorities of North-Rhine-Westphalia under the legal terms: 81-02.04.2018.A344 and 81-02.04.2016.A367.

Statistical analysis

Statistical analysis was performed with Prism V6.01 (GraphPad, San Diego, CA) using Student *t*-test or one-way ANOVA as indicated. In all Figs, *P*-values are indicated as $^*P < 0.05$, $^{**}P < 0.01$ and $^{***}P < 0.001$ when compared to control or $^{\#}P < 0.05$, $^{\#\#}P < 0.01$ and $^{\#\#\#}P < 0.001$ when compared to indicated samples. All plots show mean + standard error of mean (SEM).

The paper explained

Problem
In various inflammation-induced intestinal disorders, it has been shown that reactive enteric glia play a role in disease progression by contributing to inflammatory processes. However, less is known about the underlying pathogenic mechanism of EGC activation.

Results
Herein, we show that enteric gliosis occurs upon abdominal surgery and leads to postoperative ileus (POI), an inflammation-based intestinal motility disorder. Activation of EGC in this process depends on ATP and selective purinergic signaling in EGCs. Within a comprehensive set of *in vivo*, *ex vivo*, and *in vitro* analyses in mice and human specimens, we found that ATP is released during abdominal surgery and activates purinergic P2X2 signaling that triggers gliosis in human and murine EGC. We further identified a novel P2X2 antagonist and P2X2 antagonism with ambroxol proved to ameliorate gliosis, reduce inflammatory responses, and improve clinical symptoms of POI.

Impact
We conclude that enteric gliosis and P2X-purinergic receptors might be promising drug targets for therapeutic approaches in immune-driven intestinal diseases.

Experiments were repeated with more samples when the result was close to statistical significance, and sample sizes for animal studies were chosen following previously reported studies that have used the POI animal model, at least 6–10 independent mice per experimental setup. All animals were handled by standardized housing procedures and kept in exactly the same environmental conditions and were genotyped at 4 weeks of age and received a randomized number by which they were identified. Age- and sex-matched animals were grouped randomly and used in the POI animal model. In each experimental set, all the control or experimental mice were treated with the same procedure and manipulation. For the experimental setup with ambroxol, the treatment of mice was blinded, and all mice were randomly caged. The analysis was performed on the treatment groups without knowing what group was treated with ambroxol. By this, we avoided any group or genotype-specific effects due to timing of experiments or handling of animals.

Data availability

All RNA-seq data have been submitted to the GEO database. The datasets produced in this study are available in the following databases: RNA-Seq: mRNA from EGC and ME tissue in GSE134943 accessible here: https://www.ncbi.nlm.nih.gov/geo/query/acc.cgi?acc=GSE134943) and RNA-Seq data from mRNA of ME tissue from patients in GSE149181 accessible here: https://www.ncbi.nlm.nih.gov/geo/query/acc.cgi?acc=GSE149181; other data are available in the Expanded View Datasets or the Appendix Tables. The software tools used for this study include Partek Flow, available from https://www.partek.com/partek-flow/#features; Venn Diagramm Software, available from http://bioinformatics.psb.ugent.be/webtools/Venn/; and Gene Set

Enrichment Analysis, available from https://www.partek.com/partek-flow/#features.

Expanded View for this article is available online.

Acknowledgements
The authors thank the Next Generation Sequencing Core Facility and the Institute for Genomic Statistics and Bioinformatics of the University Clinics Bonn for supporting the RNA-Seq analysis. The authors thank the Flow Cytometry Core Facility of the University Clinics Bonn for supporting the isolation of tdTomato$^+$ EGCs. The sniffer cells (HEK mixed clone 228) were a gift from Dr. Terrance Egan, Saint Louis University to Fievos L. Christofi, The Ohio State University. The gpSox10 antibody was a kind gift of Professor Wegner, University of Erlangen. NIDDKNIHR01DK113943 to Dr. Fievos L. Christofi, an NCI Cost shared resource grant P30LA16058 for the molecular core facility in the College of Medicine, The Ohio State University. This publication was supported by a personnel grant of the German research council (DFG) to SW (WE4204/3-1), BonnNI (Q-611.0754), and the ImmunoSensation^2 Cluster of Excellence (EXC 2151–390873048).

Author contributions
RS, PL, AM, ML, IK, BS, CS, IG, EM, and EV-H performed research. RS, FLC, CEM, and SW analyzed data. RS, JCK, FLC, and SW prepared and revised the manuscript. RS, CEM, FLC, and SW designed the research. YB, CS, and CEM produced the P2X2-specific antagonists. T.G. organized the patient material.

Conflict of interest
SW and JCK receive royalties from Wolter Kluwer for contribution to the post-operative ileus section of the *UpToDate* library. All other authors declare no competing interests.

References

Abdo H, Derkinderen P, Gomes P, Chevalier J, Aubert P, Masson D, Galmiche J-P, Vanden Berghe P, Neunlist M, Lardeux B (2010) Enteric glial cells protect neurons from oxidative stress in part via reduced glutathione. *FASEB J* 24: 1082 – 1094

Andersson HC, Anderson MF, Porritt MJ, Nodin C, Blomstrand F, Nilsson M (2011) Trauma-induced reactive gliosis is reduced after treatment with octanol and carbenoxolone. *Neurol Res* 33: 614 – 624

Aubé A-C, Cabarrocas J, Bauer J, Philippe D, Aubert P, Doulay F, Liblau R, Galmiche JP, Neunlist M (2006) Changes in enteric neurone phenotype and intestinal functions in a transgenic mouse model of enteric glia disruption. *Gut* 55: 630 – 637

Baqi Y, Hausmann R, Rosefort C, Rettinger J, Schmalzing G, Müller CE (2011) Discovery of potent competitive antagonists and positive modulators of the P2X2 receptor. *J Med Chem* 54: 817 – 830

Beeh KM, Beier J, Esperester A, Paul LD (2008) Antiinflammatory properties of ambroxol. *Eur J Med Res* 13: 557 – 562

Belkind-Gerson J, Graham HK, Reynolds J, Hotta R, Nagy N, Cheng L, Kamionek M, Shi HN, Aherne CM, Goldstein AM (2017) Colitis promotes neuronal differentiation of Sox2+ and PLP1+ enteric cells. *Sci Rep* 7: 2525

Bhave S, Gade A, Kang M, Hauser KF, Dewey WL, Akbarali HI (2017) Connexin-purinergic signaling in enteric glia mediates the prolonged effect of morphine on constipation. *FASEB J* 31: 2649 – 2660

Boesmans W, Cirillo C, van den Abbeel V, van den Haute C, Depoortere I, Tack J, Vanden Berghe P (2013) Neurotransmitters involved in fast excitatory neurotransmission directly activate enteric glial cells. *Neurogastroenterol Motil* 25: e151 – e160

Boesmans W, Lasrado R, Vanden Berghe P, Pachnis V (2015) Heterogeneity and phenotypic plasticity of glial cells in the mammalian enteric nervous system. *Glia* 63: 229 – 241

Boesmans W, Hao MM, Fung C, Li Z, van den Haute C, Tack J, Pachnis V, Vanden Berghe P (2019) Structurally defined signaling in neuro-glia units in the enteric nervous system. *Glia* 67: 1167 – 1178

Brierley SM, Linden DR (2014) Neuroplasticity and dysfunction after gastrointestinal inflammation. *Nat Rev Gastroenterol Hepatol* 11: 611 – 627

Brown IAM, McClain JL, Watson RE, Patel BA, Gulbransen BD (2016) Enteric glia mediate neuron death in colitis through purinergic pathways that require connexin-43 and nitric oxide. *Cell Mol Gastroenterol Hepatol* 2: 77 – 91

Buffo A, Rite I, Tripathi P, Lepier A, Colak D, Horn A-P, Mori T, Götz M (2008) Origin and progeny of reactive gliosis: asource of multipotent cells in the injured brain. *Proc Natl Acad Sci USA* 105: 3581 – 3586

Burda JE, Sofroniew MV (2014) Reactive gliosis and the multicellular response to CNS damage and disease. *Neuron* 81: 229 – 248

Burnstock G, Jacobson KA, Christofi FL (2017) Purinergic drug targets for gastrointestinal disorders. *Curr Opin Pharmacol* 37: 131 – 141

Burnstock G (2020) Introduction to purinergic signaling. *Methods Mol Biol* 2041: 1 – 15

Bush TG, Savidge TC, Freeman TC, Cox HJ, Campbell EA, Mucke L, Johnson MH, Sofroniew MV (1998) Fulminant jejuno-ileitis following ablation of enteric glia in adult transgenic mice. *Cell* 93: 189 – 201

Canellada A, Ramirez BG, Minami T, Redondo JM, Cano E (2008) Calcium/calcineurin signaling in primary cortical astrocyte cultures: Rcan1-4 and cyclooxygenase-2 as NFAT target genes. *Glia* 56: 709 – 722

Carta S, Penco F, Lavieri R, Martini A, Dinarello CA, Gattorno M, Rubartelli A (2015) Cell stress increases ATP release in NLRP3 inflammasome-mediated autoinflammatory diseases, resulting in cytokine imbalance. *Proc Natl Acad Sci USA* 112: 2835 – 2840

Cauwels A, Rogge E, Vandendriessche B, Shiva S, Brouckaert P (2014) Extracellular ATP drives systemic inflammation, tissue damage and mortality. *Cell Death Dis* 5: e1102

Christofi FL (2008) Purinergic receptors and gastrointestinal secretomotor function. *Purinergic Signal* 4: 213 – 236

Colangelo AM, Alberghina L, Papa M (2014) Astrogliosis as a therapeutic target for neurodegenerative diseases. *Neurosci Lett* 565: 59 – 64

Cornet A, Savidge TC, Cabarrocas J, Deng WL, Colombel JF, Lassmann H, Desreumaux P, Liblau RS (2001) Enterocolitis induced by autoimmune targeting of enteric glial cells: a possible mechanism in Crohn's disease? *Proc Natl Acad Sci USA* 98: 13306 – 13311

Csóka B, Németh ZH, Törő G, Idzko M, Zech A, Koscsó B, Spolarics Z, Antonioli L, Cseri K, Erdélyi K *et al* (2015) Extracellular ATP protects against sepsis through macrophage P2X7 purinergic receptors by enhancing intracellular bacterial killing. *FASEB J* 29: 3626 – 3637

Di Virgilio F, Dal Ben D, Sarti AC, Giuliani AL, Falzoni S (2017) The P2X7 Receptor in Infection and Inflammation. *Immunity* 47: 15 – 31

Di Virgilio F, Sarti AC, Falzoni S, de Marchi E, Adinolfi E (2018) Extracellular ATP and P2 purinergic signalling in the tumour microenvironment. *Nat Rev Cancer* 18: 601 – 618

Esposito G, Capoccia E, Gigli S, Pesce M, Bruzzese E, D'Alessandro A, Cirillo C, Di Cerbo A, Cuomo R, Seguella L *et al* (2017) HIV-1 Tat-induced diarrhea evokes an enteric glia-dependent neuroinflammatory response in the central nervous system. *Sci Rep* 7: 7735

Farro G, Stakenborg M, Gomez-Pinilla PJ, Labeeuw E, Goverse G, Di Giovangiulio M, Stakenborg N, Meroni E, D'Errico F, Elkrim Y *et al* (2017) CCR2-dependent monocyte-derived macrophages resolve inflammation and restore gut motility in postoperative ileus. *Gut* 66: 2098 – 2109

Fujita A, Yamaguchi H, Yamasaki R, Cui Y, Matsuoka Y, Yamada K-I, Kira J-I (2018) Connexin 30 deficiency attenuates A2 astrocyte responses and induces severe neurodegeneration in a 1-methyl-4-phenyl-1,2,3,6-tetrahydropyridine hydrochloride Parkinson's disease animal model. *J Neuroinflammation* 15: 227

Furness JB (2012) The enteric nervous system and neurogastroenterology. *Nat Rev Gastroenterol Hepatol* 9: 286 – 294

Galligan JJ (2008) Purinergic signaling in the gastrointestinal tract. *Purinergic Signal* 4: 195 – 196

Germouty J, Jirou-Najou JL (1987) Clinical efficacy of ambroxol in the treatment of bronchial stasis. Clinical trial in 120 patients at two different doses. *Respiration* 51(Suppl 1): 37 – 41

Gomes P, Chevalier J, Boesmans W, Roosen L, van den Abbeel V, Neunlist M, Tack J, Vanden Berghe P (2009) ATP-dependent paracrine communication between enteric neurons and glia in a primary cell culture derived from embryonic mice. *Neurogastroenterol Motil* 21: 870 .e62

Grubišić V, Gulbransen BD (2017) Enteric glia: the most alimentary of all glia. *J Physiol (Lond)* 595: 557 – 570

Grubišić V, Perez-Medina AL, Fried DE, Sevigny J, Robson SC, Galligan JJ, Gulbransen BD (2019) NTPDase1 and -2 are expressed by distinct cellular compartments in the mouse colon and differentially impact colonic physiology and function after DSS-colitis. *Am J Physiol Gastrointest Liver Physiol* 317): G314 – G332

Grubišić V, McClain JL, Fried DE, Grants I, Rajasekhar P, Csizmadia E, Ajijola OA, Watson RE, Poole DP, Robson SC *et al* (2020) Enteric glia modulate macrophage phenotype and visceral sensitivity following inflammation. *Cell Rep* 32: 108100

Gulbransen BD, Sharkey KA (2009) Purinergic neuron-to-glia signaling in the enteric nervous system. *Gastroenterology* 136: 1349 – 1358

Gulbransen BD, Bashashati M, Hirota SA, Gui X, Roberts JA, MacDonald JA, Muruve DA, McKay DM, Beck PL, Mawe GM *et al* (2012) Activation of neuronal P2X7 receptor-pannexin-1 mediates death of enteric neurons during colitis. *Nat Med* 18: 600 – 604

Gulbransen BD, Christofi FL (2018) Are we close to targeting enteric glia in gastrointestinal diseases and motility disorders? *Gastroenterology* 155: 245 – 251

Hama AT, Plum AW, Sagen J (2010) Antinociceptive effect of ambroxol in rats with neuropathic spinal cord injury pain. *Pharmacol Biochem Behav* 97: 249 – 255

Hara M, Kobayakawa K, Ohkawa Y, Kumamaru H, Yokota K, Saito T, Kijima K, Yoshizaki S, Harimaya K, Nakashima Y *et al* (2017) Interaction of reactive astrocytes with type I collagen induces astrocytic scar formation through the integrin-N-cadherin pathway after spinal cord injury. *Nat Med* 23: 818 – 828

Hedrick TL, McEvoy MD, Mythen MMG, Bergamaschi R, Gupta R, Holubar SD, Senagore AJ, Gan TJ, Shaw AD, Thacker JKM *et al* (2018) American Society for Enhanced Recovery and Perioperative Quality Initiative Joint Consensus Statement on postoperative gastrointestinal dysfunction within an enhanced recovery pathway for elective colorectal surgery. *Anesth Analg* 126: 1896 – 1907

Idzko M, Ferrari D, Eltzschig HK (2014) Nucleotide signalling during inflammation. *Nature* 509: 310 – 317

Iyer S, Saunders WB, Stemkowski S (2009) Economic burden of postoperative ileus associated with colectomy in the United States. *J Manag Care Pharm* 15: 485 – 494

Liddelow SA, Guttenplan KA, Clarke LE, Bennett FC, Bohlen CJ, Schirmer L, Bennett ML, Münch AE, Chung W-S, Peterson TC *et al* (2017) Neurotoxic reactive astrocytes are induced by activated microglia. *Nature* 541: 481 – 487

Liñán-Rico A, Turco F, Ochoa-Cortes F, Harzman A, Needleman BJ, Arsenescu R, Abdel-Rasoul M, Fadda P, Grants I, Whitaker E *et al* (2016) Molecular signaling and dysfunction of the human reactive enteric glial cell phenotype: implications for GI infection, IBD, POI, neurological, motility, and GI disorders. *Inflamm Bowel Dis* 22: 1812 – 1834

Livne-Bar I, Lam S, Chan D, Guo X, Askar I, Nahirnyj A, Flanagan JG, Sivak JM (2016) Pharmacologic inhibition of reactive gliosis blocks TNF-α-mediated neuronal apoptosis. *Cell Death Dis* 7: e2386

Magalhaes J, Gegg ME, Migdalska-Richards A, Schapira AH (2018) Effects of ambroxol on the autophagy-lysosome pathway and mitochondria in primary cortical neurons. *Sci Rep* 8: 1385

Mathys H, Davila-Velderrain J, Peng Z, Gao F, Mohammadi S, Young JZ, Menon M, He L, Abdurrob F, Jiang X *et al* (2019) Single-cell transcriptomic analysis of Alzheimer's disease. *Nature* 570: 332 – 337

McClain J, Grubišić V, Fried D, Gomez-Suarez RA, Leinninger GM, Sévigny J, Parpura V, Gulbransen BD (2014) Ca^{2+} responses in enteric glia are mediated by connexin-43 hemichannels and modulate colonic transit in mice. *Gastroenterology* 146: 497 – 507.e1

Migdalska-Richards A, Daly L, Bezard E, Schapira AHV (2016) Ambroxol effects in glucocerebrosidase and α-synuclein transgenic mice. *Ann Neurol* 80: 766 – 775

Ochoa-Cortes F, Turco F, Linan-Rico A, Soghomonyan S, Whitaker E, Wehner S, Cuomo R, Christofi FL (2016) Enteric glial cells: a new frontier in neurogastroenterology and clinical target for inflammatory bowel diseases. *Inflamm Bowel Dis* 22: 433 – 449

de Oliveira S, López-Muñoz A, Candel S, Pelegrín P, Calado Â, Mulero V (2014) ATP modulates acute inflammation *in vivo* through dual oxidase 1-derived H2O2 production and NF-κB activation. *J Immunol* 192: 5710 – 5719

Pacheco-Pantoja EL, Dillon JP, Wilson PJM, Fraser WD, Gallagher JA (2016) c-Fos induction by gut hormones and extracellular ATP in osteoblastic-like cell lines. *Purinergic Signal* 12: 647 – 651

Pekny M, Pekna M (2014) Astrocyte reactivity and reactive astrogliosis: costs and benefits. *Physiol Rev* 94: 1077 – 1098

Pekny M, Pekna M (2016) Reactive gliosis in the pathogenesis of CNS diseases. *Biochim Biophys Acta* 1862: 483 – 491

Rakers C, Schleif M, Blank N, Matušková H, Ulas T, Händler K, Torres SV, Schumacher T, Tai K, Schultze JL *et al* (2019) Stroke target identification guided by astrocyte transcriptome analysis. *Glia* 67: 619 – 633

Rao M, Rastelli D, Dong L, Chiu S, Setlik W, Gershon MD, Corfas G (2017) Enteric glia regulate gastrointestinal motility but are not required for maintenance of the epithelium in mice. *Gastroenterology* 153: 1068 – 1081.e7

Rao M (2020) An increasingly complex view of intestinal motility. *Nat Rev Gastroenterol Hepatol* 17: 72 – 73

Riteau N, Baron L, Villeret B, Guillou N, Savigny F, Ryffel B, Rassendren F, Le Bert M, Gombault A, Couillin I (2012) ATP release and purinergic signaling: a common pathway for particle-mediated inflammasome activation. *Cell Death Dis* 3: e403

Rosenbaum C, Schick MA, Wollborn J, Heider A, Scholz C-J, Cecil A, Niesler B, Hirrlinger J, Walles H, Metzger M (2016) Activation of myenteric glia during acute inflammation *in vitro* and *in vivo*. *PLoS One* 11: e0151335

Roy Choudhury G, Ryou M-G, Poteet E, Wen Y, He R, Sun F, Yuan F, Jin K, Yang S-H (2014) Involvement of p38 MAPK in reactive astrogliosis induced by ischemic stroke. *Brain Res* 1551: 45 – 58

Schirmer L, Velmeshev D, Holmqvist S, Kaufmann M, Werneburg S, Jung D, Vistnes S, Stockley JH, Young A, Steindel M *et al* (2019) Neuronal vulnerability and multilineage diversity in multiple sclerosis. *Nature* 573: 75 – 82

Sharkey KA (2015) Emerging roles for enteric glia in gastrointestinal disorders. *J Clin Invest* 125: 918 – 925

Silveira CRA, MacKinley J, Coleman K, Li Z, Finger E, Bartha R, Morrow SA, Wells J, Borrie M, Tirona RG *et al* (2019) Ambroxol as a novel disease-modifying treatment for Parkinson's disease dementia: protocol for a single-centre, randomized, double-blind, placebo-controlled trial. *BMC Neurol* 19: 20

Stein K, Lysson M, Schumak B, Vilz T, Specht S, Heesemann J, Roers A, Kalff JC, Wehner S (2018) Leukocyte-derived interleukin-10 aggravates postoperative ileus. *Front Immunol* 9: 2599

Stoffels B, Hupa KJ, Snoek SA, van Bree S, Stein K, Schwandt T, Vilz TO, Lysson M, Veer CV't, Kummer MP *et al* (2014) Postoperative ileus involves interleukin-1 receptor signaling in enteric glia. *Gastroenterology* 146: 176 – 187.e1

Su X, Wang L, Song Y, Bai C (2004) Inhibition of inflammatory responses by ambroxol, a mucolytic agent, in a murine model of acute lung injury induced by lipopolysaccharide. *Intensive Care Med* 30: 133 – 140

Turco F, Sarnelli G, Cirillo C, Palumbo I, de Giorgi F, D'Alessandro A, Cammarota M, Giuliano M, Cuomo R (2014) Enteroglial-derived S100B protein integrates bacteria-induced Toll-like receptor signalling in human enteric glial cells. *Gut* 63: 105 – 115

Villumsen M, Aznar S, Pakkenberg B, Jess T, Brudek T (2019) Inflammatory bowel disease increases the risk of Parkinson's disease: a Danish nationwide cohort study 1977–2014. *Gut* 68: 18 – 24

Wehner S, Schwarz NT, Hundsdoerfer R, Hierholzer C, Tweardy DJ, Billiar TR, Bauer AJ, Kalff JC (2005) Induction of IL-6 within the rodent intestinal muscularis after intestinal surgical stress. *Surgery* 137: 436 – 446

Wehner S, Behrendt FF, Lyutenski BN, Lysson M, Bauer AJ, Hirner A, Kalff JC (2007) Inhibition of macrophage function prevents intestinal inflammation and postoperative ileus in rodents. *Gut* 56: 176 – 185

Wehner S, Straesser S, Vilz TO, Pantelis D, Sielecki T, La Cruz VF, de la Cruz VF, Hirner A, Kalff JC (2009) Inhibition of p38 mitogen-activated protein kinase pathway as prophylaxis of postoperative ileus in mice. *Gastroenterology* 136: 619 – 629

Weiser T (2008) Ambroxol: a CNS drug? *CNS Neurosci Ther* 14: 17 – 24

Yoo BB, Mazmanian SK (2017) The Enteric Network: Interactions between the Immune and Nervous Systems of the Gut. *Immunity* 46: 910 – 926

Zamanian JL, Xu L, Foo LC, Nouri N, Zhou L, Giffard RG, Barres BA (2012) Genomic analysis of reactive astrogliosis. *J Neurosci* 32: 6391 – 6410

Zhang M, Wang S, Yu L, Xu X, Qiu Z (2020) The role of ATP in cough hypersensitivity syndrome: new targets for treatment. *J Thorac Dis* 12: 2781 – 2790

3.4 Publication 4: *Schneider et al. 2022*, IL-1-dependent enteric gliosis guides intestinal inflammation and dysmotility and modulates macrophage function, DOI: 10.1038/s42003-022-03772-4

communications biology

ARTICLE

https://doi.org/10.1038/s42003-022-03772-4 OPEN

IL-1-dependent enteric gliosis guides intestinal inflammation and dysmotility and modulates macrophage function

Reiner Schneider[1], Patrick Leven[1], Shilpashree Mallesh[1], Mona Breßer[1], Linda Schneider[1], Elvio Mazzotta[2], Paola Fadda[2], Tim Glowka[1], Tim O. Vilz[1], Philipp Lingohr[1], Jörg C. Kalff[1], Fievos L. Christofi[2,3] & Sven Wehner[1,3]✉

Muscularis Externa Macrophages (*ME*-Macs) and enteric glial cells (EGCs) are closely associated cell types in the bowel wall, and important interactions are thought to occur between them during intestinal inflammation. They are involved in developing postoperative ileus (POI), an acute, surgery-induced inflammatory disorder triggered by IL-1 receptor type I (IL1R1)-signaling. In this study, we demonstrate that IL1R1-signaling in murine and human EGCs induces a reactive state, named enteric gliosis, characterized by a strong induction of distinct chemokines, cytokines, and the colony-stimulating factors 1 and 3. Ribosomal tagging revealed enteric gliosis as an early part of POI pathogenesis, and mice with an EGC-restricted IL1R1-deficiency failed to develop postoperative enteric gliosis, showed diminished immune cell infiltration, and were protected from POI. Furthermore, the IL1R1-deficiency in EGCs altered the surgery-induced glial activation state and reduced phagocytosis in macrophages, as well as their migration and accumulation around enteric ganglia. In patients, bowel surgery also induced IL-1-signaling, key molecules of enteric gliosis, and macrophage activation. Together, our data show that IL1R1-signaling triggers enteric gliosis, which results in *ME*-Mac activation and the development of POI. Intervention in this pathway might be a useful prophylactic strategy in preventing such motility disorders and gut inflammation.

[1] Department of Surgery, University Hospital Bonn, Bonn, Germany. [2] Department of Anesthesiology, Wexner Medical Center, The Ohio State University, Columbus, OH, USA. [3] These authors contributed equally: Fievos L. Christofi, Sven Wehner. ✉email: Sven.Wehner@ukbonn.de

Abdominal surgery induces an acute intestinal inflammation within the *muscularis externa* (*ME*)[1], resulting in functional motility disturbances, clinically known as postoperative ileus (POI). POI occurs in up to 27% of patients undergoing abdominal surgery[2] and is associated with prolonged hospitalizations, increased morbidity, and a high medico-economic burden[3]. As a result, patients suffer from nausea, vomiting, increased inflammatory response, and a higher risk of anastomotic leakage after colorectal surgery[4].

Studies of the past decades demonstrated that resident muscularis macrophages (*ME*-Macs)[5] as well as enteric glial cells (EGCs)[6] are key players and early responders in the postoperative *ME* inflammation[5,7,8]. In addition, both cell types lie in close anatomical association with enteric neurons, and there is growing evidence of communication between these cell types in health and gastrointestinal diseases in the context of inflammation[9–11].

EGCs express markers including S100β, glial-fibrillary acid protein (GFAP), proteolipid-protein-1 (PLP-1), or Sox10, commonly used as glial biomarkers to identify these cells throughout the intestine[11]. EGCs are present along the entire gastrointestinal tract, are known to modulate motility[12], and contribute to neuroinflammation in the gut[13]. Notably, some studies showed that EGCs maintain gut homeostasis[14] and that deletion of EGCs driven by the GFAP-promoter led to a massive inflammatory reaction in the GI tract[15,16], indicating a crucial immune-regulatory role of EGCs in the gut. However, these findings were challenged by a recent study showing that a proteolipid-protein-1 (PLP-1) driven depletion of EGC did not affect barrier maintenance nor sensitize mice to intestinal inflammation[12]. Despite controversial findings, EGCs are still discussed as promising interventional targets in several GI diseases, including POI[13,17]. EGC presence in the mucosa[18] and the *ME*[19] requires, in turn, the presence of intestinal microbiota. Furthermore, EGCs release immune mediators like interleukin-6 (IL-6) after stimulation with innate immune stimuli, including bacterial lipopolysaccharides[13], and host-derived factors like interleukin-1 (IL-1)[11]. Our group recently demonstrated that EGCs acquire a reactive phenotype after extracellular ATP treatment[20]. That study was the first to define the molecular identity of a reactive EGC phenotype, which we named "enteric gliosis". The general term *gliosis* is a well-established part of posttraumatic injury in the CNS[21] that involves intercellular communication between classical CNS immune cells, e.g., microglia, and neural cell types, including neurons and astrocytes. Based on similar functions and transcriptional profiles[22–25], *ME*-Macs and EGCs are often compared to microglia and astrocytes, respectively, and the bidirectional communication of the latter is a well-defined mechanism determining the functional fate of both cell types during inflammation[26].

In the intestine, there is growing evidence for an interaction of *ME*-Macs and cells of the enteric nervous system. Cell-to-cell communication between enteric neurons and *ME*-Macs has been shown to involve the release of colony-stimulating factor 1 (CSF1) and bone morphogenetic protein 2, respectively, and this interaction is thought to fine-tune intestinal motility[27]. Interactions between EGCs and *ME*-Macs were also recently described, showing that EGCs are a more potent source of CSF1. EGCs modulate visceral sensitivity through mechanisms that require interleukin-1β (IL-1β) and connexin-43 hemichannels (Cx43) to release CSF1, to activate *ME*-Macs[28]. While this study was the first to provide evidence on EGC–*ME*-Macs interactions in chronic intestinal inflammation, proof for this interaction in acute inflammation, occurring during POI, remains elusive. It is also unknown whether there is a link between EGC–*ME*-Macs interactions and abnormal motility in an acute inflammatory motility disorder such as POI.

We previously demonstrated that IL-1 is an essential cytokine in POI development, and pharmacological IL-1-antagonism with the drug anakinra or a global genetic IL1R1 depletion was shown to protect mice from POI[6]. Furthermore, we elucidated the role of the two ligands, IL-1 and IL-1β, in POI with a particular focus on IL-1β[29]. EGCs express IL1R1, and IL-1 stimulation results in the release of IL-6 and CCL2, which are known to play a role in POI[30–32]. Recently, IL-1-signaling in EGCs was also suspected of exerting pro-tumorigenic functions[33]. However, these studies demonstrated IL-1-induced cytokine release by EGCs only by carrying out in vitro experiments. Moreover, an EGC-specific approach, i.e., by cell-specific depletion of IL1R1 in EGCs, has not been used so far. Therefore, solid evidence of the cell-specific role of IL-1-signaling and focused analyses of EGC reactivity in vivo are still missing.

Herein, we aimed to fill this gap using two transgenic mouse models. First, the transgenic *RiboTag* mouse model allows a comprehensive in vivo "snapshot" of actively transcribed mRNA in EGCs[34]. Secondly, we generated a mouse with a targeted depletion of IL1R1 in glial-fibrillary acid (GFAP) expressing cells, one exclusive marker of EGCs. Additionally, we investigated if and how IL-1-signaling in EGCs affects *ME*-Mac responses by a series of transcriptional and functional analyses. Finally, we aimed to confirm our findings from our mouse study in human bowel specimens taken during a duodenopancreatectomy and in primary human EGC cultures isolated from GI surgical specimens. Together, our results show that IL-1 induces stimulus-specific enteric gliosis in EGCs that affects *ME*-Mac function and accounts for POI development in mice. Furthermore, findings in mice are translatable to humans since we discovered that the same molecular pathways are activated in the *ME* of the human postoperative bowel.

Results

IL-1 induces a specific type of gliosis in enteric glial cells. Recently, we showed that surgical trauma and intestinal manipulation induce a reactive enteric glial cell (EGC) phenotype, also referred to as "enteric gliosis", coinciding with the release of various cytokines and chemokines[20]. We hypothesized that IL-1 triggers reactive gliosis, so we stimulated primary murine EGC cultures (Fig. S1a) with IL-1β and confirmed gliosis induction by validating known biomarkers that serve as hallmarks of a gliotic phenotype. IL-1β induced IL-6 release (Fig. S1b), proliferation (Fig. S1c), and changes in morphology (Fig. S1d) in EGCs. To generate a more comprehensive molecular signature profile of the IL-1 triggered alterations in gene expression in EGCs, we performed a bulk-RNA-Seq analysis. A principal component analysis (PCA) indicated a clear separation between IL-1β and vehicle-treated EGCs (Fig. 1a). Upon IL-1β treatment, 496 genes were up, and 826 were down-regulated (Fig. 1b, $p < 0.05$; fold-change 1.5). Among the 20 most highly induced genes, we found inflammatory mediators like *IL-6*, chemokines (*Cxcl2*, *Cxcl5*, *Ccl2*, *Ccl5*), and colony-stimulating factors (*Csf1*, *Csf3*) (Fig. 1b). In addition, heat map analyses of genes sorted for induced inflammatory mediators confirmed these inductions (Fig. S1e). Next, we specified the reactive EGC state by gene ontology (GO) analysis, which revealed a gene enrichment within the terms "glial activation", "IL-1-signaling", "migration", and "inflammatory response" (Fig. 1c). Concurring heat maps confirmed a clear pattern in IL-1-activated EGCs (Fig. 1d + e), underlining their reactive state. Furthermore, by implementing our previously established "enteric gliosis" gene panel identified by ATP stimulation[20], we found a unique gene expression induced by IL-1β in EGCs, vastly different from our previously published ATP-induced gene panel (Fig. S1f). Comparison of our data set to published data investigating various stimuli for EGC activation, i.e.,

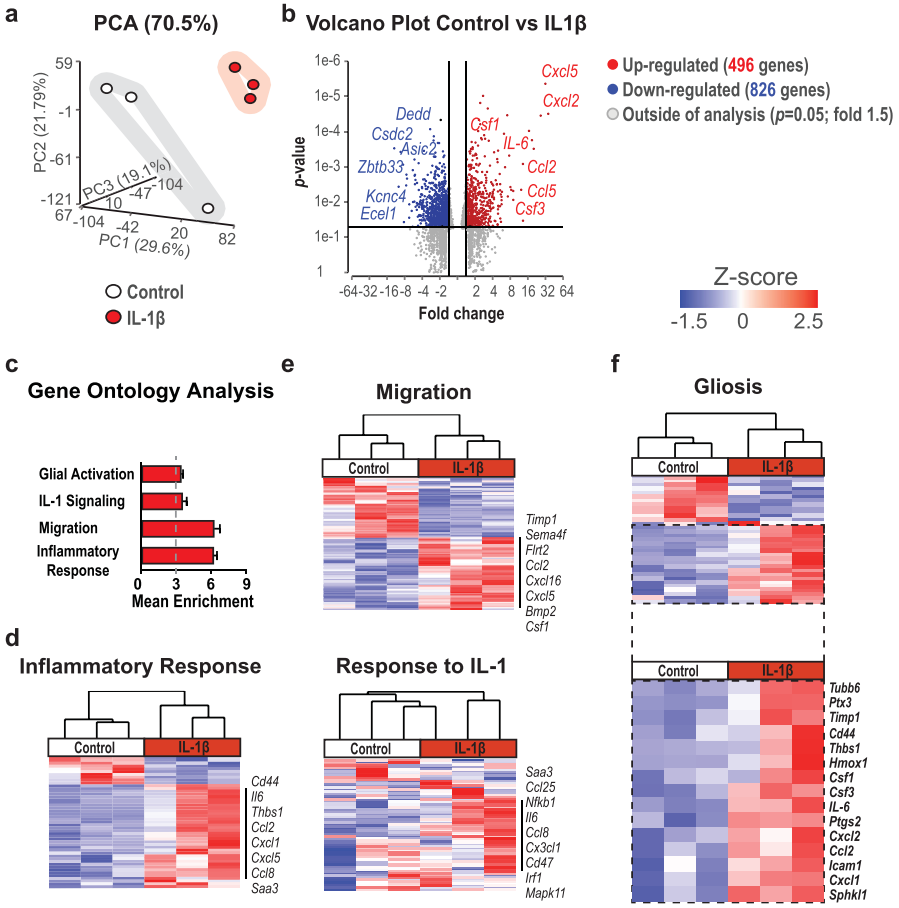

Fig. 1 IL-1 induces a specific reactive phenotype in EGCs. EGCs were treated with IL-1β (10 ng/ml) or vehicle (control) for 24 h and processed for bulk-RNA-Seq. **a** PCA plot shows a clear separation between both groups. **b** Volcano plot showing all significantly regulated genes. **c** Gene ontology (GO) analysis of IL1β-treated EGCs showing enrichment of genes connected to the indicated GO terms. **d**, **e** Heat maps of differentially expressed genes involved in "inflammatory response", "migration", and "response to IL-1" between IL-1β- and vehicle-treated EGCs. **f** Heat map of genes involved in "gliosis" highlighting the induced gene panel. Statistics were done with Fisher's exact test, $n = 3$ per group.

infection[35] or DNBS colitis[36], also revealed a distinct pattern for the IL-1β induced enteric gliosis phenotype with an inevitable overlap in key genes (Fig. S1g and Table S5). This analysis indicates that gliosis and EGC reactivity greatly depends on the inducing immune stimulus. IL-1-treated EGCs showed a prominent elevation of chemokine and cytokine levels involved in gliotic processes. Moreover, two new essential factors were identified in reactive glia in POI, *Csf1* and *Csf3* (Fig. 1f), with Csf1 recently implicated in EGC responses in a murine colitis model and human Crohn's Disease[28].

We conclude that IL-1 induces a specific transcriptome activation signature in EGCs, resulting in a distinct form of EGC gliosis leading to dysmotility and POI, with possible functions in inflammatory processes in the gut.

IL-1-induced enteric gliosis resembles the EGC reactivity profile after surgical trauma. In order to prove that the before-mentioned most prominent markers of the IL-1β-induced gliosis (see Fig. 1) are indeed selectively expressed by EGCs and not by other cell types present at low levels in EGC primary cell cultures, we used a Cre-recombinase-driven approach to analyze the expression of actively transcribed key gliosis genes. This approach is based on Cre-mediated (*Sox10*^{CreERT2}) tagging of the ribosomal Rpl22 protein with a hemagglutinin (HA) tag and subsequent immunoprecipitation of the ribosomes, including actively transcribed mRNA (Fig. 2a and ref. [34]). Immunofluorescence microscopy confirmed selective expression of the HA tag in SOX10$^+$ EGCs in cell cultures in vitro and, importantly, in vivo within *ME* whole mounts (Fig. 2b). Furthermore, after IL-1β treatment, key signature genes of gliosis (*GFAP*, *Nestin*) together with cytokines (*IL-6*, *TNFα*), chemokines (*Ccl2*, *Ccl5*, *Cxcl2*, *Cxcl5*), and growth factors (*Csf1*, *Csf3*) were selectively expressed and induced in EGCs (Figs. 2c and S2a).

As previous work implicated an immune-modulating role of EGCs in the postoperative inflammation of the *ME* resulting in POI[6,20], we next subjected *Sox10*$^{CreERT2+}$*xRpl22*$^{HA/+}$ mice to intestinal surgical manipulation (IM) to investigate the reactive state of EGCs in vivo (Figs. 2d and S2b). As expected, 24 h after IM, these mice exhibited a strong postoperative infiltration of blood-derived leukocytes within the *ME* (Fig. S2c) and impaired GI-transit time (Fig. S2d), confirming regular induction of POI. Since we expected an early activation of EGCs after surgery, we then analyzed another group of the *Sox10*$^{CreERT2+}$*xRpl22*$^{HA/+}$ mice at an early postoperative time point (IM3h). Bulk-RNA-Seq analyses of HA-precipitated EGC-specific mRNA revealed significant gene enrichment within the terms "*IL-1-signaling*", "*migration*", and "*inflammation*" (Fig. 2e). Heat maps for these GO-terms confirmed the activation pattern for an inflammatory

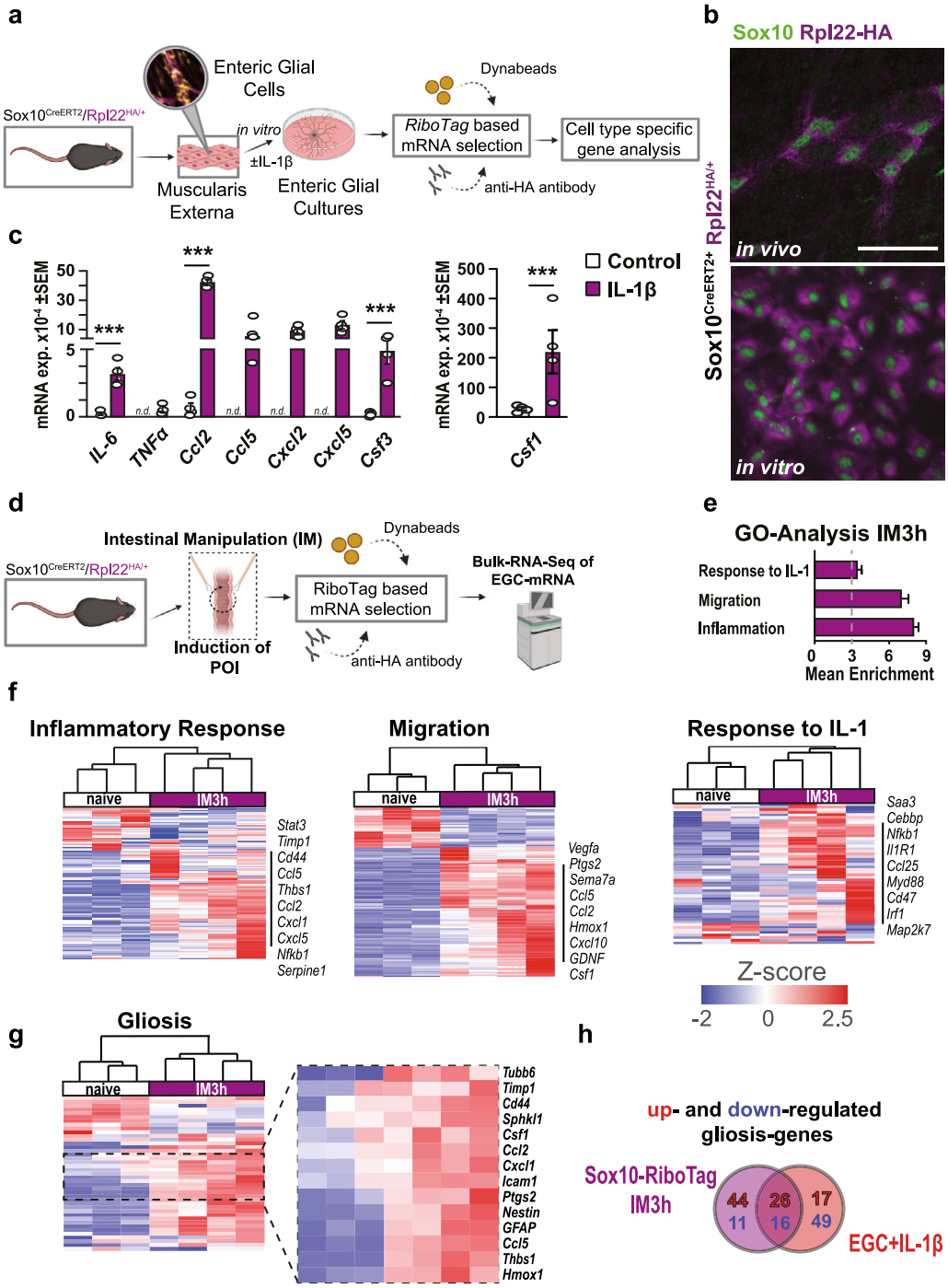

Fig. 2 IL-1-induced enteric gliosis resembles the EGC reactivity profile after surgical trauma. a Schematic overview of the *RiboTag* method applied in primary EGCs treated with IL-1β (10 ng/ml) or vehicle (control) for 3 h and processed for qPCR. $n = 4$ per group. **b** Representative immunofluorescence microscopy for EGCs (SOX10$^+$, green) and the *RiboTag* (HA$^+$, violet) in vivo (small intestine *ME*) and in vitro (EGC cultures) from *Sox10*$^{CreERT2+}$-*Rpl22*$^{HA/+}$ mice. Scale bar 50 µm. **c** qPCR analysis for gliosis-associated genes in primary EGCs treated with IL-1β. Bars showing mean gene expression compared to 18S. $n = 4$. **d** Schematic overview of the *RiboTag* method applied in the POI animal model. *Sox10*$^{CreERT2+}$-*Rpl22*$^{HA/+}$ mice underwent intestinal manipulation to induce POI, and EGC-specific mRNA was immunoprecipitated and used for bulk-RNA-Seq. $n = 3$–4 per group. **e** GO analysis of enriched genes at IM3h. **f** Heat maps of genes involved in "inflammatory response", "response to IL-1", and "migration". **g** Heat map of genes involved in "gliosis" highlighting the induced gene panel. **h** Venn-diagram of differentially expressed gliosis genes in IL-1β-treated EGCs and *Sox10*$^{CreERT2+}$-*Rpl22*$^{HA/+}$ mice at IM3h. Statistics were done with Student's *t*-test. ***<0.001, * were compared to untreated EGC cultures.

response, as well as genes involved in migration and IL-1 responsiveness (Fig. 2f). Applying our enteric gliosis gene panel, we discovered an overlap of multiple IL-1-induced and IM-induced genes in EGCs. A heat map visualized the shared, induced genes, including inflammatory mediators (e.g., *Ccl2*, *Ccl5*, *Cxcl1*), structural proteins (e.g., *GFAP*, *Nestin, Tubb6*), activation markers (e.g., *Cd44*, *Icam1*, *Hmox1*), and growth factors (*Csf1*, *Csf3*) (Fig. 2g). A Venn-diagram showed the exact transcriptional overlap in gliosis genes between IL-1β-stimulated EGCs and the reactive EGC phenotype induced by surgical trauma (Fig. 2h and Table S6). More than 20% of the up-and downregulated gliosis genes overlapped, revealing IL-1 as a substantial part of surgery-induced EGC reactivity in vivo.

EGC-restricted IL1R1 deficiency prevents postoperative macrophage activation and protects mice from POI. Given that IL-1 induces EGC reactivity in POI, we next analyzed the functional significance of IL-1-triggered EGC gliosis on POI development. We subjected mice with an EGC-restricted IL1R1-deficiency ($GFAP^{cre}xIL1R1^{fl/fl}$, Fig. S3a) and IL1R1 competent control mice ($GFAP^{WT}xIL1R1^{fl/fl}$) to IM (Fig. 3a). To validate IL1R1-deficiency, we analyzed $GFAP^{Cre+}xAi14^{fl/fl}$ mice by immunohistochemistry for SOX10 and tdtomato expression, which confirmed a 95% overlay between the glial marker and the transgenic signal, thereby validating *Gfap* as a suitable Cre-promotor for a reliable IL1R1-deficiency in EGCs (Fig. S3b). Next, we performed bulk-RNA-Seq analysis on IM3h *ME* of conditional KO mice and wild-type littermates. The PCA plot revealed a clear separation between both groups (Fig. 3b), with 287 upregulated and 437 downregulated genes in $GFAP^{cre}xIL1R1^{fl/fl}$ mice (Fig. S3c). Genes listed under the GO-terms "glial activation", "IL-1-signaling", "migration", and "inflammatory response" were enriched and more expressed in IL1R1 competent mice (Fig. 3c). A heat map of all differentially expressed genes ($p < 0.05$) revealed the downregulation of distinct gliosis genes in $GFAP^{cre}xIL1R1^{fl/fl}$ mice at IM3h, e.g., chemokines (*Ccl2*, *Cxcl1*, *Cxcl2*, *Ccl7*) and structural proteins (*GFAP*, *Cx43*, *Tubb6*) (Fig. 3d). To validate if these transcriptional alterations also affect the postoperative inflammation and the clinical outcome of POI (i.e., slow GI transit), we quantified the postoperative GI-transit and leukocyte infiltration 24 and 72 h after IM. Impressively, $GFAP^{cre+}xIL1R1^{fl/fl}$ mice were almost entirely protected from postoperative motility disturbances 24 h after IM (Fig. 3e), and leukocyte infiltration was severely reduced by more than 50% for myeloperoxidase$^+$ and 45% for CD45$^+$ leukocytes compared to $GFAP^{WT}xIL1R1^{fl/fl}$ mice (Figs. 3f and S3d). Gastrointestinal motility did not differ between genetically modified mouse strains (Fig. 3e) and C57BL6 wild-type mice upon surgery. Flow cytometry analyses confirmed reduced leukocyte infiltration by diminished numbers of F4/80$^+$ monocyte-derived macrophages, Ly6C$^+$ monocytes, activated (CD68$^+$) *ME*-Macs, and Ly6G$^+$ neutrophils in $GFAP^{cre+}xIL1R1^{fl/fl}$ mice (Figs. 3g and S3d). Notably, confocal microscopy confirmed decreased numbers of MHCII$^+$ leukocytes around ENS ganglia in the postoperative *ME* of $GFAP^{cre+}xIL1R1^{fl/fl}$ mice (Fig. 3h), an effect probably based on the diminished expression of chemokines by EGCs. Indeed, a *NanoString* inflammatory panel revealed a severely diminished gene expression of inflammatory mediators (e.g., *Ccl2*, *Cxcl2*, *Cxcl5*), cytokines (e.g., *IL-6*), and a macrophage activation marker (*Arg1*) in the postoperative *ME* of $GFAP^{cre+}xIL1R1^{fl/fl}$ mice (Fig. 3i). In line, the postoperative increase of immune cell activation markers (*CD68*, *Mip-1a*, *Csf1*, *Csf3*), as well as gliosis markers (*IL-6*, *Ccl2*, *Nestin*, and *GFAP* was abrogated in $GFAP^{cre+}xIL1R1^{fl/fl}$ mice (Figs. 3j and S3e). Notably, similar results were observed in $GFAP^{cre}xMyd88^{fl/fl}$ mice, with an EGC-restricted Myd88-deficiency, an essential adaptor molecule in the IL1R1 pathway. $GFAP^{cre+}xMyd88^{fl/fl}$ mice showed comparable downregulated gene expression patterns as $GFAP^{cre+}xIL1R1^{fl/fl}$ mice and were protected from POI (Fig. S3f + g).

Based on these data, we conclude that an IL-1-mediated macrophage-glial interaction might be critical in POI development.

Intestinal organotypic cultures demonstrate IL-1-dependent involvement in ME-Mac-EGC interactions. Previously, we and others have shown that resident *ME*-Macs also play a critical role in POI. The close anatomical relation between EGCs and resident *ME*-Macs and the multiple immune mediators released by EGCs that can activate macrophages indicate that these cells communicate with each other, and EGCs might influence *ME*-Mac activation. However, upon surgical manipulation, inflammation attracts monocyte-derived macrophages that can hardly be distinguished from resident *ME*-Macs. In order to focus exclusively on the latter's response, we established an in vitro intestinal organotypic culture (IOC) model that closely reflects the resident in vivo cell composition and structures without being compromised by infiltrating immune cells. An aseptic separation procedure of the mouse jejunum *ME* was used to simulate the mechanical activation after surgical trauma. Separated *ME* specimens were either directly used as controls or cultivated for 3 h, reflecting the IM3h time point of the in vivo model (Fig. 4a). Notably, the separation procedure produced a stronger immune response in the *ME* than the gentle in vivo IM, which was indicated by the increased gene expression of gliosis genes in IOCs than in vivo manipulated ME after 3 h (Fig. S4a). Immunofluorescence microscopy for the activation marker FOSb as well as SOX10 and β-3-tubulin (TUBB3) showed intact and activated FOSb$^+$ EGCs after 3 h incubation but no activation in control *ME* (Fig. S4b). Strong *Fosb* induction was confirmed by qPCR (Fig. S4c). Interestingly, after the 3 h incubation period, we counted significantly more activated CD68$^+$ *ME*-Macs around enteric ganglia (Figs. 4b + c and S4d). Moreover, 3D reconstruction identified the near localization of CD68$^+$ *ME*-Macs around enteric ganglia (Fig. S4e). In line with our in vivo POI mouse data, qPCR measurements of established markers for gliosis (*Nestin*, *GFAP*), intestinal inflammation (*IL-6*, *IL-1β*, *Ccl2*), and immune cell activation (*Mip-1a*, *CD68, Csf1*, *Csf3*), showed significant induction in the 3 h cultured IOCs (Fig. 4d). We transferred this model also to IOCs generated from $GFAP^{cre+}xIL1R1^{fl/fl}$ and their Cre-negative littermates. The former showed a weaker induction of gliosis, intestinal inflammation, and immune cell activation genes (Fig. 4e), indicating that the absence of EGC-specific IL-1-signaling reduces the trauma-induced *ME*-Mac activation.

The impact of EGC-derived factors on macrophage function. To further elucidate the interactions of EGCs and *ME*-Macs, we treated primary EGCs with IL-1β or vehicle and transferred the conditioned media (CM) to IL1R1-deficient bone-marrow-derived macrophage (BMDM) cultures (Fig. 5a). The primary EGC cultures consist of at least 80% glia and low amounts of neurons (Fig. S5a) and fibroblasts, verified by ICC[20] and RNA-Seq analysis for relevant cell type markers (Fig. S5b). To verify the IL-1-induced gliosis and routinely perform quality control of the CMs, we measured protein levels of prominent inflammatory markers, IL-6 and CCL2 (Fig. S5c). Moreover, to confirm that only the EGCs in our primary cultures react to the IL-1-activation by releasing inflammatory mediators, we generated primary EGCs from $GFAP^{Cre+}xIL1R1^{fl/fl}$ and $GFAP^{WT}xIL1R1^{fl/fl}$ mice. $GFAP^{Cre+}$ EGC cultures showed lower expression of inflammatory mediators on protein (Fig. S5d) and mRNA (Fig. S5e) levels,

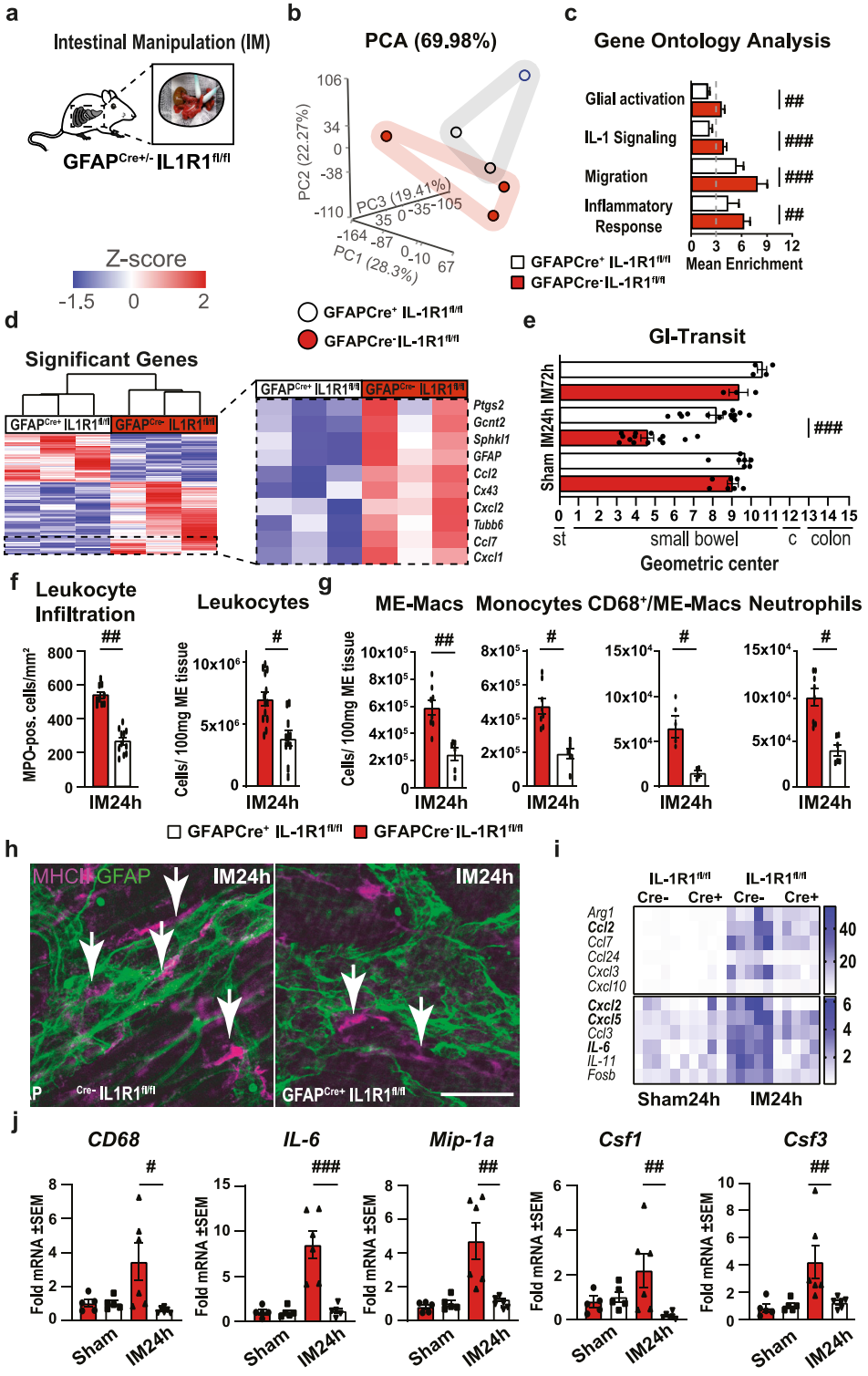

proving that these factors are released by EGCs into the CM after IL-1 treatment ($CM^{IL\text{-}1}$).

After 3 h treatment with the EGC-conditioned media, BMDMs were analyzed by bulk-RNA-Seq. The resulting PCA demonstrated a clear separation of the groups (Fig. 5b). Notably, we already observed altered functionality between naïve BMDMs and those treated with CM of vehicle-treated EGCs (CM^{Veh}). This effect was even more pronounced in BMDMs treated with the $CM^{IL\text{-}1}$ (Fig. S5f), resulting in 762 up- and 1656 downregulated genes (Fig. 5c). Within the list of differentially expressed genes, classical M1 (*Il1b*, *Tlr4*, *Sphk1*) and M2 (*Arg1*, *Socs3*, *Tgfb1*) markers showed that IL-1-triggered EGC factors affect the

Fig. 3 EGC-restricted IL1R1 deficiency prevents postoperative macrophage activation and protects mice from POI. a–d GFAP^{Cre+}-IL1R1$^{fl/fl}$ and GFAP^{Cre-}-IL1R1$^{fl/fl}$ mice underwent intestinal manipulation (IM) to induce POI. After 3 h, RNA of the ME was processed for bulk-RNA-Seq. $n = 3$ per group. **b** PCA plot of Cre$^+$ and Cre$^-$ groups. **c** GO enrichment analysis at IM3h comparing Cre$^+$ and Cre$^-$ animals, normalized to respective sham mice. **d** Heat map of differentially expressed genes highlighting induced gliosis genes. **e–j** GFAP^{Cre+}-IL1R1$^{fl/fl}$ and GFAP^{Cre-}-IL1R1$^{fl/fl}$ mice were analyzed at IM24h. **e** GI-transit analysis in IM72, IM24h, and sham24h groups of Cre$^+$ and Cre$^-$ mice. $n = 7$ (Sham); 14 (IM24h); 3–4 (IM72h). **f** Leukocyte infiltration quantification by MPO histology and FACS in IM24h groups of Cre$^+$ and Cre$^-$ mice. $n = 10$ per group. **g** FACS analysis for *ME*-Macs (CD45$^+$, F4/80$^+$), monocytes (CD45$^+$, Ly6C$^-$, Ly6G$^+$), activated ME-Macs (CD68$^+$, F4/80$^+$), and neutrophils (CD45$^+$, Ly6C$^+$, Ly6G$^-$) in IM24h groups of Cre$^+$ and Cre$^-$ mice. $n = 5$ per group. **h** Representative immunofluorescence microscopy of *ME* whole mounts showing EGCs (GFAP$^+$, green) and ME-Macs (MHCII$^+$, violet) in IM24h groups of Cre$^+$ and Cre$^-$ mice. Scale bar 50 µm. **i, j** Gene expression analysis by inflammatory *NanoString* panel (**i**) and by qPCR (**j**) for genes related to inflammation (*IL-6*) and immune cell activation (*CD68, Mip-1a, Csf1, Csf3*) at IM24h in Cre$^+$ and Cre$^-$ mice, normalized to corresponding sham groups. $n = 5$ per group. Statistics were done with Student's *t*-test and Fisher's exact test. # < 0.05, ## < 0.01, ###<0.001, # were compared to Cre$^-$ littermates.

macrophage polarization status. GO analysis and heat maps displayed substantial changes in gene clusters for "migration", "phagocytosis", and "inflammatory response" (Fig. 5d + e). Consequently, we analyzed EGC-CM-treated BMDMs for migration and phagocytosis, with the FCS treatment as a positive control. In wound-healing and transwell assays, we observed increased migration of BMDMs treated with CM^{IL-1} compared to control and CM^{Veh} (Figs. 5f + g and S5g). Phagocytosis, measured by FITC-dextran uptake after 2 h, was also increased (Fig. 5h). Overall, our data indicate that EGCs already affect macrophage function and polarization under resting conditions; however, macrophage activation and functionality are far more altered by factors released from IL-1β-stimulated EGCs.

Enteric gliosis and IL-1-signaling are involved in acute intestinal inflammation after abdominal surgery. Finally, we validated the existence of IL-1-dependent enteric gliosis in humans. Histology on intraoperatively taken jejunal specimens from patients undergoing open abdominal surgery for pancreatic head resection confirmed the close association of CD68$^+$ *ME*-Macs and GFAP$^+$ EGCs in the *ME* (Fig. 6a) and a strong IL1R1 expression in EGCs (Fig. S6a + b). Notably, this oncological surgery allowed the collection of tumor-free bowel samples at an early and a late time point during surgery (Fig. 6b). By validating the enteric gliosis status in the patient samples, we discovered the induction of inflammatory mediators (*IL-1α, IL-1β, IL-6*, *CCL2*, *CXCL2*), immune cell activators (*CSF1*, *CSF3*, *MIP-1a*), and EGC gliosis markers *(GFAP*, *NESTIN)* (Figs. 6c and S6c), previously identified in our mouse studies. To expand our understanding of ongoing mechanisms in the tissue after surgery, we performed bulk-RNA-Seq on early and late intraoperatively taken jejunal *ME* specimens and found more than 400-differentially regulated genes (Fig. 6d + e). In line with our murine data sets, gene clusters associated with "glial activation", "IL-1-signaling", "migration", and "inflammatory response" were enriched in intestinal samples from late surgery time points (Fig. 6f), correlating with corresponding heat maps (Fig. S6d). Moreover, heat map visualization of significantly regulated genes ($p < 0.05$) revealed the upregulation of distinct gliosis genes, e.g., chemokines (*CCL2*, *CXCL2*), structural proteins (*TUBB6*), and activation markers (*HMOX1*, *SOCS3*, *ICAM1*) during surgery (Fig. 6g), indicating the manifestation of enteric gliosis during surgery. To validate the effect of IL-1 on surgical samples, we prepared human jejunal IOCs from late collected patient material and incubated them with the IL1R1-antagonist anakinra for 24 h, previously used in vivo in the POI model[6]. Anakinra-treated human IOCs showed lower expression of CCL2 and IL-6 (Fig. S6e), indicating a dampened inflammatory activation response. We finally tested if primary human EGC cultures also become reactive upon IL-1β-stimulation (Fig. 6h). We detected induction of inflammatory mediators such as *IL-6*, *TNFα*, *CCL2*, *CXCL2*, and *IL-8* on mRNA level (Fig. 6i) as well as IL-6, and CCL2 on protein level (Fig. S6f) after IL-1β treatment, underlining that the gliosis phenotype is conserved across species.

Together, our data demonstrate that enteric gliosis is also induced in patients and that IL-1 induces EGC reactivity and production of various mediators that can modulate *ME*-Mac activation and functionality, thereby guiding postoperative intestinal inflammation and POI.

Overall, our investigation demonstrates that IL-1 induces a reactive phenotype in mouse EGCs. This distinct enteric gliosis state is part of the postoperative immune cascade in the *ME* in both mice and humans, and an EGC-restricted IL1R1 deficiency ameliorates POI in mice. Furthermore, mediators released by reactive EGCs alter the phenotype and function of resident *ME*-Macs towards an activated macrophage type with stronger migratory and phagocytic capabilities.

Discussion

Over the last 2 decades or so, the role of glial cells evolved from "giving structural support" to "issuing orders", especially after trauma and under inflammatory conditions, with a multitude of examples in the central[21] and enteric nervous system[11]. The present study advances our understanding of the molecular mechanisms in EGCs in an inflamed gut, and it provides an assessment of the communication between EGCs and macrophages during acute intestinal inflammation in POI. In particular, we demonstrate that EGCs acquired a reactive phenotype after surgical trauma and defined this reactive state as enteric gliosis. A key discovery is that IL1R1-signaling is a critical driver of EGC reactivity in this process. Furthermore, we found that reactive EGCs communicate with intestinal *ME*-Macs, whose cellular functions become altered towards an activated phenotype, characterized by increased migratory and phagocytic activity. Selective disruption of IL1R1-signaling in EGCs prevented reactive gliosis and protected mice from postoperative *ME* inflammation, motility disturbances, and POI.

Previously, we revealed that a pan-IL1R1 deficiency protected mice from postoperative bowel wall inflammation[6]. Our study added IL-1 signaling to a list of key factors in immune-mediated motility disorders that are used as an indicator for a successful therapy like the cytokine IL-6[30], which is also induced by IL-1[6,29], or TNFα, which is essential in the later stages of POI[37]. In POI development, various inflammatory mediators, like danger-associated molecular patterns (DAMPs: e.g., ATP[20] and IL-1α[29]) and pathogen-associated molecular patterns (PAMPs: e.g., dsRNA[7], and LPS[38]), play an essential role and contribute to the disease progression[39]. However, our recent work highlighted that IL1R1 is expressed on EGCs, and discovered that IL-1-signaling in EGCs might be a key component in intestinal inflammation and motility impairment after abdominal surgery[6].

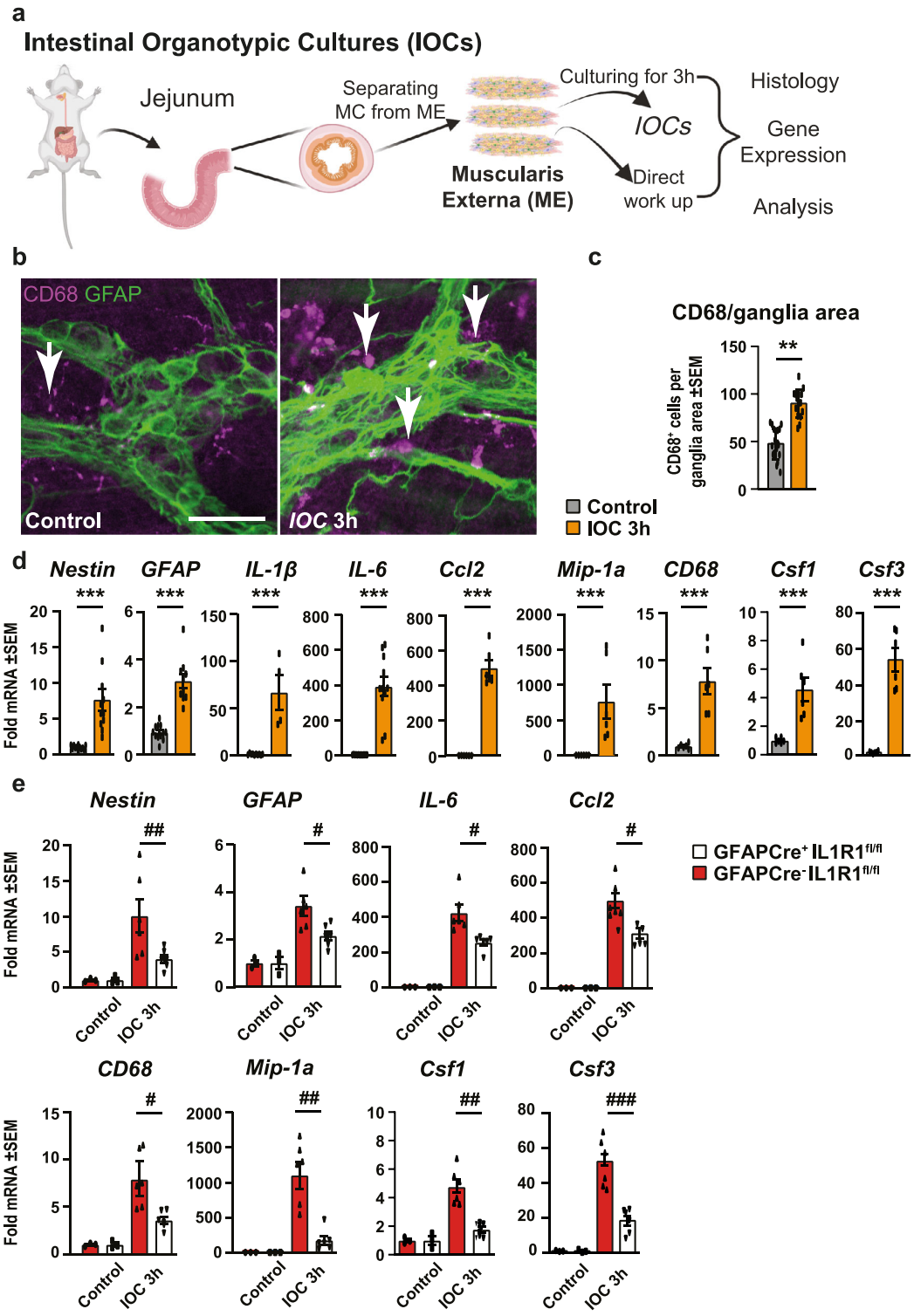

Herein, we now proved the importance of glial IL1R1-signaling with several transgenic mouse models that allowed us to precisely analyze and modify EGC reactivity in vivo and in vitro. One of these models is the *Sox10*$^{CreERT2+}$*xRpl22*$^{HA/+}$ (*RiboTag*) mouse, suitable for generating an in vivo "snapshot" of actively transcribed RNA selectively in EGCs[34,36]. Analysis of *RiboTag* mice confirmed that IL1R1-signaling is part of post-operative EGC reactivity. Around 2/3 of upregulated genes overlap between IL-1β-stimulated EGCs in vitro and the reactive EGC phenotype induced by IM in vivo. We conclude that an IL-1-induced EGC reactivity is a major trigger of surgery-induced enteric gliosis.

Fig. 4 Intestinal organotypic cultures demonstrate IL-1-dependent involvement in ME-Mac-EGC interactions. a Experimental workflow scheme. Intestinal organotypic cultures (IOC) from *muscularis externa* (*ME*) were prepared from C57BL/6 wild-type mouse jejunum by surgical dissection of the *lamina propria* and mucosa tissue, a procedure that mimics the surgical trauma in vivo. This model allows the analysis of resident cell types in the absence of any infiltrating blood-derived immune cells. IOCs were either directly processed or incubated for 3 h, corresponding to the IM3h time point in the POI mouse model. $n = 6$ per group. **b**, **c** Histological visualization (**b**) and quantification (**c**) of activated macrophages ($CD68^+$, violet) surrounding enteric ganglia (GFAP+, green). $n = 5$ mice per group; quantifying ganglia in 3–4 IOCs per mouse. Scale bar 50 µm. **d** Gene expression analysis in IOCs by qPCR for genes involved in "enteric gliosis" (*Nestin, GFAP*), *inflammation* (*IL-1β, IL-6, Ccl2*), and *immune cell activation* (*Mip-1a, CD68, Csf1, Csf3*). **e** IOCs were prepared from $GFAP^{Cre+}$-$IL1R1^{fl/fl}$ and $GFAP^{Cre-}$-$IL1R1^{fl/fl}$ mice according to the same experimental workflow shown in **a** and either directly processed or incubated for 3 h. Gene expression analysis by qPCR for genes involved in "enteric gliosis", "inflammation", and "immune cell activation". $n = 3$–8 per group. Statistics were done with Student's *t*-test. */#<0.05, **/##<0.01, ***/###<0.001, All * compared to control IOCs, all # compared to Cre^- littermates.

Further evidence for stimulus-selective reactivity in EGCs comes from the comparison of IL-1β- and ATP-stimulated EGCs. We recently showed that ATP induces enteric gliosis[20]. Compared to ATP, IL-1β caused a stronger induction of several chemokines, suggesting a specific role in reactive processes upon surgery. These findings imply that the term "reactive glia", commonly used to describe a general glial activation, does not represent a hardwired phenotype as it depends on the specific stimulus. However, some genes were upregulated in ATP-and IL-1β-stimulated EGCs, including *IL-6*, *Cxcl1*, and *Cxcl2*, prominently induced in astrogliosis[40], and *Hmox1*, a marker for neurodegeneration[41] and reactive glial cells[42]. These genes might be part of an overarching response found in multiple reactive EGC phenotypes, pointing to a core gliosis signature across various organs and stimuli. Future comparisons of enteric gliosis signatures from other glial cell populations as well as other diseases might help to specify both the core gliosis signature and the stimulus- and disease-specific responses of reactive glial cells. Usage of published data sets from activated EGCs under inflammatory conditions (infection[35] and colitis[36]) showed that IL-1 induced gliosis shares induced genes and shows individual molecular responses. However, the available data were collected with different approaches, mouse models, intestinal parts, and transcriptional analysis methods, providing only a rough initial idea of core genes and conditions leading to specific gliosis expression patterns. More comprehensive comparisons with multiple conditions are required and expected to be published in the future to allow reliable conclusions on core and conditions-specific gliosis signatures.

Given that IL-1-signaling induced the expression of a variety of immune mediators, which might preferably act on immune cells located in anatomical proximity, we focused on the interactions of EGCs and *ME*-Macs. These *ME*-Macs have previously been shown to be crucial in the postoperative immune response in POI[5,37,43]. An ex vivo IOC model allowed us to explicitly focus on the EGCs and ME-Macs interaction. In manipulated IOCs, we found an upregulation of several molecules depending on glial IL1R1-signaling known to act on macrophages and affect their function. Among these genes, we found unspecific macrophage activation markers (*Mip1* and *CD68*) and members of the *Csf1* family (*Csf1* and *Csf3*), which exert distinct functions on macrophage differentiation.

Furthermore, CSF1 was described as an essential factor in maintaining *ME*-Macs[44]. Although enteric neurons were first identified as a CSF1 source in the intestine[27], a recent study by the Gulbransen group showed that EGCs produce more *Csf1* than enteric neurons in a colitis model[28]. They also showed that IL-1 triggers CSF1 release from EGC cultures in vitro *and* increases MHCII and CD68 expression in BMDM cultures. Our IOC model and in vivo data add to this hypothesis, showing that EGCs indeed produce CSF1 and activate *ME*-Macs in their native environment. Notably, the IOCs' initial immune response was stronger than the in vivo manipulated ME response at 3 h after mechanical separation or surgical manipulation. We interpret this difference as a consequence of an increased release of additional factors due to the stronger mechanical forces applied to the IOCs during their preparation than the more gentle in vivo ME manipulation. These mediators might trigger additional immune responses independent of IL-1 release.

Consequently, IL1R1 depletion or antagonism does not dampen the cytokine production and EGC activation in the IOC model to the same extent as in the more gentle in vivo surgical manipulation approach. Here, it should be noted that the IOC does not fully reflect POI as it is missing important characteristics of POI development. First peripheral innervation of the SNS and PNS, known to modulate the ME immune response to surgery, is missing. Secondly, and more critical for the later inflammatory phase IOCs do not become infiltrated by blood-derived leukocytes, which extravasate into the *ME* after surgical manipulation. For these reasons, IOCs do not represent an ex vivo POI model but a suitable model for studying local tissue responses to mechanical or surgical trauma without systemic stimuli. Research using *ME* IOCs might be a tool to investigate how the tissue can immunologically respond in vitro to what might affect molecular and functional measurements, e.g., in pharmacological and physiological studies, respectively.

Another interesting molecule expressed by EGCs in an IL-1-dependent manner is *Csf3*. Compared to other members of the *Csf* family, *Csf3* is less well studied, and to date, it has been linked to neutrophil migration and activation[45,46]. As we also observed a prominent induction of the neutrophil chemokines *Cxcl2* and *Cxcl5* and a significant reduction of infiltrating neutrophils in $GFAP^{Cre}$x$IL1R1^{fl/fl}$ mice after surgery, EGCs might indeed affect the recruitment and maybe even the function of these cells. As neutrophils are not present at the beginning of intestinal surgery and instead infiltrate at later stages, an interaction of reactive EGCs with these infiltrating immune cell populations is likely and warrants future investigation. Importantly, recent studies showed that *Csf3* is able to alter macrophage polarization in vitro[47] and induce the expression of regulatory macrophage markers in DSS-colitis[48]. In breast cancer, *Csf3*-signaling also caused immunosuppressive behavior in macrophages[49], making *Csf3*, next to *Csf1*, one of the most promising EGC-released factors that impact the state and function of *ME*-Macs and/or infiltrating monocyte-derived macrophages.

EGC-selective IL1R1-deficiency completely abolished the expression of all the mediators directly acting on macrophages (i.e., Csf1, Csf3, Cxcl1, Cxcl2, Il6, Ccl2, and Mip1α), we expected that this would also alter macrophage transcriptomes and function. The capacity of EGCs to induce inflammatory responses in macrophages was indeed confirmed by RNA-Seq analysis showing changes in the inflammatory response and the expression of M1 and M2 markers. In addition to the general induction of immune responses, genes shaping essential macrophage functions

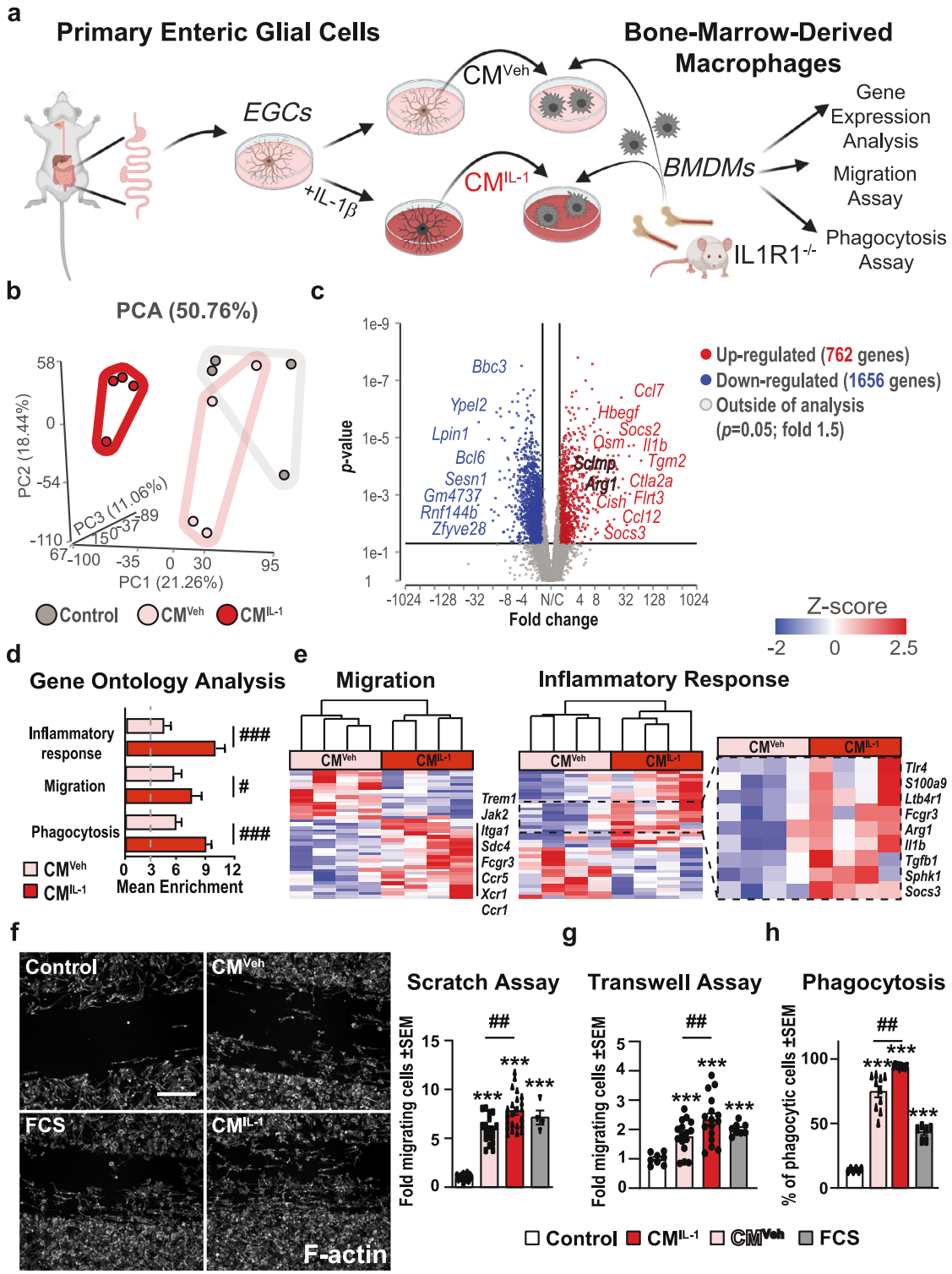

like migration and phagocytosis were also transcriptionally altered in response to reactive EGC-released factors. The accumulation of CD68^{+} *ME*-Macs around enteric ganglia and their morphological changes towards a round-shaped cell type showed that *ME*-Mac migration and activation are increased upon exposure to EGC-derived mediators. Similar to microglia in the CNS, the attraction of *ME*-Macs to the vicinity of enteric ganglia might be part of a protective mechanism involving either rapid clearance of neuronal debris or neuroprotective features against excessive inflammatory responses to restore intestinal function. Increased resident macrophage accumulation at sites of neuronal damage is also observed in models of spinal cord[50] and brain

Fig. 5 The impact of EGC-derived factors on macrophage function. a Schematic overview showing the generation of primary EGCs and production of $CM^{IL\text{-}1}$ (EGCs treated with IL-1β (10 ng/ml) for 24 h) and CM^{Veh} before transferring CM to Bone-marrow-derived macrophages (BMDMs). BMDMs were isolated from $IL1R1^{-/-}$ mice to exclude any side effects of IL1β-residues in the collected $CM^{IL\text{-}1}$. After BMDM maturation, cells were treated with $CM^{IL\text{-}1}$, $CM^{Veh,}$ or were left untreated for 3 h (RNA-Seq) and 24 h (functional assays). **b** Bulk-RNA-Seq analyses of BMDMs after 3 h incubation showed a separation between the three treatment groups in a PCA plot. $n = 4$ per group. **c** Volcano plot from bulk-RNA-Seq analyses of BMDMs after 3 h treatment with $CM^{IL\text{-}1}$ or CM^{Veh} highlighting the top 20 regulated genes (Fold 2, *p*-value 0.05). **d**, **e** GO enrichment analysis in BMDMs after $CM^{IL\text{-}1}$ and CM^{Veh} stimulation and heat maps of genes involved in "migration" and "inflammatory response" highlighting induced genes related to macrophage function. **f**–**h** BMDMs were processed 24 h after CM incubation in **f** scratch ($n = 4$ independent BMDM cultures; multiple technical replicates per culture; Control (20 readings); CM^{Veh} (20 readings); $CM^{IL\text{-}1}$ (20 readings); FCS (4 readings). **g** transwell ($n = 3$ independent BMDM cultures; multiple technical replicates per culture; Control (8 readings); CM^{Veh} (16 readings); $CM^{IL\text{-}1}$ (16 readings); FCS (8 readings), and **h** phagocytosis ($n = 3$ independent BMDM cultures; multiple technical replicates per culture; Control (6 readings); CM^{Veh} (10 readings); $CM^{IL\text{-}1}$ (10 readings); FCS (6 readings) assays. Scale bar 100 µm. Statistics were done with Student's *t*-test and Fisher's exact test. */#<0.05, **/##<0.01, ***/###<0.001, All * compared to control BMDMs, all # compared to CM^{Veh}-treated BMDMs.

injury[51,52], wherein microglia, the CNS counterparts of *ME*-Macs, accumulate in the damaged areas. Support for increased clearance of dying cells or debris comes from our observation that IL-1-triggered EGCs stimulate phagocytosis in macrophages. As ENS homeostasis is well-ordered by apoptosis and neurogenesis[53], an enhanced elimination of damaged neurons or their protection from excessive inflammation by phagocytosis of cell debris might be a conserved mechanism. Indeed, a neuroprotective role of *ME*-Macs during homeostasis[22] and infection has recently been shown[54]. When enteric gliosis is a key element of this neuroprotective response, a logical argumentation would be that its blockage might have detrimental effects. However, as we observed a clear improvement of POI and a reduction of postoperative inflammation by inhibiting IL1R1-mediated enteric gliosis, we suppose that neuroprotective mechanisms might play a minor role during acute postoperative inflammation and that compensatory pathways are activated to maintain this function. Another possibility is that *ME*-Mac migration to ganglia might be fundamentally a protective homeostatic mechanism, although a stronger reactive glial cell phenotype with more surgical trauma may cause an exaggerated response and activation of macrophages to act instead in a detrimental way to exacerbate the inflammatory response. Our previous work[5] and other investigators[31] have provided evidence that activated macrophages are essential contributors to the development of POI. We propose that glial IL1R1 knockout may protect mice from POI by causing a milder macrophage induction in these mice. However, a causative link between glia-to-macrophages-to neurons has not yet been established in our study for the glial IL1R1 knockout model and the resolution of the GI-transit phenotype in the POI model in $GFAP^{Cre}xIL1R1^{fl/fl}$ animals does not necessarily depend on a milder macrophage induction and glial-to-macrophage signaling. An alternative hypothesis to be tested is that IL1-induced EGCs directly influence enteric neurons that control peristalsis to cause POI and that a glial IL1R1 knockout prevents it. Recent studies show that EGCs can interact with enteric neurons, triggering cell death[55,56], neuronal dysregulation[57], and homeostasis functions[58]. These interesting questions need to be addressed in future studies. Notably, different subtypes of *ME*-Macs with different innate responsiveness have recently been described by us[7], and previous single-cell-RNA-Seq studies revealed four distinct clusters of *ME*-Macs[22]. Unfortunately, the individual subpopulation-specific cellular functions and interactions are largely unknown, and future studies have to investigate whether EGCs preferably interact with one of these distinct subtypes.

As already stated above, besides interacting with resident *ME*-Macs, EGCs might also act on infiltrating monocytes, which are non-exclusively attracted by EGC-released CCL2. CCL2 is a major chemoattractant for monocyte-derived leukocytes in POI[32,59]. Although three groups independently demonstrated that these cells do not affect POI 24 h after surgery, they are involved in the late-phase resolution, and CCR2-deficient mice (i.e., the receptor target for CCL2) recover more slowly from POI than wild-type animals[31,32,59]. This observation might point towards a potential beneficial role of EGC-derived CCL2 in POI resolution. However, in our view, this seems unlikely as we already observed a clear improvement of POI after 24 h and normalization of GI-transit after 72 h in $GFAP^{Cre+}$-$IL1R1^{fl/fl}$ mice. Hence, it is evident that there is no delay in POI at later stages.

The human data included in our study showed evidence that IL-1-signaling and enteric gliosis also occur during GI-tract surgery. Although the time between sampling of the early and late intraoperative specimen was less than 3 h, the earliest time point in our mouse studies, we observed a strong induction of cytokines and chemokines comparable to murine IL-1-triggered enteric gliosis. Notably, IL-1β was also strongly induced, and human EGCs had a strong transcriptional response, indicating a preserved mechanism of enteric gliosis in rodents and humans. Moreover, the GO analyses underlined the induction of common glial activation and immune-activating pathways. The data is translatable from mice to humans, and we conclude that the blockade of IL-1-triggered enteric gliosis might therefore prevent the development of POI in surgical patients. Previous preclinical data from our group already demonstrated that an antibody-mediated depletion of IL-1α or IL-1β or pharmacological inhibition of IL1R1 by Anakinra effectively prevented POI in mice[6]. Our findings in human IOCs, isolated from surgical patients, showing reduced IL-6 and CCL2 upon ex vivo stimulation in the presence of Anakinra, confirm our theory about an immediate EGC immune-responsiveness to IL-1 signaling. These findings emphasize our view that the initial inflammatory activation of the EGC/*ME*-Mac axis is crucial for POI development, and interaction with IL-1-signaling might be rather useful for prevention than treatment of existing POI. In line, multiple trials with Anakinra show anti-inflammatory effects in inflammation-associated intestinal diseases, such as mucositis (NCT03233776) and colorectal cancer (NCT02090101). Anakinra or other pharmacological interventions targeting IL1-signaling in EGCs could potentially serve as a prophylactic treatment in POI in surgical patients to add to the benefits of ERAS (enhanced recovery after surgery) protocols[60].

In conclusion, our study provides insights into the molecular mechanism of postoperative IL-1-triggered enteric gliosis and its consequence on the communication between EGCs and *ME*-Macs. Inhibition of this gliotic state ameliorated postoperative inflammation and protected mice from POI. Moreover, we confirmed the induction of enteric gliosis and activation of IL-1-signaling in surgical patients, supporting the idea of an intervention in the IL-1 pathway as a promising and clinically suitable strategy to prevent inflammation-induced motility disorders.

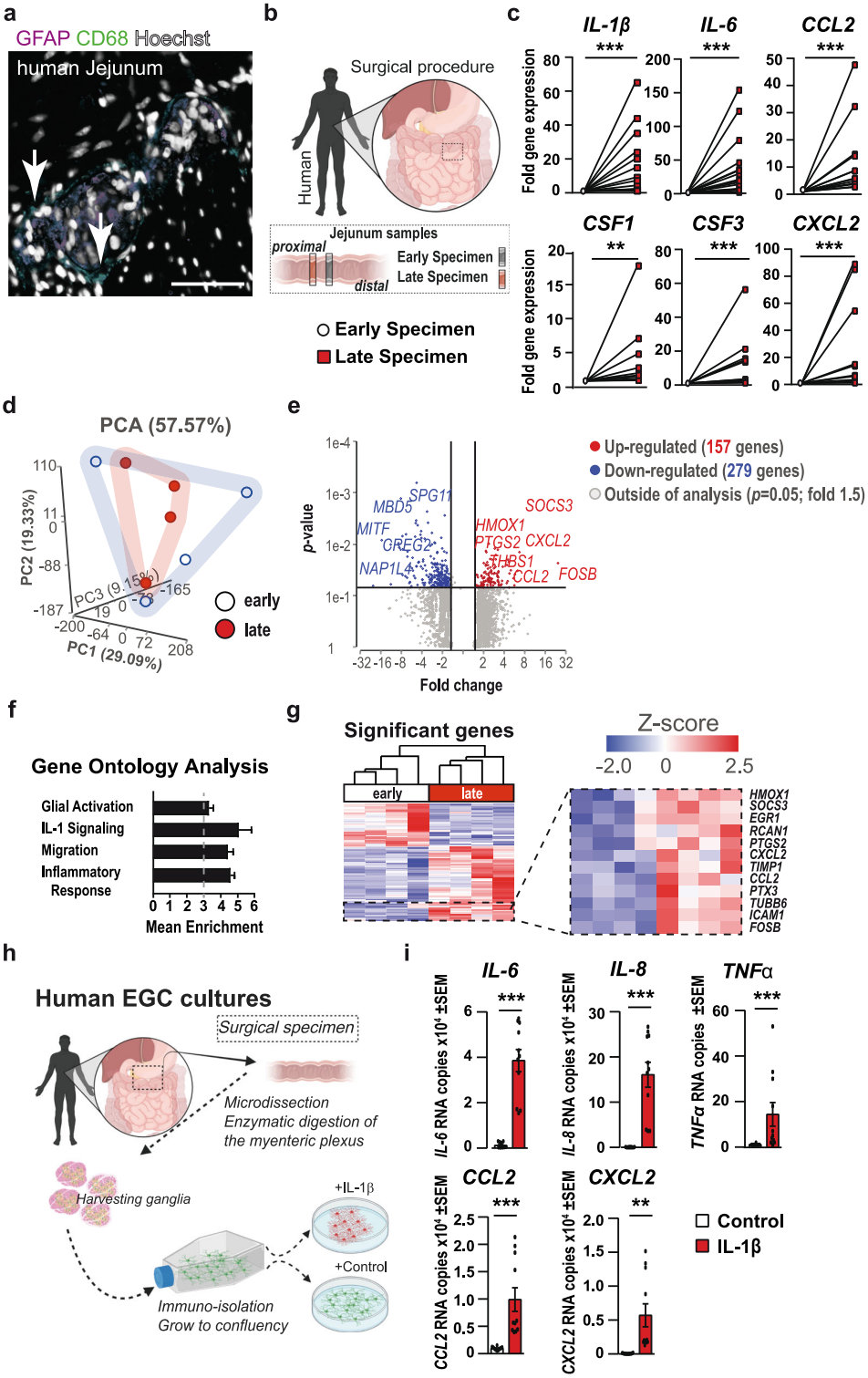

Methods

Animals. Experiments were performed using 8–12-week-old Sox10-^{CreERT2}xRpl22$^{HA/+}$ or GFAP^{cre}xIL1R1$^{fl/fl}$ mice kept in a pathogen-free animal facility with standard rodent food and tap water ad libitum. Appropriate authorities of North-Rhine-Westphalia, Germany (81-02.04.2016.A367) approved experiments.

The POI mouse model was induced by intestinal manipulation as described previously[6]. Animals were sacrificed 3 and 24 h after manipulation.

Murine enteric glia cell cultures. Primary enteric glial cell (EGC) cultures were obtained by sacrificing C57BL/6 or GFAP^{cre+} Ai14$^{fl/fl}$ mice, 8–16 weeks of age, extracting the small intestine, and cleansing it with 20 ml of oxygenated Krebs-

Fig. 6 Enteric gliosis and IL-1-signaling are involved in acute intestinal inflammation after abdominal surgery. a Immunohistochemistry for macrophages ($CD68^+$, green) and EGCs ($GFAP^+$, violet) in jejunal cross-sections. Hoechst (white) was used as counterstain. White arrows indicate ganglia-associated macrophages. Scale bar 50 µm. **b** Schematic overview showing the patient specimen collection of jejunal *ME* at an early and late time point during pancreatic head resection. **c** qPCR analysis of jejunal *ME* specimens for inflammation- and macrophage function-associated genes. $n = 10$–15; IL1β (14), IL-6 (15), CCL2 (13), CSF1 (10), CSF3 (11), CXCL2 (13). **d**–**g** Bulk-RNA-Seq analysis of jejunal *ME* specimens, including a PCA plot (**d**) and a Volcano plot visualizing differentially expressed genes (**e**) between late and early specimens ($p = 0.05$, fold: 1.5). $n = 4$. **f** GO term analysis of all differentially expressed genes between early and late specimens showed enrichment in gene clusters related to "glial activation", "IL-1-signaling", "migration", and "inflammatory response". **g** Heat map of significantly regulated genes highlighting gliosis-related genes. **h** Schematic overview of the generation and treatment of primary human EGCs from patient specimens. **i** *NanoString* analysis of primary human EGCs treated with IL1β or vehicle for 24 h. $n = 10$. Data are shown as mean RNA counts. Statistics were done with Student's *t*-test and Fisher's exact test. *<0.05, **<0.01, ***<0.001, All * compared to early *ME* specimens or untreated hEGCs.

Henseleit buffer (126 mM NaCl; 2.5 mM KCl: 25 mM NaHCO3; 1.2 mM NaH2PO4; 1.2 mM MgCl2; 2.5 mM CaCl2, 100 IU/ml Pen, 100 IU/ml Strep and 2.5 µg/ml Amphotericin). The small bowel was cut into 3–5 cm long segments and kept in oxygenated ice-cold Krebs-Henseleit buffer. Each segment was then drawn onto a sterile glass pipette, and the *ME* was stripped with forceps to collect muscle tissue for further digestion steps. After centrifugation (300xg for 5 min), the tissue was incubated for 15 min in 5 ml DMEM containing Protease Type1 (0.25 mg/ml, Sigma-Aldrich) and Collagenase A (1 mg/ml, Sigma-Aldrich) in a water bath at 37 °C, 150 rpm. The enzymatic digestion was stopped by adding 5 ml DMEM containing 10% FBS (Sigma-Aldrich), centrifugation for 5 min at 300xg, and re-suspended in proliferation medium (neurobasal medium with 100 IU/ Pen, 100 µg/ml Strep, 2.5 µg/ml Amphotericin (all Thermo Scientific), FGF and EGF (both 20 ng/ml, Immunotools). Cells in proliferation media were kept at 37 °C, 5% CO_2 for 4 days to promote the formation of enteric neurospheres. For experiments, enteric neurospheres were dissociated with trypsin (0.25%, Thermo Scientific) for 5 min at 37 °C and distributed at 50% confluency on Poly-Ornithine (Sigma-Aldrich) coated 6 well plates in differentiation medium (neurobasal medium with 100 IU/ Pen, 100 µg/ml Strep, 2.5 µg/ml Amphotericin, B27, N2 (all Thermo Scientific) and EGF (2 ng/ml, Immunotools). After 7 days in differentiation medium, mature enteric glia cells were treated with ATP (100 µM, Sigma) and IL-1 (10 ng/ml, Immunotools) and further processed for RNA isolation or their conditioned medium used for enzyme-linked immunosorbent assay (ELISA) or qPCR analysis.

Murine bone-marrow-derived macrophage cultures. Primary bone-marrow-derived macrophage (BMDM) cultures were obtained by sacrificing $IL1R1^{-/-}$ mice, 8–16 weeks of age, extracting the femoral bones and isolating bone-marrow stem cells with a syringe, and culturing the cells in RPMI supplemented with FCS (10%, Thermo Scientific), β-mercaptoethanol (1 mM, SIGMA) and 10 ng/ml rmCSF-1 (Immunotools). After 4 days in culture, the medium was changed to remove all dead cells, and on day 6, cells were used for all planned experiments.

For the scratch assays, BMDMs were transferred to 24-well plates and grown to 90% confluency. The "scratch" was performed with a 200 µl pipette tip, and damaged/dead cells were immediately removed by one wash step with PBS. BMDMs were treated with CM^{Veh}, CM^{IL-1}, neurobasal medium (NB) supplemented with 10% FCS, and NB without serum (control) for 24 h. After treatment, BMDMs were fixed with 4% PFA for 15 min and stained for F-Actin with Phalloidin FITC (Thermo Scientific) for 1 h, and processed with the fluorescence microscope Nikon TE2000 in the cell culture well plates.

For the transwell assays, BMDMs were placed in transwells (10,000 cells, Ibidi) and treated with CM^{Veh}, CM^{IL-1}, NB supplemented with 10% FBS, and NB without serum (control) for 3 h. Afterwards, transwells were fixed with 4% PFA for 15 min, and cells were stained for F-Actin with Phalloidin FITC (Thermo Scientific) and Hoechst for 1 h. Transwells were mounted on glass slights and processed with the fluorescence microscope Nikon TE2000.

For the phagocytosis assays, BMDMs were transferred to 24-well plates (10,000 cells/well) and treated with CM^{Veh}, CM^{IL-1}, neurobasal medium (NB) supplemented with 10% FBS and NB without serum (control) for 24 h. After removing the treatment medium, BMDMs were incubated with Dextran-Cascade Blue 10,000 MW (50 µg/ml, Thermo Scientific) for 1 h. Then washed two times with warmed PBS and collected by EDTA/Trypsin (0.05%) and processed by FACS analysis for high and low phagocytic cells.

Human surgical specimens. The ethics committee of the College of Medicine at the Ohio State approved the human IRB protocol[13] (Table S1).

The ethics committee of the University of Bonn, Germany, approved the collection of patient surgical specimens (*266_14*) (Table S2).

The human IRB protocol was approved by the ethics committee of the College of Medicine at The Ohio State University. Informed consent was obtained to procure viable human surgical tissue from the colon or small bowel from patients with polyps undergoing a colectomy (sigmoid colon) or patients undergoing Roux-en-Y by-pass surgery (jejunum) (Table S1). Human EGCs (hEGCs) in culture from 9 GI surgical specimens were used to study gene expression and IL1R1 immunoreactivity.

Human surgical tissue for the IOC experiments was collected from four patients undergoing pancreatectomy. Human jejunum specimens were collected in ice-cold oxygenated Krebs-Henseleit buffer during the surgical procedure and transported to the laboratory. Full-thickness jejunum specimens were incubated for 24 h with or without Anakinra (100 µg/ml) in DMEM/F12 with 10% FBS at 5%CO_2 and 37 °C. After 24 h, media were collected, centrifuged, and frozen in liquid nitrogen for ELISA analyses.

Human EGC cultures. Myenteric plexus tissue of patients was processed and cultured as described before[13,20]. Briefly, tissue collection was performed by the surgeon and immersed immediately in ice-cold oxygenated Krebs-Henseleit solution and promptly transported to the research facilities within 15 min in coordination with the Clinical Pathology Team. For isolating myenteric ganglia, tissue was pinned luminal side facing upwards under a stereoscopic microscope, and the mucosa, submucosa, and most of the circular muscle were dissected away using scissors and then flipped over to remove longitudinal muscle by dissection.

Myenteric plexus tissue was cut and enzymatically dissociated as described elsewhere (LIT) with modifications as follows: Myenteric plexus tissue was minced into 0.1–0.2 cm^2 pieces and dissociated in an enzyme solution (0.125 mg/ml Liberase, 0.5 µg/ml Amphotericin B) prepared in Dulbecco's modified Eagle's medium (DMEM)-F12, for 60 min at 37 °C with agitation. Ganglia were removed from the enzymatic solution by spinning down (twice), and re-suspending in a mixture of DMEM-F12, bovine serum albumin 0.1%, and DNase 50 µg/ml DNase (once). Solution containing the ganglia was transferred to a 100 mm culture dish, and isolated single ganglia free of smooth muscle or other tissue components were collected with a micropipette while visualized under a stereoscopic microscope and plated into wells of a 24-well culture plate and kept in DMEM-F12 (1:1) medium containing 10% fetal bovine serum (FBS) and a mixture of antibiotics (penicillin 100 U/ml, streptomycin 100 µg/ml, and amphotericin B 0.25 µg/ml) at 37 °C in an atmosphere of 5% CO_2 and 95% humidity.

After cells reach semi-confluence after 3–4 weeks (P1), hEGCs were enriched and purified by eliminating/separating fibroblasts, smooth muscle, and other cells. EGC enrichment and purification were achieved by labeling the isolated cells with magnetic microbeads linked to the anti-specific antigen, D7-Fib, and passing them through a magnetic bead separation column following the manufacturer's instructions (*Miltenyi Biotec Inc*, San Diego, CA). This purification protocol was performed twice (P2 and P3) to reach a cell enrichment of up to 10,000 fold, and 20,000 cells were plated on glass coverslips pre-coated with 20 µg/ml laminin/P-D-Lys in 50 mm bottom glass #0 culture dishes for immunostaining and imaging or 12-well plates for IL-6 or CCl2 release experiments. Cultured hEGCs were kept until confluent and harvested for additional experiments (4 to 10 days). On the day of the experiment, hEGCs were stimulated as indicated. Parallel to this, cells at each passage were split and seeded in plastic 25 mm^2 culture flasks and used for study in passages three to six.

NanoString nCounter gene expression assay. The RNA quality has been evaluated using Agilent RNA 6000 Nano Chip. NanoString nCounter technology is based on the direct detection of target molecules using color-coded molecular barcodes, providing a digital simultaneous quantification of the number of target molecules. Total (RNA 100 ng) was hybridized overnight with nCounter Reporter (20 µl) probes in hybridization buffer and excess of nCounter Capture probes (5 µl) at 65 °C for 16–20 h. The hybridization mixture containing target/probe complexes was allowed to bind to magnetic beads containing complementary sequences on the capture probe. After each target found a probe pair, excess probes were washed, followed by a sequential binding to sequences on the reporter probe. Biotinylated capture probe-bound samples were immobilized and recovered on a streptavidin-coated cartridge. The abundance of specific target molecules was then quantified using the nCounter digital analyzer. Individual fluorescent barcodes and target molecules in each sample were recorded with a CCD camera by performing a high-density scan (600 fields of view). Images were processed internally into a digital format and were normalized using the NanoString nSolver software analysis tool.

Counts were normalized for all target RNAs in all samples based on the positive control RNA to account for differences in hybridization efficiency and post-hybridization processing, including purification and immobilization of complexes. The average was normalized by background counts for each sample obtained from the average of the eight negative control counts. Subsequently, a normalization of mRNA content was performed based on internal reference housekeeping genes Gusb, TBP, NMNAT1, RBP1, STX1A, CTNNB1 using nSolver Software (NanoString Technologies, Seattle, WA).

Immunohistochemistry. Whole-mount specimens were mechanically prepared by dissection of the (sub)mucosa, fixed in 4% paraformaldehyde/PBS for 30 min, permeabilized with 1% Triton-X 100/PBS for 15 min, blocked with 5% donkey serum/PBS for 1 h, and incubated with primary IgGs mentioned in appendix Table S4 at 4 °C overnight. After three PBS washing steps, secondary antibodies (Dianova, anti-rat IgG-Cy2 1:800, anti-guinea pig IgG-Cy3, anti-chicken IgY-FITC, and anti-rabbit IgG-FITC or - Cy3 1:800 were incubated for 90 min (Table S4). Specimens were mounted in Epredia Shando Immu-Mount (Thermo Scientific) and imaged on a Leica confocal imaging system or a Nikon 2000TE fluorescent microscope.

Primary cells were fixed in 4% paraformaldehyde/PBS for 30 min, permeabilized with 0.25% Triton-X 100/PBS for 15 min, blocked with 5% donkey serum in PBS for 1 h, and incubated with primary IgGs mentioned in Table S4 at 4 °C overnight.

After three PBS washing steps, secondary antibodies (Dianova, anti-mouse IgG-Cy2 1:800, anti-guinea pig IgG-FITC, and anti-rabbit IgG-FITC or - Cy3 1:800 were incubated for 60 min. Specimens were mounted in Fluorogel-Tris and imaged using a Leica confocal imaging system or a Nikon TE 2000 fluorescent microscope.

Quantitative PCR. Total RNA was extracted from *ME* specimens at indicated time points after IM using the RNeasy Mini Kit (Qiagen, Hilden, Germany), followed by deoxyribonuclease I treatment (Ambion, Austin, TX). Complementary DNA was synthesized using the High Capacity cDNA Reverse Transcription Kit (Applied Biosystems, Darmstadt, Germany). The expression of mRNA was quantified by real-time RT-PCR with primers shown in Table S3. Quantitative polymerase chain reaction was performed with SYBR Green PCR Master Mix (Applied Biosystems, Darmstadt, Germany).

Flow cytometry (FACS). FACS analysis was performed on isolated *ME* samples of the small bowel 24 h after IM in $GFAP^{Cre}xIL1R1^{fl/fl}$ animals. Isolation of *ME* was achieved by sliding small bowel segments onto a glass rod, removing the outer muscularis circumferentially with moist cotton applicators and cutting the *ME* into fine pieces. *ME* was digested with a 0.1% collagenase type II (Worthington Biochemical, Lakewood, NJ, USA) enzyme mixture, diluted in PBS, containing 0.1 mg/ml DNase I (La Roche, Germany), 2.4 mg/ml Dispase II (La Roche, Germany), 1 mg/ml BSA (Applichem), and 0.7 mg/ml trypsin inhibitor (Applichem) for 40 min in a 37 °C shaking water bath. Afterwards single-cell suspension was obtained using a 70 µm filter mesh and cells were stained for 30 min at 4 °C with the appropriate antibodies. For antibodies used in this study see Table S4. Flow cytometry analyses were performed on *FACSCantoI*(BD Biosciences) using *FACSDiva* software and data were analyzed with the latest *FlowJo* software (Tree Star, Ashland, OR, USA).

Enzyme-linked immunosorbent assay (ELISA). Release of IL-6 and CCL2 was measured in *ME* RIPA lysates isolated from small intestine segments at the indicated time points after IM. Release of IL-6 in EGC cultures incubated with various treatments was measured at the indicated time points. All ELISAs were purchased from (Thermo Scientific) and used according to the manufacturer's instructions. Values were normalized to tissue weights or untreated EGCs. Briefly, for animal tissue, the isolated *ME* (~50 mg) was lysed with 1xRIPA buffer for 30 min, centrifuged for 30 min at maximum speed and the protein concentration was determined with a BCA kit (Thermo Scientific). 100 µg of total protein was used to measure the release of IL-6 or CCL2 in duplicates. For EGCs, cells were treated with the indicated substances for 24 h, the supernatant was collected, centrifuged at 5000 rcf for 5 min, and snap-frozen in liquid nitrogen before being processed for the IL-6 or CCL2 ELISA.

In vivo gastrointestinal transit. Gastrointestinal transit (GIT) was assessed by measuring the intestinal distribution of orally administered fluorescently labeled dextran-gavage 90 min after administration as described previously[6]. The gastrointestinal tract was divided into 15 segments (stomach to the colon). The geometric center (GC) of labeled dextran distribution was calculated as described previously. The stomach (st) correlates with a GC of 1, the small bowel correlates with a GC of 2–11, the cecum (c) correlates with a GC of 12, and the colon correlates with a GC of 13–15. GIT measurements were performed with sham and IM24h animals of $GFAP^{Cre}xIL1R1^{fl/fl}$ or $Sox10^{CreERT2}xRpl22^{HA/+}$ animals.

MPO$^+$-cell infiltration. Jejunal mucosa-free ME whole-mount specimens were fixed in ethanol and stained with Hanker Yates reagent (Polyscience Europe, Germany) to identify myeloperoxidase expressing cells (MPO$^+$). The mean number of MPO$^+$ cells/mm^2 for 5 random areas per animal was determined. MPO$^+$ measurement was performed with animals 24h after IM.

RNA-Seq. RNA samples were extracted using the RNeasy Mini Kit (*Qiagen*). RNA-Seq libraries were prepared using the QuantSeq 3′ mRNA-Seq Library Prep Kit (*Lexogen*) according to the manufacturer's instructions by the Genomics Core Facility of the University Hospital Bonn. The method has high strand specificity (>99.9%), and most sequences are generated from the last exon and the 3′ untranslated region. The technique generates only one fragment per transcript, and the number of reads mapped to a given gene is proportional to its expression. Fewer reads than in classical RNA-seq methods are needed to determine unambiguous gene expression levels, allowing a high level of multiplexing. Library preparation involved reverse transcription of RNA with oligodT primers, followed by removal of RNA and second-strand cDNA synthesis with random primers. The resulting fragments containing both linker fragments were PCR amplified with primers containing the Illumina adaptors and sample-specific barcodes. All libraries were sequenced (single-end 50 bp) on one lane of the Illumina Hiseq 2500. Only genes with an adjusted *p*-value below 0.05 and a minimum fold-change greater than 1.5 were considered to be differentially expressed between conditions.

RiboTag method. *RiboTag* IP was performed according to Leven et al.[34]. Briefly, the muscle layer of the whole small bowel tissue was mechanically separated from the mucosal layer and placed in RNA*later* (Thermo Scientific). Muscle tissue was lysed on a Precellys homogenizer [Bertin Instruments] (3 × 5000 rpm, 45 s; 5 min intermediate incubation on ice) in pre-cooled homogenization buffer (50 mM Tris/HCl, 100 mM KCl, 12 mM $MgCl_2$, 1% NP-40, 1 mg/ml Heparin, 100 µg/ml Cycloheximide, 1 mM DTT, 200 U/ml RNAsin, 1× Protease Inhibitor P8340), centrifuged (10 min, 10,000 × *g*, 4 °C), and supernatants saved. "Input" controls were generated from 50 µl cleared lysate. Supernatants were incubated with anti-HA antibody (5 µl; 1 mg/ml; Table S4; 4 h, 4 °C, 7 rpm) and conjugates added to 200 µl of equilibrated A/G dynabeads (Thermo Scientific) and incubated (overnight, 4 °C, 7 rpm). High salt buffer (50 mM Tris/HCl, 300 mM KCl, 12 mM $MgCl_2$, 1% NP-40, 100 µg/ml Cycloheximide, 0.5 mM DTT) was used to wash beads before elution of cell-specific mRNA and subsequent mRNA extraction (Qiagen RNeasy micro kit).

Software. The software tools used for this study include Partek Flow, available from https://www.partek.com/partek-flow/#features; Subread/Feature Counts[61], available from http://subread.sourceforge.net/; Venn-Diagram Software, available from http://bioinformatics.psb.ugent.be/webtools/Venn/; and Gene Set Enrichment Analysis, available from https://www.partek.com/partek-flow/#features.

Statistics and reproducibility. Statistical analysis was performed with Prism V9.01 (GraphPad, USA) using Student *t*-test or one-way ANOVA as indicated. In all figures, *p*-values are indicated as $*p < 0.05$, $**p < 0.01$ and $***p < 0.001$ when compared to control or $\#p < 0.05$, $\#\#p < 0.01$ and $\#\#\#p < 0.001$ compared to indicated samples. All plots show the means of indicated expression levels ± standard error of the mean (SEM).

For all shown RNA-seq data, the Partek software was used for all analyses. Partek software performs statistical analyses by the Fisher's exact test and provides *p*-values with multiple testing corrections (FDR).

Experiments were repeated with more samples when the result was close to statistical significance, and sample sizes for animal studies were chosen following previously reported studies that have used the POI animal model; at least 6–10 independent mice per experimental setup. All animals were handled by standardized housing procedures and kept in precisely the same environmental conditions and were genotyped at 6 weeks of age and received a randomized number by which they were identified. Age- and sex-matched animals were grouped randomly and used in the POI animal model. All the control or experimental mice in each experimental set were treated with the same procedure and manipulation. By this, we avoided any group or genotype-specific effects due to the timing of experiments or handling of animals.

Reporting summary. Further information on research design is available in the Nature Research Reporting Summary linked to this article.

Data availability

The data sets produced in this study are available upon reasonable request and in the following databases: RNA-Seq data from mRNA of *ME*-tissue from patients in GSE149181. The *RiboTag* data of control and IM3h mice is available under the accession number *GSE198889*, and the data of EGCs treated with IL1β, and BMDMs treated with conditioned media is available under the accession number *GSE205610*. All raw data used for the main figures were included in an excel sheet named supplementary data 1.

Received: 23 December 2021; Accepted: 26 July 2022;
Published online: 12 August 2022

References

1. Kalff, J. et al. Surgically induced leukocytic infiltrates within the rat intestinal muscularis mediate postoperative ileus. *Gastroenterology* **117**, 378–387 (1999).
2. Wolthuis, A. M. et al. Incidence of prolonged postoperative ileus after colorectal surgery: a systematic review and meta-analysis. *Colorectal Dis.* **18**, O1–9 (2016).
3. Asgeirsson, T. et al. Postoperative ileus. it costs more than you expect. *J. Am. Coll. Surg.* **210**, 228–231 (2010).
4. Peters, E. G. et al. Relation between postoperative ileus and anastomotic leakage after colorectal resection: a post hoc analysis of a prospective randomized controlled trial. *Colorectal Dis.* **19**, 667–674 (2017).
5. Wehner, S. et al. Inhibition of macrophage function prevents intestinal inflammation and postoperative ileus in rodents. *Gut* **56**, 176–185 (2007).
6. Stoffels, B. et al. Postoperative ileus involves interleukin-1 receptor signaling in enteric glia. *Gastroenterology* **146**, 176–87.e1 (2014).
7. Enderes, J. et al. A population of radio-resistant macrophages in the deep myenteric plexus contributes to postoperative ileus via toll-like receptor 3 signaling. *Front. Immunol.* **11**, 581111 (2020).
8. Matteoli, G. et al. A distinct vagal anti-inflammatory pathway modulates intestinal muscularis resident macrophages independent of the spleen. *Gut* **63**, 938–948 (2014).
9. Yoo, B. B. & Mazmanian, S. K. The enteric network: interactions between the immune and nervous systems of the gut. *Immunity* **46**, 910–926 (2017).
10. Wang, H., Foong, J. P. P., Harris, N. L. & Bornstein, J. C. Enteric neuroimmune interactions coordinate intestinal responses in health and disease. *Mucosal Immunol.* https://doi.org/10.1038/s41385-021-00443-1 (2021).
11. Seguella, L. & Gulbransen, B. D. Enteric glial biology, intercellular signalling and roles in gastrointestinal disease. *Nat. Rev. Gastroenterol. Hepatol.* https://doi.org/10.1038/s41575-021-00423-7 (2021).
12. Rao, M. et al. Enteric glia regulate gastrointestinal motility but are not required for maintenance of the epithelium in mice. *Gastroenterology* **153**, 1068–1081.e7 (2017).
13. Liñán-Rico, A. et al. Molecular signaling and dysfunction of the human reactive enteric glial cell phenotype: implications for GI infection, IBD, POI, neurological, motility, and GI disorders. *Inflamm. Bowel Dis.* **22**, 1812–1834 (2016).
14. Rosenberg, H. J. & Rao, M. Enteric glia in homeostasis and disease: From fundamental biology to human pathology. *iScience* **24**, 102863 (2021).
15. Bush, T. G. et al. Fulminant jejuno-ileitis following ablation of enteric glia in adult transgenic mice. *Cell* **93**, 189–201 (1998).
16. Cornet, A. et al. Enterocolitis induced by autoimmune targeting of enteric glial cells. a possible mechanism in Crohn's disease? *Proc. Natl Acad. Sci. USA* **98**, 13306–13311 (2001).
17. Gulbransen, B. D. & Christofi, F. L. Are we close to targeting enteric glia in gastrointestinal diseases and motility disorders? *Gastroenterology* **155**, 245–251 (2018).
18. Kabouridis, P. S. et al. Microbiota controls the homeostasis of glial cells in the gut lamina propria. *Neuron* **85**, 289–295 (2015).
19. Vicentini, F. A. et al. Intestinal microbiota shapes gut physiology and regulates enteric neurons and glia. *Microbiome* **9**, 210 (2021).
20. Schneider, R. et al. A novel P2X2-dependent purinergic mechanism of enteric gliosis in intestinal inflammation. *EMBO Mol. Med.* **13**, e12724 (2021).
21. Burda, J. E. & Sofroniew, M. V. Reactive gliosis and the multicellular response to CNS damage and disease. *Neuron* **81**, 229–248 (2014).
22. Schepper, S. D. et al. Self-maintaining gut macrophages are essential for intestinal homeostasis. *Cell* **175**, 400–415.e13 (2018).
23. Rao, M. et al. Enteric glia express proteolipid protein 1 and are a transcriptionally unique population of glia in the mammalian nervous system. *Glia* https://doi.org/10.1002/glia.22876 (2015).
24. Rosenbaum, C. et al. Activation of myenteric glia during acute inflammation in vitro and in vivo. *PLoS ONE* **11**, e0151335 (2016).
25. Brykczynska, U. et al. Distinct transcriptional responses across tissue-resident macrophages to short-term and long-term metabolic challenge. *Cell Rep.* **30**, 1627–1643.e7 (2020).
26. Jha, M. K., Jo, M., Kim, J.-H. & Suk, K. Microglia-astrocyte crosstalk: an intimate molecular conversation. *Neuroscientist* **25**, 227–240 (2019).
27. Muller, P. A. et al. Crosstalk between muscularis macrophages and enteric neurons regulates gastrointestinal motility. *Cell* **158**, 300–313 (2014).
28. Grubišić, V. et al. Enteric glia modulate macrophage phenotype and visceral sensitivity following inflammation. *Cell Rep.* **32**, 108100 (2020).
29. Hupa, K. J. et al. AIM2 inflammasome-derived IL-1β induces postoperative ileus in mice. *Sci. Rep.* **9**, 10602 (2019).
30. Wehner, S. et al. Induction of IL-6 within the rodent intestinal muscularis after intestinal surgical stress. *Surgery* **137**, 436–446 (2005).
31. Farro, G. et al. CCR2-dependent monocyte-derived macrophages resolve inflammation and restore gut motility in postoperative ileus. *Gut* **66**, 2098–2109 (2017).
32. Stein, K. et al. Leukocyte-derived interleukin-10 aggravates postoperative ileus. *Front. Immunol.* **9**, 2599 (2018).
33. Valès, S. et al. Tumor cells hijack enteric glia to activate colon cancer stem cells and stimulate tumorigenesis. *EBioMedicine* **49**, 172–188 (2019).
34. Leven, P., Schneider, R., Siemens, K., Jackson, W., & Wehner, S. Application of a RiboTag based approach to generate and analyze mRNA from enteric neural cells. *Neurogastroenterol. Motility* https://doi.org/10.1111/nmo.14309 (2021).
35. Progatzky, F. et al. Regulation of intestinal immunity and tissue repair by enteric glia. *Nature* **599**, 125–130 (2021).
36. Delvalle, N. M. et al. Communication between enteric neurons, glia, and nociceptors underlies the effects of tachykinins on neuroinflammation. *Cell. Mol. Gastroenterol. Hepatol.* **6**, 321–344 (2018).
37. Wehner, S. & Engel, D. R. Resident macrophages in the healthy and inflamed intestinal muscularis externa. *Pflügers Arch. Eur. J. Physiol.* **469**, 541–552 (2017).
38. Lin, S.-S. et al. Alterations in the gut barrier and involvement of Toll-like receptor 4 in murine postoperative ileus. *Neurogastroenterol. Motil.* **30**, e13286 (2018).
39. Sommer, N. P., Schneider, R., Wehner, S., Kalff, J. C. & Vilz, T. O. State-of-the-art colorectal disease: postoperative ileus. *Int. J. Colorectal Dis.* https://doi.org/10.1007/s00384-021-03939-1 (2021).
40. Hyvärinen, T. et al. Co-stimulation with IL-1β and TNF-α induces an inflammatory reactive astrocyte phenotype with neurosupportive characteristics in a human pluripotent stem cell model system. *Sci. Rep.* **9**, 1–15 (2019).
41. Muñoz, A. M., Rey, P., Parga, J., Guerra, M. J. & Labandeira-Garcia, J. L. Glial overexpression of heme oxygenase-1: a histochemical marker for early stages of striatal damage. *J. Chem. Neuroanat.* **29**, 113–126 (2005).
42. Andersson, H. C. et al. Trauma-induced reactive gliosis is reduced after treatment with octanol and carbenoxolone. *Neurological Res.* **33**, 614–624 (2011).
43. Kalff, J. C., Schraut, W. H., Simmons, R. L. & Bauer, A. J. Surgical manipulation of the gut elicits an intestinal muscularis inflammatory response resulting in postsurgical ileus. *Ann. Surg.* **228**, 652–663 (1998).
44. van Wesenbeeck, L. et al. The osteopetrotic mutation toothless (tl) is a loss-of-function frameshift mutation in the rat Csf1 gene. Evidence of a crucial role for CSF-1 in osteoclastogenesis and endochondral ossification. *Proc. Natl Acad. Sci. USA* **99**, 14303–14308 (2002).
45. Bendall, L. J. & Bradstock, K. F. G-CSF: From granulopoietic stimulant to bone marrow stem cell mobilizing agent. *Cytokine Growth Factor Rev.* **25**, 355–367 (2014).
46. Pinheiro, D., Mawhin, M.-A., Prendecki, M. & Woollard, K. J. In-silico analysis of myeloid cells across the animal kingdom reveals neutrophil evolution by colony-stimulating factors. *eLife* **9**, https://doi.org/10.7554/eLife.60214 (2020).
47. Wen, Q. et al. G-CSF-induced macrophage polarization and mobilization may prevent acute graft-versus-host disease after allogeneic hematopoietic stem cell transplantation. *Bone Marrow Transplant.* **54**, 1419–1433 (2019).
48. Meshkibaf, S., Martins, A. J., Henry, G. T. & Kim, S. O. Protective role of G-CSF in dextran sulfate sodium-induced acute colitis through generating gut-homing macrophages. *Cytokine* **78**, 69–78 (2016).
49. Hollmén, M. et al. G-CSF regulates macrophage phenotype and associates with poor overall survival in human triple-negative breast cancer. *Oncoimmunology* **5**, e1115177 (2016).
50. Fu, H. et al. Depletion of microglia exacerbates injury and impairs function recovery after spinal cord injury in mice. *Cell Death Dis.* **11**, 528 (2020).
51. Lou, N. et al. Purinergic receptor P2RY12-dependent microglial closure of the injured blood-brain barrier. *Proc. Natl Acad. Sci. USA* **113**, 1074–1079 (2016).
52. Simon, D. W. et al. The far-reaching scope of neuroinflammation after traumatic brain injury. *Nat. Rev. Neurol.* **13**, 171–191 (2017).
53. Kulkarni, S. et al. Adult enteric nervous system in health is maintained by a dynamic balance between neuronal apoptosis and neurogenesis. *Proc. Natl Acad. Sci. USA* **114**, E3709–18 (2017).
54. Ahrends, T. et al. Enteric pathogens induce tissue tolerance and prevent neuronal loss from subsequent infections. *Cell* **184**, 5715–5727.e12 (2021).
55. Brown, I. A. M., McClain, J. L., Watson, R. E., Patel, B. A. & Gulbransen, B. D. Enteric glia mediate neuron death in colitis through purinergic pathways that require connexin-43 and nitric oxide. *Cell. Mol. Gastroenterol. Hepatol.* **2**, 77–91 (2016).

56. Costa, D. V. S. et al. 5-fluorouracil induces enteric neuron death and glial activation during intestinal mucositis via a S100B-RAGE-NFκB-dependent pathway. *Sci. Rep.* **9**, 665 (2019).
57. Aube, A. C. et al. Changes in enteric neurone phenotype and intestinal functions in a transgenic mouse model of enteric glia disruption. *Gut* **55**, 630–637 (2006).
58. Gulbransen, B. D. & Sharkey, K. A. Purinergic neuron-to-glia signaling in the enteric nervous system. *Gastroenterology* **136**, 1349–1358 (2009).
59. Pohl, J. M. et al. Irf4-dependent CD103(+)CD11b(+) dendritic cells and the intestinal microbiome regulate monocyte and macrophage activation and intestinal peristalsis in postoperative ileus. *Gut* **66**, 2110–2120 (2017).
60. Mazzotta, E., Villalobos-Hernandez, E. C., Fiorda-Diaz, J., Harzman, A. & Christofi, F. L. Postoperative ileus and postoperative gastrointestinal tract dysfunction: pathogenic mechanisms and novel treatment strategies beyond colorectal enhanced recovery after surgery protocols. *Front. Pharmacol.* **11**, 583422 (2020).
61. Liao, Y., Smyth, G. K. & Shi, W. FeatureCounts: an efficient general purpose program for assigning sequence reads to genomic features. *Bioinformatics* **30**, 923–930 (2014).

Acknowledgements

The authors thank the Next Generation Sequencing Core Facility and the Institute for Genomic Statistics and Bioinformatics of the University Clinics Bonn for supporting the RNA-Seq analysis. In addition, the authors thank the Flow Cytometry Core Facility of the University Clinics Bonn for supporting all FACS experiments. We thank the technicians Patrik Efferz, Mariola Lysson, Jana Müller, and Bianca Schneiker for their support with the readouts like ELISA and qPCR and for handling the transgenic mouse lines. We thank Prof. Vachilis Pachnis for sharing the *Sox10*^{CreERT2} mice with us. We thank PD Valentin Schäfer for sharing the Anakinra substance for in vitro assays. We thank Prof. Vanda A. Lennon for sharing the ANNA-1 antibody to visualize enteric neurons in our primary cell cultures. We thank Prof. Nico Schlegel and Prof. Wouter de Jonge for reading our manuscript and providing helpful suggestions for wording our results and conclusions. Graphical visualizations were created with BioRender software. We thank the following funding organizations for supporting our research: National Institutes of Health Grant (NCI Cost shared resource for COM, The Ohio State University): P30CA16058 National Institutes of Health, National Institutes of Diabetes, Digestive and Kidney Diseases (NIH, NIDDK) Grants: R01DK113943 and R01DK125809 (F.L.C.). BonnNI medical student Grant: Q-611.0754 (S.W.). ImmunoSensation2 Cluster of Excellence: EXC 2151–390873048 (S.W.). German research council (D.F.G.): WE4204/3-1 (S.W.).

Author contributions

Conceptualization: R.S., F.L.C., and S.W. Methodology: R.S., J.C.K., F.L.C., P.L., S.M., M.B., T.G., P.h.L., T.O.V., and S.W. Investigation: R.S., P.L., M.B., S.M., L.S., E.Z., and P.F. Visualization: R.S., P.L., M.B., S.M., and P.F. Funding acquisition: J.C.K., F.L.C., and S.W. Project administration: J.C.K., F.L.C., and S.W. Patient material and clinical organization: T.G., P.h.L., T.O.V. Supervision: R.S., F.L.C., and S.W. Writing—original draft: R.S., J.C.K., F.L.C., and S.W. Writing—review & editing: R.S., J.C.K., F.L.C., P.L., S.M., T.G., P.h.L., T.O.V., L.S., M.B., and S.W.

Funding

Open Access funding enabled and organized by Projekt DEAL.

Competing interests

The authors declare the following competing interests: S.W. and J.C.K. receive royalties from Wolter Kluwer for contributing to the postoperative ileus section of the *UpToDate* library. All other authors declare no competing interests.

Additional information

Supplementary information The online version contains supplementary material available at https://doi.org/10.1038/s42003-022-03772-4.

Correspondence and requests for materials should be addressed to Sven Wehner.

Peer review information *Communications Biology* thanks Ulrika Marklund and the other, anonymous, reviewer(s) for their contribution to the peer review of this work. Primary handling editor: Zhijuan Qiu. Peer reviewer reports are available.

Reprints and permission information is available at http://www.nature.com/reprints

Publisher's note Springer Nature remains neutral with regard to jurisdictional claims in published maps and institutional affiliations.

4. Discussion

4.1 Enteric glia shape the post-surgical intestinal inflammatory environment

4.1.1 *RiboTag* optimization and overview

Our previous studies showed the involvement of different cell types [1-3] and mediators [4-8] in post-operative ileus (POI) pathogenesis, and the growing acknowledgment of various enteric glial cell (EGC) abilities [9] prompted us to investigate their role during POI. Here, we provide evidence that a cascade initiated by the first surgical incision and aggravated by the mechanical manipulation of the small bowel leads to reactive gliosis via norepinephrine (NE) derived mainly from the sympathetic nervous system (SNS) [10]. This cascade is immediately followed by interleukin-1 (IL-1) [11] signaling to EGCs and subsequent adenosine triphosphate (ATP) binding to EGCs [12], further promoting enteric gliosis and culminating in intestinal inflammation of the *muscularis externa (ME)*, impaired motility, and POI.

After the successful establishment of an optimized extraction protocol for the *ME* of the small bowel, we proved that almost all EGCs cell-specifically express the Sox10$^{iCre-ERT2}$ *RiboTag* [13], thereby enabling tissue and time point-specific analysis [14] of the glial transcriptome throughout POI [10,11].

4.1.2 Immediate adrenergic-driven reactive response of enteric glia

To elucidate the starting point of EGC reactivity, we first looked at the initial surgical incision known to cause *ME* inflammation [15] and activation of the fast-acting SNS, which controls peristalsis [16] through its innervation of the myenteric plexus [17-19]. The SNS has already been implicated in POI in regard to macrophage activation and differentiation [20] and our study extended this role by discovering that SNS disruption reduces cytokine expression and enteric gliosis and attenuates the local immune response [10], an effect similarly observed in the CNS [21,22]. As global chemical disruption of the SNS might include additional effects, we established a specific mouse line together with the group of Philipp Sasse, which enables Cre-activated control of β-adrenergic downstream targets via optogenetics. Activation of this transgen in EGCs by blue light induced FOS expression and EGC reactivity similar to that after intestinal manipulation, emphasizing the importance of adrenergic pathways in shaping immediate enteric gliosis during surgery [10]. While modulation of β-adrenergic receptors (ARs)

induced both astrogliosis [23] and enteric gliosis *in vivo* and *in vitro* [10], NE effects depend on multiple factors [24] and can evoke ambivalent outcomes [25-28], as seen when comparing chronic and acute gut diseases [20,29-33]. As this ambivalence has been observed even within chronic diseases [34,35], EGCs are highly plastic [36], and AR expression shifts during inflammation [20,23], additional studies have to be conducted to elicit this compelling interaction and the influence of NE on EGCs in pathophysiologies of gut diseases.

4.1.3 IL-1 and ATP trigger glial reactivity and induce enteric gliosis

Important signaling pathways in POI involve the cytokine IL-1 [4] and ATP, a potent damage-associated molecular pattern [37-41]. Our previous studies showed that pan-IL-1R1 deficiency protected mice from POI [4] and that IL-1 [6] induces the POI-defining cytokine IL-6 [7]. As IL-1R1 is expressed by EGCs, we ablated the receptor glia-specifically and could reduce postoperative inflammation, prevent reactive gliosis, and ultimately POI [11]. Similarly, extracellular ATP interacts with EGCs [42-45] and was speculated to be involved in gliosis [46]. Even though the origin of extracellular ATP is still elusive, we hypothesize, based on its presence during early POI [12], a release from injured cells or active release by activated [47] *ME*-macrophages [48] or enteric neurons (ENs) [45] rather than infiltrating immune cells [49]. Furthermore, reactive EGCs primed by NE and triggered by IL-1 might release ATP, a mechanism previously seen after LPS treatment [50]. Consequently, stimulation of primary EGCs with ATP or IL-1β induced multiple genes, congruent with our glia-specific *in vivo* transcripts [11,12]. Further investigation of ATP signaling revealed purine receptor P2X2, highly expressed in murine and human EGCs [12,50], and p38-MAPK, a downstream target of ATP known from CNS gliosis [51] and post-surgery gut inflammation [8], as regulators of enteric gliosis [12].

4.1.4 Enteric gliosis in POI as a dynamic, multifactorial process

Using a longitudinal analysis, we acquired distinct transcriptional patterns of EGCs at each time point, overlapping with classic POI development, namely resident cell activation, disease manifestation, and resolution [52]. Herein, EGCs become reactive and switch to an inflammatory and migration-inducing phenotype, followed by a proliferation-dominated phase that ultimately culminates in a state likely linked to anti-inflammatory effects and tissue healing. This early EGC reactivity is similar to astrocyte

changes after various insults, known as gliosis [51,53,54]. After creating [12] a gene list derived from CNS gliosis [55-61], we utilized our data of differentially expressed genes (DEG) of EGCs at POI onset for refinement and establishment of a distinct phenotype called “acute enteric gliosis” [10]. Regulated enteric gliosis genes, amongst others, included established CNS gliosis genes [55,56,59,62-64], genes known to be regulated in POI without specific EGC context [7,65,66], or ones associated with other intestinal disease conditions [67-69]. Moreover, we detected several genes of the immediate-early class, responsible for priming the transcription machinery [70,71], highlighting the swift response of EGCs. Strikingly, around 70% of DEGs at IM3h had chemotactic and inflammatory connotations, emphasizing the modulation of gut inflammation by EGCs [4,67,72].

As migratory genes were induced in our EGC-specific *in vivo* analysis and *ME*-macrophages are known as key players of POI [3,73,74], we took a closer look at EGC-macrophage interaction. One of the most prominent mediators produced by EGCs was CSF1, which is essential for *ME*-macrophage maintenance [75] and was previously shown to be released from ENs [76] and EGCs [72]. Grubišić et al. showed *ME*-macrophage activation by IL-1-stimulated EGCs through CSF1/Cx43 signaling [72], an effect we also observed by an increased abundance of phagocyting, $CD68^{+}$ *ME*-macrophages around enteric ganglia. This accumulation has been observed in gut homeostasis [77] and infection [78] and might also resemble neuroprotective mechanisms in the CNS, where microglia, often described as central nervous *ME*-macrophage counterparts, localize to areas of neurodegeneration after injury [79-81] and facilitate swift removal of dead cells. Moreover, analysis of bone-marrow-derived macrophage cultures stimulated with EGC-conditioned medium, revealed an induction of a migratory and phagocytic phenotype, emphasizing the effect of EGCs on macrophages regardless of their origin. Interestingly, all approaches targeting EGC reactivity, including adrenergic blockade, IL-1 deficiency, and P2X2 antagonism reduced the accumulation of *ME*-macrophages around ganglia, further underlining enteric gliosis as a multifactorial process. Since activated *ME*-macrophages contribute to POI [3,65] and can be separated into distinct clusters [77] with specific characteristics [1], time point-specific interactions of EGCs with those *ME*-macrophage subtypes will be crucial in devising dedicated interventions. Another closely associated resident cell type are ENs. EGCs influence ENs during inflammation[82-86] and can directly facilitate POI symptoms such as motility disturbance [87] implying interactions independent from *ME*-macrophages. While one of our

follow-up studies focussed on neurodegenerative effects during POI and interactions with *ME*-macrophages (manuscript in preparation), further studies connecting all these cells to EGCs in a comprehensive study are warranted.

Our findings indicate acute enteric gliosis as a highly dynamic process involving several signaling pathways and feedback loops. Multiple treatment schemes evoked enteric gliosis, and their blockade led to an attenuation of EGC reactivity and POI hallmarks [10-12]. Mechanistically, we propose a cascade of SNS-based NE release, induced by the first surgical incision, acting on EGCs as a primer for their reactive changes, aggravated by the manipulation of the intestine, and subsequently elevated self-perpetuating IL-1 signaling. Reactive EGCs and detrimental effects on surrounding cells then trigger increased extracellular ATP levels, further exacerbating enteric gliosis and shaping the entire *ME* inflammatory microenvironment. As blockage of these pathways reduces gliosis [10] and POI hallmarks [11,12,20], we believe acute enteric gliosis to be a detrimental event in POI.

In summary, sympathetic adrenergic signaling acts as a priming factor of early EGC reactivity, amplified by later actions of IL-1 and ATP, resulting in changes to the inflammatory microenvironment and surrounding cells, especially during the immediate POI onset (**Figure 3**).

4.2 Enteric glia involvement in later POI stages

During POI progression, EGCs undergo a phenotypical switch from an active pro-inflammatory to a proliferative and ultimately resolution-associated phenotype, emphasizing their plasticity [88,89] and specific intestinal functions [90]. However, the reason why EGCs undergo gliosis is still unclear, and while countermeasures improved POI symptoms during the disease peak, the implications for regeneration are unknown. While gliosis is treated in CNS disorders [91,92] to improve neural functions, the verdict is still out for the ENS. As EGCs can be stimulated by the mediators they release themselves, such as ATP and IL-1, feedback loops might present a way to shape certain temporally and spatially defined actions. When the milieu changes, e.g., through

either the loss of early signals due to changed receptor expression [24] or released mediators of infiltrating cells [49,65,93,94], these feedback loops are interrupted, prompting EGC adaptation. EGC proliferation was observed at peak inflammation, and the glial capacity to replenish ENs [88] might be the first indicator of their regenerative potential. Immune cell migration into the *ME* is a crucial part of the later POI stages and disruption of glial IL-1 signaling reduced infiltration. CSF3, a glial-derived chemoattractant recently implicated in *ME*-macrophages modulation [95,96] and neutrophil migration and activation [97,98], highlights potential interactions of infiltrating immune cells and EGCs during POI resolution and thus warrants future investigations. A closer look at the resolution phase and involved mediators, molecular mechanisms, and cell types interacting with EGCs will improve POI understanding. This will be especially important, as both preventive and curative approaches will be needed to minimize POI incidence and strength in the clinic.

4.3 Translation to the clinic and potential glia-targeting remedies

Even though murine studies contributed to significant advancements in disease research in the past decade, physiological and metabolic differences between rodents and humans impede exact translation between species [99,100]. Nonetheless, we verified our murine gliosis signature in human specimens [11,12], suggesting a conserved gliosis mechanism. Additionally, human and mouse primary glia showed similar receptor profiles and could be activated by the same stimuli [12,50]. As next-generation sequencing techniques, such as single-cell [101-104] and single-nuclei sequencing become more common [105], we will be able to corroborate and refine our *in vivo* gliosis signature of murine POI more thoroughly in surgical patient gut specimens.

EGCs have been discussed as potential targets for inflammatory intestinal diseases for some time [106], and our studies suggest that treatments interacting with either of the analyzed pathways might help ameliorate POI. Earlier antagonistic studies with propranolol reported ambivalent effects on POI [107,108], but modern pharmacology might be able to generate specifically tailored antagonists and mimic the effects seen in animal models [10,20,109]. Moreover, clinical relevance has to be assessed for adrenergic modulation, as other cells expressing β-ARs, such as immune cells, must be considered. Similarly, interaction with purinergic signaling should be clinically tested. Interestingly,

our studies implicated Ambroxol, a potent P2X2 antagonist [110] effective in other inflammatory models [111-113] and already clinically used for lung inflammation [114], as a partial counter to acute enteric gliosis, immune cell infiltration, and motility disturbances. Due to the high impact of purines on inflammation [115] and the proven efficacy and safety in multiple gut and gut-brain axis-related diseases [116-118] Ambroxol and similar clinically proven drugs [119] should be studied for POI treatment in patients and subsequently optimized towards highly-selective P2 antagonism [120]. As this system is highly complex and involves various receptors on different cell types, exact effects will have to be closely monitored and should be carefully studied. Lastly, antibody or drug-based interaction with IL-1 signaling not only reduced murine POI, e.g., by Anakinra [4], but also positively affected human samples [11], and Anakinra is already applied in intestinal clinical trials (NCT03233776 [121]; NCT02090101). Therefore, we believe peri-operative IL-1 antagonism to be a potentially important method of preventing POI according to established protocols [122]. Of note, studies also showed IL-1-dependent intestinal regeneration in acute colitis [123] and infection models [124,125], emphasizing the need to meticulously study the optimal point of administration. These strategies are especially promising as current treatments of POI focus on recovery rather than prevention and rely on antagonism of analgesics and unspecific interventions such as acupuncture, probiotics, and gum chewing [126-128].

4.4 Caveats, conclusions, and prospects

Despite our findings, the exact connotation of enteric gliosis is still unclear. While a rather detrimental effect is likely due to the improved hallmarks of POI after the blockade of each investigated pathway, other effects not immediately recognizable could be at hand. The overall detrimental environment might mask neuroprotective modulation by EGCs, and a constantly aggravated glial activation might drive *ME*-macrophages to forego their protective functions and act destructively. One must remember the tightly orchestrated actions present throughout this acute disorder, involving multiple resident and infiltrating immune cells. Direct causation between the actions of EGCs, ENs, and *ME*-macrophages needs to be further assessed to comprehend the exact mechanisms that shape inflammatory reactions during POI progression. To this end, there is also a need to identify genes restricted to EGCs during postoperative inflammation. Modern

single-nuclei RNA-Seq studies might assist in identifying these genes and providing disease but also overarching profiles of EGC reactivity, which can then be used as potential biomarkers of the disease state or treatment efficacy.

Although we aimed to elucidate the pathways affecting EGCs in POI by various *in vivo*, *ex vivo*, and *in vitro* approaches in both murine and human specimens, final confirmation of P2X2 and β-AR involvement requires glial-specific, inducible knockout mice. While the *RiboTag* approach was used to successfully analyze overall EGC changes, further work based on single-cell/-nuclei sequencing techniques and spatial transcriptomics, especially for human surgical samples, is required to thoroughly characterize EGC subpopulations involved in POI modulation. Similarly, translation of the gliosis profile and novel EGC-specific genes to other diseases, especially chronic inflammatory bowel diseases or oncological conditions, will require additional *RiboTag* modifications and single-cell-/nuclei approaches to account for highly enzyme-laden tissues and the limited tissue amounts, respectively.

In conclusion, this thesis provides a longitudinal transcriptomic profile of reactive EGCs throughout the course of acute, post-surgical inflammation associated with the term enteric gliosis. Furthermore, purinergic, IL-1R1 and adrenergic signaling have been identified as triggers of glial reactivity during different phases of postoperative inflammation. These pathways modulate the tissue microenvironment by expression and secretion of various mediators in EGCs, finally shaping immune cell function in the inflamed gut.

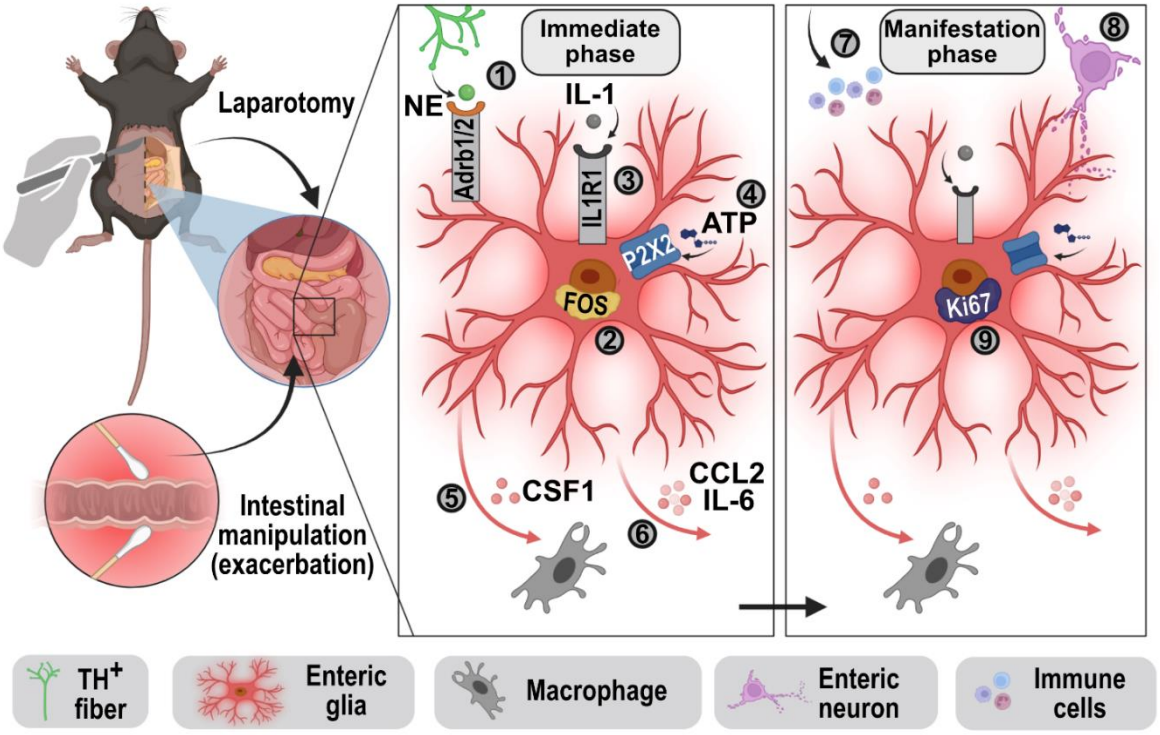

Figure 3. Schematic overview of the inflammatory reactions of EGCs after laparotomy and intestinal manipulation. Surgical incision leads to an immediate NE-mediated (adrenergic) EGC reactivity (immediate phase, left panel). Herein, NE, released from the SNS, binds to EGC adrenoceptors Adrb1/2 **(1)** triggering c-FOS upregulation **(2)**. Further (intestinal) manipulation during surgery exacerbates the initially triggered adrenergic responses by enhancing EGC reactivity via IL-1β signaling through IL1R1 **(3)** as well as extracellular ATP binding via purinergic P2X2 receptors **(4)**. These pathways lead to cytokine (IL-6) and chemokine (CCL2) release **(5)** and macrophage modulation via CSF1 **(6)**. Immunomodulation persists through later phases of POI (manifestation, right panel), while initial c-FOS reactivity drops. Peripheral immune cells infiltrate **(7)**, neurons and their synapses degenerate **(8)**, and EGCs initiate proliferative profiles, such as Ki67 upregulation **(9)**. This image was created with BioRender.com.

4.5 References

1. Enderes J, Mallesh S, Schneider R, et al. A Population of Radio-Resistant Macrophages in the Deep Myenteric Plexus Contributes to Postoperative Ileus Via Toll-Like Receptor 3 Signaling. *Front Immunol*. 2020;11:581111. doi:10.3389/fimmu.2020.581111
2. Engel DR, Koscielny A, Wehner S, et al. T helper type 1 memory cells disseminate postoperative ileus over the entire intestinal tract. *Nat Med*. 2010;16(12):1407-1413. doi:10.1038/nm.2255
3. Wehner S, Behrendt FF, Lyutenski BN, et al. Inhibition of macrophage function prevents intestinal inflammation and postoperative ileus in rodents. *Gut*. 2007;56(2):176-185. doi:10.1136/gut.2005.089615
4. Stoffels B, Hupa KJ, Snoek SA, et al. Postoperative ileus involves interleukin-1 receptor signaling in enteric glia. *Gastroenterology*. 2014;146(1):176-87.e1. doi:10.1053/j.gastro.2013.09.030
5. Wehner S, Vilz TO, Stoffels B, Kalff JC. Immune mediators of postoperative ileus. *Langenbecks Arch Surg*. 2012;397(4):591-601. doi:10.1007/s00423-012-0915-y
6. Hupa KJ, Stein K, Schneider R, et al. AIM2 inflammasome-derived IL-1β induces postoperative ileus in mice. *Sci Rep*. 2019;9(1):10602. doi:10.1038/s41598-019-46968-1
7. Wehner S, Schwarz NT, Hundsdoerfer R, et al. Induction of IL-6 within the rodent intestinal muscularis after intestinal surgical stress. *Surgery*. 2005;137(4):436-446. doi:10.1016/j.surg.2004.11.003
8. Wehner S, Straesser S, Vilz TO, et al. Inhibition of p38 mitogen-activated protein kinase pathway as prophylaxis of postoperative ileus in mice. *Gastroenterology*. 2009;136(2):619-629. doi:10.1053/j.gastro.2008.10.017
9. Seguella L, Gulbransen BD. Enteric glial biology, intercellular signalling and roles in gastrointestinal disease. *Nat Rev Gastroenterol Hepatol*. 2021. doi:10.1038/s41575-021-00423-7
10. Leven P, Schneider R, Schneider L, et al. β-adrenergic signaling triggers enteric glial reactivity and acute enteric gliosis during surgery. *J Neuroinflammation*. 2023;20(1):255. doi:10.1186/s12974-023-02937-0
11. Schneider R, Leven P, Mallesh S, et al. IL-1-dependent enteric gliosis guides intestinal inflammation and dysmotility and modulates macrophage function. *Commun Biol*. 2022;5(1):811. doi:10.1038/s42003-022-03772-4
12. Schneider R, Leven P, Glowka T, et al. A novel P2X2-dependent purinergic mechanism of enteric gliosis in intestinal inflammation. *EMBO Mol Med*. 2021;13(1):e12724. doi:10.15252/emmm.202012724
13. Leven P, Schneider R, Siemens KD, Jackson WS, Wehner S. Application of a RiboTag -based approach to generate and analyze mRNA from enteric neural cells. *Neurogastroenterology & Motility*. 2021. doi:10.1111/nmo.14309

14. Sanz E, Bean JC, Carey DP, Quintana A, McKnight GS. RiboTag: Ribosomal Tagging Strategy to Analyze Cell-Type-Specific mRNA Expression In Vivo. *Curr Protoc Neurosci*. 2019;88(1):e77. doi:10.1002/cpns.77

15. Kalff JC, Türler A, Schwarz NT, et al. Intra-abdominal activation of a local inflammatory response within the human muscularis externa during laparotomy. *Ann Surg*. 2003;237(3):301-315. doi:10.1097/01.SLA.0000055742.79045.7E

16. Lomax AE, Sharkey KA, Furness JB. The participation of the sympathetic innervation of the gastrointestinal tract in disease states. *Neurogastroenterol Motil*. 2010;22(1):7-18. doi:10.1111/j.1365-2982.2009.01381.x

17. Gulbransen BD, Bains JS, Sharkey KA. Enteric glia are targets of the sympathetic innervation of the myenteric plexus in the guinea pig distal colon. *J Neurosci*. 2010;30(19):6801-6809. doi:10.1523/JNEUROSCI.0603-10.2010

18. Matheis F, Muller PA, Graves CL, et al. Adrenergic Signaling in Muscularis Macrophages Limits Infection-Induced Neuronal Loss. *Cell*. 2020;180(1):64-78.e16. doi:10.1016/j.cell.2019.12.002

19. Gabanyi I, Muller PA, Feighery L, Oliveira TY, Costa-Pinto FA, Mucida D. Neuro-immune Interactions Drive Tissue Programming in Intestinal Macrophages. *Cell*. 2016;164(3):378-391. doi:10.1016/j.cell.2015.12.023

20. Mallesh S, Schneider R, Schneiker B, et al. Sympathetic Denervation Alters the Inflammatory Response of Resident Muscularis Macrophages upon Surgical Trauma and Ameliorates Postoperative Ileus in Mice. *IJMS*. 2021;22(13):6872. doi:10.3390/ijms22136872

21. Tong F, He Q, Du W-J, et al. Sympathetic Nerve Mediated Spinal Glia Activation Underlies Itch in a Cutaneous T-Cell Lymphoma Model. *Neurosci Bull*. 2021. doi:10.1007/s12264-021-00805-6

22. Sutin J, Griffith R. Beta-adrenergic receptor blockade suppresses glial scar formation. *Exp Neurol*. 1993;120(2):214-222. doi:10.1006/exnr.1993.1056

23. Imura T, Shimohama S, Sato M, et al. Differential Expression of Small Heat Shock Proteins in Reactive Astrocytes after Focal Ischemia: Possible Role of β-Adrenergic Receptor. *J Neurosci*. 1999;19(22):9768-9779. doi:10.1523/JNEUROSCI.19-22-09768.1999

24. Straub RH, Wiest R, Strauch UG, Härle P, Schölmerich J. The role of the sympathetic nervous system in intestinal inflammation. *Gut*. 2006;55(11):1640-1649. doi:10.1136/gut.2006.091322

25. Vardjan N, Horvat A, Anderson JE, et al. Adrenergic activation attenuates astrocyte swelling induced by hypotonicity and neurotrauma. *Glia*. 2016;64(6):1034-1049. doi:10.1002/glia.22981

26. Yoshioka Y, Negoro R, Kadoi H, et al. Noradrenaline protects neurons against H2 O2 -induced death by increasing the supply of glutathione from astrocytes via β3 -adrenoceptor stimulation. *J Neurosci Res*. 2021;99(2):621-637. doi:10.1002/jnr.24733

27. Danková M, Domoráková I, Fagová Z, Stebnický M, Kunová A, Mechírová E. Bradykinin and noradrenaline preconditioning influences level of antioxidant

enzymes SOD, CuZn-SOD, Mn-SOD and catalase in the white matter of spinal cord in rabbits after ischemia/reperfusion. *Eur J Histochem*. 2019;63(4). doi:10.4081/ejh.2019.3045

28. Laureys G, Gerlo S, Spooren A, Demol F, Keyser J de, Aerts JL. β_2-adrenergic agonists modulate TNF-α induced astrocytic inflammatory gene expression and brain inflammatory cell populations. *J Neuroinflammation*. 2014;11:21. doi:10.1186/1742-2094-11-21

29. Willemze RA, Welting O, van Hamersveld P, et al. Loss of intestinal sympathetic innervation elicits an innate immune driven colitis. *Mol Med*. 2019;25(1). doi:10.1186/s10020-018-0068-8

30. Willemze RA, Welting O, van Hamersveld HP, et al. Neuronal control of experimental colitis occurs via sympathetic intestinal innervation. *Neurogastroenterol Motil*. 2018;30(3). doi:10.1111/nmo.13163

31. Willemze RA, Bakker T, Pippias M, Ponsioen CY, Jonge WJ de. β-Blocker use is associated with a higher relapse risk of inflammatory bowel disease: a Dutch retrospective case-control study. *Eur J Gastroenterol Hepatol*. 2018;30(2):161-166. doi:10.1097/MEG.0000000000001016

32. Schiller M, Azulay-Debby H, Boshnak N, et al. Optogenetic activation of local colonic sympathetic innervations attenuates colitis by limiting immune cell extravasation. *Immunity*. 2021;54(5):1022-1036.e8. doi:10.1016/j.immuni.2021.04.007

33. Schneider KM, Blank N, Alvarez Y, et al. The enteric nervous system relays psychological stress to intestinal inflammation. *Cell*. 2023;186(13):2823-2838.e20. doi:10.1016/j.cell.2023.05.001

34. Deng L, Guo H, Wang S, et al. The Attenuation of Chronic Ulcerative Colitis by (R)-salbutamol in Repeated DSS-Induced Mice. *Oxid Med Cell Longev*. 2022;2022:9318721. doi:10.1155/2022/9318721

35. Clemente-Moragón A, Gómez M, Villena-Gutiérrez R, et al. Metoprolol exerts a non-class effect against ischaemia-reperfusion injury by abrogating exacerbated inflammation. *Eur Heart J*. 2020;41(46):4425-4440. doi:10.1093/eurheartj/ehaa733

36. Sanchini G, Vaes N, Boesmans W. Mini-review: Enteric glial cell heterogeneity: Is it all about the niche? *Neuroscience Letters*. 2023;812:137396. doi:10.1016/j.neulet.2023.137396

37. Carta S, Penco F, Lavieri R, et al. Cell stress increases ATP release in NLRP3 inflammasome-mediated autoinflammatory diseases, resulting in cytokine imbalance. *Proceedings of the National Academy of Sciences*. 2015;112(9):2835-2840. doi:10.1073/pnas.1424741112

38. Csóka B, Németh ZH, Törő G, et al. Extracellular ATP protects against sepsis through macrophage P2X7 purinergic receptors by enhancing intracellular bacterial killing. *The FASEB Journal*. 2015;29(9):3626-3637. doi:10.1096/fj.15-272450

39. Cauwels A, Rogge E, Vandendriessche B, Shiva S, Brouckaert P. Extracellular ATP drives systemic inflammation, tissue damage and mortality. *Cell Death & Disease*. 2014;5(3):e1102. doi:10.1038/cddis.2014.70

40. Grubišić V, Perez-Medina AL, Fried DE, et al. NTPDase1 and -2 are expressed by distinct cellular compartments in the mouse colon and differentially impact colonic physiology and function after DSS colitis. *American Journal of Physiology-Gastrointestinal and Liver Physiology*. 2019;317(3):G314-G332. doi:10.1152/ajpgi.00104.2019

41. Galligan JJ. Purinergic signaling in the gastrointestinal tract. *Purinergic Signalling*. 2008;4(3):195-196. doi:10.1007/s11302-008-9109-z

42. Gulbransen BD, Sharkey KA. Purinergic neuron-to-glia signaling in the enteric nervous system. *Gastroenterology*. 2009;136(4):1349-1358. doi:10.1053/j.gastro.2008.12.058

43. Boesmans W, Hao MM, Fung C, et al. Structurally defined signaling in neuro-glia units in the enteric nervous system. *Glia*. 2019;67(6):1167-1178. doi:10.1002/glia.23596

44. Boesmans W, Cirillo C, van den Abbeel V, et al. Neurotransmitters involved in fast excitatory neurotransmission directly activate enteric glial cells. *Neurogastroenterol Motil*. 2013;25(2):e151-60. doi:10.1111/nmo.12065

45. gomes p, chevalier j, Boesmans W, et al. ATP-dependent paracrine communication between enteric neurons and glia in a primary cell culture derived from embryonic mice. *Neurogastroenterol Motil*. 2009;21(8):870-e62. doi:10.1111/j.1365-2982.2009.01302.x

46. Burda JE, Sofroniew MV. Reactive gliosis and the multicellular response to CNS damage and disease. *Neuron*. 2014;81(2):229-248. doi:10.1016/j.neuron.2013.12.034

47. Oliveira S de, López-Muñoz A, Candel S, Pelegrín P, Calado Â, Mulero V. ATP modulates acute inflammation in vivo through dual oxidase 1-derived H2O2 production and NF-κB activation. *The Journal of Immunology*. 2014;192(12):5710-5719. doi:10.4049/jimmunol.1302902

48. Riteau N, Baron L, Villeret B, et al. ATP release and purinergic signaling: a common pathway for particle-mediated inflammasome activation. *Cell Death & Disease*. 2012;3(10):e403. doi:10.1038/cddis.2012.144

49. Stein K, Lysson M, Schumak B, et al. Leukocyte-Derived Interleukin-10 Aggravates Postoperative Ileus. *Front Immunol*. 2018;9. doi:10.3389/fimmu.2018.02599

50. Liñán-Rico A, Turco F, Ochoa-Cortes F, et al. Molecular Signaling and Dysfunction of the Human Reactive Enteric Glial Cell Phenotype: Implications for GI Infection, IBD, POI, Neurological, Motility, and GI Disorders. *Inflamm Bowel Dis*. 2016;22(8):1812-1834. doi:10.1097/MIB.0000000000000854

51. Roy Choudhury G, Ryou M-G, Poteet E, et al. Involvement of p38 MAPK in reactive astrogliosis induced by ischemic stroke. *Brain Research*. 2014;1551:45-58. doi:10.1016/j.brainres.2014.01.013

52. Boeckxstaens GE, Jonge WJ de. Neuroimmune mechanisms in postoperative ileus. *Gut*. 2009;58(9):1300-1311. doi:10.1136/gut.2008.169250

53. Andersson HC, Anderson MF, Porritt MJ, Nodin C, Blomstrand F, Nilsson M. Trauma-induced reactive gliosis is reduced after treatment with octanol and

carbenoxolone. *Neurological Research*. 2011;33(6):614-624. doi:10.1179/1743132810Y.0000000020

54. Pekny M, Pekna M. Astrocyte reactivity and reactive astrogliosis: costs and benefits. *Physiological Reviews*. 2014;94(4):1077-1098. doi:10.1152/physrev.00041.2013

55. Zamanian JL, Xu L, Foo LC, et al. Genomic analysis of reactive astrogliosis. *Journal of Neuroscience*. 2012;32(18):6391-6410. doi:10.1523/JNEUROSCI.6221-11.2012

56. Hara M, Kobayakawa K, Ohkawa Y, et al. Interaction of reactive astrocytes with type I collagen induces astrocytic scar formation through the integrin-N-cadherin pathway after spinal cord injury. *Nat Med*. 2017;23(7):818-828. doi:10.1038/nm.4354

57. Liddelow SA, Guttenplan KA, Clarke LE, et al. Neurotoxic reactive astrocytes are induced by activated microglia. *Nature*. 2017;541(7638):481-487. doi:10.1038/nature21029

58. Fujita A, Yamaguchi H, Yamasaki R, et al. Connexin 30 deficiency attenuates A2 astrocyte responses and induces severe neurodegeneration in a 1-methyl-4-phenyl-1,2,3,6-tetrahydropyridine hydrochloride Parkinson's disease animal model. *J Neuroinflammation*. 2018;15(1):227. doi:10.1186/s12974-018-1251-0

59. Mathys H, Davila-Velderrain J, Peng Z, et al. Single-cell transcriptomic analysis of Alzheimer's disease. *Nature*. 2019;570(7761):332-337. doi:10.1038/s41586-019-1195-2

60. Rakers C, Schleif M, Blank N, et al. Stroke target identification guided by astrocyte transcriptome analysis. *Glia*. 2019;67(4):619-633. doi:10.1002/glia.23544

61. Schirmer L, Velmeshev D, Holmqvist S, et al. Neuronal vulnerability and multilineage diversity in multiple sclerosis. *Nature*. 2019;573(7772):75-82. doi:10.1038/s41586-019-1404-z

62. Nieves MD, Furmanski O, Doughty ML. Sensorimotor dysfunction in a mild mouse model of cortical contusion injury without significant neuronal loss is associated with increases in inflammatory proteins with innate but not adaptive immune functions. *J Neurosci Res*. 2021;99(6):1533-1549. doi:10.1002/jnr.24766

63. Hyvärinen T, Hagman S, Ristola M, et al. Co-stimulation with IL-1β and TNF-α induces an inflammatory reactive astrocyte phenotype with neurosupportive characteristics in a human pluripotent stem cell model system. *Sci Rep*. 2019;9(1):16944. doi:10.1038/s41598-019-53414-9

64. Penkowa M, Espejo C, Ortega-Aznar A, Hidalgo J, Montalban X, Martínez Cáceres EM. Metallothionein expression in the central nervous system of multiple sclerosis patients. *Cell Mol Life Sci*. 2003;60(6):1258-1266. doi:10.1007/s00018-003-3021-z

65. Farro G, Stakenborg M, Gomez-Pinilla PJ, et al. CCR2-dependent monocyte-derived macrophages resolve inflammation and restore gut motility in postoperative ileus. *Gut*. 2017;66(12):2098-2109. doi:10.1136/gutjnl-2016-313144

66. Docsa T, Bhattarai D, Sipos A, Wade CE, Cox CS, Uray K. CXCL1 is upregulated during the development of ileus resulting in decreased intestinal contractile activity. *Neurogastroenterol Motil*. 2020;32(3):e13757. doi:10.1111/nmo.13757

67. Progatzky F, Shapiro M, Chng SH, et al. Regulation of intestinal immunity and tissue repair by enteric glia. *Nature*. 2021;599(7883):125-130. doi:10.1038/s41586-021-04006-z

68. Howarth GS, Bastian SEP, Dunbar AJ, Goddard C. Betacellulin promotes growth of the gastrointestinal organs and effects a diuresis in normal rats. *Growth Factors*. 2003;21(2):79-86. doi:10.1080/08977190310001605779

69. Chen F, Yang W, Huang X, et al. Neutrophils Promote Amphiregulin Production in Intestinal Epithelial Cells through TGF-β and Contribute to Intestinal Homeostasis. *The Journal of Immunology*. 2018;201(8):2492-2501. doi:10.4049/jimmunol.1800003

70. Bahrami S, Drabløs F. Gene regulation in the immediate-early response process. *Adv Biol Regul*. 2016;62:37-49. doi:10.1016/j.jbior.2016.05.001

71. Cruz-Mendoza F, Jauregui-Huerta F, Aguilar-Delgadillo A, García-Estrada J, Luquin S. Immediate Early Gene c-fos in the Brain: Focus on Glial Cells. *Brain Sci*. 2022;12(6). doi:10.3390/brainsci12060687

72. Grubišić V, McClain JL, Fried DE, et al. Enteric Glia Modulate Macrophage Phenotype and Visceral Sensitivity following Inflammation. *Cell Rep*. 2020;32(10):108100. doi:10.1016/j.celrep.2020.108100

73. Wehner S, Engel DR. Resident macrophages in the healthy and inflamed intestinal muscularis externa. *Pflugers Arch - Eur J Physiol*. 2017;469(3-4):541-552. doi:10.1007/s00424-017-1948-4

74. Kalff JC, Schraut WH, Simmons RL, Bauer AJ. Surgical Manipulation of the Gut Elicits an Intestinal Muscularis Inflammatory Response Resulting in Postsurgical Ileus. *Ann Surg*. 1998;228(5):652-663. doi:10.1097/00000658-199811000-00004

75. Mischopoulou M, Cipriani G. Muscularis Macrophages in Healthy and Diseased Gut. In: Shamsadin Athari S, Mehrabi Nasab E, eds. *Phagocytosis: Main Key of Immune System*. IntechOpen; 2023.

76. Muller PA, Koscsó B, Rajani GM, et al. Crosstalk between Muscularis Macrophages and Enteric Neurons Regulates Gastrointestinal Motility. *Cell*. 2014;158(5):1210. doi:10.1016/j.cell.2014.08.002

77. Schepper S de, Verheijden S, Aguilera-Lizarraga J, et al. Self-Maintaining Gut Macrophages Are Essential for Intestinal Homeostasis. *Cell*. 2018;175(2):400-415.e13. doi:10.1016/j.cell.2018.07.048

78. Ahrends T, Aydin B, Matheis F, et al. Enteric pathogens induce tissue tolerance and prevent neuronal loss from subsequent infections. *Cell*. 2021;184(23):5715-5727.e12. doi:10.1016/j.cell.2021.10.004

79. Fu H, Zhao Y, Hu D, Wang S, Yu T, Zhang L. Depletion of microglia exacerbates injury and impairs function recovery after spinal cord injury in mice. *Cell Death & Disease*. 2020;11(7):528. doi:10.1038/s41419-020-2733-4

80. Lou N, Takano T, Pei Y, Xavier AL, Goldman SA, Nedergaard M. Purinergic receptor P2RY12-dependent microglial closure of the injured blood-brain barrier. *Proceedings of the National Academy of Sciences*. 2016;113(4):1074-1079. doi:10.1073/pnas.1520398113

81. Simon DW, McGeachy MJ, Bayır H, Clark RSB, Loane DJ, Kochanek PM. The far-reaching scope of neuroinflammation after traumatic brain injury. *Nat Rev Neurol*. 2017;13(3):171-191. doi:10.1038/nrneurol.2017.13

82. Brown IAM, McClain JL, Watson RE, Patel BA, Gulbransen BD. Enteric glia mediate neuron death in colitis through purinergic pathways that require connexin-43 and nitric oxide. *Cell Mol Gastroenterol Hepatol*. 2016;2(1):77-91. doi:10.1016/j.jcmgh.2015.08.007

83. Luo P, Liu D, Li C, He W-X, Zhang C-L, Chang M-J. Enteric glial cell activation protects enteric neurons from damage due to diabetes in part via the promotion of neurotrophic factor release. *Neurogastroenterol Motil*. 2018;30(10):e13368. doi:10.1111/nmo.13368

84. Delvalle NM, Dharshika C, Morales-Soto W, Fried DE, Gaudette L, Gulbransen BD. Communication Between Enteric Neurons, Glia, and Nociceptors Underlies the Effects of Tachykinins on Neuroinflammation. *Cell Mol Gastroenterol Hepatol*. 2018;6(3):321-344. doi:10.1016/j.jcmgh.2018.05.009

85. Li N, Xu J, Gao H, et al. *Reactive Enteric Glial Cells Participate in Paralytic Ileus by Damaging Nitrergic Neurons During Endotoxemia*. 2021.

86. Fung C, Boesmans W, Cirillo C, Foong JPP, Bornstein JC, Vanden Berghe P. VPAC Receptor Subtypes Tune Purinergic Neuron-to-Glia Communication in the Murine Submucosal Plexus. *Front Cell Neurosci*. 2017;11:118. doi:10.3389/fncel.2017.00118

87. Mazzotta E, Grants I, Villalobos-Hernandez E, et al. BQ788 reveals glial ETB receptor modulation of neuronal cholinergic and nitrergic pathways to inhibit intestinal motility: Linked to postoperative ileus. *Br J Pharmacol*. 2023;180(19):2550-2576. doi:10.1111/bph.16145

88. Boesmans W, Nash A, Tasnády KR, Yang W, Stamp LA, Hao MM. Development, Diversity, and Neurogenic Capacity of Enteric Glia. *Front Cell Dev Biol*. 2021;9:775102. doi:10.3389/fcell.2021.775102

89. Boesmans W, Lasrado R, Vanden Berghe P, Pachnis V. Heterogeneity and phenotypic plasticity of glial cells in the mammalian enteric nervous system. *Glia*. 2015;63(2):229-241. doi:10.1002/glia.22746

90. Guyer RA, Stavely R, Robertson K, et al. Single-cell multiome sequencing clarifies enteric glial diversity and identifies an intraganglionic population poised for neurogenesis. *Cell Rep*. 2023;42(3):112194. doi:10.1016/j.celrep.2023.112194

91. Colangelo AM, Alberghina L, Papa M. Astrogliosis as a therapeutic target for neurodegenerative diseases. *Neuroscience Letters*. 2014;565:59-64. doi:10.1016/j.neulet.2014.01.014

92. Livne-Bar I, Lam S, Chan D, et al. Pharmacologic inhibition of reactive gliosis blocks TNF-α-mediated neuronal apoptosis. *Cell Death & Disease*. 2016;7(9):e2386. doi:10.1038/cddis.2016.277

93. Jonge WJ de, van den Wijngaard RM, The FO, et al. Postoperative ileus is maintained by intestinal immune infiltrates that activate inhibitory neural pathways

in mice. *Gastroenterology*. 2003;125(4):1137-1147. doi:10.1016/s0016-5085(03)01197-1

94. Kalff JC, Carlos TM, Schraut WH, Billiar TR, Simmons RL, Bauer AJ. Surgically induced leukocytic infiltrates within the rat intestinal muscularis mediate postoperative ileus. *Gastroenterology*. 1999;117(2):378-387. doi:10.1053/GAST.1999.0029900378

95. Wen Q, Kong Y, Zhao H-Y, et al. G-CSF-induced macrophage polarization and mobilization may prevent acute graft-versus-host disease after allogeneic hematopoietic stem cell transplantation. *Bone Marrow Transplant*. 2019;54(9):1419-1433. doi:10.1038/s41409-019-0449-9

96. Meshkibaf S, Martins AJ, Henry GT, Kim SO. Protective role of G-CSF in dextran sulfate sodium-induced acute colitis through generating gut-homing macrophages. *Cytokine*. 2016;78:69-78. doi:10.1016/j.cyto.2015.11.025

97. Bendall LJ, Bradstock KF. G-CSF: From granulopoietic stimulant to bone marrow stem cell mobilizing agent. *Cytokine Growth Factor Rev*. 2014;25(4):355-367. doi:10.1016/j.cytogfr.2014.07.011

98. Pinheiro D, Mawhin M-A, Prendecki M, Woollard KJ. In-silico analysis of myeloid cells across the animal kingdom reveals neutrophil evolution by colony-stimulating factors. *Elife*. 2020;9. doi:10.7554/eLife.60214

99. Agoston DV. How to Translate Time? The Temporal Aspect of Human and Rodent Biology. *Front Neurol*. 2017;8:92. doi:10.3389/fneur.2017.00092

100. Radermacher P, Haouzi P. A mouse is not a rat is not a man: species-specific metabolic responses to sepsis - a nail in the coffin of murine models for critical care research? *Intensive Care Med Exp*. 2013;1(1):26. doi:10.1186/2197-425X-1-7

101. Drokhlyansky E, Smillie CS, van Wittenberghe N, et al. The Human and Mouse Enteric Nervous System at Single-Cell Resolution. *Cell*. 2020;182(6):1606-1622.e23. doi:10.1016/j.cell.2020.08.003

102. Zeisel A, Hochgerner H, Lönnerberg P, et al. Molecular Architecture of the Mouse Nervous System. *Cell*. 2018;174(4):999-1014.e22. doi:10.1016/j.cell.2018.06.021

103. Elmentaite R, Kumasaka N, Roberts K, et al. Cells of the human intestinal tract mapped across space and time. *Nature*. 2021;597(7875):250-255. doi:10.1038/s41586-021-03852-1

104. Fawkner-Corbett D, Antanaviciute A, Parikh K, et al. Spatiotemporal analysis of human intestinal development at single-cell resolution. *Cell*. 2021;184(3):810-826.e23. doi:10.1016/j.cell.2020.12.016

105. Satam H, Joshi K, Mangrolia U, et al. Next-Generation Sequencing Technology: Current Trends and Advancements. *Biology (Basel)*. 2023;12(7). doi:10.3390/biology12070997

106. Gulbransen BD, Christofi FL. Are We Close to Targeting Enteric Glia in Gastrointestinal Diseases and Motility Disorders? *Gastroenterology*. 2018;155(2):245-251. doi:10.1053/j.gastro.2018.06.050

107. Hallerbäck B, Carlsen E, Carlsson K, et al. Beta-adrenoceptor blockade in the treatment of postoperative adynamic ileus. *Scand J Gastroenterol*. 1987;22(2):149-155. doi:10.3109/00365528708991872

108. Ferraz AA, Wanderley GJ, Santos MA, Mathias CA, Araújo JG, Ferraz EM. Effects of propranolol on human postoperative ileus. *Dig Surg*. 2001;18(4):305-310. doi:10.1159/000050157

109. Tan S, Zhou F, Zhang Z, et al. Beta-1 blocker reduces inflammation and preserves intestinal barrier function after open abdominal surgery. *Surgery*. 2021;169(4):885-893. doi:10.1016/j.surg.2020.11.004

110. Baqi Y, Hausmann R, Rosefort C, Rettinger J, Schmalzing G, Müller CE. Discovery of potent competitive antagonists and positive modulators of the P2X2 receptor. *Journal of Medicinal Chemistry*. 2011;54(3):817-830. doi:10.1021/jm1012193

111. Migdalska-Richards A, Daly L, Bezard E, Schapira AHV. Ambroxol effects in glucocerebrosidase and α-synuclein transgenic mice. *Annals of Neurology*. 2016;80(5):766-775. doi:10.1002/ana.24790

112. Hama AT, Plum AW, Sagen J. Antinociceptive effect of ambroxol in rats with neuropathic spinal cord injury pain. *Pharmacol Biochem Behav*. 2010;97(2):249-255. doi:10.1016/j.pbb.2010.08.006

113. Su X, Wang L, Song Y, Bai C. Inhibition of inflammatory responses by ambroxol, a mucolytic agent, in a murine model of acute lung injury induced by lipopolysaccharide. *Intensive Care Medicine*. 2004;30(1):133-140. doi:10.1007/s00134-003-2001-y

114. Beeh KM. Antiinflammatory properties of ambroxol. *Eur J Med Res*. 2008;13:557.

115. Burnstock G. *Introduction to Purinergic Signaling*. Springer New York. *Methods Mol Biol*. 2020;2041:1-15. Methods in Molecular Biology.

116. Germouty J, Jirou-Najou JL. Clinical efficacy of ambroxol in the treatment of bronchial stasis. Clinical trial in 120 patients at two different doses. *Respiration*. 1987;51 Suppl 1(1):37-41. doi:10.1159/000195273

117. Mullin S, Smith L, Lee K, et al. Ambroxol for the Treatment of Patients With Parkinson Disease With and Without Glucocerebrosidase Gene Mutations: A Nonrandomized, Noncontrolled Trial. *JAMA Neurol*. 2020;77(4):427-434. doi:10.1001/jamaneurol.2019.4611

118. Silveira CRA, MacKinley J, Coleman K, et al. Ambroxol as a novel disease-modifying treatment for Parkinson's disease dementia: protocol for a single-centre, randomized, double-blind, placebo-controlled trial. *BMC Neurology*. 2019;19(1):20. doi:10.1186/s12883-019-1252-3

119. Richards D, Gever JR, Ford AP, Fountain SJ. Action of MK-7264 (gefapixant) at human P2X3 and P2X2/3 receptors and in vivo efficacy in models of sensitisation. *Br J Pharmacol*. 2019;176(13):2279-2291. doi:10.1111/bph.14677

120. Burnstock G, Jacobson KA, Christofi FL. Purinergic drug targets for gastrointestinal disorders. *Current Opinion in Pharmacology*. 2017;37:131-141. doi:10.1016/j.coph.2017.10.011

121. Wardill HR, Mooij CEM de, Da Silva Ferreira AR, et al. Supporting the gastrointestinal microenvironment during high-dose chemotherapy and stem cell transplantation by inhibiting IL-1 signaling with anakinra. *Sci Rep*. 2022;12(1):6803. doi:10.1038/s41598-022-10700-3

122. Mazzotta E, Villalobos-Hernandez EC, Fiorda-Diaz J, Harzman A, Christofi FL. Postoperative Ileus and Postoperative Gastrointestinal Tract Dysfunction: Pathogenic Mechanisms and Novel Treatment Strategies Beyond Colorectal Enhanced Recovery After Surgery Protocols. *Front Pharmacol*. 2020;11:583422. doi:10.3389/fphar.2020.583422

123. Bersudsky M, Luski L, Fishman D, et al. Non-redundant properties of IL-1α and IL-1β during acute colon inflammation in mice. *Gut*. 2014;63(4):598-609. doi:10.1136/gutjnl-2012-303329

124. Cox CB, Storm EE, Kapoor VN, et al. IL-1R1-dependent signaling coordinates epithelial regeneration in response to intestinal damage. *Sci Immunol*. 2021;6(59). doi:10.1126/sciimmunol.abe8856

125. Wu W-JH, Kim M, Chang L-C, et al. Interleukin-1β secretion induced by mucosa-associated gut commensal bacteria promotes intestinal barrier repair. *Gut Microbes*. 2022;14(1):2014772. doi:10.1080/19490976.2021.2014772

126. Chen H-T, Hung K-C, Huang Y-T, et al. Efficacy of electroacupuncture in improving postoperative ileus in patients receiving colorectal surgery: a systematic review and meta-analysis. *Int J Surg*. 2024;110(2):1113-1125. doi:10.1097/JS9.0000000000000848

127. Cui Y, Zhang C, Zhang H, et al. Effect evaluation of different preventive measures for ileus after abdominal operation: A systematic review and network meta-analysis. *Heliyon*. 2024;10(4):e25412. doi:10.1016/j.heliyon.2024.e25412

128. Emile SH, Horesh N, Garoufalia Z, Gefen R, Ray-Offor E, Wexner SD. Strategies to reduce ileus after colorectal surgery: A qualitative umbrella review of the collective evidence. *Surgery*. 2024;175(2):280-288. doi:10.1016/j.surg.2023.10.005

5. Acknowledgements

I extend my heartfelt appreciation to Prof. Sven Wehner, for his invaluable guidance, mentorship, and support during my work in his group. His feedback and unwavering belief in my scientific abilities assisted me in driving my career and shaped me as a scientist.

Similarly, I want to express my utmost gratitude to Dr. Reiner Schneider as my mentor and constant companion during all the long lab hours and struggles of scientific work. Without his insightful feedback in numerous discussions and his constructive criticism, I would not be the person I am today. Additionally, I would like to thank him for his positive attitude, all the non-work-related talks and after-work excursions in the decade I have known him, which always brightened my mood and lifted me up whenever I was faltering.

I would like to express my gratitude to the members of my dissertation committee, Prof. Steinhäuser, Prof. Wilhelm, and Prof. Jackson, for their thoughtful insights and constructive suggestions. Especially Prof. Jackson was an immense help during the revision of two of my publications and thereby provided valuable contributions to my thesis.

I would like to thank the wonderful team of AG Wehner for the countless hours we spent together; you enriched all the little moments and made them more memorable. I thank my amazing technicians Bianca Schneiker, Mariola Lysson, Jana Müller, and Patrik Efferz, who acted as my faerie godparents and could always be relied upon. Their constant support and friendly attitude made the days brighter and work more enjoyable. I appreciate Svenja Gysser, Xenia Zoller, and Dr. Alex Seinsche for all the assistance in planning and communicating with the various departments of the UKB. I express my gratitude towards Dr. Ivan Kuzmanov for sharing his knowledge and reassuring me when I was down, and Dr. Balbina Garcia Reyes for her valuable scientific input and all the discussion about geek culture. I would like to thank all the cheerful and ambitious technicians in training (Ariane und Emily Thielisch, Julian Lehmann, Lisa Enns, Melissa Jürgens) and our fabulous students over the years (Hannah Neuhaus, Stefanie Lück-Fuhrmann, Tawfik Abou Assale, Kevin Siemens, Mona Breßer, Jonah Lunnebach, Akram Abdulkadyrov, and Yasin Abdel Galil). They all helped me grow as

a leader, were valuable assets in my lab work and provided a good working atmosphere. Similarly, I would like to thank my fellow PhD students (Shilpashree Mallesh, Lilly Bantavi, Hilal Sengül, Ebrahim Hamza, and Linda Schneider) for all the lively discussions, friendly banter, shared long hours, and general camaraderie. Especially fellow night owls Linda and Mona were always reliable, lightened my mood, and helped me stay sane.

I thank all my friends, especially my former flatmate Fabian Wälter and my fellow PhDs Patrick Wunder and Eileen C. Haring for all the support throughout the 20 or more years of our friendships.

I am grateful for the support my parents, in-laws, grandparents, sister, and brother-in-law provided me with, not only throughout this journey but throughout my entire life. Thanks to your care and love I am the man I am today.

Lastly, I want to thank my wonderful wife Wiebke, and my amazing daughter Nele for their unrelenting support, immeasurable patience, and all-encompassing love throughout this intense journey. Your sacrifices, both big and small have made this possible and I am deeply thankful. Without you, none of this would have been possible and you two have my eternal love.